NAVAL POSTGRADUATE SCHOOL
Monterey, California

THESIS

R122

TURBULENCE EFFECTS ON THE HIGH ANGLE OF ATTACK AERODYNAMICS OF A VERTICALLY LAUNCHED MISSILE

by

M. Peter Rabang

June 1988

Thesis Advisor Richard M. Howard

Approved for public release; distribution is unlimited.

T242275

nclassified

urity classification of this page

REPORT DOCUMENTATION PAGE

a Report Security Classification Unclassified		1b Restrictive Markings
a Security Classification Authority		3 Distribution Availability of Report Approved for public release; distribution is unlimited.
b Declassification Downgrading Schedule		
Performing Organization Report Number(s)		5 Monitoring Organization Report Number(s)
a Name of Performing Organization Naval Postgraduate School	6b Office Symbol *(if applicable)* 33	7a Name of Monitoring Organization Naval Postgraduate School
c Address *(city, state, and ZIP code)* Monterey, CA 93943-5000		7b Address *(city, state, and ZIP code)* Monterey, CA 93943-5000
a Name of Funding Sponsoring Organization	8b Office Symbol *(if applicable)*	9 Procurement Instrument Identification Number
c Address *(city, state, and ZIP code)*		10 Source of Funding Numbers

Program Element No	Project No	Task No	Work Unit Accession No

1 Title *(include security classification)* TURBULENCE EFFECTS ON THE HIGH ANGLE OF ATTACK AERODYNAMICS OF A VERTICALLY LAUNCHED MISSILE

2 Personal Author(s) M. Peter Rabang

13a Type of Report	13b Time Covered	14 Date of Report *(year, month, day)*	15 Page Count
Master's Thesis	From To	June 1988	165

16 Supplementary Notation The views expressed in this thesis are those of the author and do not reflect the official policy or position of the Department of Defense or the U.S. Government.

17 Cosati Codes			18 Subject Terms *(continue on reverse if necessary and identify by block number)*
Field	Group	Subgroup	Vortex, Vertical Launch, Surface to Air Missile, High Angle of Attack Aerodynamics, Turbulence, Body of Revolution

19 Abstract *(continue on reverse if necessary and identify by block number)*

A subsonic wind tunnel investigation was conducted at the Naval Postgraduate School Wind Tunnel Test Facility to examine the effects of grid generated turbulence on the high angle of attack aerodynamics of a vertically launched missile. Four turbulence generating grids produced turbulence with length scale to missile model diameter ratios of 1.05, 0.89, 0.62, and 0.15 with respective turbulence intensities of 3.31%, 2.78%, 1.88%, and 0.47%. The test model is representative of current cruciform wing missiles with low aspect ratio wings and long root chords. The tangent ogive nose has a nose fineness ratio of 2.29. Three separate body configurations were tested with and without the turbulence generating grids. One configuration was a body in isolation and the other two were wing and tail configurations at 0° and 45° roll angles. All test runs were conducted at $Re_d \approx 1.1 \times 10^5$ over an angle of attack range of -5° to 95°. Results indicate that as turbulence length scales approach body diameter size, the angle of attack for the onset of asymmetric vortices was delayed and the side force magnitude was reduced. The vortices generated by the nose of the missile continue to dominate the afterbody vortices for body configurations with and without wings regardless of the turbulence conditions.

20 Distribution Availability of Abstract	21 Abstract Security Classification	
☒ unclassified unlimited ☐ same as report ☐ DTIC users	Unclassified	
22a Name of Responsible Individual Richard M. Howard	22b Telephone *(include Area code)* (408) 646-2870	22c Office Symbol 67Ho

DD FORM 1473,84 MAR 83 APR edition may be used until exhausted
All other editions are obsolete

security classification of this page

Unclassified

Approved for public release; distribution is unlimited.

Turbulence Effects on the High Angle of Attack Aerodynamics of a Vertically Launched Missile

by

M. Peter Rabang
Lieutenant, United States Navy
B.S., University of South Carolina, 1981

Submitted in partial fulfillment of the
requirements for the degree of

MASTER OF SCIENCE IN ENGINEERING SCIENCE

from the

NAVAL POSTGRADUATE SCHOOL
June 1988

ABSTRACT

A subsonic wind tunnel investigation was conducted at the Naval Postgraduate School Wind Tunnel Test Facility to examine the effects of grid generated turbulence on the high angle of attack aerodynamics of a vertically launched missile. Four turbulence generating grids produced turbulence with length scale to missile model diameter ratios of 1.05, 0.89, 0.62, and 0.15 with respective turbulence intensities of 3.31%, 2.78%, 1.88%, and 0.47%. The test model is representative of current cruciform wing missiles with low aspect ratio wings and long root chords. The tangent ogive nose has a nose fineness ratio of 2.29. Three separate body configurations were tested with and without the turbulence generating grids. One configuration was a body in isolation and the other two were wing and tail configurations at 0° and 45° roll angles. All test runs were conducted at $Re_d \approx 1.1 \times 10^5$ over an angle of attack range of -5° to 95°. Results indicate that as turbulence length scales approach body diameter size, the angle of attack for the onset of asymmetric vortices was delayed and the side force magnitude was reduced. The vortices generated by the nose of the missile continue to dominate the afterbody vortices for body configurations with and without wings regardless of the turbulence conditions.

THESIS DISCLAIMER

The reader is cautioned that computer programs developed in this research may not have been exercised for all cases of interest. While every effort has been made, within the time available, to ensure that the programs are free of computational and logic errors, they cannot be considered validated. Any application of these programs without additional verification is at the risk of the user.

TABLE OF CONTENTS

I. INTRODUCTION 1
A. BACKGROUND 1
B. HIGH ANGLE OF ATTACK AERODYNAMICS 2
1. Vortex Regions. 2
a. Regime I - [$0° \leq \alpha < \alpha_{SV}$] 4
b. Regime II - [$\alpha_{SV} \leq \alpha < \alpha_{AV}$] 4
c. Regime III - [$\alpha_{AV} \leq \alpha < \alpha_{UV}$] 4
d. Regime IV - [$\alpha_{UV} \leq \alpha < 90°$] 4
2. Two Dimensional Crossflow. 5
3. Three Dimensional Vortices. 8
C. LIFTING SURFACE EFFECTS 10
1. Wings. 10
2. Strakes 11
3. Tails 12
D. TURBULENCE 12
1. Intensity and Length Scale 12
2. Boundary Layer Effects 14
3. Vortex effects 15
E. VSLAM LAUNCH ENVIRONMENT 15
1. The Marine Environment 15
2. Turbulence 16
3. Crosswind 17
4. Ship Airwake. 17
5. Additional launch considerations 18

II. EXPERIMENT AND PROCEDURES 19
A. APPARATUS 19
1. Wind Tunnel 19
2. VSLAM Model 21
3. Balance 23
4. Model Balance Support 23

5. Turbulence Grids 25
6. Data Acquisition Hardware 29
7. Data Acquisition Software 31
B. EXPERIMENTAL CONDITIONS 31
C. EXPERIMENTAL PROCEDURE 33
1. Balance Calibration 33
2. Prerun Calibration and Test 33
3. Data Collection 34
4. Preliminary Runs 34
D. EXPERIMENTAL CORRECTIONS 35

III. RESULTS 37
A. VARIATIONS IN NOSE ROLL ANGLE 37
B. DATA REPEATABILITY 39
C. BODY IN ISOLATION 40
D. WINGS AND STRAKES WITHOUT TURBULENCE. 44
E. WINGS AND STRAKES WITH TURBULENCE. 51
F. NORMAL FORCE RESULTS 52
G. SIDE FORCE TO NORMAL FORCE RATIO 52

IV. CONCLUSIONS AND RECOMMENDATIONS 69

APPENDIX A. BALANCE CALIBRATION CONSTANTS 71

APPENDIX B. RUN MATRIX 73

APPENDIX C. NUMERICAL DATA LISTING 76

APPENDIX D. DATA ACQUISITION PROGRAM 129

APPENDIX E. COEFFICIENTS TRANSLATION PROGRAM 139

LIST OF REFERENCES 144

INITIAL DISTRIBUTION LIST 149

LIST OF TABLES

Table 1. BALANCE CHANNELS 23
Table 2. GRID SPECIFICATIONS 26
Table 3. GRID TURBULENCE PARAMETERS 27
Table 4. VLSAM MODEL BLOCKAGE 36

LIST OF FIGURES

Figure 1. Vortex Generation Regimes 3
Figure 2. Two dimensional crossflow about a cylinder 5
Figure 3. Side force to normal force ratio 6
Figure 4. Flow over a delta wing 11
Figure 5. Naval Postgraduate School Low Speed Wind Tunnel 20
Figure 6. Drawing of VLSAM model. 22
Figure 7. Photograph of VLSAM model in the test section. 24
Figure 8. Planview of VLSAM model in the test section. 25
Figure 9. Grid Turbulence Intensity 26
Figure 10. Grid Turbulence Length Scales 27
Figure 11. Turbulence Grids 2, 3, and 4. 28
Figure 12. Turbulence Grid 1 installed in the wind tunnel. 29
Figure 13. Data Acquisition Hardware 30
Figure 14. Body configurations and reference system. 32
Figure 15. Blockage factors 36
Figure 16. Side force variations with nose roll angle 38
Figure 17. Side force variations with nose roll angle 38
Figure 18. Data Repeatability Runs 39
Figure 19. R0B802 40
Figure 20. R1B801 42
Figure 21. R2B801 42
Figure 22. R3B801 43
Figure 23. R4B801 43
Figure 24. R0A803 45
Figure 25. R0C802 45
Figure 26. R1A804 46
Figure 27. R2A801 46
Figure 28. R3A801 47
Figure 29. R4A801 47
Figure 30. R1C802 48
Figure 31. R2C801 48

Figure 32. R3C801 49
Figure 33. R4C801 49
Figure 34. R0B802 53
Figure 35. R1B801 54
Figure 36. R2B801 54
Figure 37. R3B801 55
Figure 38. R4B801 55
Figure 39. R0A803 56
Figure 40. R0C802 56
Figure 41. R1A804 57
Figure 42. R2A801 57
Figure 43. R3A801 58
Figure 44. R4A801 58
Figure 45. R1C802 59
Figure 46. R2C801 59
Figure 47. R3C801 60
Figure 48. R4C801 60
Figure 49. R0B802 61
Figure 50. R1B801 61
Figure 51. R2B801 62
Figure 52. R3B801 62
Figure 53. R4B801 63
Figure 54. R0A803 63
Figure 55. R1A804 64
Figure 56. R2A801 64
Figure 57. R3A801 65
Figure 58. R4A801 65
Figure 59. R0C802 66
Figure 60. R1C802 66
Figure 61. R2C801 67
Figure 62. R3C801 67
Figure 63. R4C801 68
Figure 64. Balance Calibration Constants 71
Figure 65. Balance Calibration Constants 72

NOMENCLATURE

A	axial force
A_d	base area
AOA	angle of attack
C_n	normal force coefficient, $\frac{N}{q_\infty A_d}$
C_y	side force coefficient, $\frac{S}{q_\infty A_d}$
C_{ax}	axial force coefficient, $\frac{A}{q_\infty A_d}$
C_{pt}	pitching moment coefficient, $\frac{M_P}{q_\infty A_d l_B}$
C_{rl}	rolling moment coefficient, $\frac{M_R}{q_\infty A_d l_B}$
C_{yw}	yawing moment coefficient, $\frac{M_Y}{q_\infty A_d l_B}$
d	base diameter of the missile body
l_B	balance reference length, (= 1)
l_N	nose length
$(l_N/d)_{nose}$	nose fineness ratio
$(l_M/d)_{missile}$	missile fineness ratio
L_d	missile diameter scale
L_l	missile length scale
L_u	turbulence length scale
M_P	pitching moment
M_R	rolling moment
M_Y	yawing moment
N	normal force
q	test section dynamic pressure
q_M	measured reference pressure

q_R	reference pressure
q_∞	free-stream dynamic pressure,
Re_d	Reynolds number, $\frac{\rho U_\infty d}{\mu}$
S	side force
T_u	turbulence intensity
u′	root-mean-square (rms) velocity fluctuation
U	horizontal velocity
U_M	measured velocity
U_∞	longitudinal mean velocity
V_v	vertical velocity
z_0	roughness length
α	angle of attack
α_{AV}	angle of attack for asymmetric vortices
α_{SV}	angle of attack for symmetric vortices
α_{UV}	angle of attack for unsteady vortices
ε	blockage factor
θ_A	nose semi-vertex angle
μ	coefficient of viscosity
ϕ	angle from crossflow
ϕ_R	roll angle
ρ	air density

ACKNOWLEDGEMENTS

My sincere gratitude goes to my advisor Dr. Richard Howard for providing me the opportunity to study and work with wind tunnel experimental techniques in high angle of attack aerodynamics. His wisdom and encouragement throughout the many months of research provided me with a knowledgeable and rewarding experience.

The assistance of the NAVY-NASA Joint Institute of Aeronautics and the following NASA-Ames Research Facility Personnel is acknowledged:

Mr. Chuck Pronty, Aerodynamic Facilities Branch

Mr. Jim McMahon, Balance Calibration Laboratory

Mr. Doug McMurchy, Balance Calibration Laboratory

I would also like the thank the many people here at the Naval Postgraduate School who supported this experimental research. In particular:

Mr. Jack King, Aerolab

Mr. John Moulton, Aeronautics Shop

Mr. Ron Ramaker, Aeronautics Shop

LT. Randy Langmead, USN, Aeronautics Microcomputer Lab

DEDICATION

In memory of Julia Mateo Rabang.

I. INTRODUCTION

A. BACKGROUND

The development of missiles capable of operating at high angles of attack has prompted numerous investigations and experiments in high angle of attack research. Much interest is due to the demands for highly maneuverable missiles at supersonic speeds. In cases where the missile is launched from the ground or at sea from a ship, the missile's initial velocity for all practical purposes is zero. From this initial state, the missile must fly over a wide range of Mach numbers from subsonic to supersonic speeds. The aerodynamic characteristics of the missile may vary greatly as it transitions through these operating speeds. All surface-to-air missiles follow a three phase operation: launch, midcourse, and terminal. Each phase represents a different missile flight regime owing to the changing flight control requirements and airflow about the missile, thus presenting a challenge to the missile designer who must develop a missile capable of operating throughout each regime.

Vertical launch for missiles is by no means a novel idea. It has been the primary means of launching large rockets and missiles from land. Vertical launch of surface-to-air missiles at sea is a recent development. Conventional launch systems utilize a trainable launcher consisting of a rail or tube adjustable in azimuth and elevation. The vertical launch surface-to-air missile (VLSAM) uses a canister container which stores and launches the missile. The canister system eliminates the cumbersome trainable launcher and associated specialized storage facilities and loading mechanisms. Other advantages of the VLSAM are the 360° coverage provided without interference from the ship's superstructure, a higher firing rate since launcher availability is no longer a factor, and space and weight savings [Ref. 1].

VLSAMs have their own unique trajectories, allowing them to *point* at their targets after launch. Two flight control methods are currently used: thrust vectored control, and aerodynamic surface control [Ref. 2]. Thrust vectored control is used with short range missiles which must *pitch over* quickly to engage targets at close range. Long range missiles maneuver with aerodynamic control surfaces. In each case, as the VLSAM exits the canister it enters the open ocean environment at low velocity and is subject to potentially significant crosswinds. The resultant of the missile and crosswind velocities is a potential high angle of attack flow about the missile [Ref. 3]. This high angle of attack flow may

cause asymmetric vortices to form on the missile nose and afterbody which induces side forces as discussed later in this chapter. These side forces could give flight control problems to the VLSAM at launch.

The launch environment may contain some degree of turbulence, both from the atmospheric boundary layer, and the airflow about the ship. Understanding the effect of this turbulence on the aerodynamic characteristics of a VLSAM during launch is the goal of a continuing effort of research and experiments conducted at the Naval Postgraduate School (NPS). In earlier work, Roane [Ref. 3] developed a system of modelling the flowfield turbulence by a series of four grids to generate turbulence in the NPS low speed wind tunnel. The goal of this thesis is to experimentally examine the effects of this turbulence on the asymmetric vortex induced forces generated on a VLSAM model.

B. HIGH ANGLE OF ATTACK AERODYNAMICS

Flow separation from the body, wing, and tail surfaces is an important phenomenon encountered in high angle of attack aerodynamics since asymmetric vortices may form to induce side forces. Primary factors which influence flow separation from the missile body are: the angle of attack, crossflow Reynolds number (Re_d) [1], nose geometry, and nose length to diameter ratio (also called the nose fineness ratio). Secondary factors include roll angle and roll rate, free stream turbulence, surface roughness, acoustic environment (pressure waves), and vibration [Refs. 4, 5, 6]. This section discusses how the factors mentioned above influence the mechanisms responsible for vortex generation and disposition.

1. Vortex Regions.

As a slender unyawed body changes angle of attack α from 0° to 90°, the airflow over the missile body transitions through four regimes as described by Ericsson and Reding [Ref. 7: pp. 246-247]. These regimes [Figure 1] are characterized by the changing vortex patterns and the resulting induced in-plane (normal), and out-of-plane (side) forces and moments which act on the missile at zero side-slip and at high angles of attack [2] [Refs. 2, 4, 8, 9]. These regimes are bounded by:

α_{SV} - the angle of attack at which steady symmetric vortices are formed.

α_{AV} - the angle of attack where steady asymmetric vortices are formed.

α_{UV} - the angle of attack where unsteady vortices are formed.

---

1 The crossflow Reynolds number is set by the base diameter of the missile.

2 Without wings and tails.

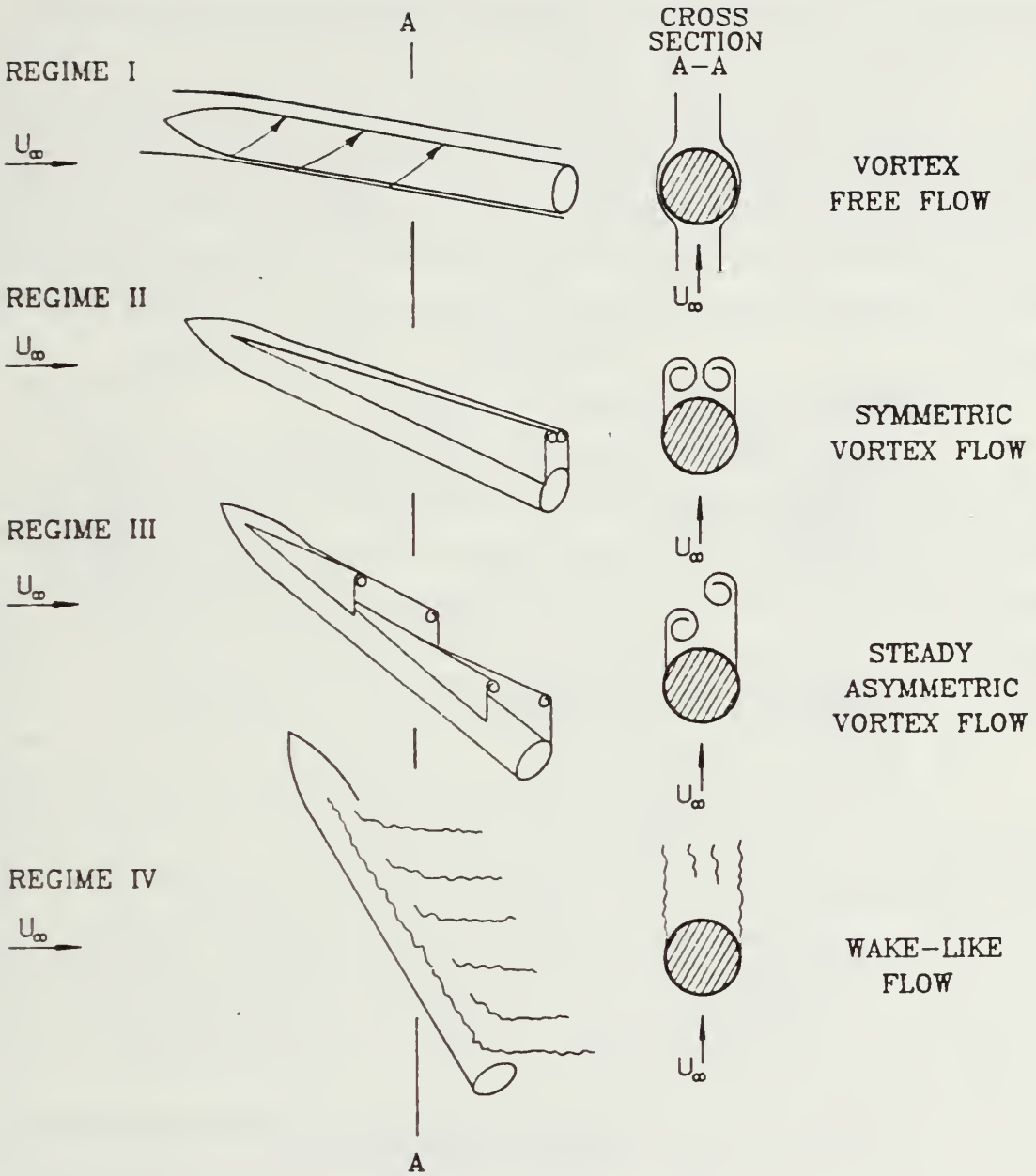

Figure 1. Vortex Generation Regimes: [Ref. 10]

a. Regime I - $[0° \leq \alpha < \alpha_{SV}]$

The axial flow dominates and flow around the body remains attached for pointed noses. If the nose is blunted, a separation bubble may occur (discussed below).

b. Regime II - $[\alpha_{SV} \leq \alpha < \alpha_{AV}]$

The crossflow begins to push the boundary layer to the leeward side where it separates and a system of two or more pairs of symmetric vortices are formed. These vortices originate at the nose of the body. For long bodies, more pairs of symmetric vortices are generated along the body length. The number and strength of the symmetric vortices increase with angle of attack. Symmetric vortices typically start at $\alpha_{SV} \approx 5°$ [Ref. 4].

c. Regime III - $[\alpha_{AV} \leq \alpha < \alpha_{UV}]$

Crossflow begins to dominate, shedding asymmetric vortices which induce out-of-plane or side forces on the body. These asymmetric vortices are relatively steady, but may change from side to side at higher angles of attack near the maximum side force magnitude [Ref. 11]. In some cases the side forces may exceed the normal force. The vortices which are the most asymmetric yield the highest side force magnitude [Ref. 12]. This regime typically starts at $\alpha_{AV} \approx 20°$ [Ref. 4].

d. Regime IV - $[\alpha_{UV} \leq \alpha < 90°]$

The crossflow dominates completely and flow separation becomes unsteady and dependent on Reynolds number. At the critical Reynolds number the boundary layer separates then re-attaches as a turbulent vortex sheet (discussed later). The boundary layer is shed as a random wake at supercritical Reynolds numbers, or a von Karman vortex sheet at subcritical Reynolds numbers. Normal force magnitude will plateau and side force magnitude decreases to zero. This regime has been observed to begin at $\alpha_{UV} \approx 60°$ [Ref. 4].

Asymmetric vortex induced side forces are dependent on the strength and disposition of the vortex patterns which are, according to Ericsson and Reding [Ref. 7], a result of boundary layer transition on the surfaces of the missile. The analogy most often used to describe flow separation deals with boundary layer transition on a two-dimensional cylinder in a normal crossflow. Three dimensional effects due to nose and afterbody geometry must also be understood as they dictate the formation of the vortex structure.

2. Two Dimensional Crossflow.

Airflow over the missile body can be divided into normal and axial components. The axial flow component follows along the missile body length and the crossflow is essentially a two dimensional flow normal to a cylinder. The crossflow analogy provides information for cylinder lift and drag which act in the direction of the crossflow. Side forces may exist at right angles to the crossflow depending on the type of flow separation on opposite sides of the cylinder. Mechanisms behind boundary layer transition and separation provide an explanation for flow separation and subsequent asymmetric vortex generation effects.

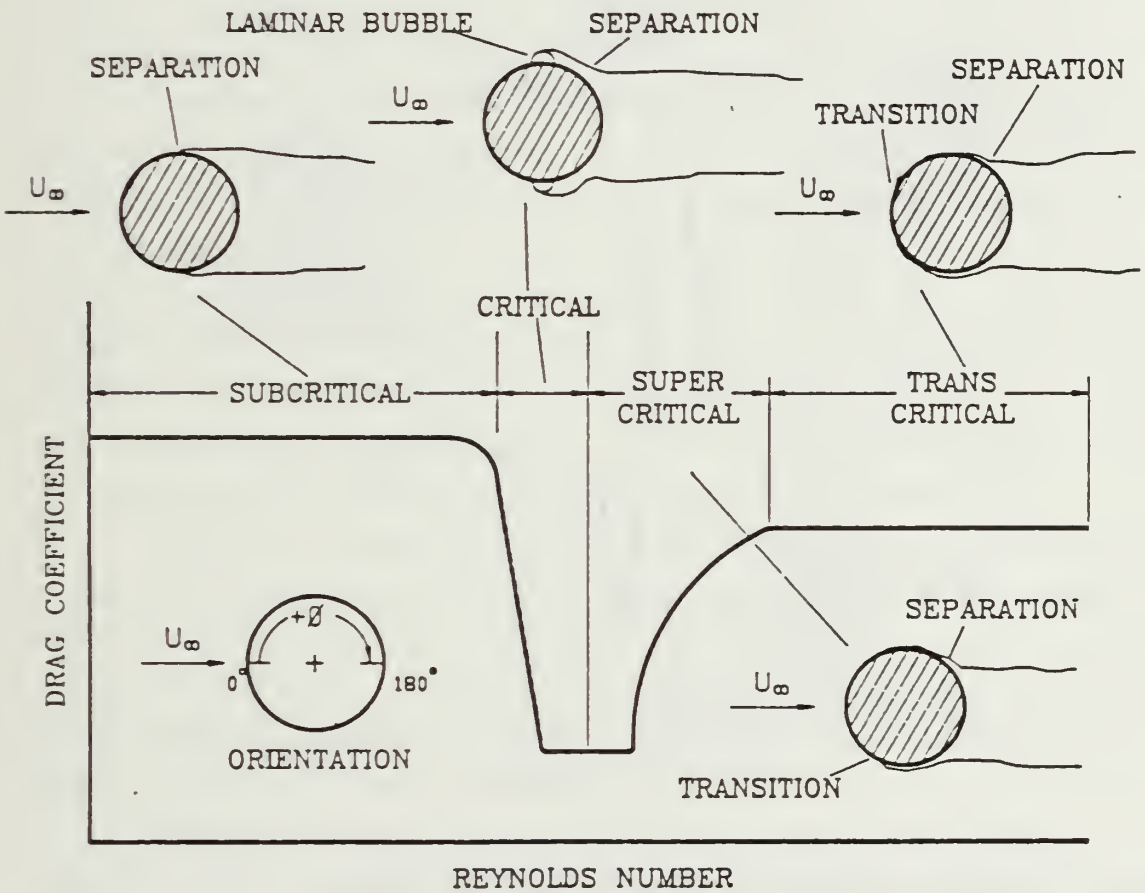

Figure 2. Two dimensional crossflow about a cylinder: [Refs. 13, 14].

The crossflow Reynolds number is the primary factor which influences the separation point of the boundary layer. Viscous flow, surface roughness, and turbulence

are other factors which influence boundary layer separation. Achenbach classified the flow around a cylinder into four distinct regions deliniated by differing flow separation and drag behavior [Ref. 13]. These regions are shown in Figure 2and discussed below.

In the subcritical range, the boundary layer is laminar and flow separation occurs close to to the lateral meridian where ϕ, defined as the angle from the direction of the crossflow, varies from 80° to 90°. Asymmetric subcritical separation occurs at $\phi \approx 90°$, where the side force just begins to reach a noticeable magnitude.

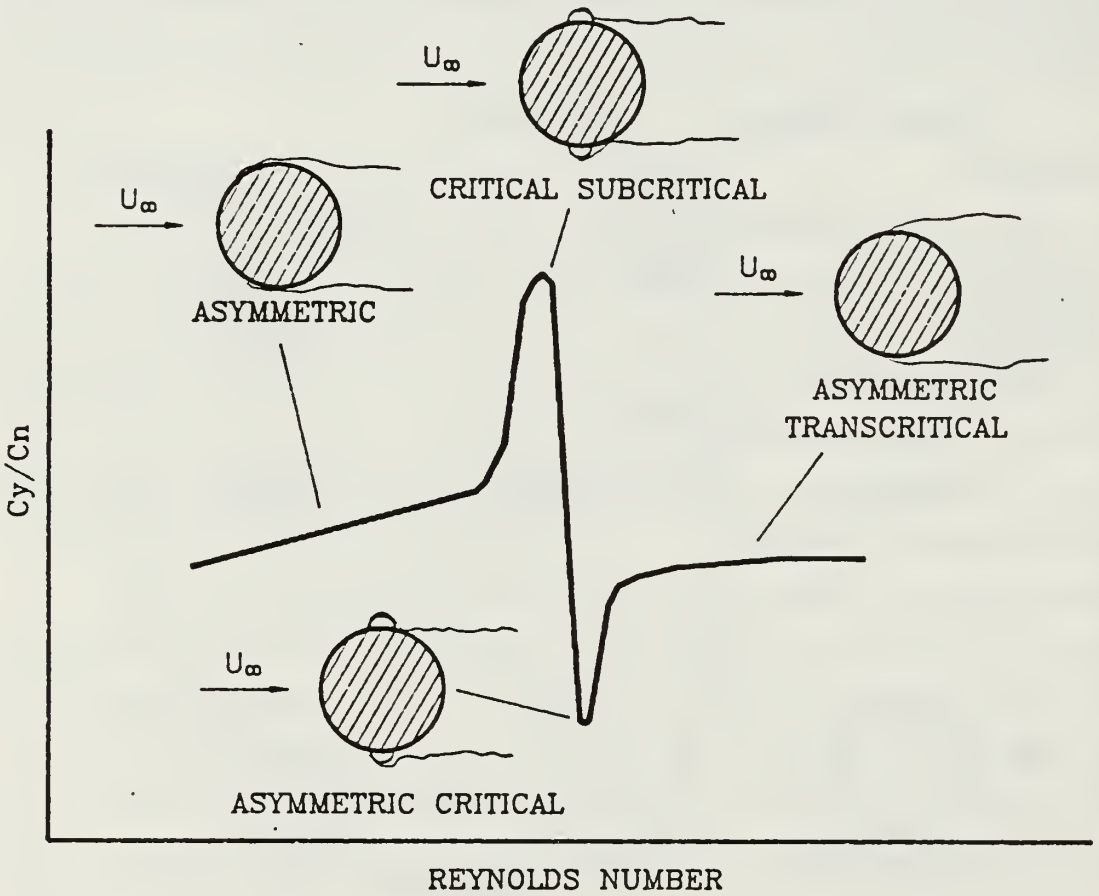

Figure 3. Side force to normal force ratio: [Ref. 7: p. 260].

When the Reynolds number enters the critical range, the laminar boundary layer separates from the body at $\phi \approx 90°$ and re-attaches as a turbulent boundary layer which separates again from the surface at $\phi \approx 140°$. Between the laminar separation and the turbulent re-attachment, a laminar bubble is formed. In this region, the flow separation

can easily change back and forth from critical to subcritical for small changes in Reynolds number. The changes occur on opposite sides of the cylindrical section and when critical separation exists on one side of the body and subcritical separation on the opposite side, a large difference in ϕ from opposite transition points is possible. When this critical and subcritical combination occurs, an asymmetry is observed in the generated vortices. The pressure difference on opposite sides of the lateral meridian will produce the side force. For the largest difference in ϕ, the vortices will be at maximum asymmetry, and the side force at the highest magnitude as seen in Figure 3. The asymmetric vortices may also become susceptible to altering back and forth, hence the change in the direction of the induced side forces. Maximum side force occurs at the critical Reynolds number, making it an important parameter. [Ref. 15]

Next, as the Reynolds number increases into the fully critical range, laminar transition moves towards the direction of the crossflow. Turbulent separation will move forward to $\phi < 140°$ and the laminar bubble is no longer formed. Asymmetric critical separation occurs simultaneously on opposite sides of the body. The asymmetric vortices produce nearly equal surface pressures at the lateral meridian because the separation asymmetry only affects the surface pressures at $\phi > 140°$. In this range the vortices are ineffective at producing a significant side force and a sudden decrease in magnitude occurs as shown by the curve in Figure 3. The boundary layer thickens and viscous properties of the fluid are the dominant factor. Drag reaches a minimum.

Finally, as the Reynolds number increases further to supercritical and into the transcritical range, the laminar transition point works towards $\phi \approx 0°$ and turbulent separation occurs at $\phi \approx 100°$. The asymmetric transcritical separation point moves towards the lateral meridian where the asymmetric vortices once again produce a significant side force. Drag will continue to rise and settle out at a level lower than subcritical conditions. [Refs. 7: pp. 247-261, 13]

The Reynolds number dictates the greatest influence on the normal force and drag characteristics, especially within the critical range. Maximum normal forces on the missile should occur when the boundary layer flow is completely laminar or completely turbulent, because crossflow drag is high. Surface roughness and viscous effects are also present. Experiments by Lamont [Ref. 16] and Wardlaw [Ref. 17] show that maximum asymmetric loads follow the same behavior as the normal force, with the lowest vortex induced side forces occurring at transcritical conditions. The largest lift to drag ratio occurs at the critical Reynolds number where drag is a minimum. Maximum vortex

asymmetry has been observed to occur at the critical/subcritical Reynolds number explained above. Thus the maximum side force to normal force ratio may be expected to be found at the critical Reynolds number. [Ref. 14]

3. **Three Dimensional Vortices.**

The initial separation point of the shed vortices occurs at the nose of the slender body. Many researchers have observed that these vortices shed from the nose will dominate other vortices shed along the body length [Refs. 18, 19, 20]. Thus, the nose geometry becomes an important factor in vortex generation and disposition. Axisymmetric missile nose geometry falls into two shapes: cones and ogives, both pointed and blunt. Noses are dimensionalized for comparison by their length to base diameter ratio or fineness ratio, $(l_N/d)_{nose}$.

For pointed conical and ogive noses, observations indicate that α_{AV} occurs as a function of the semi-vertex angle θ_A . At all Mach numbers, asymmetric vortex shedding begins when the the angle of incidence α is greater than the apex angle of the nose, where $\theta_A = \theta_C$ for a conical nose.

$$\alpha_{AV} \approx 2\theta_A \qquad \{1\}$$

For a tangent ogive nose[3], with length l_N and base diameter d:

$$\theta_A = \tan^{-1}\left[\frac{\frac{l_N}{d}}{\frac{l_N^2}{d} - 0.25} \right] \qquad \{2\}$$

A close approximation for slender bodies is:

$$\theta_A \approx \frac{d}{l_N} \qquad \{3\}$$

Blunting the nose may cause a second type of asymmetric vortex shedding to develop at the rear of the nose. The blunt nose causes a separation bubble to form on the leeward side of the nose. Asymmetric vortices originate at the rear of the blunted nose, and tend to dominate the induced effects from the afterbody vortices [Ref. 21]. The asymmetric vortices generated by a blunted nose do not alternate from side to side

---

[3] A tangent ogive nose is constructed from a constant radius arc with the center of the arc lying in the plane of the base of the nose and some distance away from the nose axis.

as readily as those generated a pointed nose. Side force magnitudes are also reduced. Afterbody vortices from a blunt nose missile remain closer to the body and are easily shed throughout the missile length [Ref. 4]. Thus, blunting the nose will reduce the effects of vortex asymmetry and the induced side force.

Nose fineness ratio has been shown to have an effect on the asymmetric vortex induced side force [Refs. 18, 19, 22]. In general, side force magnitude increases with larger nose fineness ratio [Ref. 18]. As the nose fineness ratio increases, the nose apex angle decreases and the angle of attack for the onset of asymmetric vortices will decrease. Thus, a missile with high nose fineness ratio may become more susceptible to induced side forces at a lower angle of attack than a missile having a lower nose fineness ratio. Jorgensen demonstrated that decreasing the nose fineness ratio is more beneficial in reducing side force than blunting the nose [Ref. 18].

The presence of the afterbody at a constant roll angle has almost no effect on vortex generation from the pointed nose of slender bodies [Ref. 23]. The first pair of vortices generated by a pointed nose will set the pattern for vortices shed along the body [Ref. 24]. The afterbody will also shed asymmetric vortices, but these will not effect the nose vortices generation, although the afterbody forces will contribute to the overall magnitude of induced forces from the nose-body combination.

Should the afterbody roll angle change, with nose roll angle remaining constant, the afterbody vortices will change the side force magnitude and direction as shown in research by Kruse [Ref. 25]. Since the nose and body of a missile do not rotate independently of each other, the vortex system generated by the nose should still dominate afterbody vortices on a axisymmetric missile configuration.

Experimental results for pointed ogive-cylinders with and without afterbodies show that small variations in roll angle alter the asymmetric vortex structure and side forces. Researchers believe that surface imperfections and deviations in the nose axisymmetric geometry are the sources of this phenomenon. The direction and magnitude of the side force becomes unpredictable, a detriment to anyone attempting to generate a model. [Ref. 26]

The preceding section on the two dimensional flow separation analogy discussed four flow separation mechanisms. Keener identified that three of these flow separation mechanisms occurred simultaneously along the length of a nose and forebody at angles of attack greater than 20° and transcritical Reynolds number of $Re_d = 0.8 \times 10^6$. These mechanisms were observed from surface flow patterns on tangent ogive noses.

1. Primary laminar separation near the nose.
2. Primary transitional separation at the nose midsection consisting of a laminar bubble.
3. Primary turbulent separation near the base of the nose.

The extent of the transitional separation region grew with increasing angles of attack and constant Reynolds number while the turbulent separation region decreased. [Ref. 11]

Ongoing investigations have not fully revealed the exact cause of vortex asymmetry. The general consensus among high angle of attack researchers is that vortex asymmetry is induced by the location of boundary layer separation [Refs. 7, 9]. Keener also considers the possibility that vortex asymmetry may be caused by an inviscid instability in the pair of separated vortices. [Ref. 11] There are many other three dimensional effects which must be considered to complete a flowfield analysis which include roll, pitch, and yaw rate; and yaw angle.

C. LIFTING SURFACE EFFECTS

1. Wings.

Compared to aircraft, missiles generally use low aspect ratio wings. Mutual effects from a wing-body combination are important since in some cases the missile wing span approaches body diameter.

As discussed earlier, nose vortices dictate flow behavior over the missile body at high angles of attack. In turn, the effects may also be felt by the wings. Without wings, the nose and body vortices tend to move away from the body with increasing angle of attack. The addition of wings causes the vortices to take a different trajectory, moving them closer to the body. As the vortices move closer to the body, the result is comparable to increasing the effective angle of attack causing unsteady asymmetric vortices. [Ref. 27]

A significant fraction of the normal force from a missile wing is proportional to the square of the angle of attack. This is attributed to the vortex lift effects from flow around a sharp leading edge delta wing [4]. As vortices curl around the wing leading edge, a low pressure area forms on top of the wing providing lift as shown in Figure 4. Since a cruciform missile has an equilateral wing arrangement, equal lift may be provided in the normal and side directions depending on the wing angle of attack to the flow. For

---

[4] A common wing planform shared by numerous missiles.

wings with low aspect ratio, a large proportion of the lift generated by the wing will be due to vortex lift. [Ref. 28]

The net effect of the wing-body combination seems to be a reduction in the effective angle of attack for the onset of asymmetric vortices and side forces.

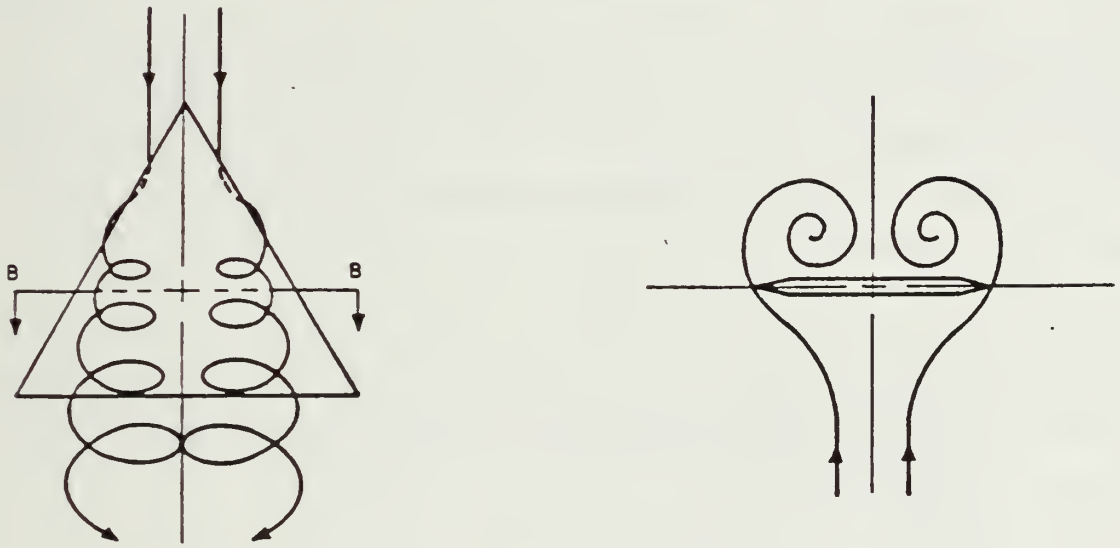

Figure 4. **Flow over a delta wing:** The left drawing shows the vortices curling over the sharp leading edge for low Reynolds numbers. The right drawing is the cross section B-B. [Ref. 29].

2. Strakes

For an aircraft, the addition of strakes is to improve the aerodynamic characteristics by enhancing lift at high angles of attack. Vortices generated by flow separation from the aircraft's forebody interacts with the flow over the main wing. The addition of strakes will generate additional vortices improving the interaction between body vortices and airflow over the wings. The effects of wing strakes are different on a low aspect ratio wing missile since missile forebodies are comparatively longer and wing half span is smaller when compared to body radius. The flow becomes separated from the body at a moderate angle of attack before passing over the strakes [Ref. 30]. The strakes on a

missile may lessen the effect of asymmetric body vortices since the strakes would cause interference with the crossflow component around the body. The real benefit of incorporating strakes with low aspect ratio wings is from the strong vortices produced by the strake which enhance vortex lift effects.

3. Tails

The tails of a missile have little influence on flowfields on the forebody, especially at low angles of attack. At high angles of attack interference on the flowfield caused by wings and the afterbody may effect tailflow which depends a great deal on the placement of the wings, the length of the afterbody between the wings and tails, and the missile's angle of attack. For higher angles of attack, nose and wing vortices may be sufficiently displaced away from the body to have only a slight effect on the tailflow. Should a large distance between wings and tails exist, afterbody vortices may dominate the airflow over the tail surfaces. Hence, most missile configurations with long afterbodies utilize canard or wing control while missiles employing tail control have short afterbodies and low aspect ratio wings with long root chords. The additional asymmetric vortices from the afterbody will also contribute to the overall side force on the missile. [Ref. 28: p. 172]

D. TURBULENCE

1. Intensity and Length Scale

Turbulence denotes an irregular fluctuation or disturbance of a fluid changing motion when superimposed on a flowfield. In terms of scale (size and energy), the flowfield may be magnitudes higher than turbulence. The disturbance exists when fluid particles overcome the constraining effects of viscosity and are able to fluctuate in the flowfield. Turbulence exists for large Reynolds numbers where longer flowfield length scales are present. A horizontal wind or crosswind may be considered as a large scale flowfield and turbulence becomes a smaller component of the crosswind. Further, when a flowfield contains turbulence, it can be considered a turbulent flowfield and so a crosswind can be though of as a turbulent crosswind. It should be understood that any wind for practical purposes is turbulent, but since crosswind size and energy scales are magnitudes larger than the turbulence scales contained in the crosswind, we can treat the crosswind as homogeneous and two dimensional.

As a large scale homogeneous flowfield, the crosswind can be viewed as exerting a uniform flow over the missile body. Flow separation mechanisms discussed earlier for a two dimensional cylinder in a steady flowfield apply in the crosswind. Understanding

the effects of small scale turbulence on the flow separation mechanisms is important since vortex generation and asymmetry determine side force direction and magnitude. Small scale turbulence effects are dependent on turbulence length scale and intensity which will be discussed below. Turbulence intensity and length scale components exists in the streamwise and spanwise directions relative to the flowfield. For purposes of this and following discussions only the streamwise component in the flowfield will be discussed.

Turbulence intensity is the measure of the relative magnitude of velocity fluctuations in the flowfield. Mathematically, for a horizontal flowfield or crosswind, the turbulence intensity T_u is the ratio of the root-mean-square (rms) velocity fluctuation u′, to the mean velocity component in the flowfield, U_∞.

$$T_u = \frac{u'}{U_\infty} \qquad \{4\}$$

Since the turbulence intensity measures the magnitude of velocity fluctuation, a higher intensity indicates higher kinetic energy and correlates to *more turbulent* flow.

Turbulence length scale L_u describes the time average measure of the fluid disturbance eddies. The measure is time averaged since these disturbances constantly change size. The size of the disturbances are determined by external conditions associated with the flow. An example of large scale turbulence are flow disturbances caused by flowfields over large buildings in a city, while small scale turbulence is generated by flow through mesh screens. [Ref. 31: p. 557]

Turbulence length scale to body size ratio may dictate the manner in which turbulence affects the VLSAM flowfield. The turbulence length scale can be compared to missile length, L_u:L_l , or missile diameter, L_u:L_d . When the turbulence length scale is many times larger than the missile length, $L_u \gg L_l$, the effect on the missile is somewhat like a uniform time independent steady-state flowfield, especially at low turbulence intensities. The effects of the flowfield on vortex development are largely dictated by those conditions and factors discussed earlier for a two dimensional cylinder. When the turbulence length scale is comparable to the body length, $L_u \approx L_l$, the flowfield is distinctly non-uniform and may cause unwanted rolling, pitching and yawing motion [Ref. 32]. In both cases, the missile body motion results from the actual flowfield conditions about the missile body.

Perhaps the most significant turbulence condition is when the turbulence length scale is smaller than the body, $L_u \ll L_l$, and most important, when it is comparable or smaller than missile diameter, $L_u \lesssim L_d$. The small scale turbulence present in the flowfield may change the boundary layers present on the missile surface, particularly when the turbulence length scale is the same size or smaller than the boundary layer thickness. An important parameter for small scale turbulence is the turbulence intensity, since the energy in the turbulence may trigger the boundary layer. In contrast to larger turbulence scales where the primary influence is on the flowfield, the effects of small scale turbulence is felt on the boundary layer and flow separation on the surface of the missile. [Ref. 33]

Both large and small scale turbulence length scales actually coexist in the flowfield since the turbulence length scale is the mean of the disturbances in the flowfield. The combination of different length scales may add complexity to the qualitative analysis of the flowfield. The cascade effect explains how turbulence in varying length scales exists in the flowfield. As the disturbances in the flowfield experience strain, the disturbances will break up into finer disturbances of smaller scale and decreasing energy. The process repeats itself or cascades until the small disturbances eventually disappear owing to viscosity. When the disturbances decrease in size and energy, their individual intensities will decrease at a faster rate. Thus, the turbulence length scale average will be biased towards the larger turbulence scales in the flowfield and gives an accurate quantitative representation of all the length scales within the flowfield since the energy and intensity of the larger scale turbulence predominate. [Ref. 34]

2. Boundary Layer Effects

Turbulence length scales on the order of boundary layer thickness may change the boundary layer on the missile surface. This small scale turbulence will be referred to as *boundary layer scale* turbulence, and although three dimensional and inhomogeneous, can be visualized as two dimensional crossflow components over a cylinder. When the boundary layer scale turbulence in the crossflow reaches the missile surface boundary layer, it contributes energy as it dissipates into the boundary layer.[5] This turbulence interaction results in an earlier laminar transition and delays separation of the turbulent boundary layer. This causes flow separation to occur below the critical Reynolds number for laminar flow, postponing asymmetric vortex shedding. Reynolds number effects dominate at low turbulence intensities for smooth surfaces. When surface roughness in-

---

5 In accordance with the laws of momentum and energy conservation.

creases, the boundary layer separation becomes less dependent on Reynolds number and more dependent on turbulence intensity. The net effect postpones the side force induced by the asymmetric vortices and allows the missile to operate at higher angles of attack without induced side forces. [Refs. 33, 35]

The application of boundary layer scale turbulence to add energy to the boundary layer is a well known method of inducing earlier flow transition and delayed flow separation to eliminate or reduce the effects of asymmetric vortex induced side forces. Among the numerous methods implemented to add turbulence to the boundary layer are placing roughness strips in various patterns at noses of the missile models utilized in wind tunnel experiments. [Refs. 11, 26]

3. Vortex effects

When the vortices from the missile body are formed, they become detached from the body at high angles of attack. The interaction of turbulence on the order of the vortex size may give additional insight to the disposition of asymmetric vortices. This small scale turbulence will be referred to as *vortex scale turbulence* and is magnitudes larger than boundary scale turbulence. Vortex scale turbulence may be compared to body diameter size $L_v \approx L_d$. Objects in the flowfield, much larger then roughness strips, may be used to generate vortex scale turbulence. Vortex scale turbulence may be generated by strakes, support hardpoints, or inlets. The effects of vortex scale turbulence may influence the position of the asymmetric vortices and may contribute dissipated turbulence energies as with boundary layer turbulence. Since the relative positioning and magnitude of the vortex structure governs the pressure distribution on the surface of the missile, the vortex scale turbulence could dictate the position and magnitude of the asymmetric induced side forces. Research into this phenomenon has been conducted as another means of alleviating asymmetric vortex induced side forces. Methods include adding nose strakes, nose helical vortex generators, and nose booms to missile models. [Refs. 11, 18, 36]

E. VSLAM LAUNCH ENVIRONMENT

1. The Marine Environment

Conditions in the marine atmospheric environment may have a significant effect on the VLSAM. In the atmosphere, turbulence conditions exist almost everywhere, in particular, within the atmospheric boundary layer (ABL) which is the lowest part of the atmosphere [Ref. 37: p. 179]. The conditions in the ABL are the result of atmospheric flow over the sea surface. The flowfield cannot be strictly classified as a boundary layer

flow since non-uniform boundary conditions under constant fluctuation and changes almost always exist [Ref. 32].

The lowest ten percent of the ABL is referred to as the surface layer and is typically 50 meters in height but may vary from 5-200 meters. The surface layer is characterized by distinct variations in wind speed, nearly vertical heat and mass fluxes, and other meteorological fluctuations with height [Ref. 38: p. 236]. Fluctuations in wind variations, especially at sea may reach fifty percent of the mean wind speed [Ref. 31: p. 557]. The surface layer is also characterized by intense small scale turbulence which is mechanically produced by surface roughness or friction from waves on the ocean surface.[6] The lowest portion of the surface layer is termed the roughness layer and is where the surface has the greatest effect on generating turbulence and influencing fluid motion. Mean flow in the roughness layer in largely three dimensional and inhomogeneous in nature. Small scale turbulence dominates flow near the surface. As altitude increases, small scale turbulence decreases rapidly as large scale turbulence formed by convective conditions in the atmosphere prevail. Several roughness heights above the surface, the mean flowfield becomes nearly horizontally homogeneous and two dimensional. Over sea, the mean surface layer and especially the roughness layer are more inhomogeneous and three dimensional than over land.

2. Turbulence

The roughness length z_o is a measure of surface roughness as a function of the mean wind velocity and height above the surface. Surface layer turbulence length scale and intensity can be empirically determined from the aforementioned parameters. For typical open ocean roughness lengths in the range $10^{-3} < z_o < 10^{-2}$ meters, turbulence intensities are on the order of 13 to 17 percent at a 10 meter elevation and mean wind speed of approximately 25 m sec [Ref. 39]. These high turbulence intensities are for high crosswind velocities and rough seas; extreme conditions which may be encountered. Tieleman states an average turbulence intensity of 6 to 12 percent to exist below a 20 meter height above the ocean surface [Ref. 32].

From previous discussions, the turbulence length scale to body scale ratio is an important parameter for flowfield behavior. For the conditions stated in the preceding paragraph, the longitudinal turbulence length scales L_u are in the range $80 < L_u < 90$ meters (or $262 < L_u < 295$ feet). For a typical missile with a 1.1 foot diameter, the turbulence to missile diameter length scale ratio is about $L_u : L_d \approx 280:1$ and would have

---

6 This small scale turbulence is larger than the missile length.

little effect on boundary layer development. Yet the possibility exists where boundary layer and vortex scale turbulence may be present due to the cascade effect from large scale turbulence and from crosswind interaction with the ship's superstructure, lending themselves to vortex and boundary layer interactions.

3. Crosswind

A typical VLSAM launching with a 10g acceleration reaches an altitude of approximately 56 feet travelling at a vertical velocity of $V_v \approx 164$ ft/sec. The VLSAM is still well within the surface layer environment (50 m) and subject to crosswind and turbulence effects. The preceding paragraph indicates turbulence length scales are relatively long in the surface layer. In such a case, the large scale flowfield or crosswind may dictate aerodynamic effects on the VLSAM. As an example, if a ship travels at 20 knots and a mean wind speed of 20 m/sec are combined with the VLSAM launch velocity, the resultant vector is at 191 ft/sec at an angle of 31° from the missile direction. The result is that the VLSAM flies at an effective angle of attack of 31° at 191 ft/sec, placing it in Regime III, the asymmetric vortex region, as it travels through the surface layer. [Ref. 3]

A missile at a lower altitude, closer to the ship, will have a lower velocity and therefore it will be flying at an even greater effective angle of attack. Gregoriou states that a VLSAM that pitches over towards a target may experience an effective angle of attack up to $\alpha \approx 50°$ [Ref. 2]. These examples should illustrate the distinct possibility of asymmetric vortex induced side forces on a VLSAM during launch phase.

4. Ship Airwake.

Changing flowfields and turbulence may be dictated by the ship's hull and superstructure. This flowfield or ship airwake may increase the crosswind velocity, cause significant crosswind gradients, and non-uniformities in the flowfield increasing turbulence intensities while decreasing turbulence length scales. These effects occur in and around the vicinity of the ship which acts as a turbulence generator. Results of earlier discussions produced the following parameters in the marine surface layer:

$$\text{Mean crosswind velocity} - \quad 20 < U_\infty < 30 \quad \text{(m/sec)}$$

$$\text{Turbulence intensity} - \quad 13 < T_u < 17 \quad \text{(percent)}$$

$$\text{Turbulence length scale} - \quad 80 < L_u < 90 \quad \text{(meters)}$$

These values may change due to ship airwake effects in favor of higher turbulence intensities and smaller length scales, conditions prone to affect the missile boundary layer causing delayed separation. [Ref. 39]

5. Additional launch considerations

Other considerations which may influence the VLSAM at launch are dependent on the launch platform, the mechanics of a canister launch, and the aerodynamic effects of the the missile controlling itself. These conditions are essential to the overall aerodynamic effects on the VLSAM as it exits the canister.

The launch platform undergoes constant roll, pitch and yaw motion and transmits this motion to the VLSAM as it travels through the the guide mechanism in the canister. Increased severity of the ship's motion adds complexity to the initial velocity vector as the VLSAM leaves the guide.

The launch feature unique to a VLSAM is that the canister used for storage is also the launcher. Unlike a rail launched missile where motor exhaust dissipates into the surroundings, a canister or tube constrains a portion of the rocket motor gases resulting in a muzzle blast effect. As the VLSAM rocket motor ignites, most of the exhaust gases are typically vented via a plenum and uptake arrangement. Still, there is a significant amount of backflow which flows around the VLSAM as it leaves the canister. The rocket motor exhaust from the uptake may also interact with the flowfields about the missile. The environment of a rocket motor ignition is severe in itself, with high magnitudes of heat, shocks, and vibration. [Ref. 40]

The VLSAM itself may impose some form of flight control, aerodynamic or thrust vector, to maintain flight attitude during the launch phase. Should the missile change flight attitude, the flowfield around it will be altered.

These considerations are introduced to bring out the numerous factors which may influence the VLSAM flowfield and cause in-plane and out-of-plane forces and moments during the launch phase. They will add complexity to a fully comprehensive flowfield analysis of the VLSAM which is beyond the scope of the present investigation.

II. EXPERIMENT AND PROCEDURES

A. APPARATUS

The experimental investigation was conducted at the Naval Postgraduate School wind tunnel test facility. The VLSAM model was mounted on a six-component strain gage balance and sting support assembly. Turbulence generating grids and the test facility steady-state data acquisition hardware/software complete the experimental apparatus discussed in this section.

1. Wind Tunnel

The horizontal-flow low-speed tunnel used for this experiment is located in the Naval Postgraduate School wind tunnel test facility and shown in Figure 5. The wind tunnel is powered by a one-hundred horsepower electric motor driving a three blade variable-pitch propeller via a four-speed Dodge truck transmission. Immediately following the propeller blades are a set of stator blades to help straighten the flow. Turning vanes installed at each corner, and two fine wire mesh screens placed at the entrance to the settling chamber smoothen the airflow and reduce turbulence. The settling chamber to test section contraction ratio is approximately 10:1. A heavy wire mesh screen is installed at the end of the test section diffuser to prevent foreign object damage to the fan section. [Ref. 41: pp.3-1 to 3-2]

The test section operates at atmospheric pressure and measures 45 inches by 32 inches. Corner fillets house the test section lighting and help reduce synergetic boundary layer effects at the wall interactions.[7] To counteract a reduction in freestream pressure due to boundary layer growth, the walls of the test section are slightly diverged. Immediately downstream of the test section are breather slots around the perimeter of the wind tunnel. These slots allow air to enter and leave the tunnel unhindered, replenishing air lost through leaks and ensuring a uniform test section pressure. A reflection plane located in the center of the test section provides a horizontal surface to the flowfield and reduces the test section available height to 28 inches. A flush turntable at the center allows model the operator to change model pitch or angle of attack during wind tunnel operation.[Ref. 41: pp. 3-3 to 3-4]

---

[7] The fillets reduce the area of the test section from 10 ft.^{2} to 9.88 ft.^{2} Fillets are employed throughout the wind tunnel at wall interactions.

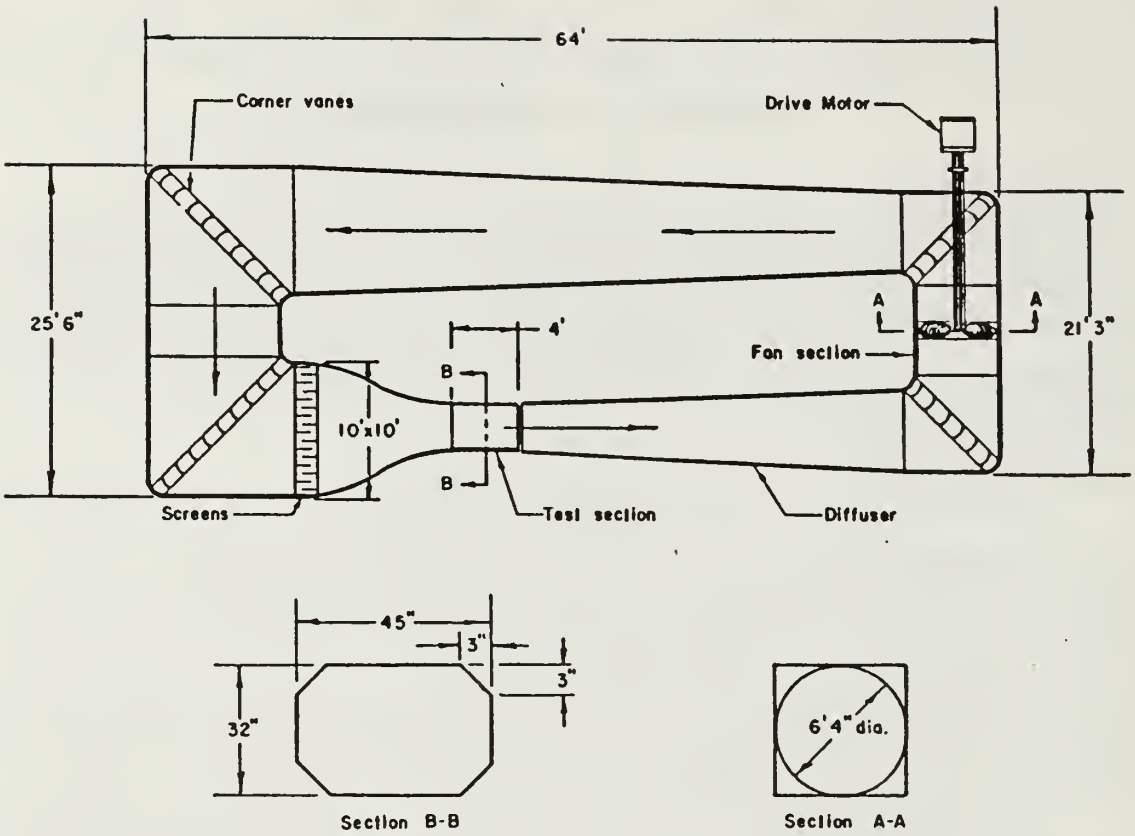

Figure 5. Naval Postgraduate School Low Speed Wind Tunnel: [Ref. 41: p. 3-7]

Flow measurement components utilized with the wind tunnel are a dial thermometer, manometer, and pitot static tube. Temperature in the wind tunnel is measured by a dial thermometer extending into the settling chamber. Dynamic pressure in the wind tunnel is measured by the static pressure difference between the test section and the settling chamber using a water filled manometer. Static pressure in the settling chamber is measured by four static pressure taps, one on each wall. The test section has another four static pressure taps, one on each wall, upstream of the test section to preclude interference from the model. The pressure taps at each section are connected via a common manifold prior to feeding into the manometer. The manometer measures pressure differences in centimeters of water, which is the test section dynamic pressure, and is converted to the actual wind tunnel velocity by equation [5].

$$U_M = \sqrt{\frac{2 \cdot 2.046 \cdot \text{cm } H_2O}{0.93 \cdot \rho}} \quad \{5\}$$

Where:

U_M = measured velocity ($\frac{ft}{sec}$)
2.046 = conversion factor
cm H_2O = manometer reading in cm of H_2O
0.93 = calibration factor.[8]
ρ = air density ($\frac{lb_m}{ft^3}$)

A pressure transducer circuit, connected to the manometer displays test section dynamic pressure on a digital readout. Once calibrated, the digital manometer has a greater accuracy than the manometer and was used to measure the dynamic pressure. The pitot static tube is read from a aircraft airspeed indicator and is used only for test section velocity approximations when starting and stopping the wind tunnel.

2. VSLAM Model

The VLSAM model was designed to be representative of a cruciform tail-control missile with very low aspect ratio wings or dorsal fins. The model was fabricated from 6061 and 2024 aluminum alloy by Naval Postgraduate School personnel. The model accommodates the one-inch precision balance and sleeve used in the experiment and has internal reserve space for fitting pressure measurement instrumentation. Four sections form the major parts of the model. The body section is a hollow cylinder with locating pin attachment points for the balance, sleeve, wings and tails. The body mounts on the balance, or by an adapter for use without the balance to mount the model on the support or sting. Body roll angle, with or without the balance, can be varied in 90° increments. The nose piece attaches to the body forward of the balance. Nose roll angle may be varied in 45° increments independent of the body. The nose is a pointed ogive shape with a short constant diameter section aft of the ogive which provides an interference free interface between the ogive shape and the body section. Four very low aspect ratio wings with strakes comprise the cruciform wing section and are mounted equilaterally in fixed position along the model axis. Likewise, in the tail section, are four tail control fins which are fixed in postion at 0° incidence relative to the model axis mounted aft of each wing. All parts are rigidly connected to the model body by countersunk machine

---

8 Total pressure correction for the settling chamber.

screws. The surface of the VLSAM model is free from proturberances and is buffed to a polished finish. Detailed dimensions of the VLSAM model are shown in Figure 6. A short summary of key dimensions are listed below:

Total length	=	22.85 in.
Base diameter	=	1.75 in.
Length diameter ratio	=	13.06
Ogive nose length	=	4.0 in.
Ogive diameter ratio	=	2.29
Wing span/root chord	=	3.13 in./13.55 in.
Tail span/root chord	=	5.50 in./1.70 in.
Center of pressure	=	13.5 inches aft of nose tip (approx.)

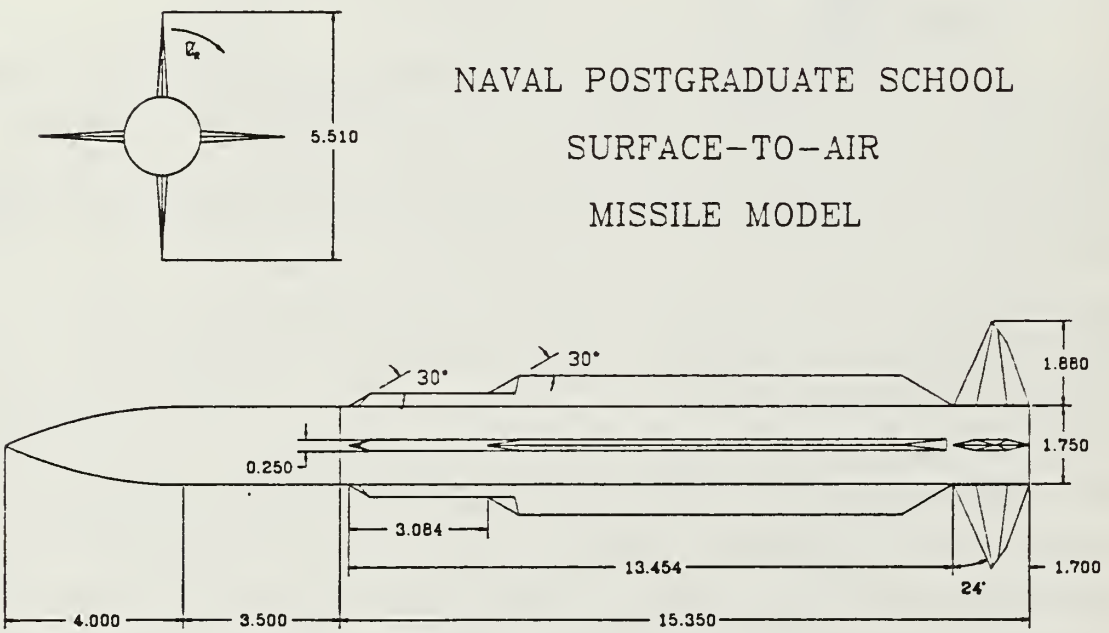

Figure 6. Drawing of VLSAM model.

3. Balance

Force and moment measurements were taken by a six-component, one-inch, strain-gage precision balance. The balance was on loan from the NASA-Ames Research Center under the Navy-NASA Joint Institute of Aeronautics. Balance calibration was performed by NASA-Ames. Calibration data and data conversion values were also provided and are listed in Appendix A [Ref. 42]. A wheatstone bridge circuit capable of measuring positive and negative strain comprises each channel and is oriented to measure strain in a chosen direction. The directions relative to the balance axis are normal, side, and axial with one gage measuring rolling moment. Channel capacities and accuracies are listed in Table 1. Individual channel accuracies are based on full scale (maximum) load.

Table 1. BALANCE CHANNELS: [Ref. 42].

Channel	Component	Maximum Load	% Accuracy
N1	Normal Force	400 lbs.	0.056
N2	Normal Force	400 lbs.	0.049
S1	Side Force	200 lbs.	0.115
S2	Side Force	200 lbs.	0.132
A	Axial Force	100 lbs.	0.153
R	Roll Moment	21 ft-lbs.	0.204

A machined sleeve provides a close tolerance fit between the balance and the interior of the VLSAM model. The model is seated to the balance by locating pins such that the balance center coincides with the approximate center of pressure of the model. Since the balance supports the model, it provides the mechanical interface between the model and sting support.

4. Model/Balance Support

The VLSAM model and balance support, also called the sting mount, is rigidly fixed in the wind tunnel test section by the reflection plane turntable at the base and an aluminum reinforced clear plexiglas section at the top. The sting mount changes model pitch in the horizontal direction with the pivot point located to coincide with the ap-

proximate centers of the VLSAM model and balance. Heavy duty construction in stainless steel and aluminum keeps deflections and vibrations to a minimum. The presented cross-sectional area of the sting mount to the test section flow is minimal for all pitch angles to reduce blockage effects. The reflection plane turntable rests on a heavy-weight pedestal to prevent deflections and vibration. The entire assembly rotates via a chain gear drive powered by an electric motor. Pitch and pitch rate are set by the operator on the motor controller, or by a relay actuator controlled by the data acquisition system. A ring scale on the pedestal indicates model pitch in 1/10 degree increments.

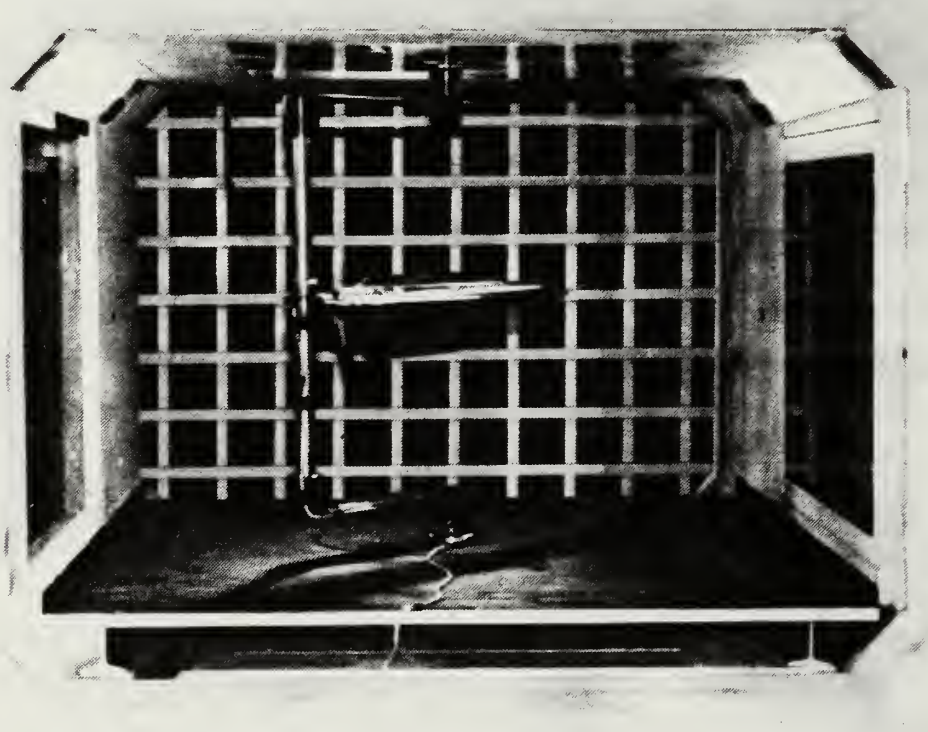

Figure 7. Photograph of VLSAM model in the test section.

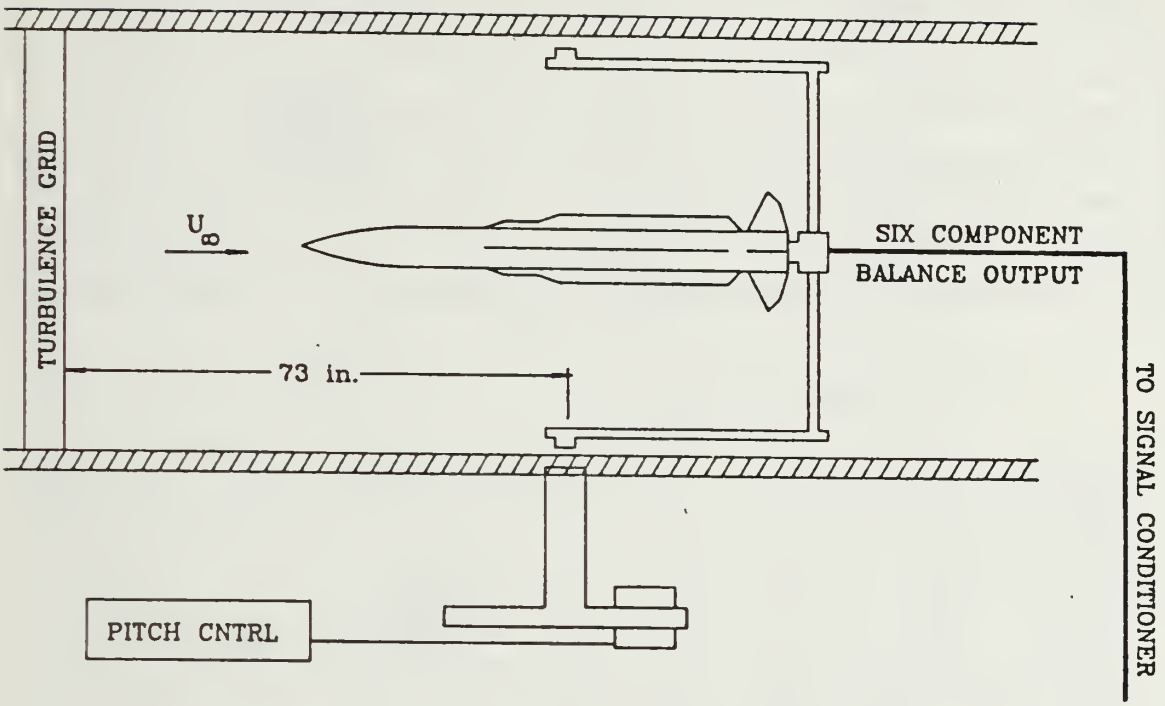

Figure 8. Planview of VLSAM model in the test section.

5. Turbulence Grids

The turbulence grids were designed for use in the low speed wind tunnel to generate turbulence in varying intensities and length scales. Each of the four grids or screens is mounted in a wooden frame and placed 73 inches forward of the model sting mount pivot point. The specifications for the four grids are listed in Table 2. Three of the four grids are square-mesh square-bar and fabricated from wood. They employ bi-plane construction which generates a nearly isotropic homogeneous turbulence. The fourth grid is also square mesh, but was fabricated from round wire. Two wire screens are attached together for a fine mesh. Turbulence intensities and length scale for each of the grids are shown in Figure 9 and Figure 10. These grids were constructed by Roane who also measured the turbulence intensities and length scales.

Table 2. GRID SPECIFICATIONS: [Ref. 3 : p.28]

Grid	Mesh Width (in.)	Bar Diameter (in.)	Mesh/Diameter	Material
One	5.00	1.00	5	Wood
Two	3.75	0.75	5	Wood
Three	2.50	0.50	5	Wood
Four	1.00	0.0625	16	Wire

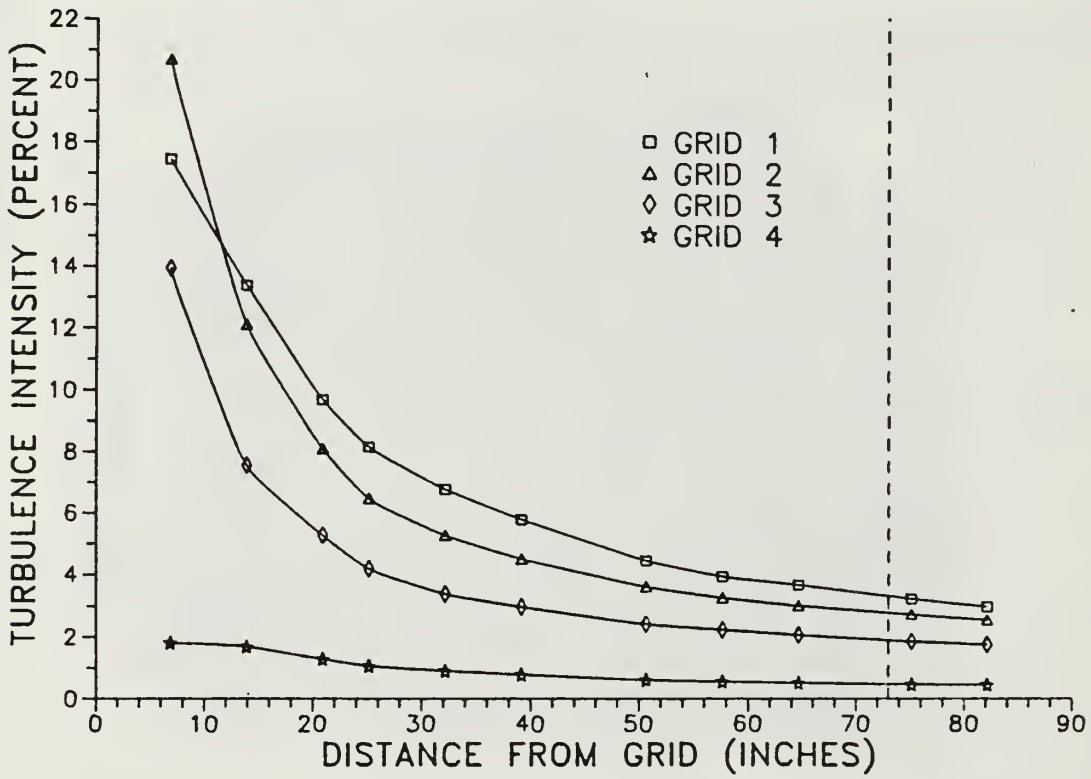

Figure 9. Grid Turbulence Intensity: The dashed line indicates the model pivot axis. [Ref. 3: pp. 45]

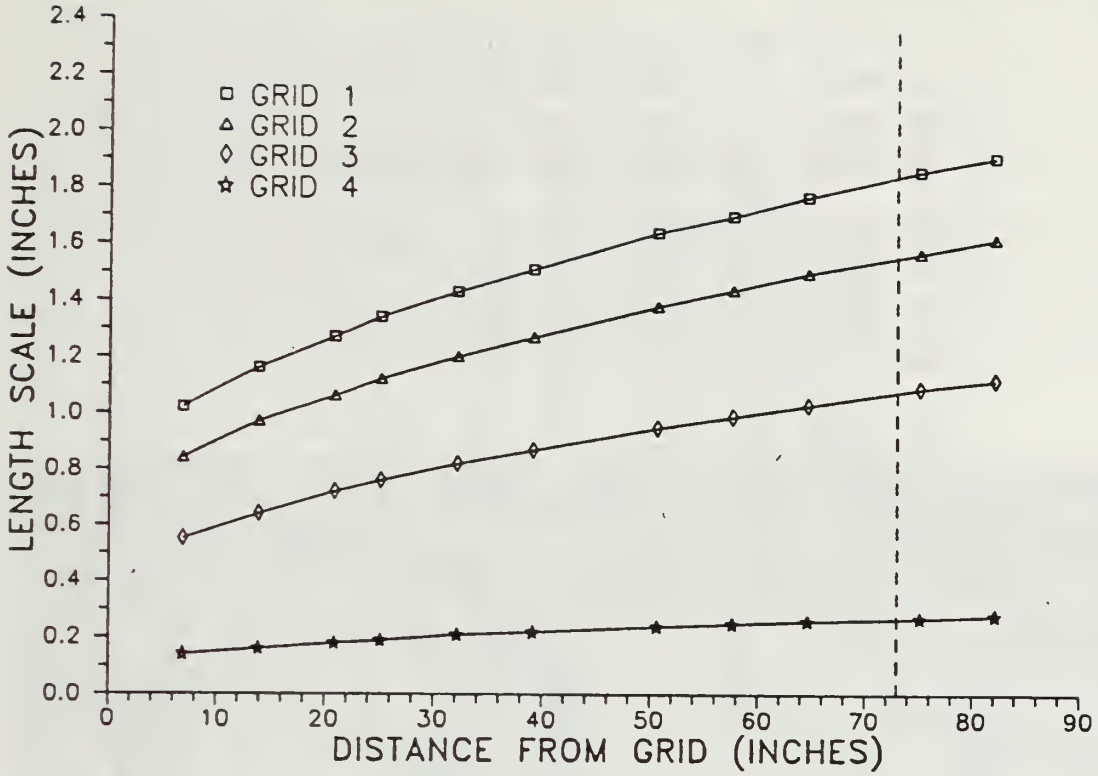

Figure 10. Grid Turbulence Length Scales: The dashed line indicates the model pivot axis. [Ref. 3: pp. 48]

Table 3. GRID TURBULENCE PARAMETERS: At the model pivot axis. [Ref. 3: pp. 44-49]

Grid	Intensity (percent)	Length Scale (in.)	Turbulence/ Model Dia.	Dynamic Pressure (lb/ft^2)
One	3.31	1.84	1.05	15.35
Two	2.78	1.56	0.89	14.88
Three	1.88	1.08	0.62	16.38
Four	0.47	0.27	0.15	15.61
None	0.23	-	-	15.85

The dynamic pressures shown in Table 3 are the true dynamic pressure in the test section from Roane [Ref. 3: pp. 44-49]. The grid generated turbulence length scales to missile length ratios at the test section are smaller than 1:12 which suggests that the turbulence effects on the flowfield and vortices may be due to boundary layer scale and/or vortex scale turbulence. The turbulence length scales to body diameter ratios are on the order of and smaller than one as seen in Table 3. Conclusions on the effects of the grid generated turbulence with regards to changing length scales at constant intensity or changing intensities with constant length scale are not possible with the present grid turbulence parameters.

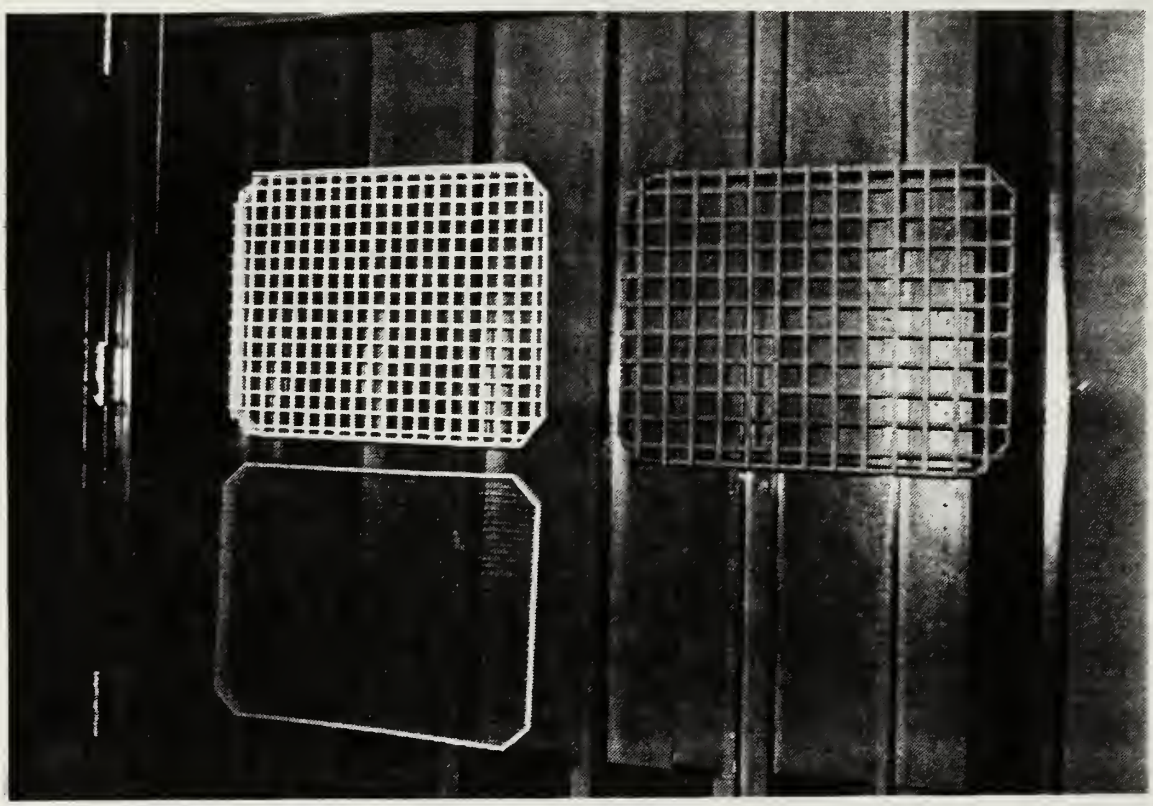

Figure 11. Turbulence Grids 2, 3, and 4.: Clockwise from lower left hand corner; Grid 4, Grid 3, Grid 2.

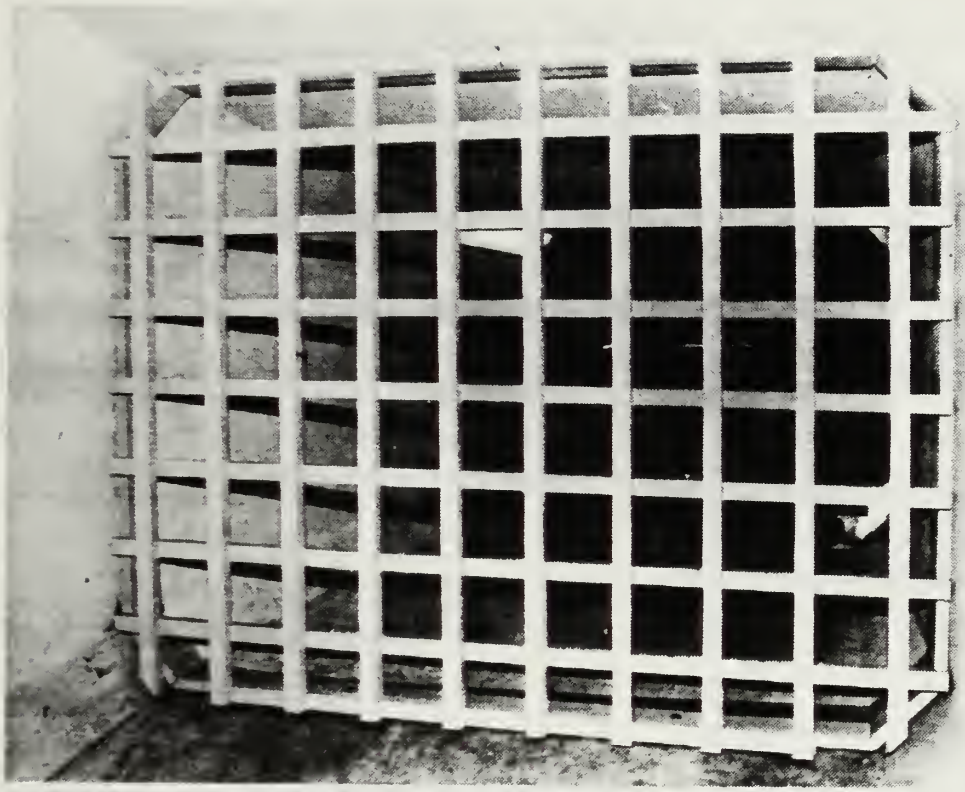

Figure 12. Turbulence Grid 1 installed in the wind tunnel.

6. Data Acquisition Hardware

The data acquisition hardware consists of test facility components to operate the precision balance in the wind tunnel. Each strain-gage in the balance is supported by a signal conditioning circuit which supplies excitation voltage and allows zeroing and calibration of the balance circuit. Each balance channel from the signal conditioner unit is fed into a Hewlett-Packard relay multiplexer which sequences through each channel as required by the data acquisition software. Prior to being measured, the balance signal is fed through a 1000 gain low-noise amplifier to improved resolution for small magnitude signals. A Hewlett-Packard digital multimeter converts the analog voltage signal into a digital signal for use by the data acquisition program. An IBM-AT microcomputer executes the data acquisition software and stores the collected data. Other items utilized in the data acquisition process are the wind tunnel measurement apparatus discussed earlier. Data acquisition hardware components are shown in Figure 13.

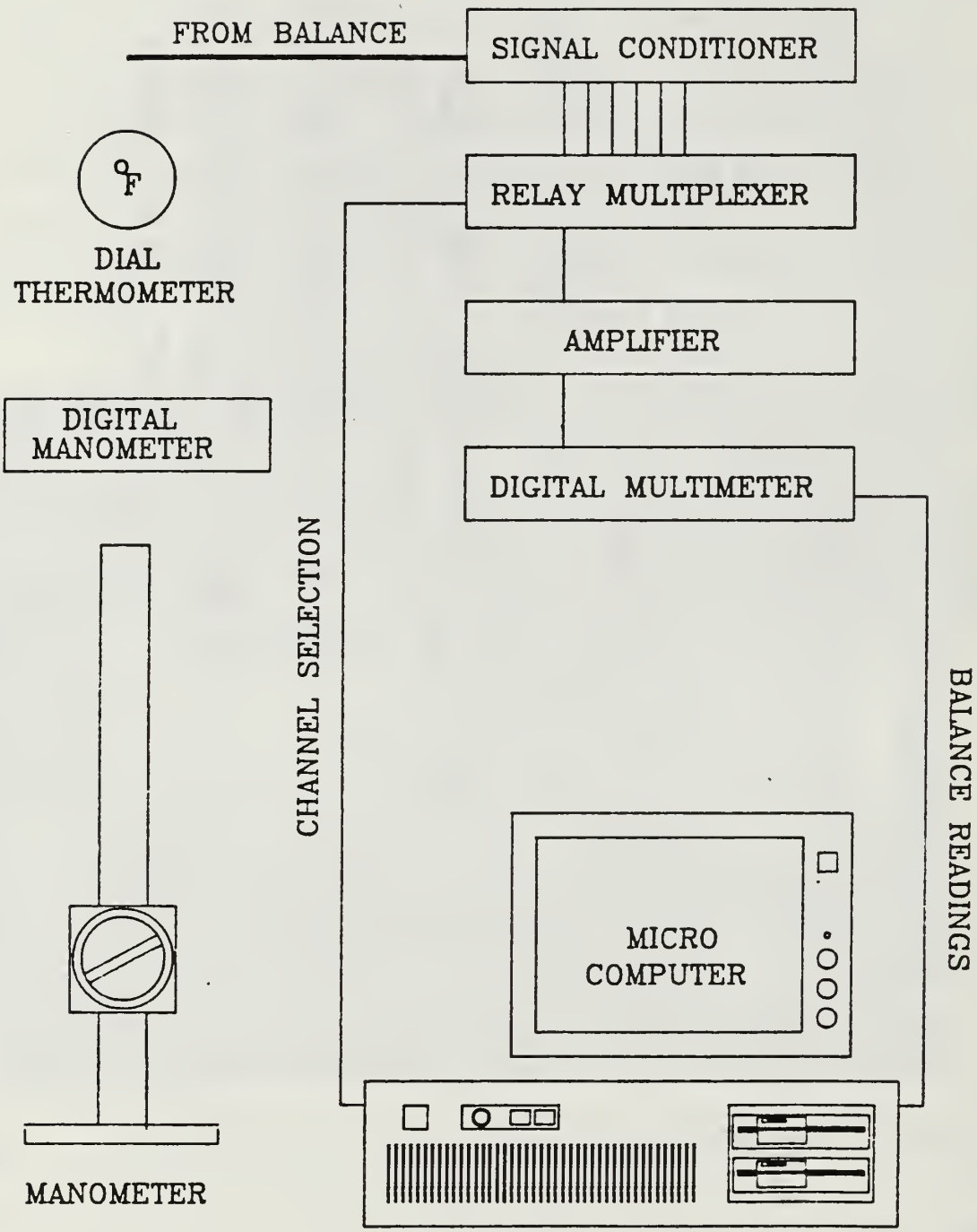

Figure 13. Data Acquisition Hardware

7. Data Acquisition Software

The data acquisition software consists of a shell program to control the Hewlett-Packard instruments and a data conversion program to convert the raw balance readings into a usable form and store them. All readings are time averaged and represent steady state measurements. The initial balance reading in volts is manipulated with the balance calibration constants to give force values in pounds and moment values in foot-pounds. Another program translates the force and moment values into a coefficient form accounting for test conditions and corrections in the wind tunnel. The data acquisition programs are listed in Appendix C and Appendix D.

B. EXPERIMENTAL CONDITIONS

The introduction discussed many variables which could affect flow separation and vortex structure at high angles of attack. To simplify the various outcomes of the test due to numerous perturbations, the following variables were kept as constant as experimental conditions would allow:

1. Reynolds number
2. Test section dynamic pressure.
3. Test section velocity.
4. Nose geometry and roll angle.

The experimental reference pressures used in the turbulence mapping by Roane [Ref. 3] were duplicated in this experiment in order to use the turbulence grid length scales and intensities shown in Table 3, Reference dynamic pressures for the grid and no grid conditions are listed below. These reference pressures ensure a similar test section velocity since the total pressure difference measured by manometer is in error due to the disturbances caused by the screens. Since actual dynamic pressure in the test section is determined by the test section velocity, the velocities in the test section from Roane's turbulence mapping were used to calculate the actual dynamic pressures. These reference pressures are:

NO GRID: q_R = 7.20 (cm. H_2O)
GRID 1: q_R = 10.00 (cm. H_2O)
GRID 2: q_R = 10.00 (cm. H_2O)
GRID 3: q_R = 10.00 (cm. H_2O)
GRID 4: q_R = 5.40 (cm. H_2O)

The dynamic pressure conditions for the experiment would give a subcritical Reynolds number of $Re_d \approx 1.1X10^5$ and actual dynamic pressures in the test section shown in Table 3. Test conditions for individual runs are listed in Appendix B. Other variables were altered to make comparisons:

1. Angle of attack.
2. Wing/tail configuration.
3. Afterbody roll angle.

Three different VLSAM model afterbody configurations were chosen to compare the effects of turbulence on the VLSAM model with and without wings and at two different roll angles.

1. BODY A - Wings and tails at zero roll angle in a "+" configuration.
2. BODY B - No wings or tails. Body roll angle set at $\phi_R = 45°$.
3. BODY C - Wings and tails at $\phi_R = 45°$ roll angle in a "X" configuration.

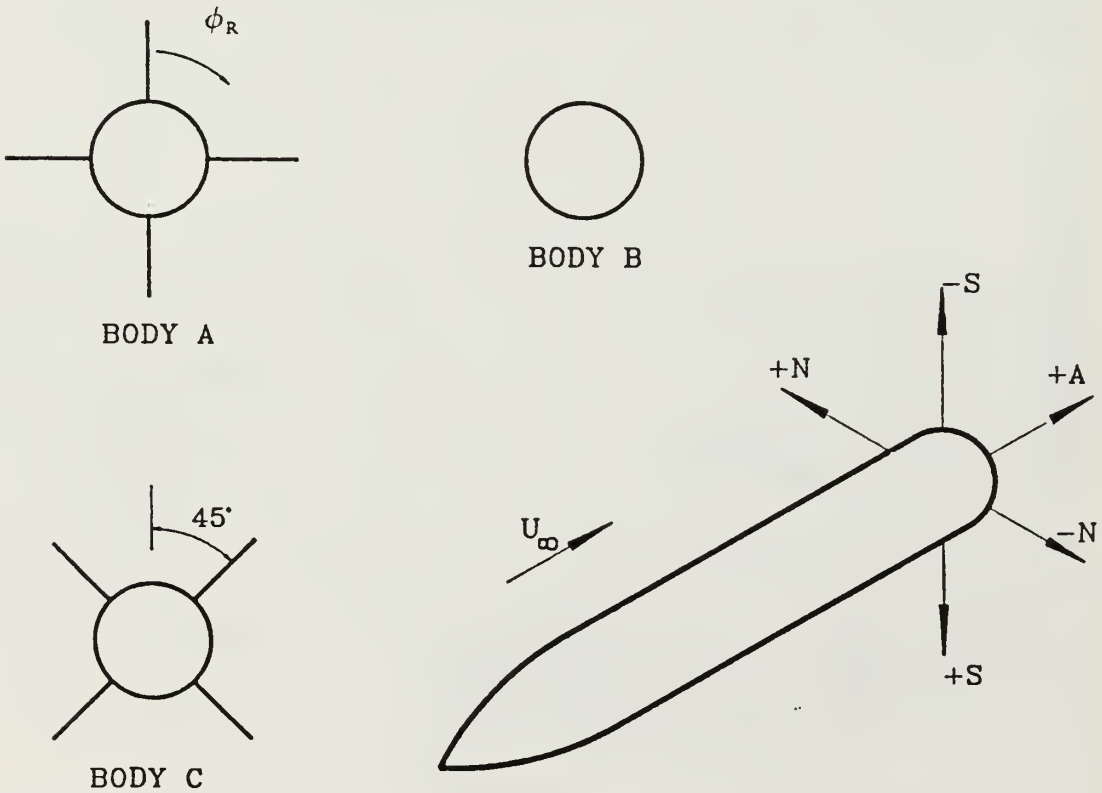

Figure 14. Body configurations and reference system.

In all cases, as the afterbody roll angle changes, the nose roll angle remains fixed to the reference plane. BODY A and BODY C configurations were chosen to be certain that measurements would indicate the presence of vortex asymmetry by any side force magnitude. The wings and tails in the "+" and "X" roll angles are the only wing attitudes where, in the absence of asymmetric vortices, zero side forces, rolling moments, and yawing moments occur. [Ref. 43]

The goal of the experiment was to measure the effects of the grid generated turbulence on the high angle of attack aerodynamics on the VLSAM model, in particular the affect on side force magnitude and direction.

C. EXPERIMENTAL PROCEDURE

1. Balance Calibration

The precision balance was calibrated by the NASA Ames Calibration Laboratory which determined balance constants for the data acquisition program and gave individual channel or circuit accuracy. The balance was fixed to the model/balance support in the test section without the sleeve and VLSAM model. After all electrical connections were made and checked the data acquisition hardware was energized and balance excitation voltage for each channel was set to 5.00 ± 0.003 DC volts via the signal conditioner. The entire data acquisition system was allowed to warm up and settle out for one hour. Next, the amplifier was zeroed at a 1000 gain setting followed by zeroing each balance circuit to 0 ± 200 nanovolts across the wheatstone bridge. The balance sleeve was fitted along with a cradle for static weights. The data acquisition software was run to obtain the initial tare readings. Finally calibrated weights were added to the cradle and measured by the balance to compare readings with balance calibration specifications. Normal and side force readings were found to be accurate to within 0.05% of full scale readings. After this initial test was completed, the signal conditioner was never de-energized to maintain the excitation voltages to the balance circuits.

2. Prerun Calibration and Test

Prior to each run, the data acquisition system was fully energized and allowed to settle out for half an hour. During the settling period, the data acquisition system was cycled repeatedly by the software to bring the relay multiplexer, digital multimeter, and amplifier to operating temperature conditions. Next, the static weight test was repeated with the mounted VLSAM model, to ensure the balance circuits were remaining within calibration accuracy. If not, the model was removed, the balance circuits were zeroed, and the static weight test procedure completed without and with the model.

3. Data Collection

When the prerun calibration results were satisfactory, the wind tunnel was started and test section reference pressure set at 110% of the data run reference pressure. The model pitch or angle of attack was slowly cycled from -10° to 110° and back at approximately 2° per second. This procedure tested the safety of the support assembly with the balance and the model and let the mechanical interfaces settle out. The pitch angles where noticable model vibration occurred were noted.

The wind tunnel was put into a no wind condition (zero dynamic pressure) with the motor running and the model set at -5° pitch.[9] The data acquisition software recorded the initial tare readings. The intial settling chamber temperature and barometric pressure were recorded. The wind tunnel was brought up to operating reference pressure and the actual data acquisition began. Missile angle of attack was manually set and entered into the data acquisition program for each set of readings. Test section reference pressure was kept constant as the model angle of attack increased adding blockage. The microcomputer reduced the balance readings to force and moment values and stored the data on disk. At the end of each run, reference pressure was set at zero and several readings recorded to measure any shift between initial and final readings.

The force and moment data are translated into coefficient form by another program which also corrects for blockage and test conditions. Data were graphed for comparative analysis and graphs are found in the results section.

4. Preliminary Runs

Previous experiments showed that variations in nose roll angle would alter the asymmetric vortex structure, thus changing side force direction and magnitude. Non-repeatability of data points is another area often encountered in earlier investigations. Prior to conducting the actual experimental data runs, preliminary runs were made to determine which nose roll angle produced the largest side force magnitude. Data runs were also conducted to examine the repeatability of data without changing test conditions. The preliminary runs would also indicate data trends and would give some degree of confidence in the data collected in the subsequent runs.

Preliminary test runs were short and durations ran approximately 30 minutes. Temperature increases were small, from 2°F to 5°F, giving a smaller temperature gradient and allowing test section air density to remain in a narrow range. When the experiment proceeded to the actual test runs, test time durations typically lasted 4.5 hours.

---

9 This conditon will be referred to as the model's zero condition.

In order to keep test section air density as uniform as possible, the test procedure was interrupted at least once during the run cycle to cool the air in the wind tunnel. Settling chamber temperatures rose about 10°F to 20°F with larger increases for coarser turbulence generating grids. When the the settling chamber temperature increased to 20°F above the start temperature, the wind tunnel was cooled down by air exchange. Once the tunnel had cooled down to within 5°F of the start temperature, the run continued at 2° below the interrupt angle of attack to overlap readings.

Other test conditions that were beyond the control of the experiment include the turbulence and vibrations produced by the wind tunnel itself during operation and vibrations and deflections of the model balance support.

D. EXPERIMENTAL CORRECTIONS

Model blockage corrections for changing angle of attack were made by equations [6], [7], and [8], from [Ref. 44]

$$q = q_M(1 + 2\varepsilon) \quad \{6\}$$

$$U = U_M(1 + \varepsilon) \quad \{7\}$$

where:

q = dynamic pressure (lb/ft^2)
q_M = measured reference pressure (lb/ft^2)
U = horizontal velocity (ft/sec)
U_M = measured horizontal velocity (ft/sec)
ε = blockage factor

and:

$$\varepsilon = \frac{1}{4}\frac{\text{model frontal area}}{\text{test section area}} \quad \{8\}$$

Model frontal area varies for each body configuration and angle of attack with minimum blockage at 0° and maximum blockage at 90° as shown in Figure 15.

Blockage equations for each body configuration were developed as a function of model angle of attack. These equations are shown in Figure 15 and Table 4, and are implemented in the data conversion program listed in Appendix E.

Table 4. VLSAM MODEL BLOCKAGE

Configuration	Minimum Blockage (percent)	Maximum Blockage (percent)
BODY A	3.10	9.76
BODY C	3.10	6.74
BODY B	3.10	6.37

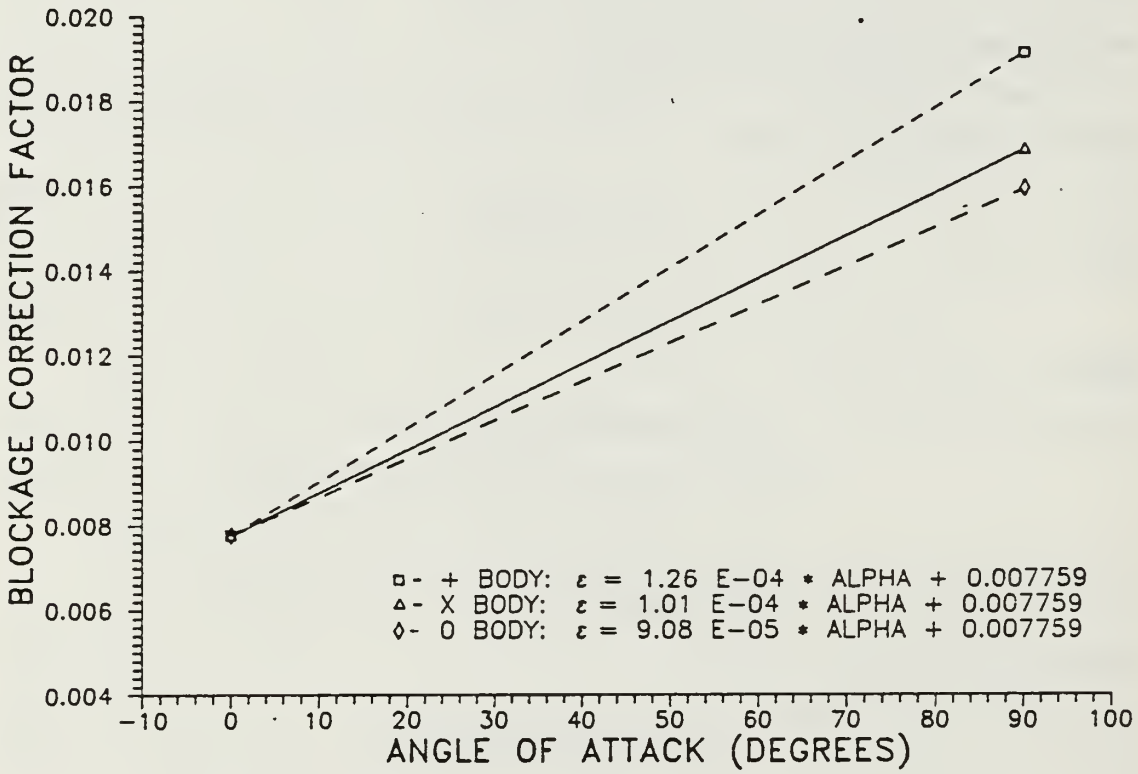

Figure 15. Blockage factors

III. RESULTS

Several important factors must be kept in mind as the results are presented. These factors are conclusions from previous high angle of attack studies on slender bodies in low turbulence environments and may apply to these results. The nose fineness ratio of the VLSAM model is 2.29. Results by Keener [Ref. 11] dictate that the vortex cores from the nose at fineness ratio 3.5 should not be as crowded together as in higher fineness ratio noses at 5.0. Since the nose is pointed, no blunt nose effects are expected. From equation [2], vortices should become asymmetric when the angle of attack is $\alpha_{AV} \approx 24°$ for the given apex angle of the VLSAM model. Flow separation throughout the length of the nose should remain laminar at all angles of attack for $Re_d \leq 3.0 \times 10^5$ [Ref. 11]. Conditions for all data runs are stated in the previous chapter and listed in Appendix B are stated in the previous chapter. All data represent steady-state conditions and are expressed in coefficient form.

A. VARIATIONS IN NOSE ROLL ANGLE

Previous research showed that variations in nose geometry and roll angle altered the vortex structure shedding from the nose and afterbody at high angles of attack. The objective of the first set of preliminary runs was to determine the nose geometry which produced the highest side force magnitude. Since the model used in the experiment used only one nose, variations in nose roll angle became the single variable affecting nose geometry. The nose with the highest side force magnitude would be fixed in the same position regardless of afterbody configuration for all subsequent runs. Both sets of runs were conducted under identical conditions, $Re_d = 1.33 \times 10^5$ and test section dynamic pressure at q = 22.2 lbs ft^2. Angle of attack was varied from 0° to 90° in 10° and 5° increments. Model configuration was BODY A and no grids were used. Nose roll angle was changed in 45° increments for each run. Results for each set of runs are plotted in Figure 16 and Figure 17.

In both cases, changes in nose roll angle alone produced variations in side force magnitude and direction. The plots also show a some repeatability of the data points. Nose eight, in both run sets, produced the largest side force magnitude in the negative direction. The angle of attack when side force magnitude became noticeable at $\alpha \approx 30°$ was the same for all nose roll angles within each set of runs, which is also true for the angle of attack $\alpha \approx 80°$ where side force magnitude decreases to negligible values.

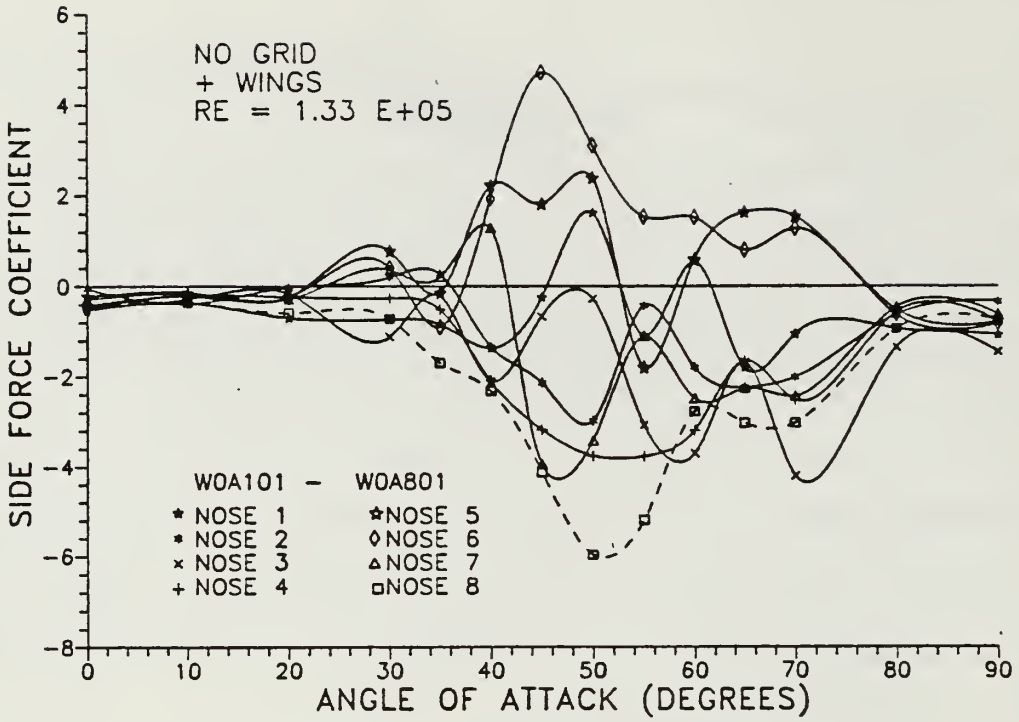

Figure 16. Side force variations with nose roll angle: Runs W0A101 to W0A801.

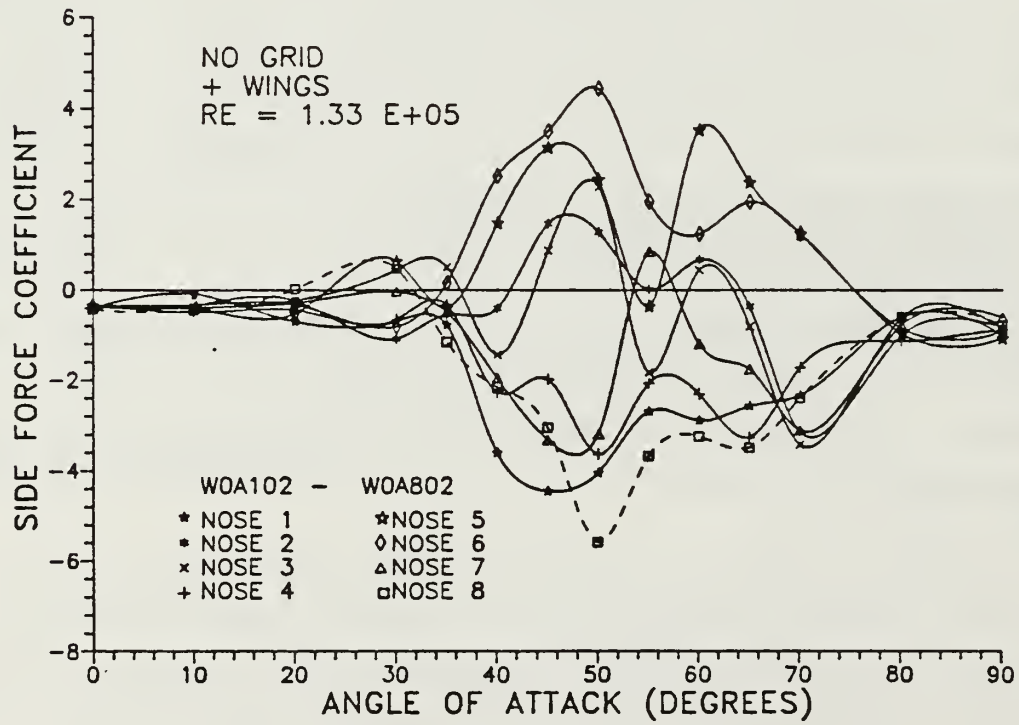

Figure 17. Side force variations with nose roll angle: Runs W0A102 to W0A802.

These side force measurements suggest that vortices become asymmetric at $\alpha_{AV} \approx 30°$ and end at $\alpha_{CV} \approx 80°$, which is true for all roll angles. The angle of attack increments are large. Smaller increments would give better observations of data trends and all subsequent data collection runs are in one degree increments.

B. DATA REPEATABILITY

A recurring problem dealing with side force measurements from asymmetric vortices is the non-repeatability of data except in Keener [Ref. 23] where repeatability of results was good. In this experiment, all readings are an average of ten separate measurements taken within a 40 second interval, so any signs of repeatability could indicate that the data is statistically accurate. As shown in Figure 16 and Figure 17, the nose roll angle which gave the maximum side force magnitude for all roll angles is nose eight, which is true for both run sets. The objective of the repeatability runs was to determine if any repeatability existed, and if not, what degree of fluctuation existed. After prerun calibrations, the model was pitched to 20° angle of attack from 0° at test dynamic pressure. Readings were taken at 20° then the dynamic pressure reduced to zero and readings taken again. The wind was turned on and off for readings as the model remained at a fixed angle of attack.

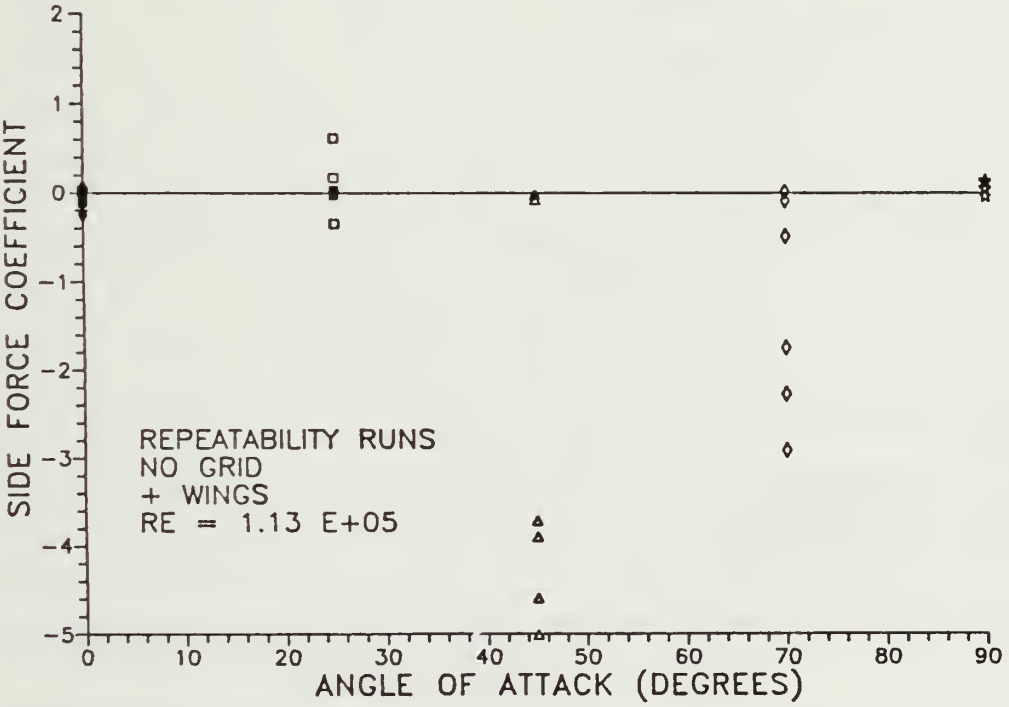

Figure 18. Data Repeatability Runs

After several readings, the model was slewed to the the zero condition for a final calibration check. This procedure was repeated for 45°, 70°, and 90° angles of attack and all results are plotted in Figure 18. Variation in side force magnitude is obvious at 20°, 45°, and 70°. Measurements at 90° show negligible fluctuation. This agrees with accepted side force fluctuation phenomenon. Statistically, the mean value of any data, will be improved if an increasing population of readings are taken. Time and record keeping limitations allowed only ten readings per channel to be recorded. Some degree of experimental accuracy may be lost with the data fluctuation, but the data point trends are useful in making comparisons between different run conditions. Comparing Figure 16 and Figure 17, the side force follows a general trend which will be useful for comparing the data runs discussed in the following sections.

C. BODY IN ISOLATION

The baseline test run was made for BODY B with no grids shown in Figure 19. The asymmetric vortices begin at $\alpha_{AV} \approx 26°$ which concurs with the value $\alpha_{AV} \approx 24°$ from equation [2]. The unsteady vortices begin to form at $\alpha_{UV} \approx 80°$. Between these two an-

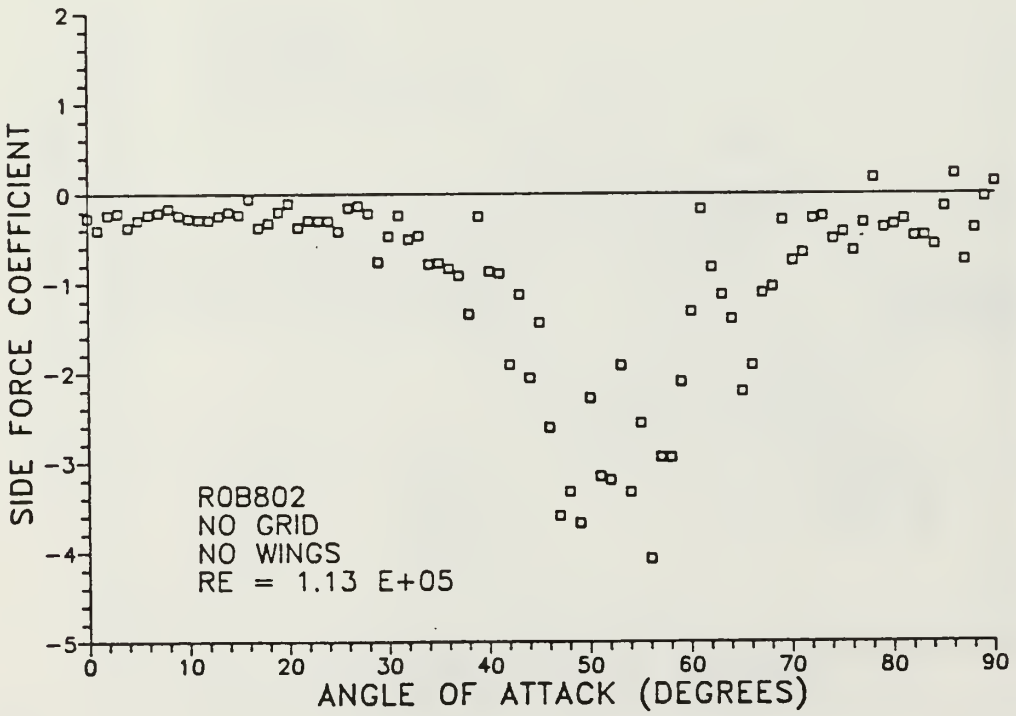

Figure 19. R0B802: Side Force Coefficient.

gles of attack the side force changes magnitude but not direction. The data points scatter suggests a strong possibility of fluctuations in the steady state side force readings. The data trend shows the maximum side force occurring at $\alpha \approx 56°$ and $C_y = 4.1$ then tapers off to nearly $C_y = 0$ after which it increases back to $C_y = -2.0$ then tapers off into the unsteady vortex region. Since there are no wings or tails, the side force is due entirely from the nose and afterbody vortices. The smaller angle of attack interval in Figure 19 does not show any data smoothness when compared to Figure 16 and Figure 17, which were run at larger increments. The data trends are similar which illustrates the dominance of the nose generated vortices. The side force magnitudes in Figure 16 and Figure 17, are just over 30% of those in Figure 19 which may be due to wing vortex effects discussed later in the results section.[10]

The BODY B configuration with Grid 1 generated turbulence is shown in Figure 20. The onset of asymmetric vortices is delayed to $\alpha_{AV} \approx 42°$ and unsteady asymmetric vortices $\alpha_{UV} \approx 82°$. In general the side force direction remains the same but there is a considerable reduction in magnitude by about 77%. One possible cause of this decrease in side force is the change in positioning of the asymmetric vortices caused by the turbulence. The turbulence length scale to missile diameter ratio is 1.08 and can be classified as *vortex scale turbulence* which may suppress the asymmetry of the nose vortex pair. Perhaps this is the reason behind the delayed angle of attack for the onset of asymmetric vortices. Another reason may be due to turbulence intensity since GRID 1 turbulence intensity is the highest.

Comparing the results from the remaining grids in Figure 21 thru Figure 23, the trends are similar to GRID 1 and the vortex asymmetry seems to be depressed by longer turbulence scales. For GRID 4 where the turbulence length scale is the smallest and side force magnitude is the highest, α_{AV} occurs at an earlier angle of attack. The data trend in Figure 23 has a closer similarity to Figure 19, although side force magnitude is reduced by 55%. Turbulence intensity does not seem to factor as much as the length scale to control asymmetric vortices since turbulence of any intensity might be expected to eliminate asymmetric vortex effects and especially in the case of GRID 1 with the highest turbulence intensities, yet GRID 1 results show the side force is not eliminated.

---

10 The axisymmetric wing and tail arrangement of BODY A and BODY B should not contribute any side force lift from the lifting surfaces.

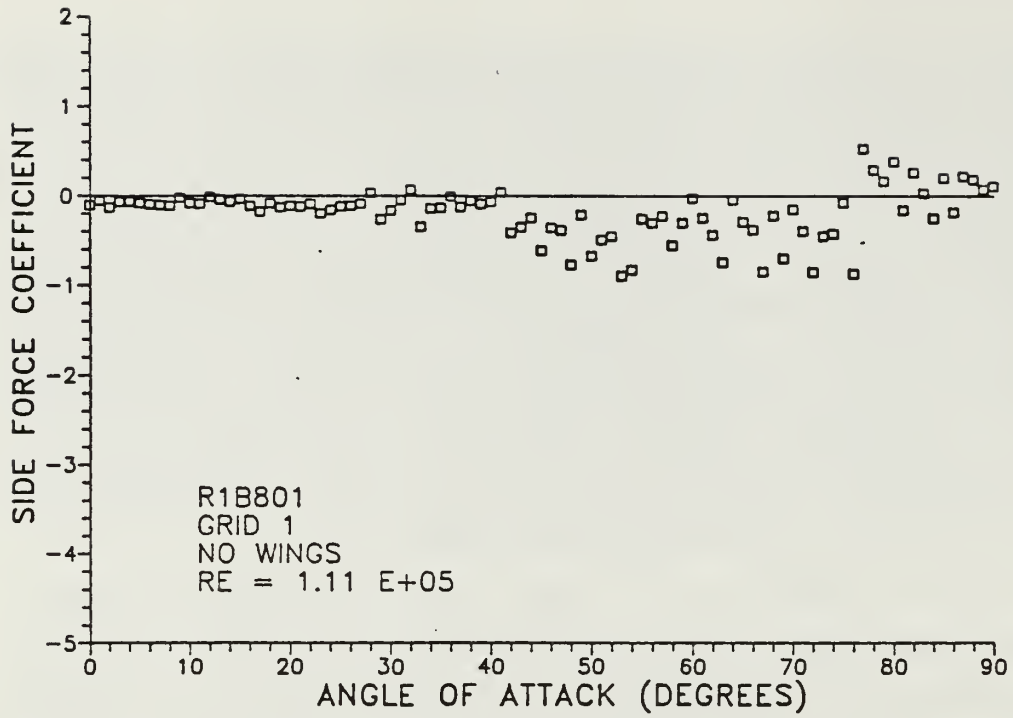

Figure 20. R1B801: Side Force Coefficient.

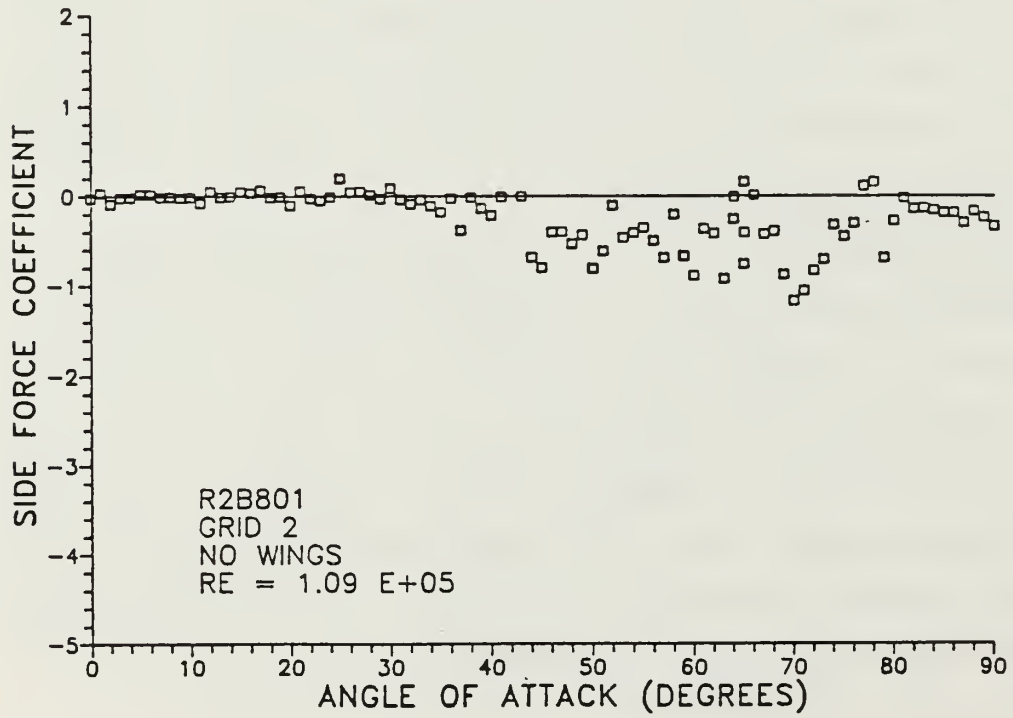

Figure 21. R2B801: Side Force Coefficient.

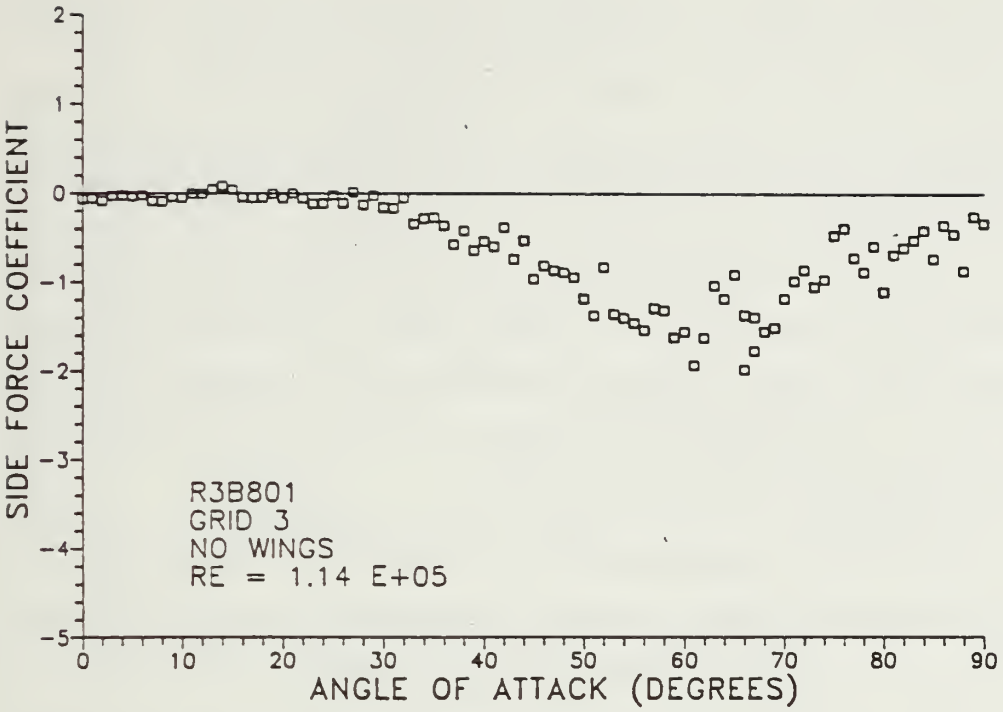

Figure 22. R3B801: Side Force Coefficient.

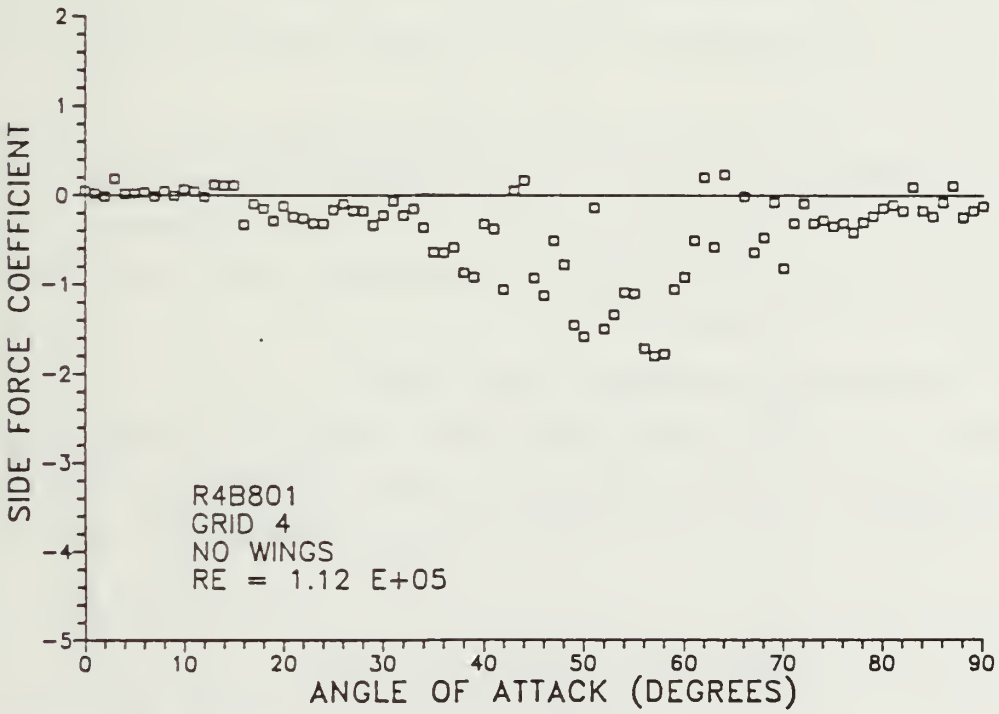

Figure 23. R4B801: Side Force Coefficient.

A correlation between turbulence length scale and turbulence intensities to the vortices is not possible since the turbulence intensities for the grids are not equal.

In previous research, Wardlaw produced 2% turbulence intensity by a wire mesh grid [Ref. 12].[11] His results showed that side force distribution was not effected by the turbulence and side force magnitude increased by 10%. If the turbulence length scales were small enough to affect the boundary layer, the side force magnitude should decrease. On the other hand, larger turbulence length scales should also suppress side forces as indicated by the results in this experiment. Since the small scale low intensity turbulence from GRID 4 does not appear to suppress side force magnitude, results from increasing GRID 4 turbulence intensity could settle whether turbulence intensity contributes anything significant to the vortex structures.

In another investigation by Clark, he showed that a single rod place upstream from the stagnation point on an ogive nose may have the same effect as grid generated turbulence. He injected a thin stream of bubbles into the flowfield upstream of the model which *forced* flow separation into steadiness [Ref. 45].[12] His results indicated that when bubbles were injected at the point of the nose, the vortices were forced to remain in a fixed separation condition. When Clark injected the bubble stream on the afterbody, there was no effect on the vortex structure or side force magnitude. He concluded that the wake from the bubble probe, rather than the bubbles themselves, *forced* the flow separation into steadiness.

Conjecture at this point would indicate that turbulence length scales of vortex size may have a greater influence on the vortex structure than turbulence intensity. The smaller scale low intensity turbulence does not seem to attenuate the asymmetric vortex structure since maximum side force magnitudes are nearly equal, but does seem to cause a steadier flow evidenced by the data scatter.

D. WINGS AND STRAKES WITHOUT TURBULENCE.

The addition of wings and strakes in the BODY A and BODY C configurations show changing trends in side force direction and magnitude.[13] BODY A in Figure 24 shows larger side force, a lower angle of attack for the onset of asymmetric vortices,

---

11 $Re_d = 1.5 \times 10^5$. No turbulence length scale given.

12 $Re_d = 0.4 \times 10^5$. No turbulence length scale or intensity given.

13 The following discussion centers on the wings and strakes since the tails are not expected to contribute any significant effects.

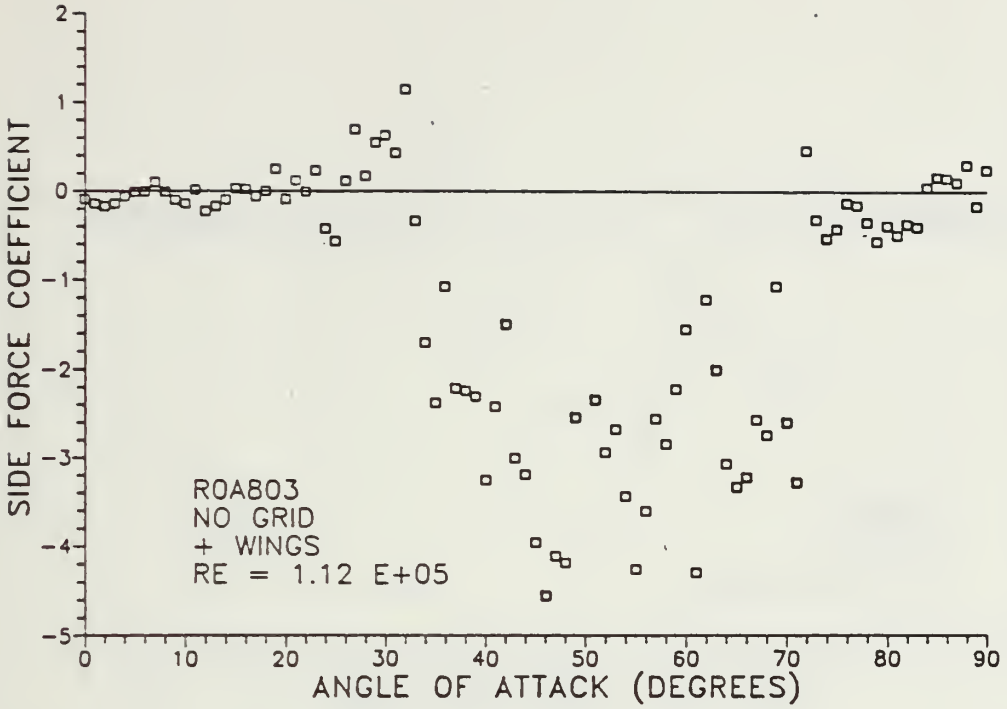

Figure 24. R0A803: Side Force Coefficient.

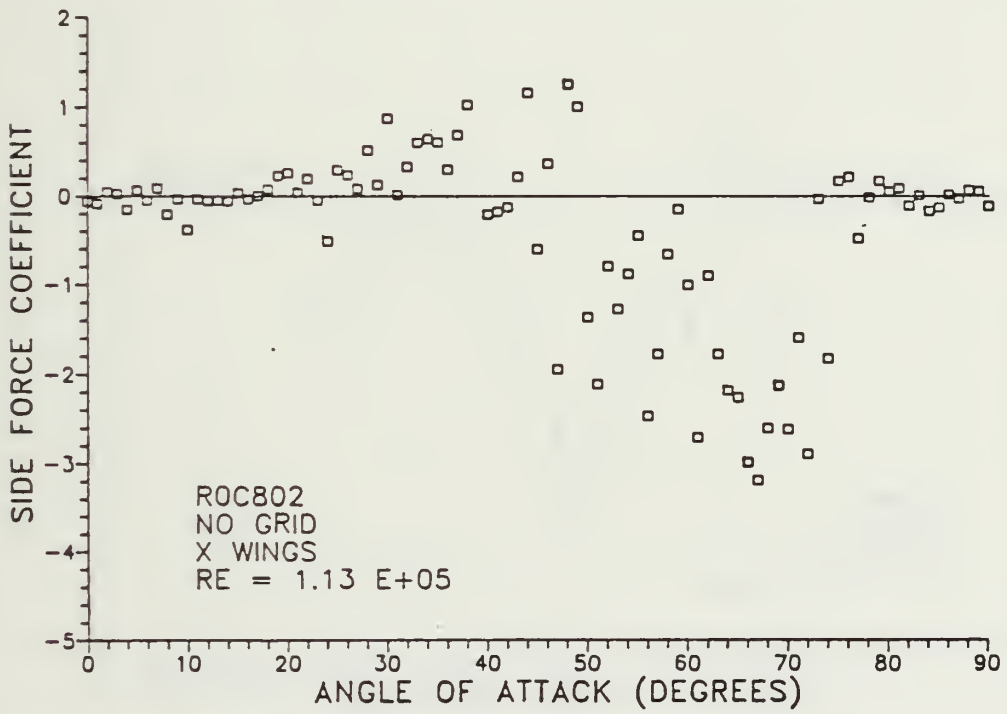

Figure 25. R0C802: Side Force Coefficient.

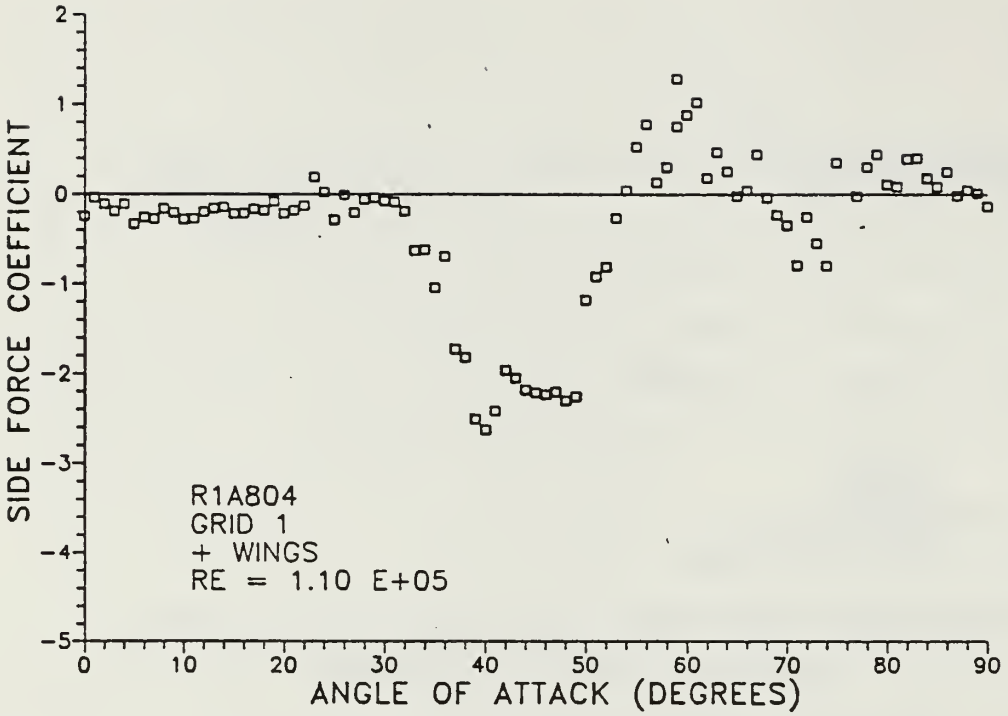

Figure 26. R1A804: Side Force Coefficient.

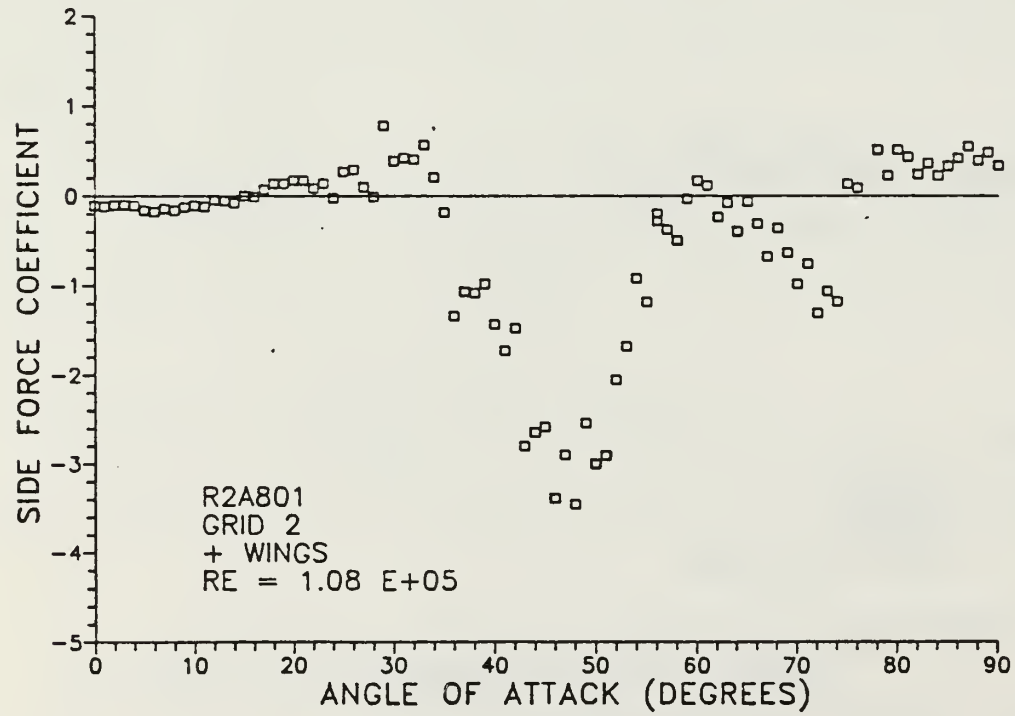

Figure 27. R2A801: Side Force Coefficient.

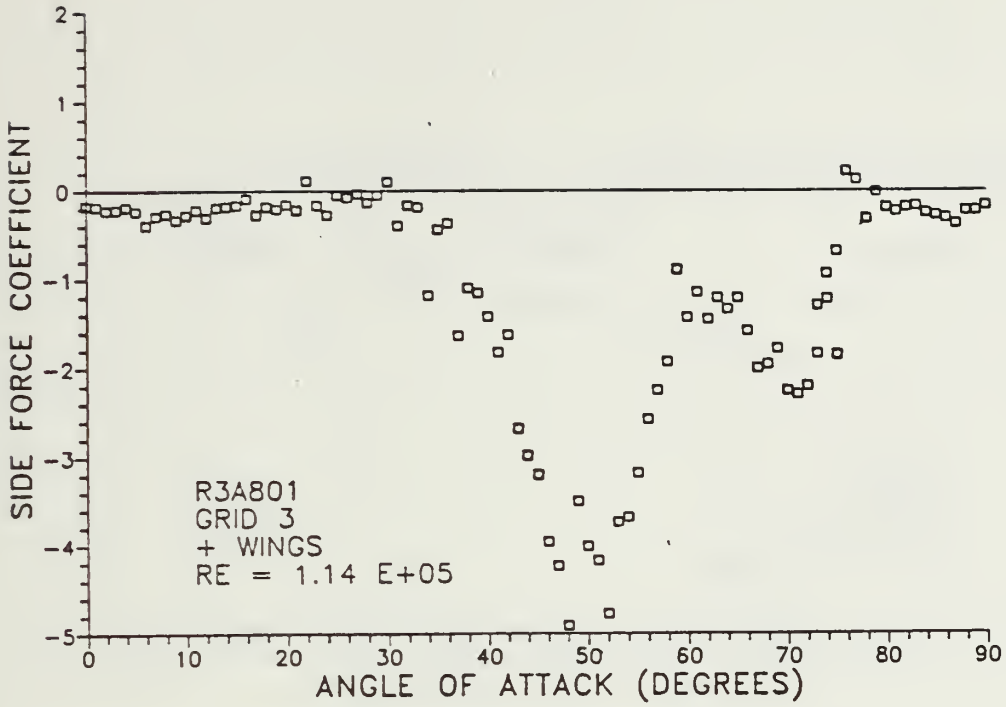

Figure 28. R3A801: Side Force Coefficient.

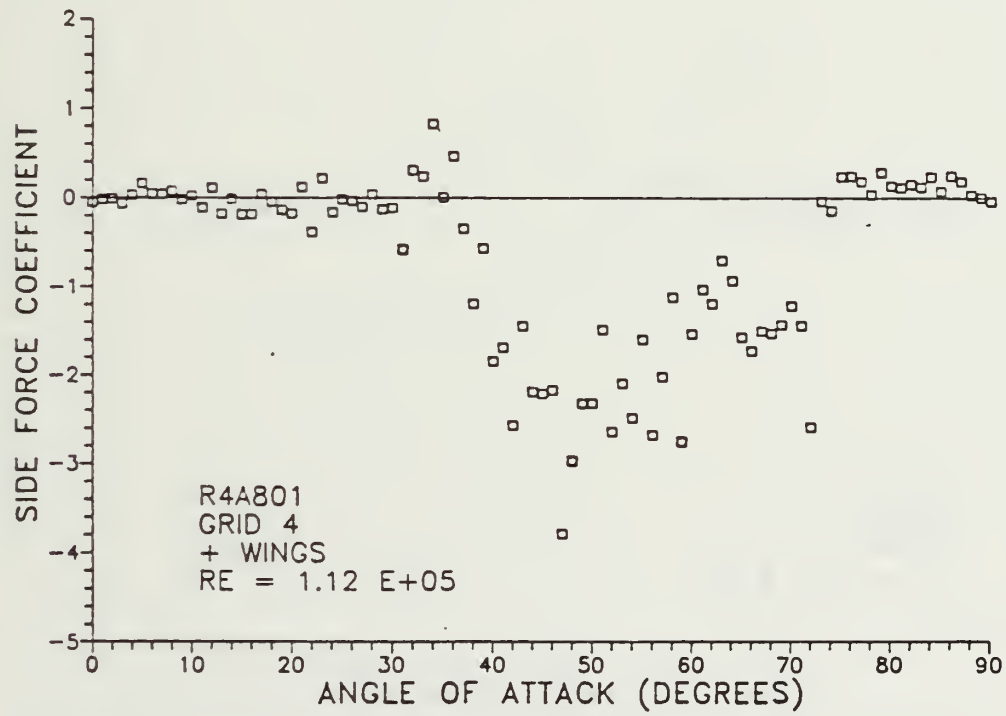

Figure 29. R4A801: Side Force Coefficient.

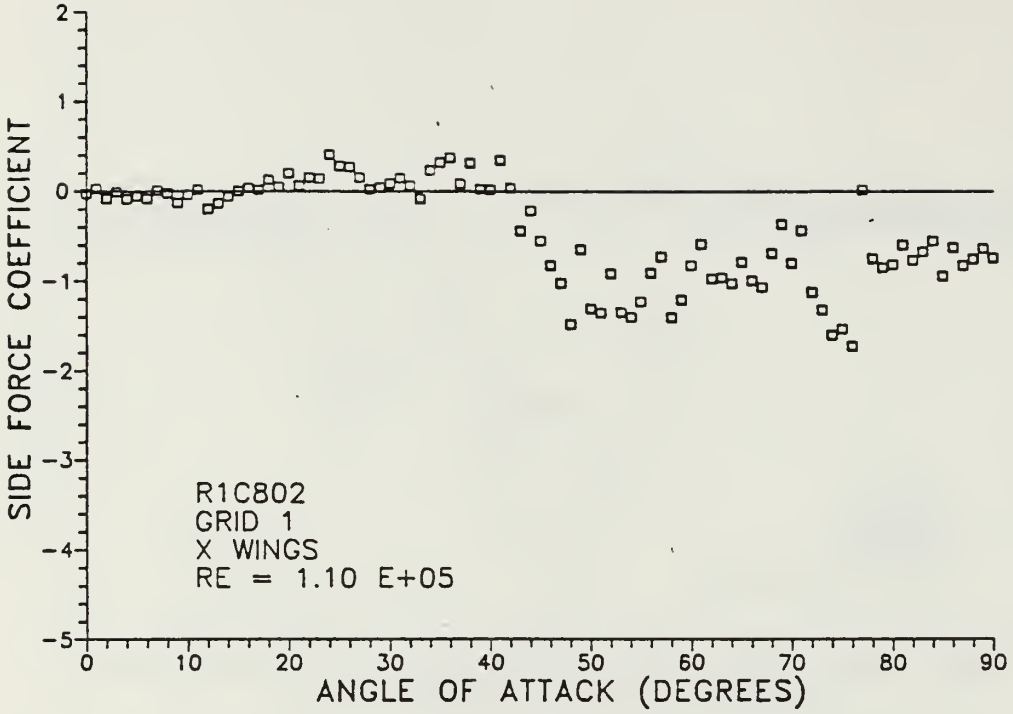

Figure 30. **R1C802:** Side Force Coefficient.

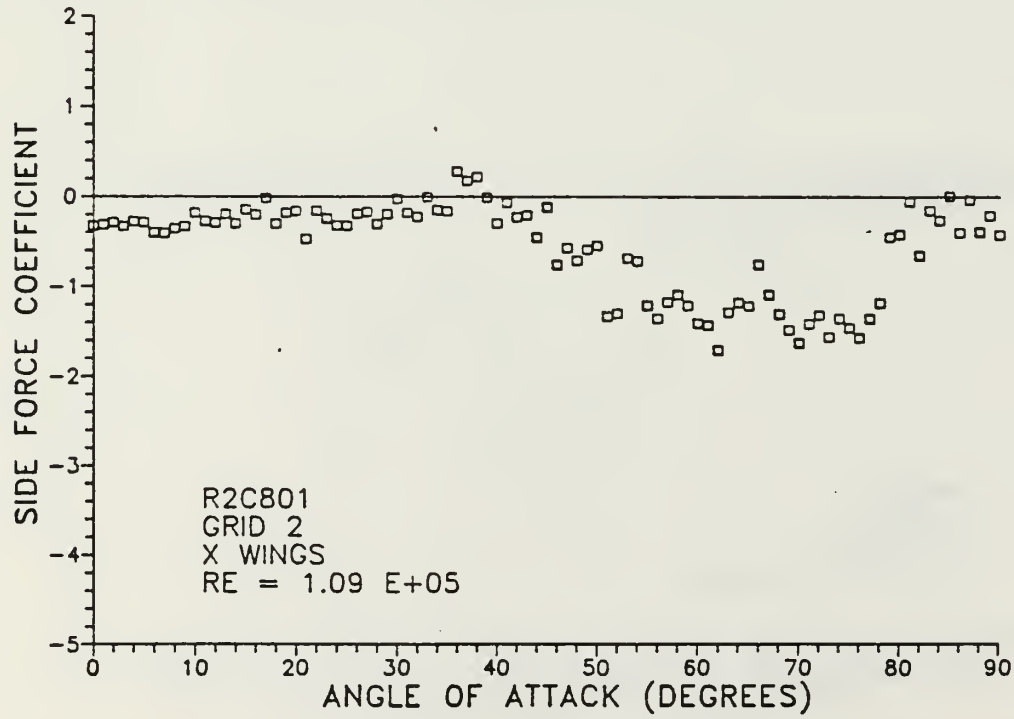

Figure 31. **R2C801:** Side Force Coefficient.

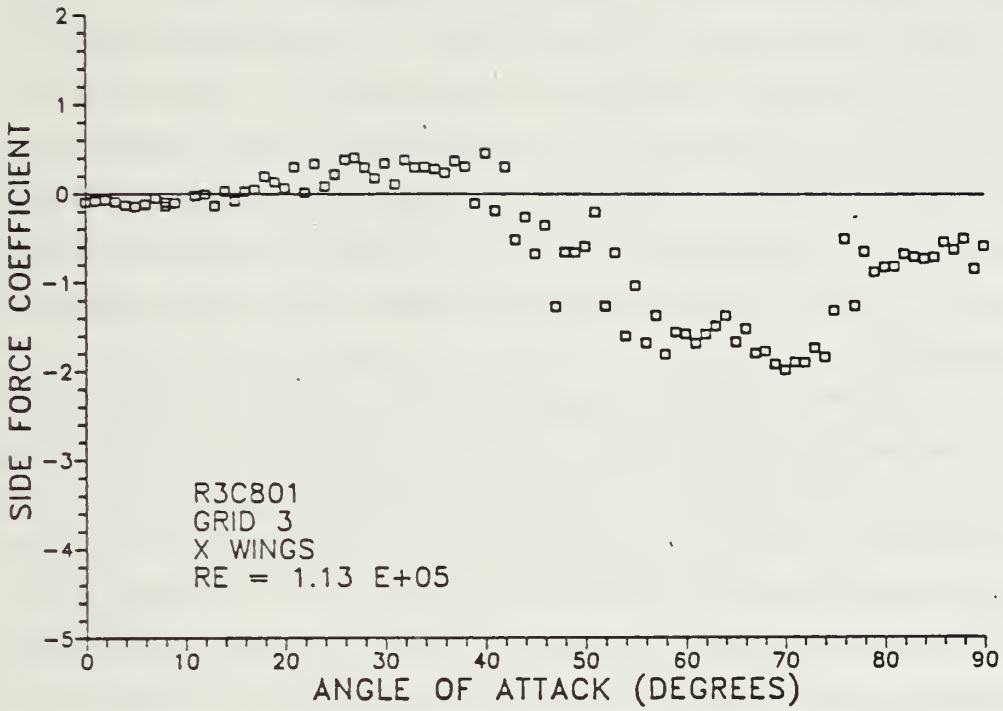

Figure 32. R3C801: Side Force Coefficient.

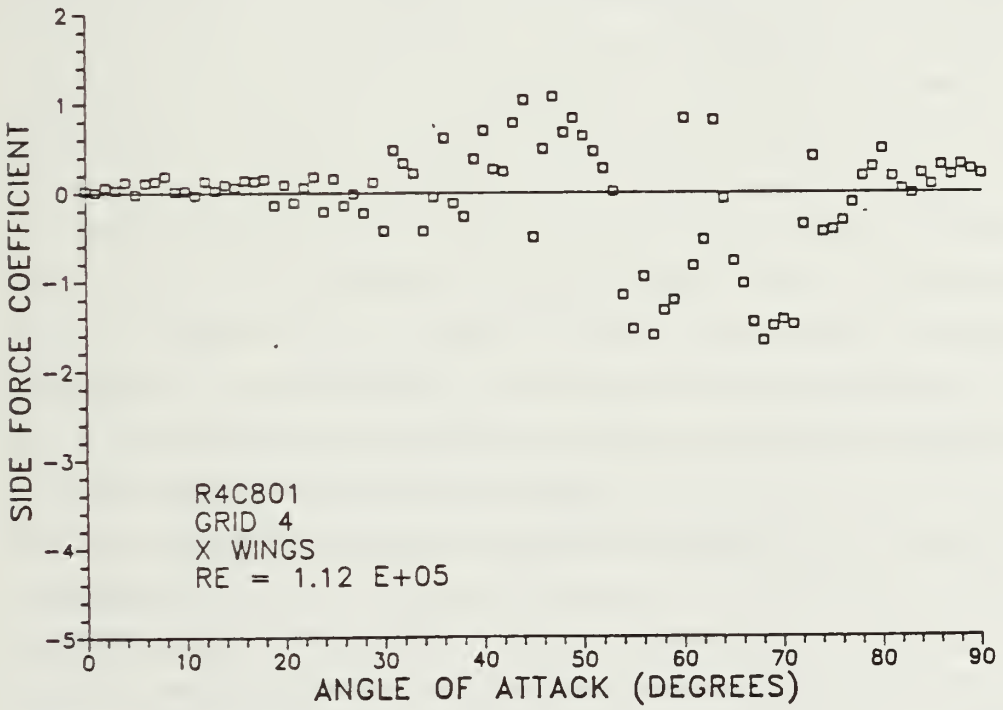

Figure 33. R4C801: Side Force Coefficient.

larger side force magnitudes by 12% when compared to BODY B in Figure 19, and greater flow unsteadiness seen in the data scatter. BODY C in Figure 25, while showing an equal degree of unsteadiness, has even lower side force magnitudes than BODY B and pronounced changes in the direction of the side forces seen from the positive side force values between $\alpha \approx 18°$ and $\alpha \approx 50°$. These results suggest that the addition of wings do not significantly alter side force magnitude. The nose vortices continue to dominate, but the wings and strakes do influence side force direction which could be caused by other flow mechanisms.

The afterbody vortices of the BODY B configuration are expected to contribute side force to the overall magnitude which raises questions as to what, if any, are the position of afterbody vortices in the BODY A and BODY C configurations. The symmetry of BODY A and BODY C configurations are not expected to contribute any side force lift from the wings and tail in the absence of asymmetric vortices. Since side force magnitude and direction trends are generally similar but not alike for all cases, there must be other mechanisms involved from the vortices generated by the leading edges of the strakes and wings.

The first possible effect is the strength and positioning of the wing and strake vortices. The nose vortices are always expected to dominate any downstream vortices and may drive the wing and strake vortices to asymmetry contributing to the overall side force magnitude. These wing and strake vortices could be stronger at inducing side forces than the afterbody vortices and may be the reason why BODY A has larger side force magnitudes than BODY B. The second effect may be due to the strake and wing vortices pushing the nose vortices further away from the body causing a weaker asymmetric vortex effect and reducing the overall side force magnitude which may explain why BODY C has smaller side force magnitudes than BODY B without turbulence. It may also be a combination of the two and could be dependent on the angle of attack. The third effect may be due to the nose and afterbody vortices causing side force lift on the leeward wing. As the nose vortex pair becomes asymmetric, the larger vortex could roll up and over the leeward wing causing a side force from vortex lift, a phenomenon enhanced by the strake and low aspect ratio wing. Side force vortex lift could also contribute to the rolling moment. Finally, the wings and strakes, depending on roll angle, may act as splitter plates which form a barrier between the vortex pairs preventing or attenuating an interaction.

High angle of attack experiments by Deane [Ref. 27] and Jorgensen [Ref. 46] with monoplane configurations show no increase in side force magnitudes when compared to the body in isolation. Further studies with monoplane wing configurations at 0° and 90° roll angles would be invaluable to study these possible effects. The disposition and strength of the asymmetric vortices would have to be quantified to determine how the actual vortex interactions occur.

E. WINGS AND STRAKES WITH TURBULENCE.

The effects of adding turbulence to BODY A and BODY C were similar. In both cases Figure 26 through Figure 33, the longer turbulence scales suppressed the side force magnitudes, but, for BODY C the data show more unsteadiness with the smaller scale turbulence, as opposed to the BODY B results. The larger scale turbulence delays the angle of attack for the onset of asymmetric vortices for BODY C to $\alpha_{AV} \approx 23°$ The results for BODY A are again close to BODY B with the onset of asymmetric vortices occurring earlier at $\alpha_{AV} \approx 22°$ for the no turbulence condition. The effects of the larger scale turbulence in delaying α_{AV} are apparent when GRID 1 results in Figure 26 and Figure 30 are compared to GRID 4 results in Figure 29 and Figure 33. Changes in side force magnitude are mixed although the general trend shows the lower side force magnitude at longer turbulence length scales except for BODY A and GRID 3 in Figure 28 which has a higher side force magnitude. The side force directional tendencies are also suppressed suggesting longer turbulence length scales brings more steadiness to the asymmetric vortices. Turbulence intensity effects from the graphs show that the higher intensities suppress side force magnitude but do not seem to change flow separation unsteadiness because of the data point fluctuation. The general trend of the data points are similar for all cases examined, especially when comparing each separate body configuration to each other. These trends indicate the dominating influence of the nose vortices. The side force differences between the body configurations could be attested to the presence of the wings and their roll angle.

Vortex scale turbulence may be responsible for changing the position of the vortices which explains the changing direction and magnitude of the side forces which is true for the case of BODY B with GRID 1. Here the vortex scale turbulence may contribute to the general unsteadiness of the vortex structure evidenced by the scattered data points. This contribution to unsteadiness can be compared to a missile experiencing unsteadiness with comparable turbulence length scales. Boundary layer scale turbulence may

exist due to the cascade effect but does not seem to factor into the experimental results since side force magnitudes were always larger for smaller scale turbulence.

F. NORMAL FORCE RESULTS

The normal force results are plotted in Figures 33 through 47 and show the characteristic trend of a steady increase to a maximum where the values level off. The normal force is largest for the BODY A configuration and the smallest for BODY B. The maximum normal force value of the BODY A configuration is $C_n = 32.3$ which is 22% higher than BODY C at $C_n = 26.4$ and 101% higher than BODY B at $C_n = 16.1$ The normal force curve for BODY A is much steeper and levels off at the higher value and lower angle of attack than the other configurations. This may be due to the wings producing more lift at lower angles of attack and more drag at higher angles of attack than for BODY C. The addition of grid generated turbulence causes a decrease in slope of the normal force curves. The curves without turbulence show a sharp turn at a maximum value where the curve levels off. The curves become rounded with the turbulence. There does not appear to be any significant effect on the overall magnitude of the normal force in the presence of turbulence. The variation in turbulence length scale and intensity do not appear to affect the normal force values as in the results for side forces. There is no noticeable fluctuations in the trend of the data points since the normal force does not fluctuate with or without the presence of turbulence.

G. SIDE FORCE TO NORMAL FORCE RATIO

The side force to normal force ratio is important to slender bodies with monoplane wings such as cruise missiles and aircraft. As this ratio increases, the slender body must be able to cope with the increasing side forces, thus requiring large amounts of yaw control. Since yaw control does not equal lift control due to the available control surface area in monoplane configurations, side forces can be a problem. Cruciform missiles should be able to cope with high side force to normal force ratios since their wing and tail arrangement gives equal lift capability in the pitch and yaw directions.

Since the normal force components are not as effected by the addition of grid generated turbulence, the side force to normal force ratios should follow the side force trends. The lowest normal force values of all the tested body configurations was BODY B which also had a substantial side force value, and therefore should be expected to have the highest side force to normal force ratio which is the case as shown in the plots. BODY B has a maximum ratio of $C_y / C_n = -0.369$ which is 112% higher than BODY A at $C_y / C_n = -0.174$ and 367% higher than BODY C at $C_y / C_n = -0.079$.

The side force to normal force ratios for the turbulence conditions in Figures 50 through 63. should follow the side force (with turbulence) trends since the normal force components are not affected to the same degree as the side force components. The C_y / C_n plots show some resemblance to the trends in the side force plots. The wide degree of scatter, especially for the turbulence from GRID 4 is representative of the side force trends. The cruciform missile should be able to cope with higher side force to normal force ratios due to it's wing and tail configuration. From these results, the winged configurations, BODY A and BODY C have smaller side force ratios than the body in isolation of BODY B. Although the ratio is small, this may be misleading since the BODY A and BODY C configurations must be able to cope with higher normal and side forces than BODY B which can be easily accomplished by their cruciform wing configurations.

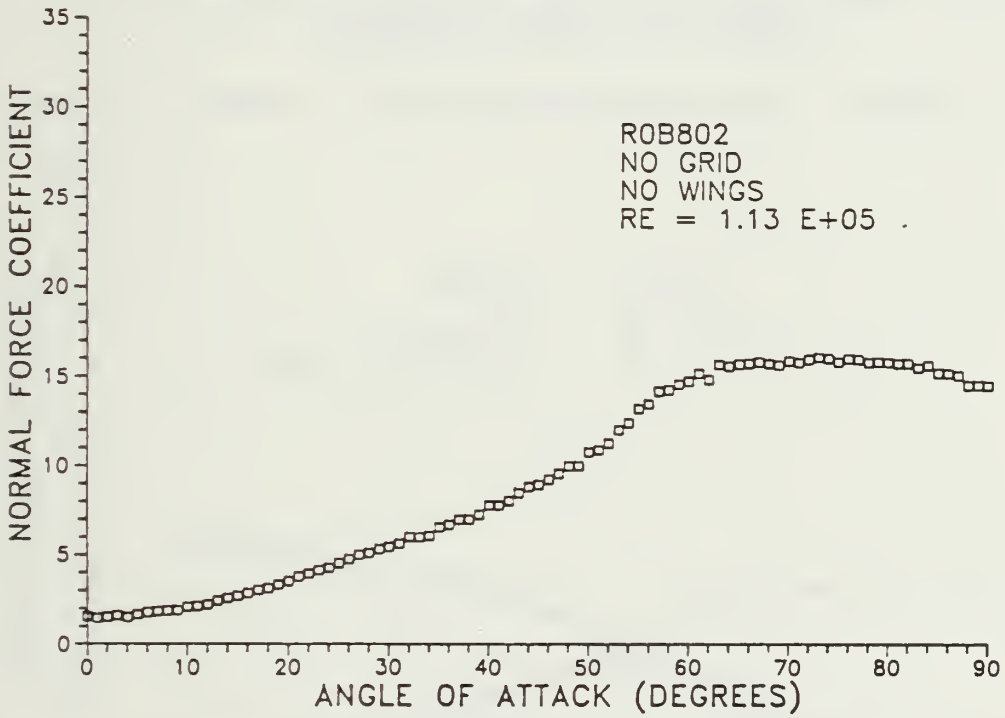

Figure 34. R0B802: Normal Force Coefficient.

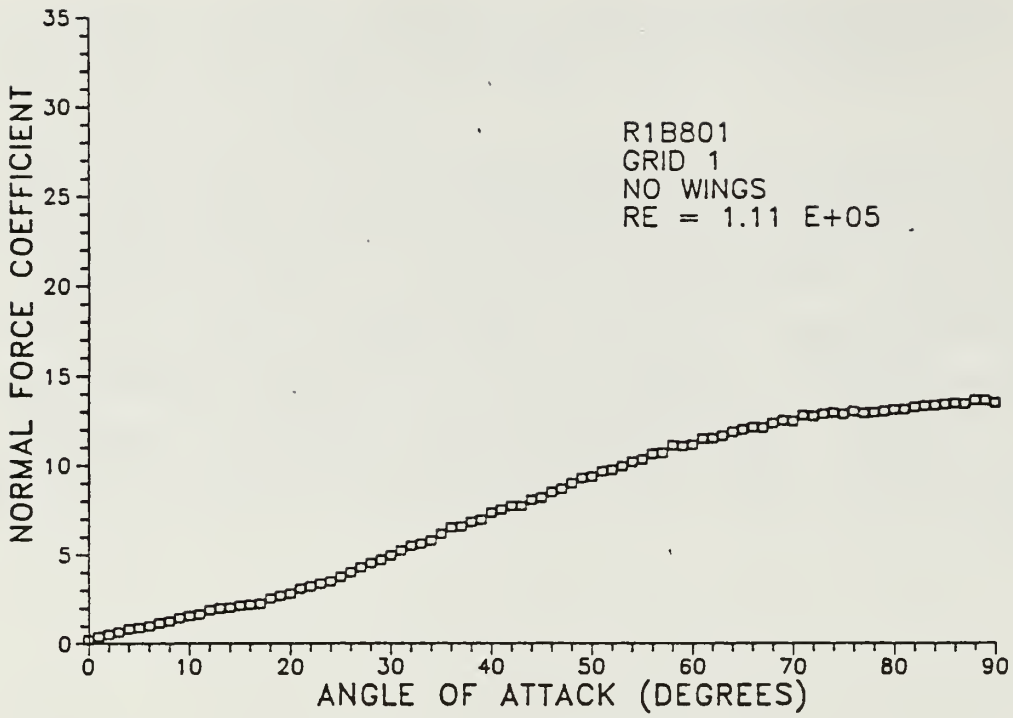

Figure 35. R1B801: Normal Force Coefficient.

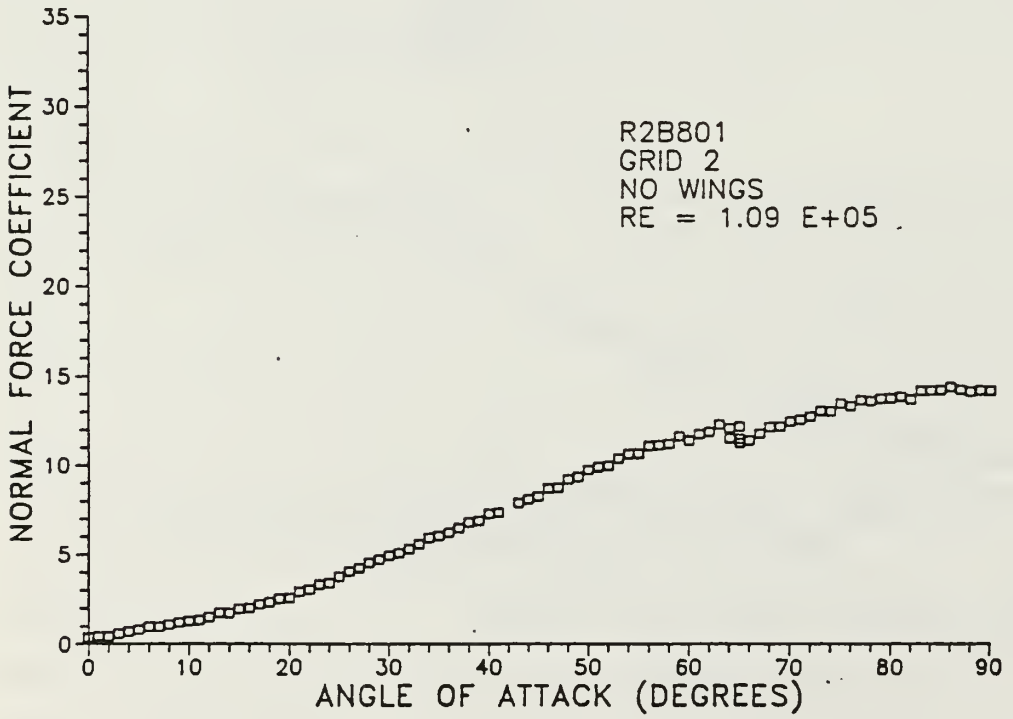

Figure 36. R2B801: Normal Force Coefficient.

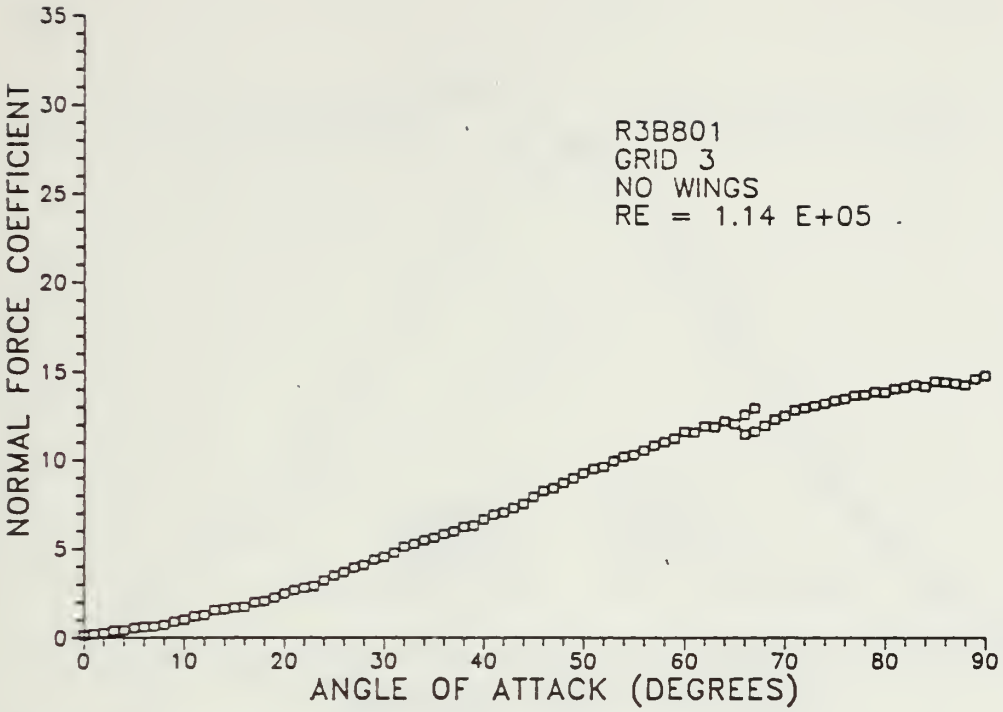

Figure 37. R3B801: Normal Force Coefficient.

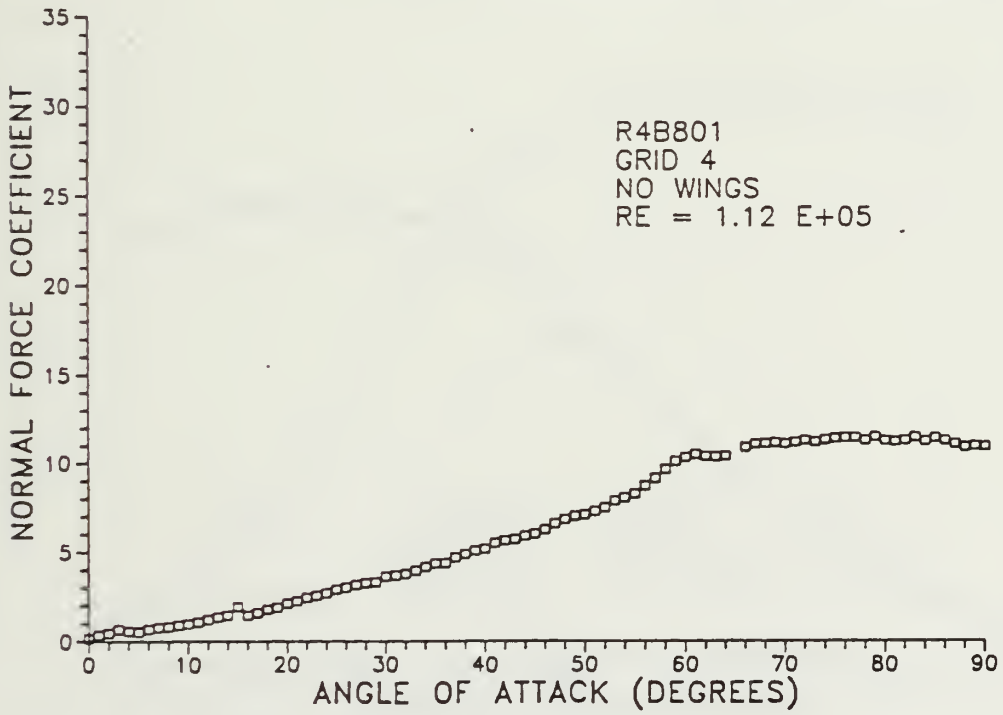

Figure 38. R4B801: Normal Force Coefficient.

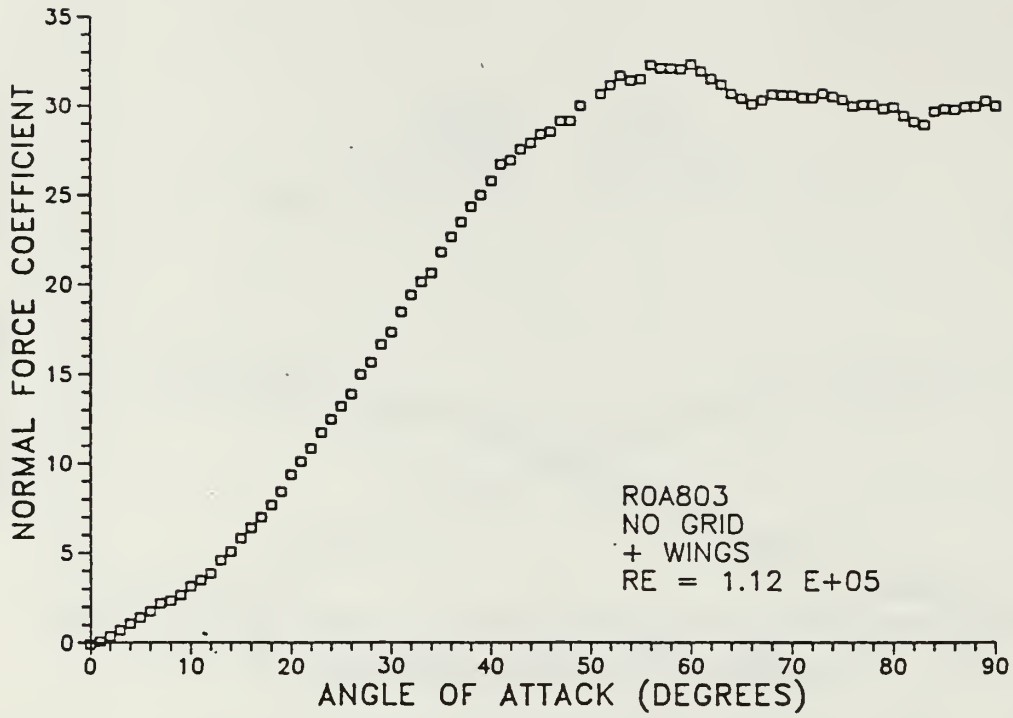

Figure 39. R0A803: Normal Force Coefficient.

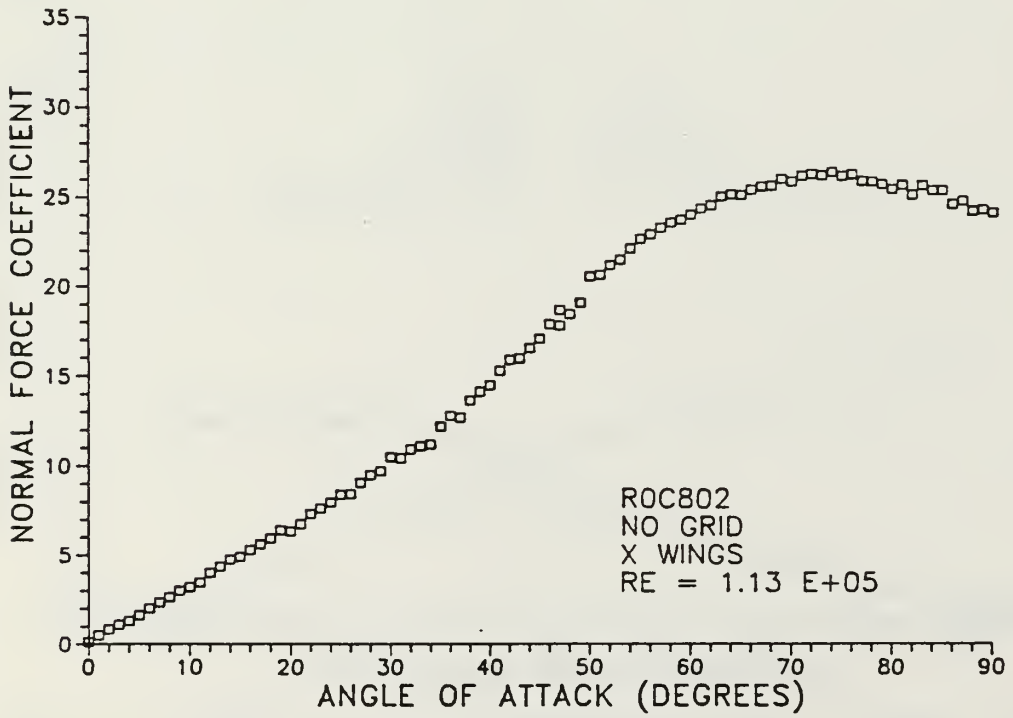

Figure 40. R0C802: Normal Force Coefficient.

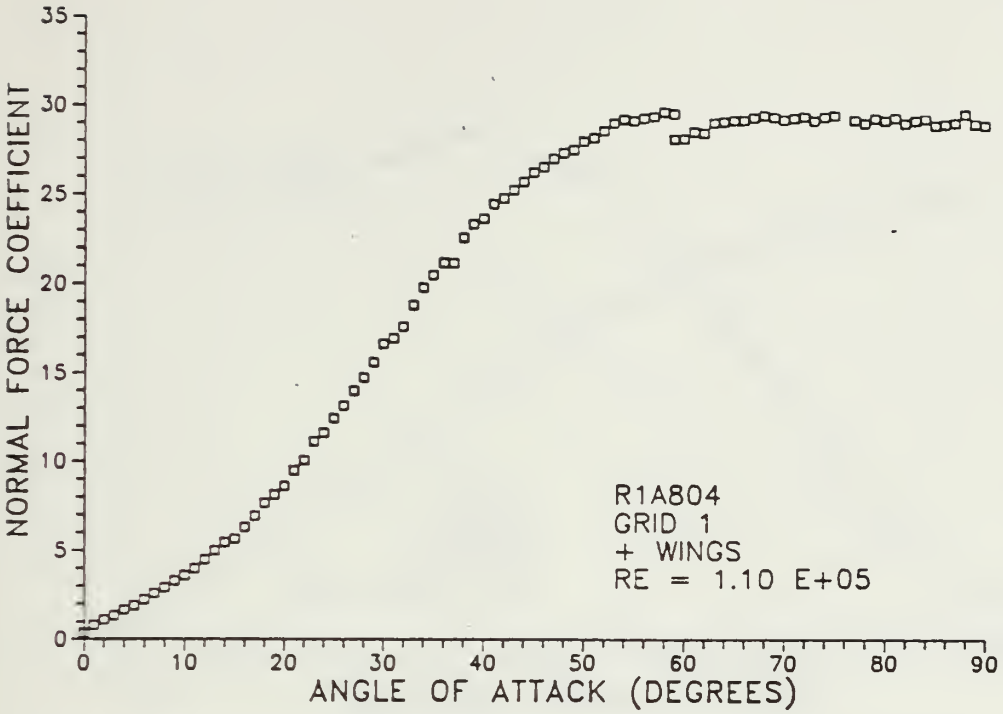

Figure 41. R1A804: Normal Force Coefficient.

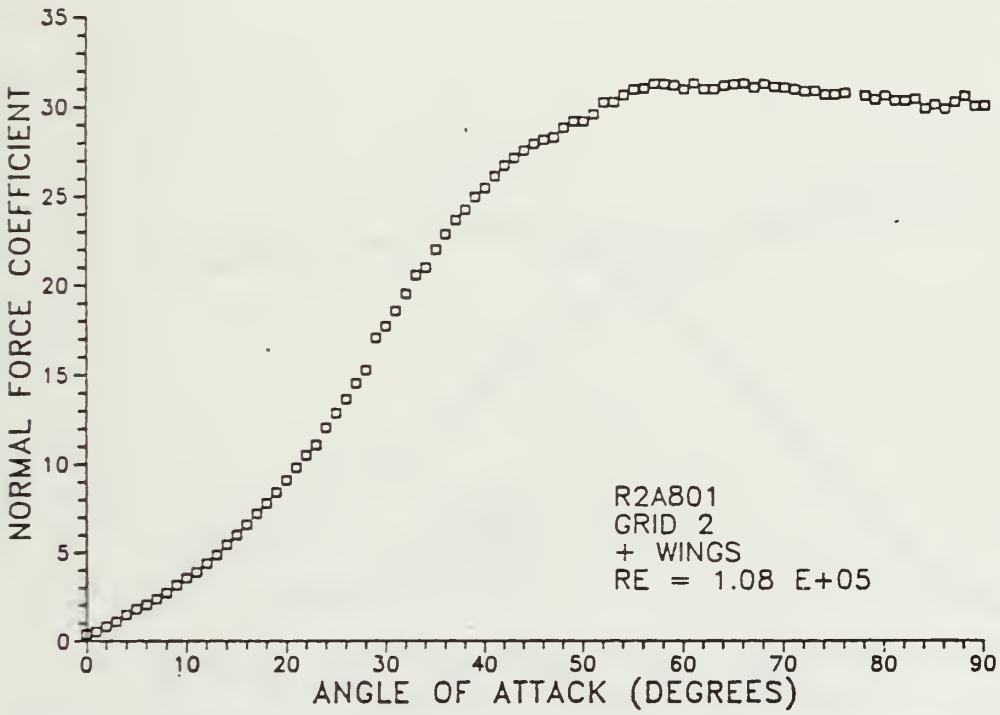

Figure 42. R2A801: Normal Force Coefficient.

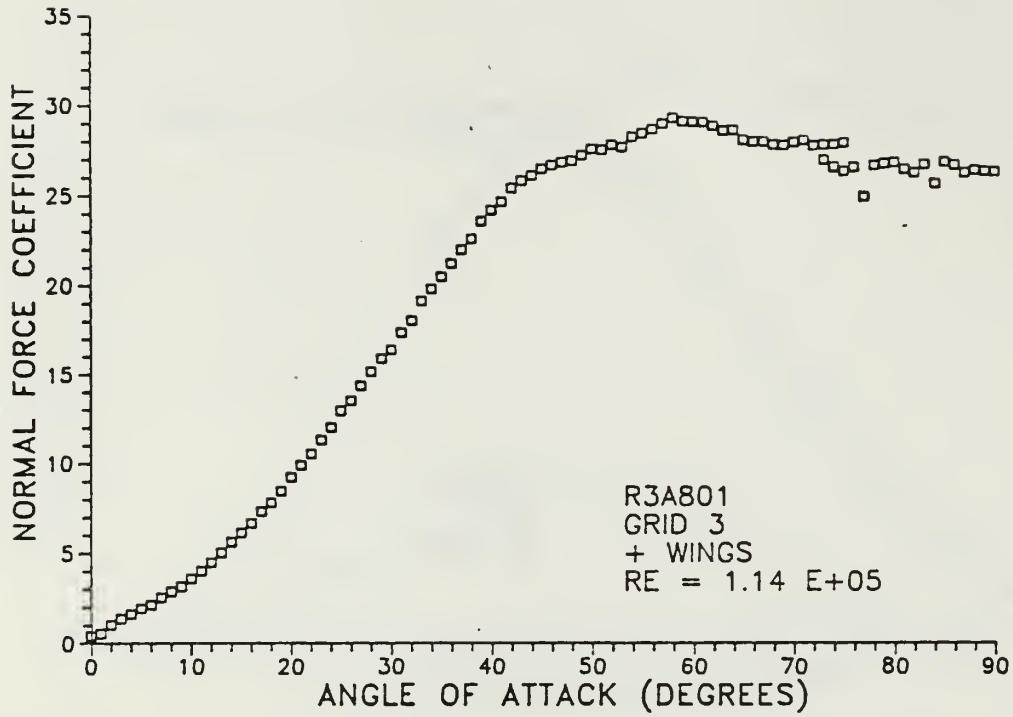

Figure 43. R3A801: Normal Force Coefficient.

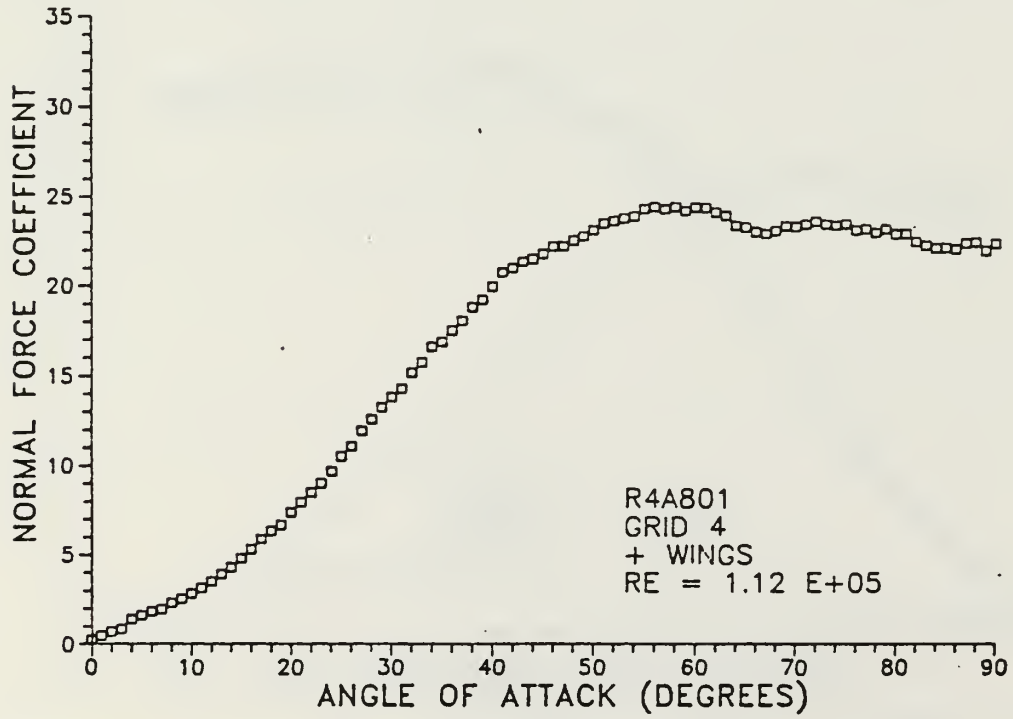

Figure 44. R4A801: Normal Force Coefficient.

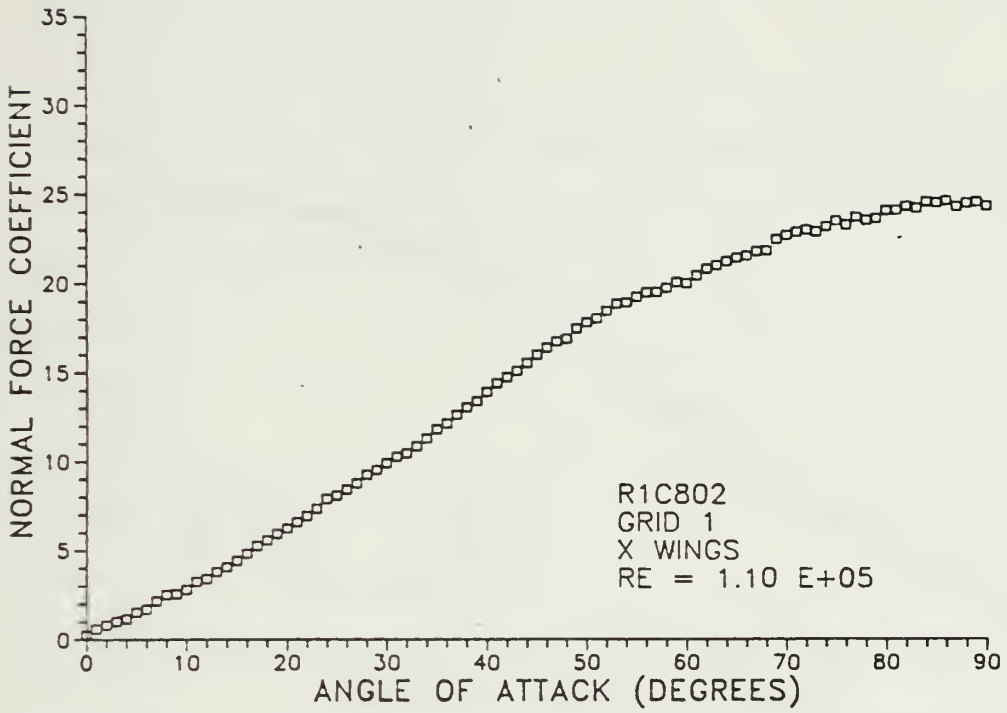

Figure 45. R1C802: Normal Force Coefficient.

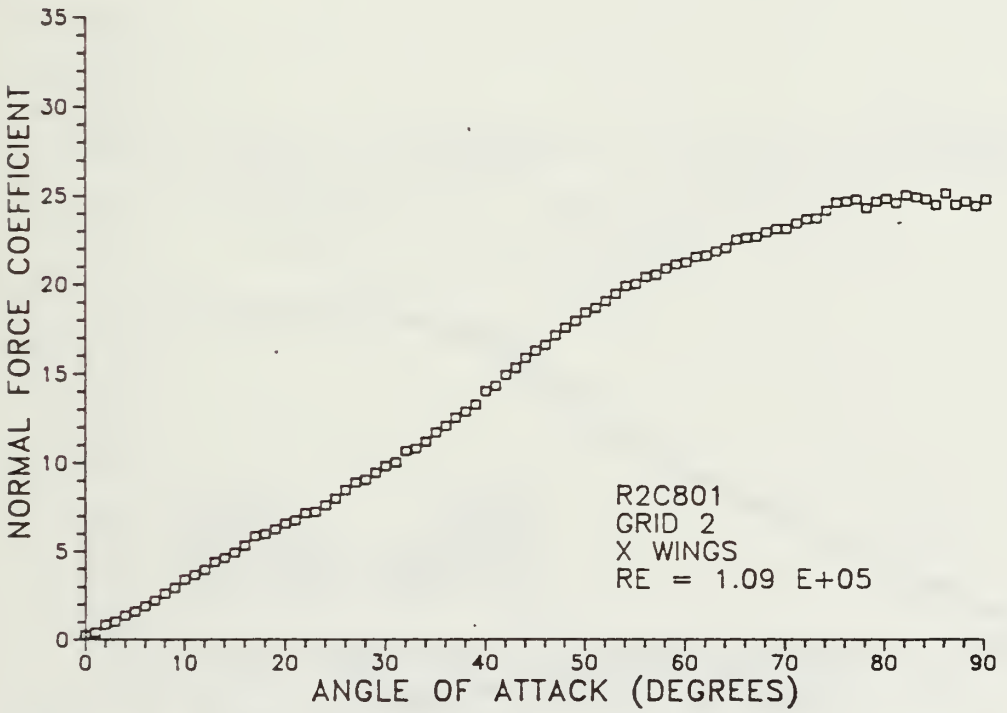

Figure 46. R2C801: Normal Force Coefficient.

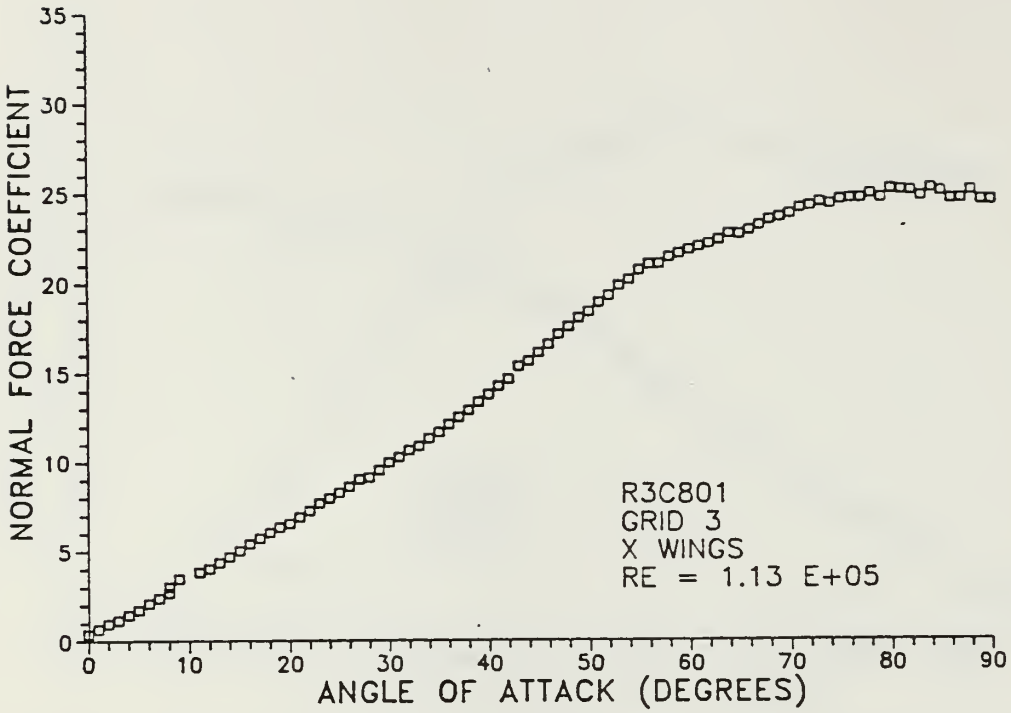

Figure 47. R3C801: Normal Force Coefficient.

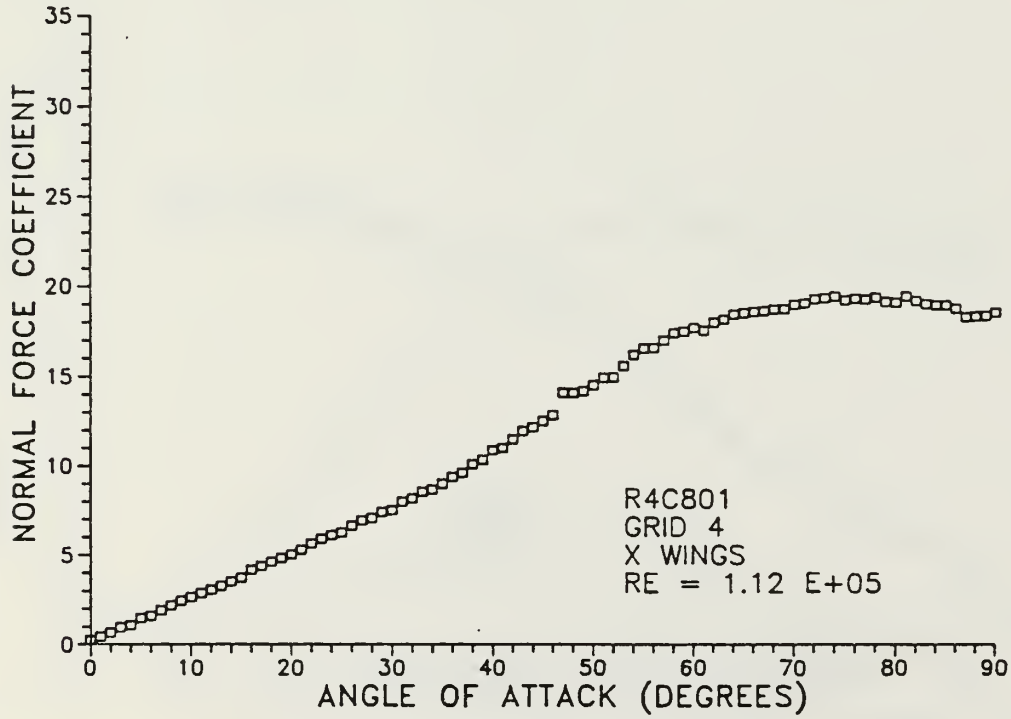

Figure 48. R4C801: Normal Force Coefficient.

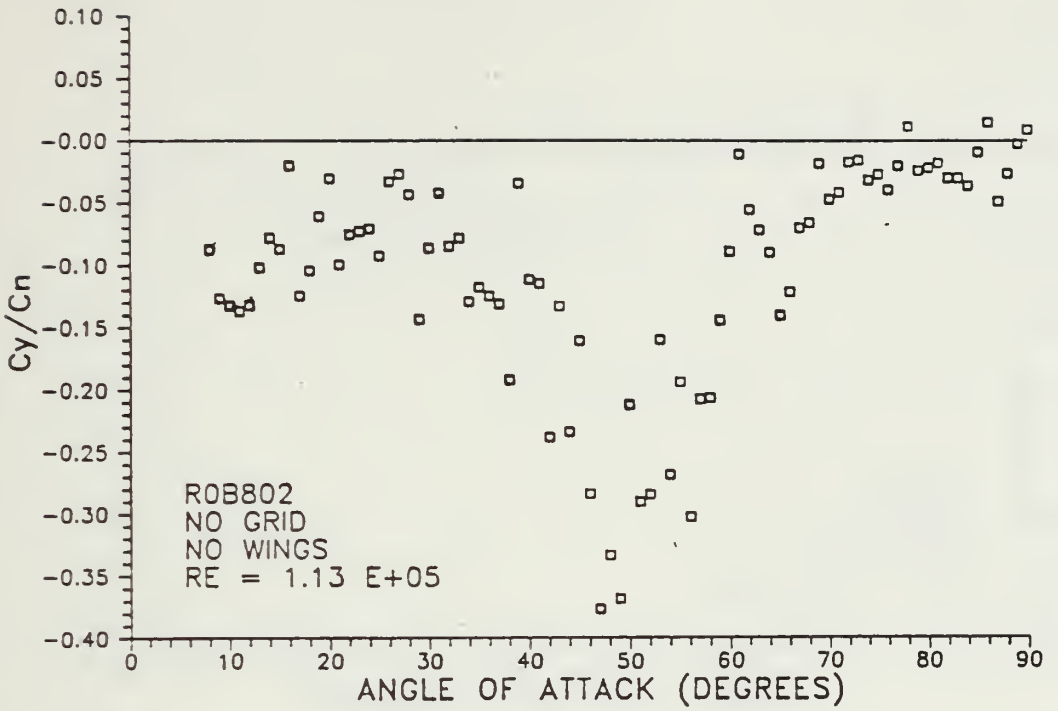

Figure 49. R0B802: Side Force to Normal Force Ratio.

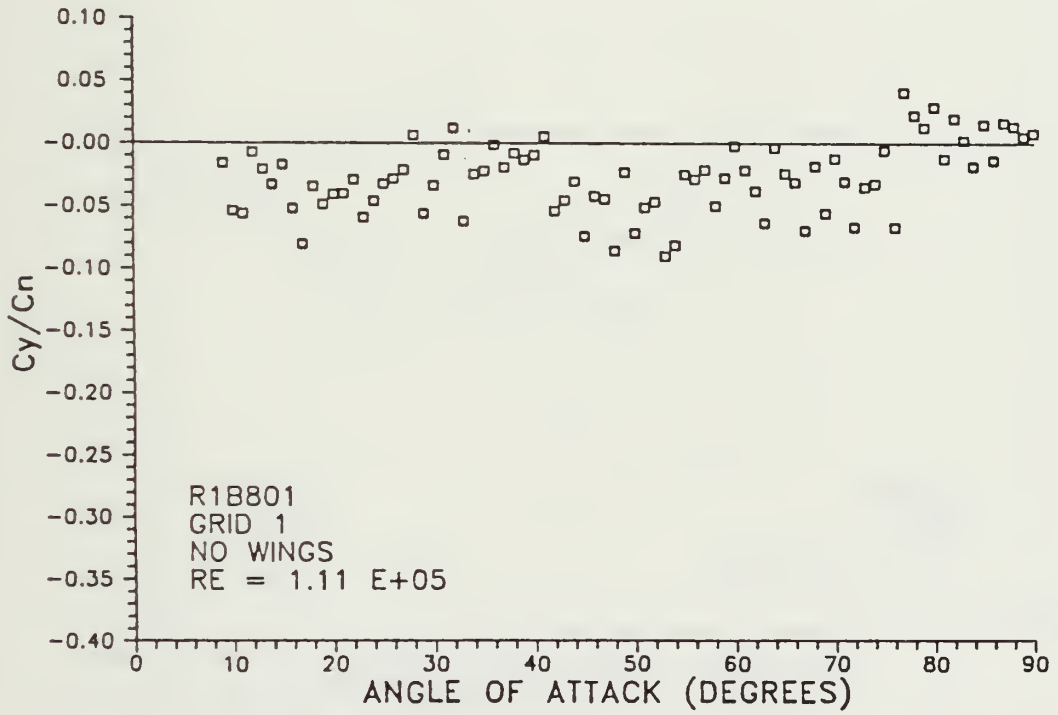

Figure 50. R1B801: Side Force to Normal Force Ratio.

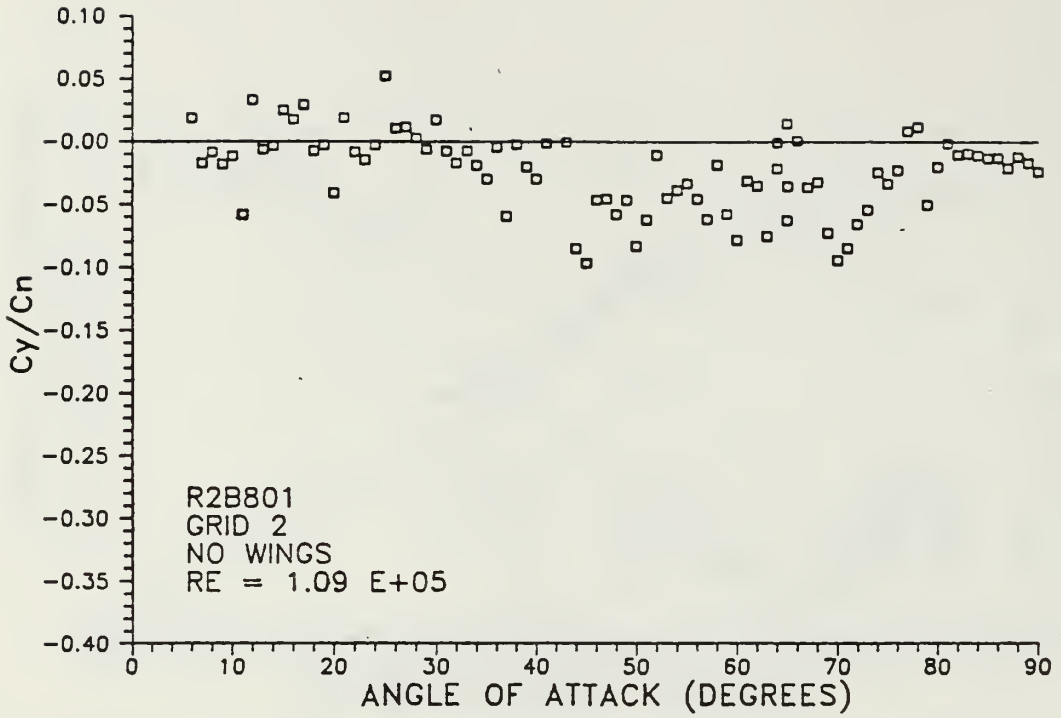

Figure 51. R2B801: Side Force to Normal Force Ratio.

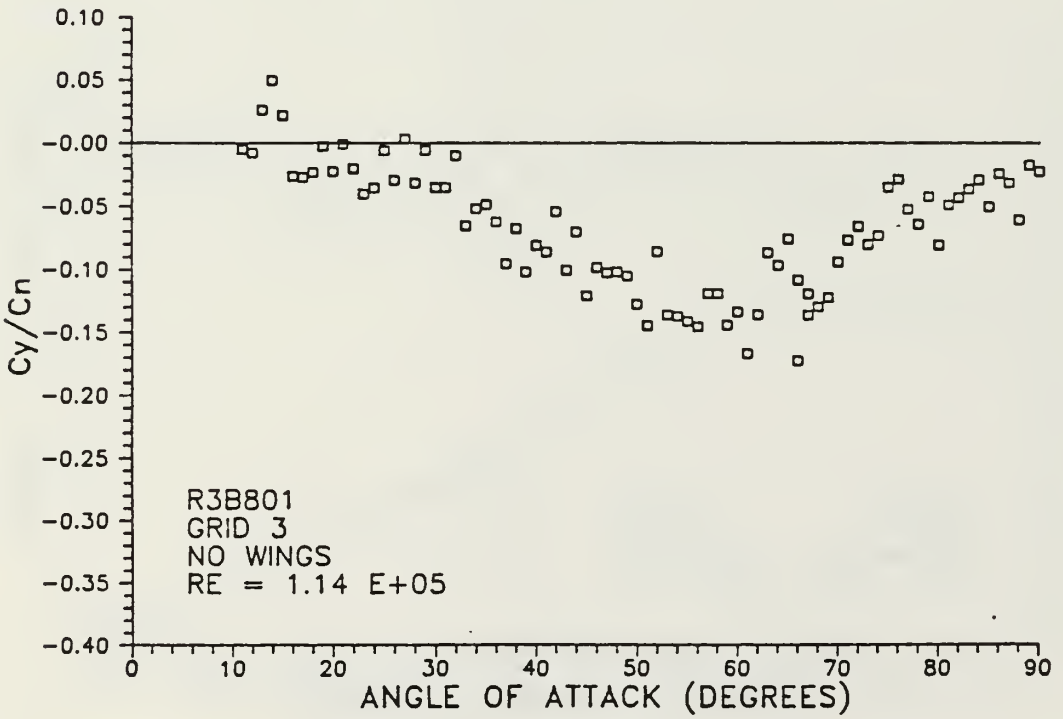

Figure 52. R3B801: Side Force to Normal Force Ratio.

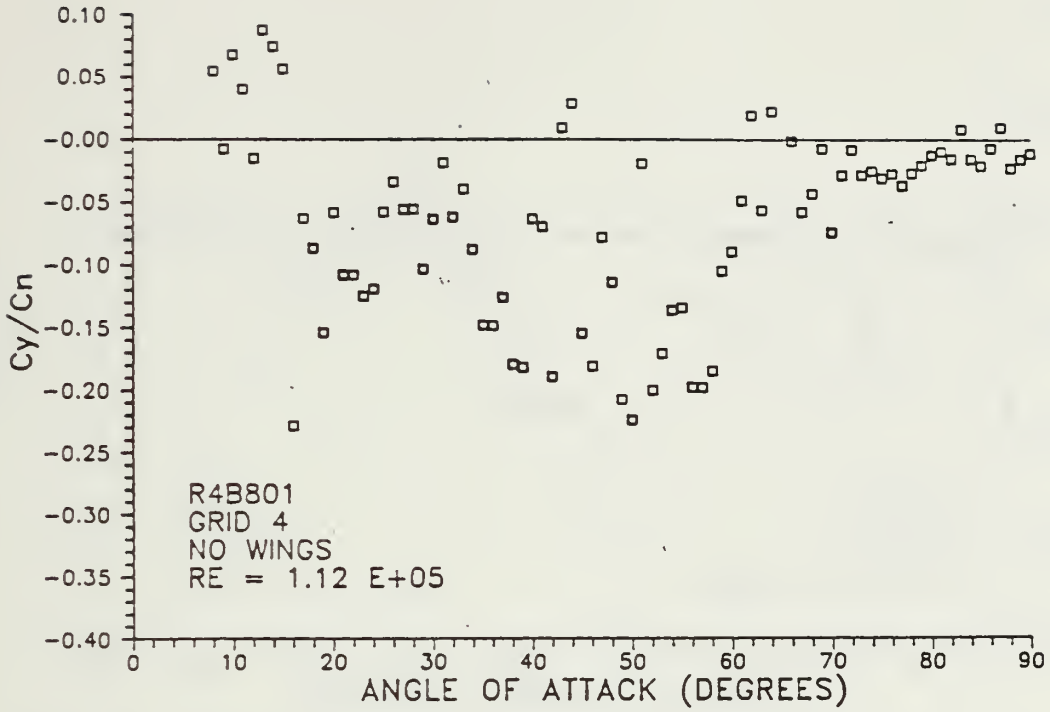

Figure 53. R4B801: Side Force to Normal Force Ratio.

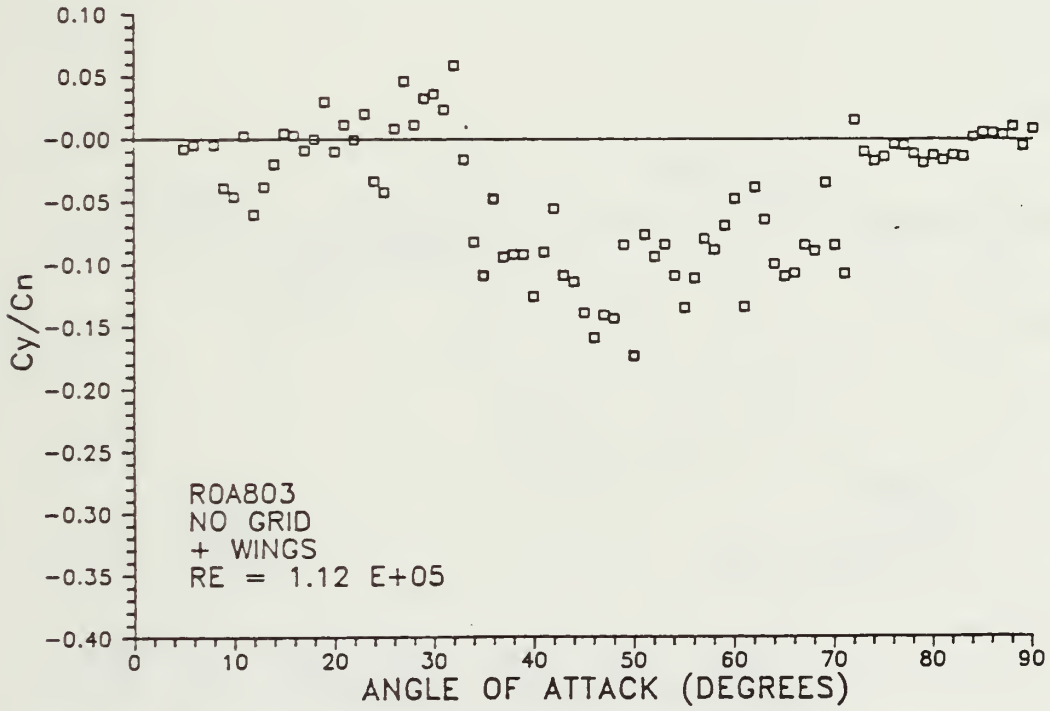

Figure 54. R0A803: Side Force to Normal Force Ratio.

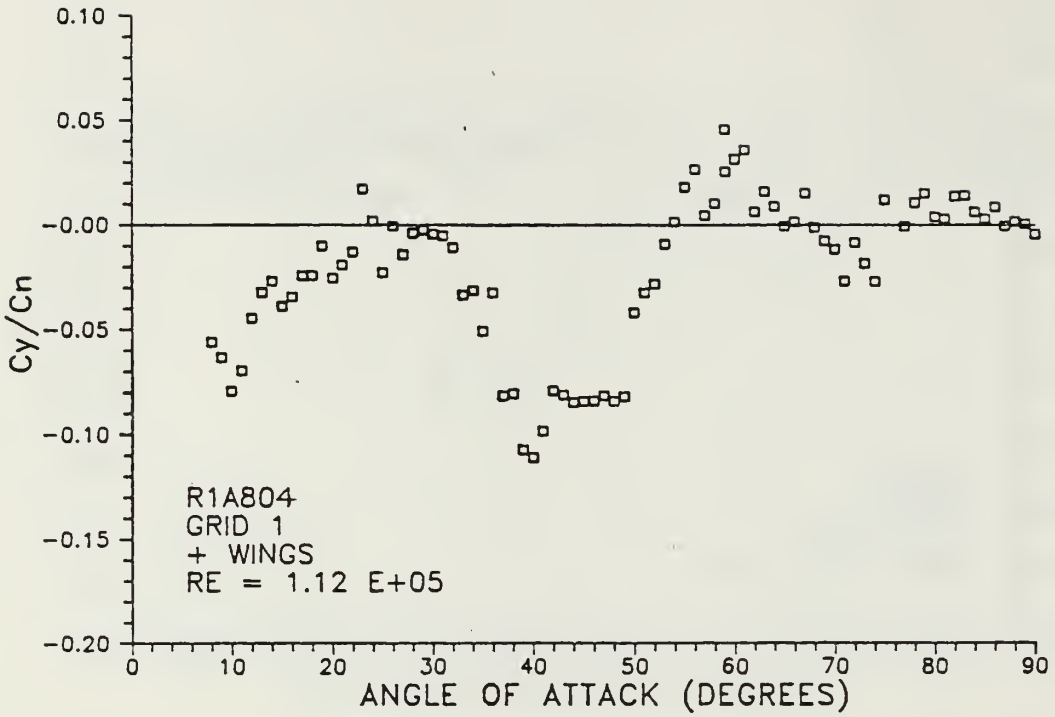

Figure 55. R1A804: Side Force to Normal Force Ratio.

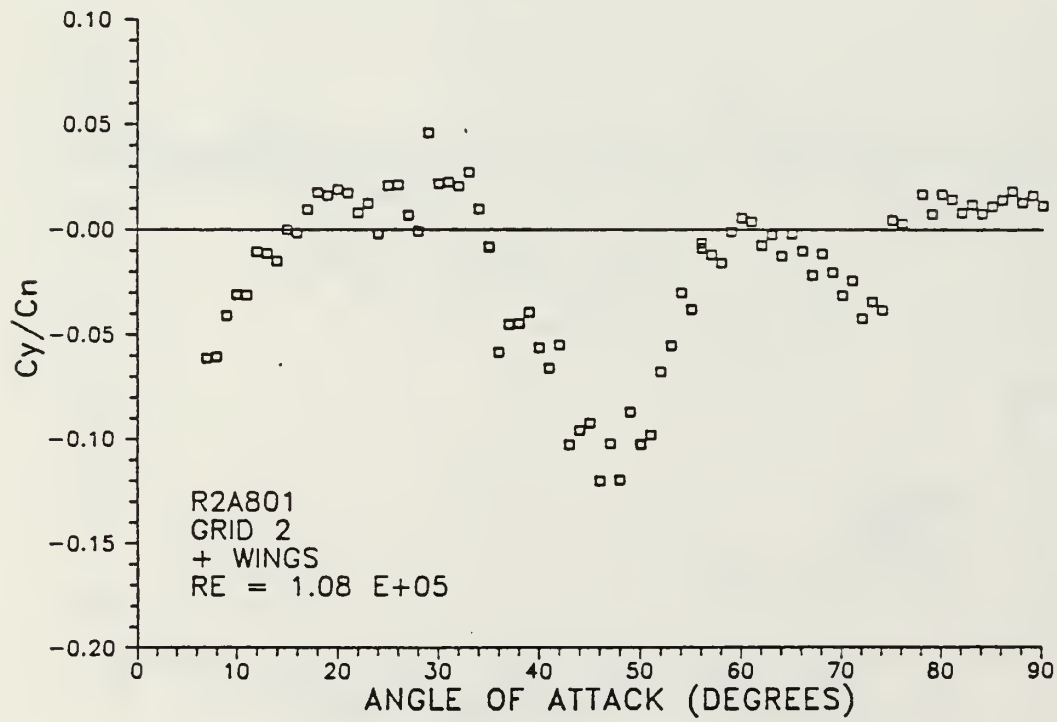

Figure 56. R2A801: Side Force to Normal Force Ratio.

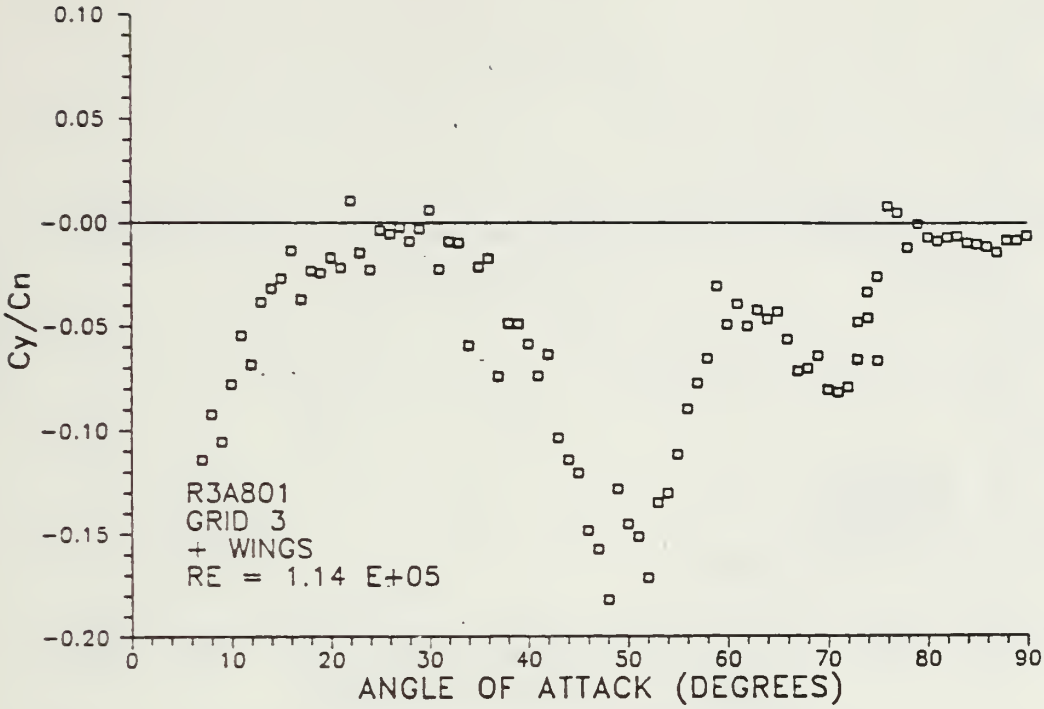

Figure 57. R3A801: Side Force to Normal Force Ratio.

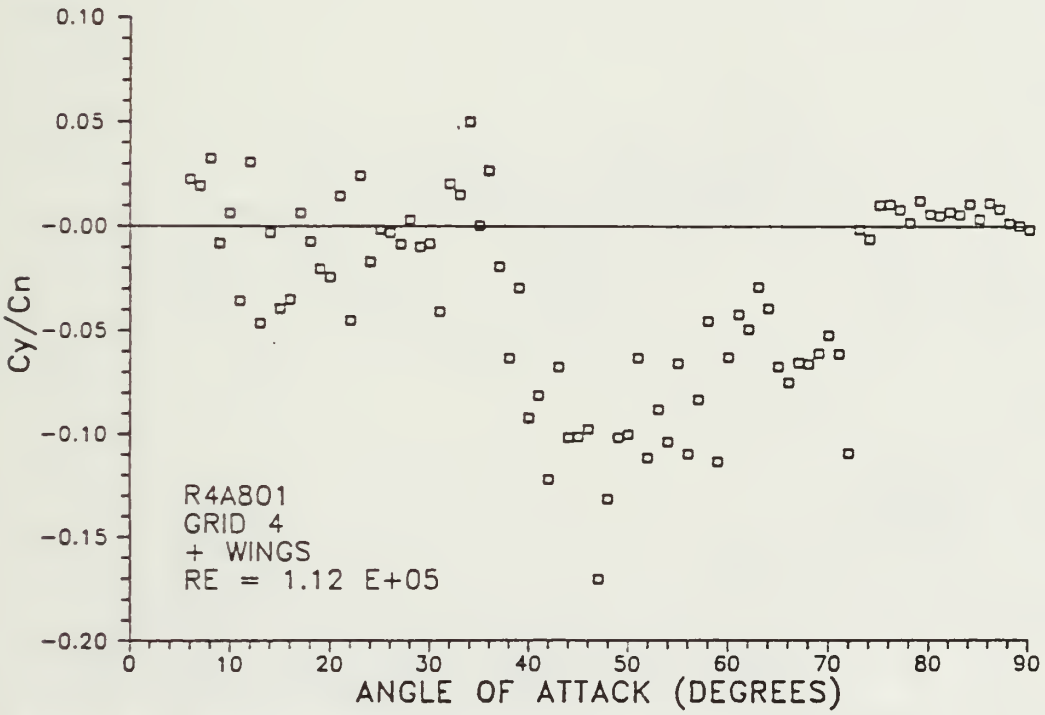

Figure 58. R4A801: Side Force to Normal Force Ratio.

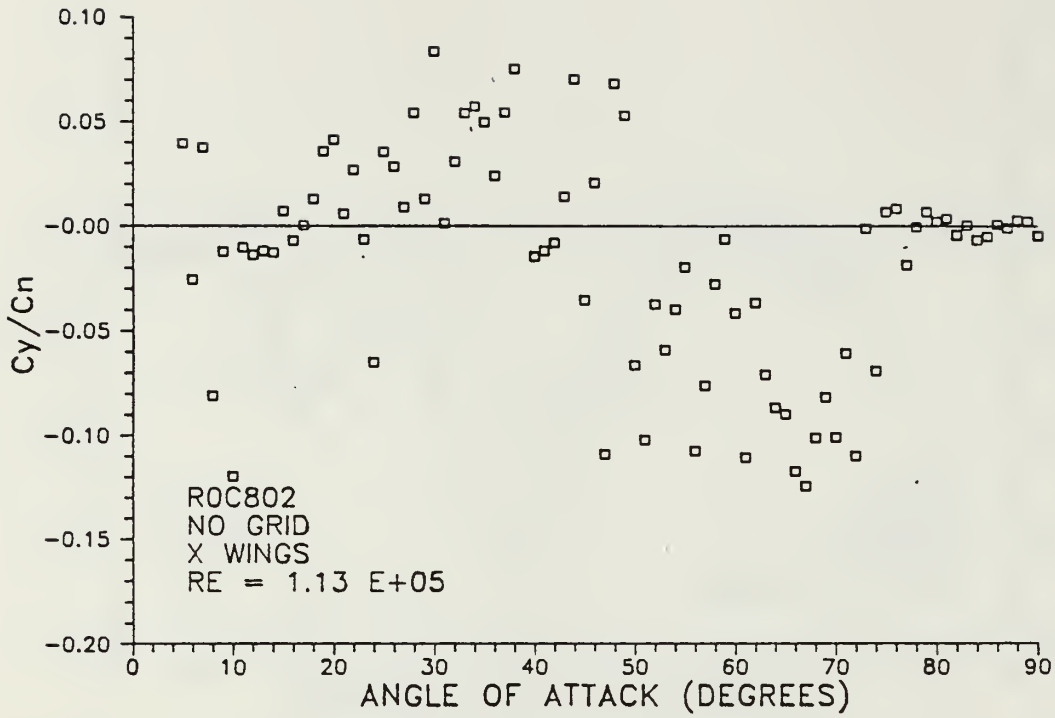

Figure 59. R0C802: Side Force to Normal Force Ratio.

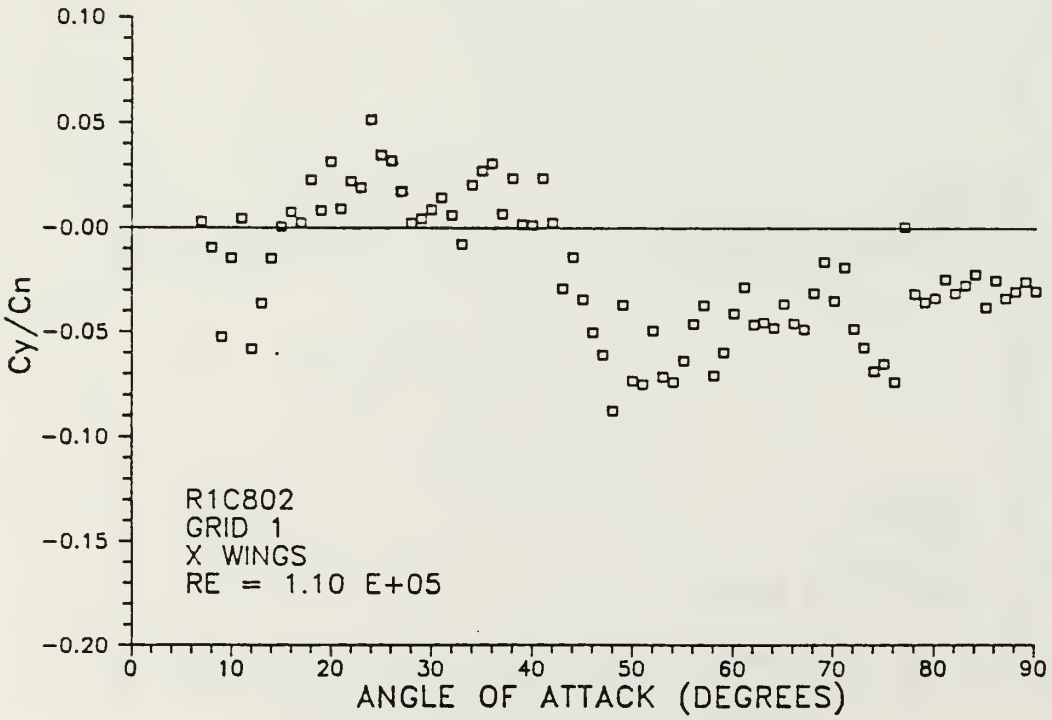

Figure 60. R1C802: Side Force to Normal Force Ratio.

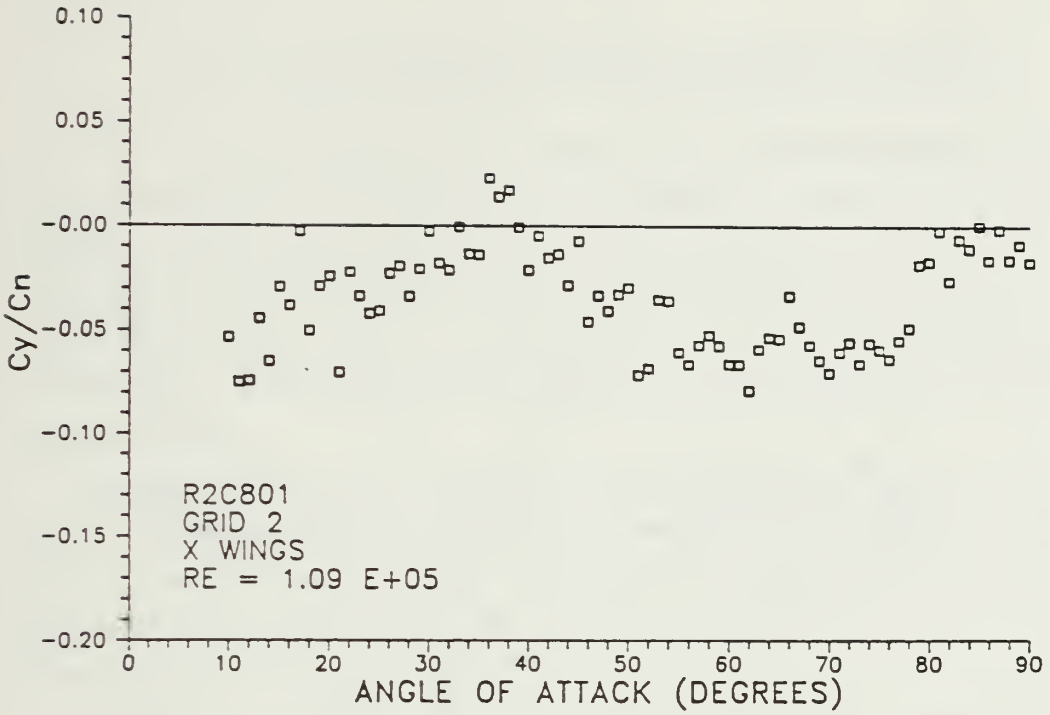

Figure 61. R2C801: Side Force to Normal Force Ratio.

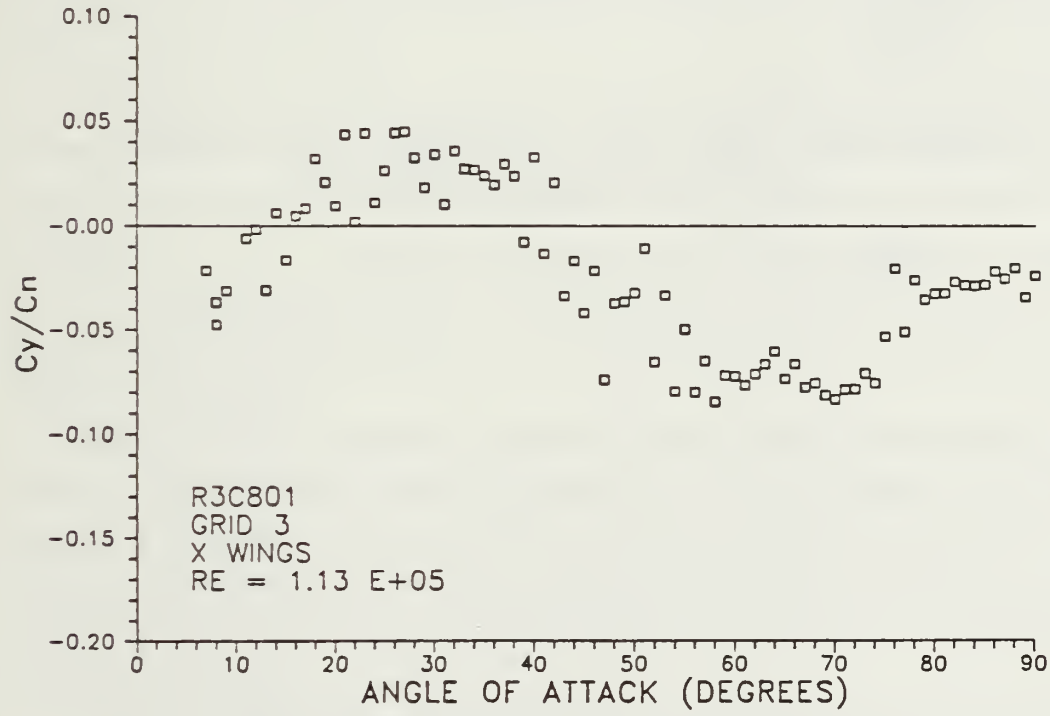

Figure 62. R3C801: Side Force to Normal Force Ratio.

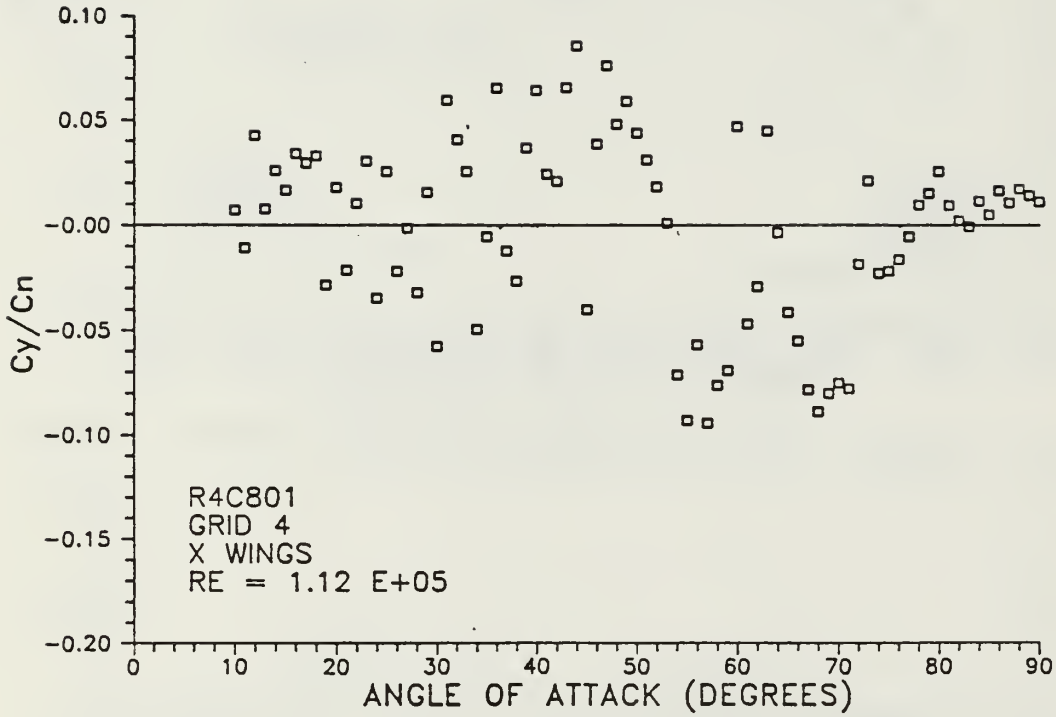

Figure 63. R4C801: Side Force to Normal Force Ratio.

IV. CONCLUSIONS AND RECOMMENDATIONS

The VLSAM in the marine environment may encounter turbulence during the launch phase at high angles of attack. The turbulence intensities in the marine environment are higher than produced in the experiment, as are the turbulence length scales which are on on the order of L_u:$L_d \approx 280$:1 for a typical VLSAM. Cascading and/or ship airwake may produce smaller low intensity turbulence on the order of missile diameter or vortex size. These turbulence scales relative to the model diameter may be produced in the wind tunnel.

Subsonic wind tunnel investigations were performed on a cruciform wing missile model with different grid generated turbulence length scales and intensities. The model was tested with three different body configurations with and without wings at 0° to 90° angle of attack. The results from the experimental runs with no turbulence yield the following conclusions:

1. Side force magnitude and direction change with variations in nose roll angle.

2. There is a general trend in the repeatability of data points and to some degree for all data points (for the steady state condition) which suggests the dominating influence of the nose generated vortices.

3. Strake and wing vortices may play an important role to influence the disposition of nose generated vortices. While the low pressure on the top of the wing may pull the nose vortices closer to the body, leading edge vortices from strakes and wings may push them away.

4. The maximum side force-to-normal force ratio was observed for the body in isolation configuration, although normal and side force values were actually lower than the winged configurations.

The results of the turbulence experiments indicate that turbulence effects for side forces may vary with length scale and intensity. Two turbulence length scales, boundary layer scale turbulence and vortex scale turbulence, are particularly important as the former may have large effect on flow separation mechanisms which generate the asymmetric vortices and the latter on the disposition of the vortices in the flowfield. Turbulence results conclude:

1. Longer turbulence length scales decrease side force magnitude and possibly any flow unsteadiness in the asymmetric vortex structure.

2. The angle of attack for the onset of asymmetric vortices is postponed by longer turbulence length scales. Since these length scales are quite large when compared to the boundary layer, the asymmetric vortex structure may be suppressed by the interaction between the inviscid vortex flowfield and the vortex scale free stream turbulence.

3. Higher turbulence intensities cause less flow unsteadiness for missiles with wings.

4. Turbulence had little effect on the normal force values. Maximum lift values were nearly identical and there was no fluctuation in normal force values for all turbulence conditions.

Further recommendations for a continued study of wing and turbulence interactions include:

1. Perform flow visualization, hotwire, surface flow, laser doppler, and water tunnel tests to quantify the various flowfields about the missile model at high angles of attack.

2. Test monoplane wing configurations at 0° and 90° roll.

3. Compare the effects of turbulence length scales at the same intensities and with longer and shorter turbulence length scales than those used in this experiment.

4. Compare the effects of turbulence intensities at the same length scale and with higher intensities than those used in this experiment.

5. Model the rocket motor plume to study the interaction with flowfields about the missile.

APPENDIX A. BALANCE CALIBRATION CONSTANTS

BALANCE CALIBRATION CA. DATE 7247 COMP DATE 7287

INV #440517

KIND FORCE PIN NO. 3

SIZE 1.00

MAKE TASK 140 RIG NO. 2

GA	CAPACITY	MAX LOAD	IMMS	K_GAGE	CAL SHUNT	CAL ROS
N1	400.00	400.00	350.	0.1667	100K	4625
N2	400.00	400.00	350.	0.1667	100K	4626
A	100.00	100.00	175.		50K	4618
S1	200.00	200.00	350.	0.1375	00K	4623
S2	200.00	200.00	350.	0.1375	100K	4597
RM	21.00	20.83	175.		50K	4623

GA	K_POS(1)	K_POS(2)	K_NEG(1)	K_NEG(2)	MAX DEV	% ACC
N1	5.0861E-02	-5.4826E-09	5.1591E-02	1.7157E-08	0.224	0.056
N2	4.7211E-02	-1.7015E-08	4.7763E-02	8.9153E-09	0.196	0.049
A	1.4309E-02	-7.1962E-10	1.4290E-02	-1.3322E-09	0.115	0.115
S1	3.1309E-02	-3.8153E-08	3.2073E-02	-8.9316E-09	-0.263	0.132
S2	3.0366E-02	-3.8607E-08	3.1167E-02	-7.2517E-09	0.305	0.153
RM	3.0885E-03	2.5672E-09	3.0908E-03	-2.4769E-09	0.042	0.204

DEG OF FIT = 2 ACCURACY = 15

INT-DEG-OF-FIT = 2

N1/N2+ =-5.6035E-03
N1/A + = 0.0000E+00
N1/S1+ =-4.1655E-03
N1/S2+ = 0.0000E+00
N1/RM+ =-5.8079E-02
N2/N1+ =-4.6218E-02
N2/A + = 2.8393E-03
N2/S1+ = 8.1694E-03
N2/S2+ =-4.1463E-03
N2/RM+ =-7.7279E-02
A /N1+ =-8.6893E-04
A /N2+ = 0.0000E+00
A /S1+ =-6.0359E-04
A /S2+ =-7.7722E-05
A /RM+ = 1.1115E-01
S1/N1+ = 6.3459E-04
S1/N2+ = 0.0000E+00
S1/A + = 0.0000E+00
S1/S2+ = 0.0000E+00

N1/N2- =-1.0257E-02
N1/A - = 0.0000E+00
N1/S1- = 4.5396E-03
N1/S2- = 0.0000E+00
N1/RM- = 4.4940E-02
N2/N1- =-5.1778E-02
N2/A - = 4.4056E-03
N2/S1- = 9.0395E-03
N2/S2- = 0.0000E+00
N2/RM- = 6.1125E-02
A /N1- = 2.1217E-03
A /N2- =-9.1524E-04
A /S1- = 0.0000E+00
A /S2- = 0.0000E+00
A /RM- = 9.7188E-02
S1/N1- = 7.1275E-03
S1/N2- = 0.0000E+00
S1/A - = 8.9235E-03
S1/S2- = 0.0000E+00

Figure 64. Balance Calibration Constants: [Ref. 42]

```
S1/RM+ = 1.1148E-01
S2/N1+ = 2.4237E-03
S2/N2+ = 0.0000E+00
S2/A  + =-2.2455E-03
S2/S1+ =-6.6785E-03
S2/RM+ = 2.6377E-01
RM/N1+ = 0.0000E+00
RM/N2+ = 1.9928E-06
RM/A  + = 0.0000E+00
RM/S1+ = 0.0000E+00
RM/S2+ = 2.5893E-06
N1/N2*N2+ = 7.1926E-07
N1/A  *A  + = 0.0000E+00
N1/S1*S1+ =-4.0352E-06
N1/S2*S2+ = 0.0000E+00
N1/RM*RM+ = 6.7860E-04
N2/N1*N1+ = 6.8577E-07
N2/A  *A  + = 1.7735E-05
N2/S1*S1+ =-2.1719E-06
N2/S2*S2+ =-1.8592E-06
N2/RM*RM+ = 1.9294E-03
A  /N1*N1+ =-4.4537E-07
A  /N2*N2+ = 0.0000E+00
A  /S1*S1+ =-4.7936E-06
A  /S2*S2+ = 4.1033E-06
A  /RM*RM+ =-2.0697E-04
S1/N1*N1+ =-5.5350E-06
S1/N2*N2+ = 0.0000E+00
S1/A  *A  + = 0.0000E+00
S1/S2*S2+ = 0.0000E+00
S1/RM*RM+ =-2.4592E-03
S2/N1*N1+ =-1.7099E-06
S2/N2*N2+ = 0.0000E+00
S2/A  *A  + =-1.2072E-05
S2/S1*S1+ = 2.7825E-06
S2/RM*RM+ =-6.2217E-03
RM/N1*N1+ = 0.0000E+00
RM/N2*N2+ =-1.1512E-07
RM/A  *A  + = 0.0000E+00
RM/S1*S1+ = 0.0000E+00
RM/S2*S2+ = 5.1560E-08
```

```
S1/RM- = 5.2630E-02
S2/N1- = 3.7176E-03
S2/N2- = 5.2619E-03
S2/A  - =-7.2915E-03
S2/S1- =-6.3560E-03
S2/RM- = 5.2581E-02
RM/N1- =-3.5945E-06
RM/N2- = 0.0000E+00
RM/A  - = 0.0000E+00
RM/S1- = 0.0000E+00
RM/S2- = 0.0000E+00
   N1/N2*N2- =-7.9499E-07
   N1/A  *A  - = 0.0000E+00
   N1/S1*S1- = 1.9679E-06
   N1/S2*S2- = 0.0000E+00
   N1/RM*RM- = 3.3320E-04
   N2/N1*N1- =-5.2897E-06
   N2/A  *A  - =-1.0467E-05
   N2/S1*S1- = 6.8493E-07
   N2/S2*S2- = 0.0000E+00
   N2/RM*RM- = 1.1773E-03
   A  /N1*N1- = 6.2547E-06
   A  /N2*N2- =-6.5946E-06
   A  /S1*S1- = 0.0000E+00
   A  /S2*S2- = 0.0000E+00
   A  /RM*RM- = 7.5001E-04
   S1/N1*N1- = 1.2723E-05
   S1/N2*N2- = 0.0000E+00
   S1/A  *A  - = 6.0345E-05
   S1/S2*S2- = 0.0000E+00
   S1/RM*RM- = 9.3969E-04
   S2/N1*N1- = 5.2110E-07
   S2/N2*N2- = 8.6265E-06
   S2/A  *A  - =-3.7054E-05
   S2/S1*S1- =-9.9830E-06
   S2/RM*RM- =-5.0075E-04
   RM/N1*N1- =-1.5697E-07
   RM/N2*N2- = 0.0000E+00
   RM/A  *A  - = 0.0000E+00
   RM/S1*S1- = 0.0000E+00
   RM/S2*S2- = 0.0000E+00
```

Figure 65. Balance Calibration Constants: [Ref. 42]

APPENDIX B. RUN MATRIX

The run matrix lists all runs conducted for this thesis research. All runs were conducted by the author in the Naval Postgraduate School Wind Tunnel Test Facility. Not all of the runs were discussed in the results section and were essential trial runs to familiarize the author with the data acquisition system and observe the general trend of the data.

These runs are listed by a sequence code as in:

R0B802

where:

1. The first letter is a run code.

   "W" - Nose roll angle runs.
   "E" - Data repeatability run.
   "R"- Data collection run.

2. The next digit is the grid number

   0 - NO GRID
   1 - GRID 1
   2 - GRID 2
   3 - GRID 3
   4 - GRID 4

3. The next digit is the nose number.
   Nose 1 is at 0° roll angle.
   Each nose represents a 45° roll angle increment.

4. The last two digits are the run number.

RUN	BODY	SCREEN	$RE_D \times 10^5$	DYNAMIC PRESSURE (lbs/ft²)	VELOCITY (ft/sec)	TEMPERATURE (°F)	ANGLE OF ATTACK (degrees)	INCREMENT (degrees)
W0A101	A	0	1.33	22.2	130.2	68.0	0→90	10,5
W0A201	A	0	1.33	22.2	130.2	68.0	0→90	10,5
W0A301	A	0	1.33	22.2	130.2	68.0	0→90	10,5
W0A401	A	0	1.33	22.2	130.2	68.0	0→90	10,5
W0A501	A	0	1.33	22.2	130.2	68.0	0→90	10,5
W0A601	A	0	1.33	22.2	130.2	68.0	0→90	10,5
W0A701	A	0	1.33	22.2	130.2	68.0	0→90	10,5
W0A801	A	0	1.33	22.2	130.2	68.0	0→90	10,5
W0A101	A	0	1.33	22.2	130.2	68.0	0→90	10,5
W0A201	A	0	1.33	22.2	130.2	68.0	0→90	10,5
W0A301	A	0	1.33	22.2	130.2	68.0	0→90	10,5
W0A401	A	0	1.33	22.2	130.2	68.0	0→90	10,5
W0A501	A	0	1.33	22.2	130.2	68.0	0→90	10,5
W0A601	A	0	1.33	22.2	130.2	68.0	0→90	10,5
W0A701	A	0	1.33	22.2	130.2	68.0	0→90	10,5
W0A801	A	0	1.33	22.2	130.2	68.0	0→90	10,5
E0A8251	A	0	1.13	15.8	109.9	62.5	25	
E0A8451	A	0	1.13	15.8	110.9	63.5	45	
E0A8701	A	0	1.13	15.8	109.9	62.5	70	

E0A8901	A	0	1.13	15.8	110.1	64.0	90	
R0A801	A	0	1.13	15.9	110.6	66.3	0→92	2
R0A802	A	0	1.13	15.9	110.6	66.5	-10→100	5
R0A803	A	0	1.12	15.8	110.5	68.0	-5→95	1
R1A801	A	1	1.10	15.4	109.9	79.0	0→92	2
R1A802	A	1	1.10	15.4	109.2	72.5	92→-4	2
R1A803	A	1	1.10	15.4	109.5	75.0	-5→95	1
R1A804	A	1	1.10	15.4	110.2	72.0	-5→95	1
R2A801	A	2	1.08	14.9	107.7	74.0	-5→95	1
R3A801	A	3	1.14	16.4	112.7	71.0	-5→95	1
R4A801	A	4	1.12	15.6	109.4	66.0	-5→95	1
R0C801	C	0	1.13	15.9	110.8	68.0	0→90	10.5
R0C802	C	0	1.13	15.8	110.1	64.0	-5→95	1
R1C801	C	1	1.10	15.4	109.1	71.0	-5→95	1
R1C802	C	1	1.10	15.4	109.0	70.5	-5→95	1
R2C801	C	2	1.09	14.9	107.5	72.0	-5→95	1
R3C801	C	3	1.13	16.4	113.0	74.0	-5→95	1
R4C801	C	4	1.12	15.6	109.6	67.0	-5→95	1
R0B801	B	0	1.13	15.8	110.0	63.0	-5→95	1
R0B802	B	0	1.13	15.8	110.2	65.5	95→-5	1
R1B801	B	1	1.11	15.4	108.9	68.5	-5→95	1
R2B801	B	2	1.09	14.9	107.4	71.0	-5→95	1
R3B801	B	3	1.14	16.4	112.7	71.0	-5→95	1
R4B801	B	4	1.12	15.6	109.2	64.0	-5→95	1

APPENDIX C. NUMERICAL DATA LISTING

The following data was collected during the data collection runs. A complete list of all the runs and respective experimental conditions is found in the RUN MATRIX of Appendix B.

RUNFILE> W0A101

AOA	Cn	Cy	Cy/Cn	Cax	Cpt	Crl	Cyw
0.0	-0.091	-0.050	0.554	-0.009	0.001	0.000	-0.002
1.0	-0.137	-0.060	0.440	-0.010	0.000	0.000	-0.002
2.0	-0.144	-0.062	0.430	-0.021	-0.001	0.000	-0.002
10.0	2.600	-0.398	-0.153	0.238	-0.023	0.031	-0.010
20.0	8.254	-0.024	-0.003	0.282	-0.061	-0.006	-0.013
30.0	15.948	0.195	0.012	0.139	0.064	-0.051	-0.020
35.0	20.241	0.271	0.013	-0.021	0.214	-0.066	-0.019
40.0	23.307	-1.338	-0.057	-0.132	0.420	0.057	0.038
45.0	26.572	-2.147	-0.081	-0.162	0.497	0.103	0.039
50.0	26.997	-2.990	-0.111	-0.168	0.523	-0.141	-0.013
55.0	27.879	-0.432	-0.016	-0.333	0.530	-0.062	0.054
60.0	28.805	-1.807	-0.063	-0.489	0.661	-0.502	0.051
65.0	27.747	-2.249	-0.081	-0.528	0.651	-0.553	0.053
70.0	26.748	-2.026	-0.076	-0.620	0.459	-0.710	0.046
80.0	26.091	-0.634	-0.024	-0.766	0.138	0.006	0.035
90.0	25.256	-0.351	-0.014	-0.227	-0.781	0.030	0.012

RUNFILE> W0A201

AOA	Cn	Cy	Cy/Cn	Cax	Cpt	Crl	Cyw
0.0	-0.065	-0.044	0.686	-0.009	0.000	0.001	-0.003
0.0	-0.306	-0.545	1.784	0.255	-0.002	0.052	-0.010
10.0	2.458	-0.374	-0.152	0.216	-0.023	0.029	-0.018
20.0	8.685	-0.709	-0.082	0.213	-0.077	0.003	-0.029
30.0	16.323	-0.741	-0.045	0.095	0.046	-0.055	-0.041
35.0	20.455	-0.845	-0.041	-0.063	0.219	-0.010	-0.058
40.0	24.255	-1.379	-0.057	-0.157	0.394	0.007	-0.100
45.0	26.546	-0.255	-0.010	-0.146	0.503	0.040	-0.107
50.0	27.550	1.616	0.059	-0.181	0.527	0.093	-0.071
55.0	28.214	-1.099	-0.039	-0.341	0.544	0.058	-0.068
60.0	28.591	0.539	0.019	-0.419	0.638	0.655	-0.059
65.0	28.311	-1.821	-0.064	-0.561	0.666	0.093	-0.075
70.0	26.655	-1.068	-0.040	-0.617	0.436	-0.106	-0.061
80.0	26.367	-0.946	-0.036	-0.758	0.084	0.026	-0.088
90.0	25.102	-1.091	-0.043	-0.150	-0.885	0.064	-0.102

RUNFILE> W0A301

AOA	Cn	Cy	Cy/Cn	Cax	Cpt	Crl	Cyw
0.0	-0.043	-0.004	0.083	0.002	-0.001	0.000	0.000
0.0	-0.215	-0.501	2.332	0.270	-0.003	0.062	-0.010
10.0	2.601	-0.287	-0.110	0.242	-0.024	0.041	-0.005
20.0	8.595	-0.175	-0.020	0.246	-0.066	-0.010	0.001
30.0	16.874	-1.122	-0.067	0.125	0.106	0.012	0.132
35.0	21.081	-0.215	-0.010	0.015	0.262	-0.043	0.176
40.0	25.104	-2.107	-0.084	-0.149	0.485	0.013	0.225
45.0	27.283	-0.669	-0.025	-0.168	0.574	-0.010	0.178
50.0	28.326	-0.274	-0.010	-0.204	0.593	-0.014	0.191
55.0	29.232	-3.079	-0.105	-0.370	0.624	-0.016	0.201
60.0	29.462	-3.712	-0.126	-0.511	0.707	-0.084	0.182
65.0	28.826	-1.684	-0.058	-0.601	0.721	0.095	0.150
70.0	27.417	-4.210	-0.154	-0.655	0.493	-0.565	0.133
80.0	26.820	-1.355	-0.051	-0.786	0.180	0.016	0.093
90.0	25.566	-1.463	-0.057	-0.277	-0.730	0.097	0.059

RUNFILE> W0A401

AOA	Cn	Cy	Cy/Cn	Cax	Cpt	Crl	Cyw
0.0	-0.068	-0.024	0.353	-0.004	-0.002	0.001	-0.002
0.0	-0.230	-0.422	1.836	0.282	-0.002	0.058	0.059
10.0	3.010	-0.202	-0.067	0.277	-0.020	0.031	-0.038
20.0	8.969	-0.244	-0.027	0.282	-0.075	0.001	-0.105
30.0	17.113	-0.267	-0.016	0.162	0.060	-0.014	-0.110
35.0	21.443	-0.518	-0.024	-0.015	0.253	-0.059	-0.108
40.0	24.944	-2.098	-0.084	-0.093	0.414	0.126	-0.110
45.0	27.542	-3.180	-0.115	-0.125	0.497	0.037	-0.106
50.0	28.297	-3.771	-0.133	-0.162	0.497	-0.112	-0.136
55.0	29.916	-3.775	-0.126	-0.334	0.466	-0.472	-0.068
60.0	29.556	-3.198	-0.108	-0.467	0.675	-0.744	-0.078
65.0	28.311	-1.656	-0.059	-0.567	0.656	-0.368	-0.089
70.0	27.768	-2.530	-0.091	-0.634	0.451	-0.705	-0.090
80.0	26.989	-0.580	-0.021	-0.774	0.087	0.041	-0.099
90.0	25.423	-0.770	-0.030	-0.138	-0.933	0.094	-0.124

RUNFILE> W0A501

AOA	Cn	Cy	Cy/Cn	Cax	Cpt	Crl	Cyw
0.0	0.000	0.027	-96.508	0.002	-0.002	-0.002	0.002
0.0	-0.030	-0.222	7.336	0.300	-0.003	0.049	0.001
10.0	2.778	-0.138	-0.050	0.271	-0.027	0.037	-0.009
20.0	9.184	-0.235	-0.026	0.284	-0.102	0.012	-0.022
30.0	16.839	0.779	0.046	0.186	0.043	-0.048	-0.005
35.0	21.164	-0.141	-0.007	0.048	0.217	-0.099	-0.041
40.0	25.155	2.221	0.088	-0.073	0.400	-0.179	-0.091
45.0	27.802	1.814	0.065	-0.081	0.496	-0.065	-0.123
50.0	28.500	2.378	0.083	-0.171	0.507	0.117	-0.065
55.0	29.545	-1.806	-0.061	-0.340	0.586	-0.118	-0.063
60.0	29.907	0.590	0.020	-0.465	0.691	0.598	-0.040
65.0	29.149	1.626	0.056	-0.569	0.672	0.535	-0.039
70.0	27.817	1.542	0.055	-0.661	0.433	0.760	-0.099
80.0	27.235	-0.518	-0.019	-0.804	0.133	0.032	-0.090
90.0	25.562	-0.764	-0.030	-0.189	-0.848	0.070	-0.114

RUNFILE> W0A601

AOA	Cn	Cy	Cy/Cn	Cax	Cpt	Crl	Cyw
0.0	0.029	0.004	0.124	0.007	0.001	0.001	0.002
0.0	-0.081	-0.479	5.884	0.287	-0.007	0.054	-0.004
10.0	3.009	-0.225	-0.075	0.293	-0.021	0.026	0.006
20.0	8.930	-0.255	-0.029	0.319	-0.077	0.016	-0.001
30.0	16.993	0.406	0.024	0.177	0.062	-0.067	-0.031
35.0	21.059	-0.914	-0.043	0.006	0.239	-0.099	0.006
40.0	24.996	1.930	0.077	-0.070	0.376	-0.125	-0.039
45.0	26.694	4.708	0.176	-0.076	0.481	-0.130	-0.030
50.0	27.084	3.092	0.114	-0.165	0.457	0.211	0.029
55.0	28.965	1.533	0.053	-0.342	0.429	0.885	0.053
60.0	28.538	1.517	0.053	-0.419	0.678	0.805	0.055
65.0	27.466	0.793	0.029	-0.507	0.617	0.785	0.053
70.0	27.061	1.276	0.047	-0.628	0.482	0.824	0.036
80.0	26.666	-0.638	-0.024	-0.779	0.114	0.042	0.023
90.0	25.381	-0.832	-0.033	-0.194	-0.881	0.075	-0.006

RUNFILE> W0A701

AOA	Cn	Cy	Cy/Cn	Cax	Cpt	Crl	Cyw
0.0	-0.064	-0.002	0.031	-0.002	-0.002	0.001	0.001
0.0	0.063	-0.294	-4.671	0.281	-0.006	0.047	-0.004
10.0	3.082	-0.165	-0.053	0.272	-0.019	0.032	0.003
20.0	8.978	-0.295	-0.033	0.286	-0.066	-0.002	0.015
30.0	16.764	0.359	0.021	0.172	0.054	-0.046	0.038
35.0	20.937	0.199	0.009	-0.009	0.210	-0.043	0.012
40.0	24.792	1.287	0.052	-0.093	0.418	-0.141	0.068
45.0	26.860	-3.952	-0.147	-0.103	0.499	0.119	0.111
50.0	27.828	-3.431	-0.123	-0.147	0.502	-0.106	0.083
55.0	28.785	-1.112	-0.039	-0.325	0.528	-0.266	0.061
60.0	29.201	-2.495	-0.085	-0.451	0.658	-0.641	0.064
65.0	28.198	-2.276	-0.081	-0.535	0.662	-0.458	0.061
70.0	27.327	-2.445	-0.089	-0.612	0.451	-0.728	0.052
80.0	26.521	-0.468	-0.018	-0.755	0.114	0.018	0.045
90.0	25.352	-0.624	-0.025	-0.157	-0.874	0.051	0.022

RUNFILE> W0A801

AOA	Cn	Cy	Cy/Cn	Cax	Cpt	Crl	Cyw
0.0	-0.009	-0.005	0.592	0.002	-0.001	0.000	0.000
0.0	-0.073	-0.441	6.017	0.269	-0.010	0.049	-0.007
10.0	2.959	-0.365	-0.123	0.263	-0.015	0.033	-0.003
20.0	9.295	-0.595	-0.064	0.295	-0.074	0.027	0.037
30.0	17.193	-0.725	-0.042	0.173	0.051	-0.018	0.049
35.0	21.435	-1.701	-0.079	-0.003	0.260	0.047	0.069
40.0	25.132	-2.326	-0.093	-0.097	0.422	0.116	0.114
45.0	27.504	-4.127	-0.150	-0.083	0.511	0.125	0.086
50.0	28.173	-5.973	-0.212	-0.182	0.481	-0.127	0.108
55.0	29.492	-5.202	-0.176	-0.352	0.493	-0.761	0.084
60.0	29.473	-2.778	-0.094	-0.449	0.724	-0.838	0.098
65.0	27.741	-3.041	-0.110	-0.523	0.593	-0.768	0.081
70.0	27.842	-3.034	-0.109	-0.656	0.481	-0.790	0.090
80.0	26.911	-0.946	-0.035	-0.798	0.105	0.028	0.080
90.0	25.780	-0.775	-0.030	-0.163	-0.912	0.071	0.058

RUNFILE> W0A102

AOA	Cn	Cy	Cy/Cn	Cax	Cpt	Crl	Cyw
0.0	0.019	-0.011	-0.568	0.003	0.001	0.001	0.001
0.0	-0.118	-0.413	3.512	0.270	0.004	0.054	0.002
10.0	3.004	-0.092	-0.031	0.245	-0.028	0.022	-0.004
20.0	8.933	-0.711	-0.080	0.229	-0.057	0.006	-0.016
30.0	17.164	-0.699	-0.041	0.090	0.053	-0.072	-0.014
35.0	21.827	-0.784	-0.036	-0.019	0.222	-0.023	-0.013
40.0	25.762	-3.610	-0.140	-0.126	0.435	0.185	0.018
45.0	28.625	-4.455	-0.156	-0.092	0.511	0.031	0.022
50.0	30.416	-4.048	-0.133	-0.188	0.560	-0.147	-0.027
55.0	32.201	-2.693	-0.084	-0.380	0.572	-0.614	0.057
60.0	32.570	-2.894	-0.089	-0.509	0.724	-0.676	0.074
65.0	31.178	-2.576	-0.083	-0.553	0.659	-0.778	0.060
70.0	31.233	-2.337	-0.075	-0.674	0.483	-0.801	0.062
80.0	31.019	-0.583	-0.019	-0.808	0.065	-0.006	-0.047
90.0	29.868	-1.006	-0.034	-0.054	-1.114	0.064	-0.055
0.0	0.861	-0.844	-0.981	0.131	-0.009	0.043	0.001

RUNFILE> W0A202

AOA	Cn	Cy	Cy/Cn	Cax	Cpt	Crl	Cyw
0.0	-0.061	-0.252	4.145	0.273	-0.003	0.047	-0.003
10.0	2.879	-0.369	-0.128	0.253	-0.034	0.021	-0.009
20.0	8.783	-0.237	-0.027	0.256	-0.086	-0.006	0.009
30.0	17.026	-1.090	-0.064	0.130	0.035	-0.002	0.035
35.0	21.632	-0.548	-0.025	-0.013	0.198	-0.048	0.046
40.0	25.550	-0.402	-0.016	-0.106	0.402	-0.030	0.013
45.0	28.532	1.469	0.051	-0.125	0.518	-0.022	0.045
50.0	30.308	1.282	0.042	-0.237	0.545	0.110	0.066
55.0	31.328	0.011	0.000	-0.437	0.624	0.269	0.074
60.0	31.976	0.674	0.021	-0.572	0.737	0.498	0.080
65.0	32.018	-0.370	-0.012	-0.707	0.722	0.098	0.081
70.0	30.740	-3.143	-0.102	-0.762	0.482	-0.535	0.062
80.0	30.829	-1.011	-0.033	-0.882	0.039	0.007	0.057
90.0	28.845	-0.837	-0.029	-0.113	-1.120	0.074	0.026
0.0	0.333	-0.053	-0.158	0.032	-0.028	0.012	-0.005

RUNFILE> W0A302

AOA	Cn	Cy	Cy/Cn	Cax	Cpt	Crl	Cyw
0.0	0.030	0.017	0.562	0.010	0.002	0.000	-0.002
0.0	-0.018	-0.381	21.059	0.278	0.004	0.056	0.000
10.0	2.835	-0.396	-0.140	0.240	-0.036	0.023	0.004
20.0	8.893	-0.226	-0.025	0.257	-0.083	0.010	0.010
30.0	17.045	0.452	0.027	0.100	0.040	-0.114	0.026
35.0	21.627	0.510	0.024	-0.034	0.208	-0.091	0.042
40.0	25.781	-1.440	-0.056	-0.137	0.422	-0.024	0.061
45.0	28.590	0.878	0.031	-0.155	0.512	-0.063	0.053
50.0	29.771	2.273	0.076	-0.271	0.556	0.094	0.063
55.0	31.914	-1.837	-0.058	-0.475	0.627	-0.061	-0.031
60.0	32.395	0.449	0.014	-0.644	0.774	0.331	0.085
65.0	31.817	-0.809	-0.025	-0.742	0.718	0.066	0.085
70.0	30.741	-3.424	-0.111	-0.796	0.492	-0.273	0.076
80.0	30.122	-0.621	-0.021	-0.939	0.061	0.023	0.062
90.0	28.647	-0.878	-0.031	-0.169	-1.092	0.055	0.035
0.0	0.233	-0.877	-3.765	-0.014	-0.003	0.059	0.006

RUNFILE> W0A402

AOA	Cn	Cy	Cy/Cn	Cax	Cpt	Crl	Cyw
0.0	-0.012	0.004	-0.307	-0.003	0.000	0.001	0.001
0.0	-0.216	-0.331	1.531	0.228	-0.006	0.041	-0.006
10.0	2.666	-0.505	-0.190	0.219	-0.025	0.025	-0.008
20.0	8.329	-0.453	-0.054	0.198	-0.079	-0.017	-0.002
30.0	16.756	-0.653	-0.039	0.071	0.032	-0.079	0.029
35.0	21.215	-0.322	-0.015	-0.089	0.210	-0.012	0.002
40.0	26.011	-2.282	-0.088	-0.216	0.421	0.115	-0.011
45.0	28.622	-1.983	-0.069	-0.245	0.521	0.016	-0.007
50.0	29.554	-3.638	-0.123	-0.265	0.556	-0.133	-0.020
55.0	31.913	-2.071	-0.065	-0.554	0.523	-0.652	0.064
60.0	31.676	-2.313	-0.073	-0.690	0.744	-0.773	0.072
65.0	31.362	-3.265	-0.104	-0.811	0.702	-0.517	0.070
70.0	30.758	-1.723	-0.056	-0.894	0.484	-0.709	0.062
80.0	29.772	-1.142	-0.038	-1.037	0.049	-0.017	0.057
90.0	28.623	-0.892	-0.031	-0.252	-1.081	0.056	-0.054
0.0	-0.016	-0.988	60.145	-0.104	0.007	0.049	0.005

RUNFILE> W0A502

AOA	Cn	Cy	Cy/Cn	Cax	Cpt	Crl	Cyw
0.0	-0.077	-0.048	0.625	-0.009	0.001	-0.002	-0.001
0.0	-0.063	-0.352	5.622	0.251	0.009	0.052	0.006
10.0	2.839	-0.423	-0.149	0.213	-0.027	0.020	-0.006
20.0	8.690	-0.523	-0.060	0.214	-0.082	-0.002	-0.019
30.0	16.959	0.641	0.038	0.079	0.027	-0.111	-0.036
35.0	21.235	-0.390	-0.018	-0.132	0.238	-0.117	0.023
40.0	25.089	1.487	0.059	-0.269	0.405	-0.132	-0.024
45.0	28.142	3.148	0.112	-0.222	0.498	-0.097	0.016
50.0	29.573	2.443	0.083	-0.392	0.527	0.118	-0.040
55.0	30.916	-0.356	-0.012	-0.557	0.625	0.104	-0.026
60.0	31.881	3.536	0.111	-0.762	0.749	0.484	-0.024
65.0	31.249	2.376	0.076	-0.856	0.707	0.566	-0.021
70.0	30.491	1.249	0.041	-0.946	0.485	0.782	-0.020
80.0	29.884	-0.970	-0.032	-1.065	0.084	0.001	-0.038
90.0	28.417	-1.067	-0.038	-0.274	-1.093	0.050	-0.050
0.0	0.092	-0.845	-9.152	-0.140	0.012	0.013	0.006

RUNFILE> W0A602

AOA	Cn	Cy	Cy/Cn	Cax	Cpt	Crl	Cyw
0.0	0.052	0.005	0.093	-0.001	-0.002	0.000	0.002
0.0	-0.105	-0.344	3.280	0.249	0.007	0.052	0.004
10.0	2.953	-0.327	-0.111	0.234	-0.035	0.024	-0.001
20.0	8.965	-0.323	-0.036	0.215	-0.079	-0.023	-0.022
30.0	17.203	-0.820	-0.048	0.068	0.027	-0.018	0.013
35.0	21.505	0.154	0.007	-0.078	0.216	-0.114	-0.043
40.0	25.362	2.513	0.099	-0.200	0.427	-0.210	0.023
45.0	28.067	3.503	0.125	-0.192	0.462	-0.095	0.007
50.0	29.227	4.441	0.152	-0.359	0.490	0.252	-0.031
55.0	31.312	1.949	0.062	-0.537	0.490	1.006	0.001
60.0	31.776	1.238	0.039	-0.636	0.775	0.911	-0.003
65.0	30.524	1.946	0.064	-0.736	0.640	0.869	0.000
70.0	30.770	1.245	0.040	-0.898	0.532	0.857	-0.014
80.0	30.375	-0.853	-0.028	-1.017	0.063	0.049	-0.036
90.0	28.691	-0.915	-0.032	-0.269	-1.065	0.075	-0.051
0.0	0.335	-0.937	-2.793	-0.103	0.015	0.042	0.009

RUNFILE> W0A702

AOA	Cn	Cy	Cy/Cn	Cax	Cpt	Crl	Cyw
0.0	-0.020	0.009	-0.447	-0.002	0.002	-0.001	0.001
0.0	-0.056	-0.379	6.753	0.249	0.007	0.052	0.000
10.0	2.897	-0.384	-0.133	0.227	-0.031	0.017	-0.007
20.0	8.870	-0.290	-0.033	0.217	-0.088	0.005	-0.029
30.0	16.961	-0.037	-0.002	0.094	0.053	-0.058	-0.033
35.0	21.542	-0.499	-0.023	-0.094	0.251	-0.025	-0.013
40.0	25.526	-1.963	-0.077	-0.261	0.409	0.040	-0.013
45.0	28.431	-3.326	-0.117	-0.257	0.516	0.075	0.021
50.0	29.908	-3.194	-0.107	-0.331	0.564	-0.050	-0.011
55.0	31.696	0.845	0.027	-0.514	0.624	-0.108	-0.034
60.0	32.462	-1.204	-0.037	-0.697	0.762	0.010	-0.028
65.0	31.970	-1.763	-0.055	-0.789	0.738	-0.187	-0.036
70.0	30.668	-3.114	-0.102	-0.878	0.490	-0.771	-0.049
80.0	30.570	-0.787	-0.026	-0.996	0.078	0.002	-0.037
90.0	29.139	-0.612	-0.021	-0.225	-1.093	0.035	-0.046
0.0	0.099	-0.972	-9.769	-0.090	0.014	0.040	0.005

RUNFILE> W0A802

AOA	Cn	Cy	Cy/Cn	Cax	Cpt	Crl	Cyw
0.0	-0.026	-0.014	0.526	-0.007	-0.001	0.000	0.000
0.0	-0.186	-0.441	2.366	0.240	0.005	0.055	0.000
10.0	2.767	-0.461	-0.167	0.224	-0.033	0.023	-0.008
20.0	8.803	0.018	0.002	0.216	-0.092	-0.031	-0.025
30.0	17.013	0.474	0.028	0.091	0.022	-0.123	-0.041
35.0	21.567	-1.157	-0.054	-0.094	0.218	-0.030	-0.030
40.0	25.496	-2.157	-0.085	-0.195	0.413	0.076	0.051
45.0	28.330	-3.053	-0.108	-0.221	0.501	0.025	0.030
50.0	29.706	-5.590	-0.188	-0.315	0.511	-0.245	-0.019
55.0	31.620	-3.679	-0.116	-0.546	0.548	-0.764	-0.064
60.0	31.772	-3.244	-0.102	-0.632	0.771	-0.956	-0.069
65.0	30.272	-3.491	-0.115	-0.723	0.610	-0.841	-0.068
70.0	30.949	-2.403	-0.078	-0.888	0.514	-0.791	-0.058
80.0	30.145	-0.597	-0.020	-1.019	0.075	-0.009	-0.041
90.0	28.951	-0.788	-0.027	-0.221	-1.091	0.041	-0.055
0.0	0.106	-0.818	-7.683	-0.075	0.006	0.042	0.006

RUNFILE> E0A825

AOA	Cn	Cy	Cy/Cn	Cax	Cpt	Crl	Cyw
0.0	-0.036	0.017	-0.474	-0.007	0.000	0.003	-0.002
0.0	0.055	-0.096	-1.728	0.269	-0.002	0.010	0.000
25.0	11.701	0.170	0.015	0.241	-0.065	-0.045	-0.007
25.0	0.081	-0.014	-0.171	0.006	0.001	0.001	0.001
25.0	11.756	0.013	0.001	0.236	-0.048	-0.008	0.011
25.0	0.105	-0.030	-0.286	-0.005	0.002	0.002	-0.001
25.0	11.866	-0.352	-0.030	0.234	-0.052	0.003	-0.007
25.0	0.213	0.024	0.114	0.005	0.001	0.002	0.001
25.0	12.139	0.607	0.050	0.245	-0.059	-0.029	-0.014
0.0	0.227	-0.112	-0.491	0.263	-0.004	0.005	-0.003
0.0	0.233	0.001	-0.003	-0.012	-0.002	-0.004	-0.001

RUNFILE> E0A845

AOA	Cn	Cy	Cy/Cn	Cax	Cpt	Crl	Cyw
0.0	-0.070	-0.038	0.545	0.001	0.000	0.002	-0.002
0.0	-0.031	-0.064	2.039	0.289	-0.003	0.003	-0.005
45.0	23.703	-5.013	-0.212	0.062	0.417	0.055	0.031
45.0	0.010	-0.029	-3.049	0.074	-0.001	-0.006	0.008
45.0	23.787	-3.719	-0.156	0.096	0.399	-0.026	0.048
45.0	0.077	-0.020	-0.261	0.091	-0.005	-0.008	0.019
45.0	23.583	-3.904	-0.166	-0.068	0.365	0.001	0.055
45.0	0.074	-0.083	-1.113	0.091	-0.007	-0.011	0.016
45.0	23.971	-4.599	-0.192	-0.040	0.389	-0.019	0.060
0.0	0.179	-0.056	-0.314	0.355	-0.010	0.009	0.013
0.0	0.225	0.092	0.411	0.057	-0.011	-0.002	0.011

RUNFILE> E0A870

AOA	Cn	Cy	Cy/Cn	Cax	Cpt	Crl	Cyw
0.0	-0.017	-0.015	0.911	-0.009	-0.004	0.000	0.001
0.0	-0.068	-0.252	3.711	0.255	-0.002	0.014	-0.005
70.0	30.017	-2.283	-0.076	-0.760	0.522	-0.613	-0.060
70.0	0.179	0.001	0.008	0.029	0.012	0.004	-0.004
70.0	29.783	-1.754	-0.059	-0.772	0.485	-0.669	-0.060
70.0	0.314	0.010	0.031	0.034	0.013	0.004	-0.007
70.0	30.018	-0.497	-0.017	-0.749	0.491	-0.652	-0.064
70.0	0.271	-0.091	-0.335	0.024	0.012	0.000	-0.012
70.0	30.248	-2.926	-0.097	-0.742	0.493	-0.681	-0.062
0.0	0.414	-0.096	-0.232	0.259	0.001	0.012	-0.014
0.0	0.390	-0.085	-0.217	-0.014	0.004	0.003	-0.013

RUNFILE> E0A890

AOA	Cn	Cy	Cy/Cn	Cax	Cpt	Crl	Cyw
0.0	0.035	0.022	0.620	0.009	-0.003	0.001	0.000
0.0	0.062	-0.210	-3.373	0.280	-0.003	0.018	-0.002
90.0	27.764	-0.039	-0.001	-0.065	-1.066	0.000	-0.053
90.0	0.167	0.038	0.229	0.062	-0.001	0.003	-0.001
90.0	27.962	0.120	0.004	-0.069	-1.074	0.006	-0.051
90.0	0.222	0.055	0.246	0.065	0.000	0.003	-0.001
90.0	28.331	0.139	0.005	-0.028	-1.090	0.015	-0.054
90.0	0.351	0.051	0.145	0.083	-0.002	0.006	0.000
90.0	28.076	0.045	0.002	-0.011	-1.096	0.007	-0.055
0.0	0.378	-0.050	-0.132	0.326	-0.011	0.012	-0.011
0.0	0.369	0.053	0.144	0.049	-0.006	0.004	-0.011

RUNFILE> R0A801

AOA	Cn	Cy	Cy/Cn	Cax	Cpt	Crl	Cyw
0.0	-0.064	-0.023	0.356	0.001	-0.003	-0.002	-0.002
0.0	-0.120	-0.416	3.461	0.282	0.001	0.053	-0.004
2.0	0.291	-0.392	-1.347	0.265	-0.031	0.037	-0.006
4.0	0.896	-0.457	-0.509	0.253	-0.095	0.040	-0.011
6.0	1.437	-0.370	-0.257	0.249	-0.097	0.025	-0.006
8.0	2.320	-0.427	-0.184	0.249	-0.065	0.023	-0.008
10.0	3.079	-0.553	-0.180	0.244	-0.035	0.031	-0.008
12.0	3.795	-0.680	-0.179	0.266	-0.024	0.029	0.004
14.0	5.045	-0.438	-0.087	0.278	-0.031	0.021	0.005
16.0	6.344	-0.346	-0.055	0.285	-0.049	-0.002	-0.004
18.0	7.496	-0.685	-0.091	0.274	-0.065	0.019	0.006
20.0	8.940	-0.410	-0.046	0.285	-0.082	-0.017	-0.007
22.0	10.422	-0.187	-0.018	0.271	-0.083	-0.033	0.000
24.0	12.395	-0.060	-0.005	0.266	-0.070	-0.058	-0.003
26.0	14.135	0.208	0.015	0.255	-0.050	-0.060	0.014
28.0	16.001	-0.993	-0.062	0.250	-0.015	-0.023	0.016
30.0	17.592	-0.650	-0.037	0.211	0.028	-0.006	0.036
32.0	19.292	0.181	0.009	0.177	0.070	-0.083	0.029
34.0	21.276	0.610	0.029	0.150	0.137	-0.048	0.042
36.0	22.887	-0.802	-0.035	0.078	0.236	0.003	0.114
38.0	24.526	-2.999	-0.122	0.041	0.348	0.172	0.113
40.0	25.930	0.705	0.027	0.013	0.407	-0.092	0.109
42.0	27.592	-2.656	-0.096	-0.016	0.443	0.031	0.111
44.0	28.418	-4.224	-0.149	-0.017	0.479	0.085	0.099
46.0	28.970	-3.818	-0.132	0.004	0.494	-0.005	0.118
48.0	29.735	-5.535	-0.186	0.008	0.472	-0.144	0.094
50.0	30.397	-5.015	-0.165	-0.023	0.532	-0.155	0.079
52.0	30.836	-2.819	-0.091	-0.113	0.468	-0.365	0.052
54.0	32.030	-5.369	-0.168	-0.178	0.482	-0.772	0.056
56.0	32.881	-4.591	-0.140	-0.260	0.479	-0.983	0.047
58.0	32.777	-2.600	-0.079	-0.326	0.623	-0.618	0.053
60.0	32.912	-3.284	-0.100	-0.358	0.707	-0.650	0.064
62.0	32.638	-2.871	-0.088	-0.386	0.704	-0.465	0.064
64.0	31.877	-3.309	-0.104	-0.436	0.677	-0.668	0.052
66.0	30.859	-2.682	-0.087	-0.430	0.531	-0.768	0.045
68.0	30.990	-3.088	-0.100	-0.485	0.488	-0.797	0.055
70.0	31.488	-2.541	-0.081	-0.567	0.463	-0.784	0.056
72.0	31.719	-2.812	-0.089	-0.671	0.428	-0.279	0.053
74.0	31.655	0.115	0.004	-0.718	0.388	0.047	0.055
76.0	31.271	-0.867	-0.028	-0.705	0.272	0.090	0.049
78.0	30.886	-0.708	-0.023	-0.703	0.142	0.073	0.043
80.0	30.797	-0.491	-0.016	-0.720	0.019	0.030	0.037
82.0	30.446	-0.738	-0.024	-0.654	-0.134	0.067	0.041
84.0	30.348	-1.075	-0.035	-0.537	-0.347	0.064	0.029
86.0	29.445	-0.881	-0.030	-0.388	-0.590	0.062	0.020
88.0	29.355	-0.731	-0.025	-0.175	-0.873	0.074	0.017
90.0	29.943	-1.052	-0.035	0.082	-1.140	0.094	0.014
92.0	29.477	-0.911	-0.031	0.121	-1.315	0.126	0.010
0.0	0.745	-1.194	-1.603	0.205	-0.062	0.114	-0.014
0.0	0.464	-1.335	-2.879	0.192	-0.059	0.113	-0.019

RUNFILE> R0A802

AOA	Cn	Cy	Cy/Cn	Cax	Cpt	Crl	Cyw
-20.0	-0.023	-0.015	0.658	-0.003	-0.001	0.000	0.001
-10.0	-3.443	-0.325	0.095	0.250	0.016	0.056	0.015
-5.0	-1.407	-0.348	0.247	0.259	0.094	0.060	0.006
0.0	-0.009	-0.300	32.588	0.261	0.010	0.046	-0.003
5.0	1.447	-0.467	-0.323	0.247	-0.088	0.039	-0.003
10.0	3.138	-0.451	-0.144	0.254	-0.033	0.025	-0.005
15.0	5.670	-0.533	-0.094	0.280	-0.038	0.016	-0.014
20.0	9.078	-0.255	-0.028	0.263	-0.079	-0.024	-0.021
25.0	13.323	0.344	0.026	0.233	-0.053	-0.111	-0.021
30.0	17.532	-0.048	-0.003	0.193	0.044	-0.047	0.023
35.0	21.887	-1.171	-0.053	0.069	0.219	-0.020	0.004
40.0	25.980	-1.150	-0.044	-0.073	0.406	0.065	0.012
45.0	28.784	-5.338	-0.185	-0.078	0.524	0.159	0.000
50.0	29.935	-5.611	-0.187	-0.143	0.501	-0.183	-0.027
55.0	31.924	-3.513	-0.110	-0.345	0.471	-0.924	0.054
60.0	32.173	-1.427	-0.044	-0.444	0.735	-0.628	0.072
65.0	31.106	-3.418	-0.110	-0.496	0.629	-0.786	0.059
70.0	30.668	-2.322	-0.076	-0.660	0.489	-0.793	0.063
75.0	30.704	-0.486	-0.016	-0.764	0.354	0.065	0.062
80.0	30.356	-0.870	-0.029	-0.772	0.075	0.002	0.051
85.0	29.305	-0.422	-0.014	-0.440	-0.450	0.037	-0.049
90.0	29.176	-0.380	-0.013	0.023	-1.070	0.046	-0.058
95.0	28.651	-0.530	-0.018	0.066	-1.502	0.076	-0.063
100.0	28.078	-0.890	-0.032	0.041	-1.738	0.052	0.002
95.0	28.364	-0.832	-0.029	0.085	-1.486	0.075	0.010
90.0	28.786	-1.006	-0.035	0.000	-1.056	0.081	0.022
85.0	28.764	-1.188	-0.041	-0.407	-0.453	0.082	0.035
80.0	30.636	-0.378	-0.012	-0.709	0.052	0.018	0.053
75.0	30.922	0.129	0.004	-0.704	0.358	0.051	0.061
70.0	30.626	-2.698	-0.088	-0.547	0.452	-0.776	0.058
65.0	30.940	-3.064	-0.099	-0.401	0.597	-0.839	0.050
60.0	32.066	-2.236	-0.070	-0.324	0.687	-0.395	0.064
55.0	31.741	-3.690	-0.116	-0.206	0.486	-0.979	0.046
50.0	30.116	-4.016	-0.133	0.047	0.504	-0.129	-0.035
45.0	29.214	-4.914	-0.168	0.154	0.468	0.227	0.035
40.0	26.395	-2.329	-0.088	0.170	0.377	0.051	-0.026
35.0	22.024	-0.332	-0.015	0.252	0.190	-0.097	-0.023
30.0	18.084	-0.359	-0.020	0.377	0.000	-0.028	0.021
25.0	13.638	-0.002	0.000	0.472	-0.078	-0.004	0.014
20.0	9.379	-0.540	-0.058	0.508	-0.108	0.060	-0.016
15.0	6.343	-0.548	-0.086	0.529	-0.094	0.054	-0.010
10.0	3.683	-0.257	-0.070	0.499	-0.082	0.066	-0.021
5.0	2.147	-0.294	-0.137	0.503	-0.137	0.064	-0.020
0.0	0.741	-0.069	-0.093	0.517	-0.044	0.080	-0.025
-5.0	-0.641	-0.268	0.419	0.508	0.040	0.089	-0.018
-10.0	-2.223	-0.055	0.025	0.517	-0.029	0.106	-0.008
-20.0	0.838	0.261	0.311	0.240	-0.054	0.038	-0.022
0.0	1.226	0.460	0.375	0.261	-0.057	0.042	-0.011
0.0	1.214	0.506	0.416	0.258	-0.059	0.043	-0.012

RUNFILE> R0A803

AOA	Cn	Cy	Cy/Cn	Cax	Cpt	Crl	Cyw
-5.0	0.019	0.009	0.500	0.002	0.001	0.000	0.000
-5.0	-1.571	-0.022	0.014	0.262	0.074	0.005	-0.002
-4.0	-1.133	-0.010	0.008	0.297	0.083	0.016	0.002
-3.0	-0.883	-0.081	0.091	0.297	0.078	0.014	0.000
-2.0	-0.712	-0.156	0.219	0.289	0.052	0.012	-0.002
-1.0	-0.485	-0.137	0.282	0.289	0.007	0.013	-0.001
0.0	-0.097	-0.095	0.985	0.274	0.001	0.012	-0.002
1.0	0.062	-0.145	-2.344	0.260	-0.012	0.009	0.000
2.0	0.362	-0.176	-0.485	0.260	-0.034	0.013	0.001
3.0	0.685	-0.145	-0.212	0.256	-0.090	0.014	-0.002
4.0	1.050	-0.062	-0.059	0.250	-0.094	0.009	-0.002
5.0	1.391	-0.011	-0.008	0.253	-0.101	0.005	-0.005
6.0	1.734	-0.009	-0.005	0.258	-0.099	-0.005	0.001
7.0	2.168	0.097	0.045	0.252	-0.077	0.004	-0.004
8.0	2.318	-0.011	-0.005	0.242	-0.067	-0.006	-0.004
9.0	2.629	-0.103	-0.039	0.252	-0.057	0.007	-0.027
10.0	3.110	-0.143	-0.046	0.257	-0.048	0.007	-0.003
11.0	3.457	0.008	0.002	0.263	-0.040	-0.007	0.004
12.0	3.824	-0.232	-0.061	0.277	-0.037	0.002	-0.006
13.0	4.556	-0.174	-0.038	0.286	-0.035	0.003	0.008
14.0	5.034	-0.102	-0.020	0.290	-0.045	0.008	-0.081
15.0	5.781	0.026	0.005	0.309	-0.062	-0.011	0.012
16.0	6.377	0.017	0.003	0.309	-0.077	-0.004	0.013
17.0	6.965	-0.064	-0.009	0.373	-0.096	0.004	-0.009
18.0	7.645	0.000	0.000	0.362	-0.111	-0.001	0.010
19.0	8.399	0.249	0.030	0.332	-0.110	-0.005	0.002
20.0	9.357	-0.095	-0.010	0.344	-0.101	0.007	0.010
21.0	10.089	0.116	0.011	0.339	-0.103	0.014	0.017
22.0	10.830	-0.007	0.001	0.330	-0.096	-0.013	-0.016
23.0	11.729	0.233	0.020	0.327	-0.093	-0.017	-0.010
24.0	12.480	-0.421	-0.034	0.324	-0.087	-0.021	0.021
25.0	13.198	-0.562	-0.043	0.326	-0.079	0.000	0.019
26.0	13.879	0.111	0.008	0.331	-0.084	-0.020	0.019
27.0	14.984	0.690	0.046	0.310	-0.050	-0.031	0.020
28.0	15.652	0.171	0.011	0.305	-0.031	-0.048	0.031
29.0	16.661	0.540	0.032	0.269	-0.005	-0.011	0.020
30.0	17.315	0.623	0.036	0.268	-0.003	-0.010	0.016
31.0	18.474	0.428	0.023	0.249	0.046	-0.052	0.003
32.0	19.390	1.139	0.059	0.240	0.061	-0.153	0.042
33.0	20.121	-0.332	-0.016	0.203	0.124	-0.036	-0.022
34.0	20.609	-1.704	-0.083	0.163	0.133	0.076	0.003
35.0	21.787	-2.381	-0.109	0.155	0.211	0.142	0.020
36.0	22.638	-1.079	-0.048	0.130	0.264	0.055	0.021
37.0	23.468	-2.219	-0.095	0.163	0.299	0.117	0.026
38.0	24.326	-2.246	-0.092	0.130	0.317	0.162	0.021
39.0	24.990	-2.310	-0.092	0.136	0.351	0.112	0.003
40.0	25.772	-3.255	-0.126	0.101	0.378	0.099	0.039
41.0	26.707	-2.418	-0.091	0.131	0.405	0.099	0.073
42.0	26.933	-1.499	-0.056	0.066	0.413	0.109	0.030
43.0	27.541	-3.006	-0.109	0.111	0.446	0.065	0.034
44.0	27.894	-3.189	-0.114	0.087	0.466	0.103	0.026
45.0	28.377	-3.959	-0.140	0.114	0.519	0.045	0.033

46.0	28.521	-4.553	-0.160	0.059	0.495	-0.046	0.010
47.0	29.113	-4.111	-0.141	0.069	0.469	0.003	0.017
48.0	29.123	-4.188	-0.144	0.058	0.493	-0.137	-0.015
49.0	29.985	-2.544	-0.085	0.003	0.477	-0.171	-0.024
50.0	30.283	-5.268	-0.174	-0.044	0.464	-0.371	0.072
51.0	30.627	-2.343	-0.077	-0.064	0.446	-0.391	0.065
52.0	31.124	-2.938	-0.094	-0.123	0.442	-0.551	0.061
53.0	31.663	-2.681	-0.085	-0.233	0.385	-0.793	0.055
54.0	31.377	-3.442	-0.110	-0.253	0.492	-0.821	0.049
55.0	31.470	-4.262	-0.135	-0.322	0.528	-0.806	0.054
56.0	32.256	-3.603	-0.112	-0.331	0.574	-0.878	0.058
57.0	32.078	-2.561	-0.080	-0.367	0.622	-0.938	0.064
58.0	32.058	-2.845	-0.089	-0.382	0.689	-0.823	0.065
59.0	32.015	-2.225	-0.069	-0.392	0.694	-0.622	0.070
60.0	32.287	-1.550	-0.048	-0.398	0.735	-0.541	0.072
61.0	31.894	-4.297	-0.135	-0.434	0.735	-0.521	0.075
62.0	31.463	-1.218	-0.039	-0.455	0.725	-0.517	0.074
63.0	31.136	-2.010	-0.065	-0.466	0.730	-0.528	0.065
64.0	30.627	-3.069	-0.100	-0.492	0.660	-0.633	0.062
65.0	30.363	-3.339	-0.110	-0.496	0.602	-0.664	0.061
66.0	30.044	-3.228	-0.107	-0.506	0.509	-0.712	0.059
67.0	30.268	-2.573	-0.085	-0.534	0.495	-0.760	0.068
68.0	30.598	-2.744	-0.090	-0.576	0.496	-0.781	0.069
69.0	30.547	-1.068	-0.035	-0.618	0.463	-0.632	0.061
70.0	30.541	-2.605	-0.085	-0.648	0.463	-0.661	0.059
71.0	30.397	-3.285	-0.108	-0.667	0.447	-0.383	0.063
72.0	30.379	0.461	0.015	-0.690	0.441	-0.338	0.065
73.0	30.630	-0.315	-0.010	-0.712	0.403	-0.042	0.069
74.0	30.457	-0.535	-0.018	-0.728	0.353	-0.017	0.070
75.0	30.282	-0.428	-0.014	-0.734	0.272	0.035	0.065
76.0	29.911	-0.131	-0.004	-0.724	0.207	0.036	0.061
77.0	30.002	-0.158	-0.005	-0.720	0.161	0.037	0.058
78.0	30.006	-0.351	-0.012	-0.715	0.101	0.010	0.059
79.0	29.768	-0.567	-0.019	-0.710	0.029	-0.019	0.062
80.0	29.857	-0.391	-0.013	-0.654	-0.064	-0.003	0.058
81.0	29.374	-0.497	-0.017	-0.589	-0.156	0.005	0.051
82.0	29.039	-0.373	-0.013	-0.522	-0.269	0.010	0.053
83.0	28.863	-0.402	-0.014	-0.465	-0.399	0.017	0.046
84.0	29.605	0.044	0.001	-0.387	-0.493	0.049	0.047
85.0	29.750	0.159	0.005	-0.313	-0.584	0.047	0.044
86.0	29.706	0.146	0.005	-0.247	-0.729	0.068	0.042
87.0	29.875	0.100	0.003	-0.111	-0.906	0.060	0.039
88.0	29.888	0.302	0.010	-0.006	-0.984	0.045	0.035
89.0	30.192	-0.164	-0.005	-0.019	-1.063	0.083	0.038
90.0	29.905	0.246	0.008	0.036	-1.128	0.065	-0.046
91.0	30.360	0.496	0.016	0.048	-1.231	0.071	0.036
92.0	29.862	0.339	0.011	0.076	-1.317	0.063	-0.050
93.0	29.802	0.554	0.019	0.075	-1.427	0.052	-0.057
94.0	29.251	0.006	0.000	0.074	-1.488	0.048	-0.056
95.0	29.538	0.424	0.014	0.079	-1.564	0.045	-0.058
95.0	1.157	0.203	0.175	0.160	-0.044	0.058	0.001
-5.0	1.097	0.180	0.164	0.104	-0.045	0.057	0.002

RUNFILE> R1A801

AOA	Cn	Cy	Cy/Cn	Cax	Cpt	Crl	Cyw
0.0	-0.099	-0.020	0.204	-0.010	0.001	-0.002	0.001
0.0	0.025	-0.304	-12.152	0.277	0.005	0.040	0.001
2.0	0.151	-0.416	-2.756	0.222	-0.006	0.031	-0.001
4.0	0.642	-0.483	-0.753	0.164	-0.024	0.029	-0.002
6.0	1.394	-0.479	-0.343	0.141	-0.043	0.017	0.001
8.0	2.479	-0.480	-0.194	0.132	-0.046	0.017	0.009
10.0	3.122	-0.627	-0.201	0.105	-0.018	0.007	0.003
12.0	4.184	-0.580	-0.139	0.138	-0.009	0.015	0.013
14.0	5.067	-0.556	-0.110	0.149	-0.017	0.004	0.013
16.0	6.205	-0.601	-0.097	0.145	-0.041	-0.010	0.017
18.0	7.353	-0.591	-0.080	0.153	-0.061	-0.013	0.020
20.0	8.589	-0.494	-0.057	0.161	-0.084	-0.029	0.019
22.0	9.870	-0.674	-0.068	0.165	-0.102	-0.024	0.024
24.0	11.306	-0.757	-0.067	0.160	-0.102	-0.028	0.036
26.0	12.708	-0.631	-0.050	0.158	-0.091	-0.049	0.042
28.0	14.107	-0.621	-0.044	0.132	-0.064	-0.035	0.048
30.0	15.754	-1.345	-0.085	0.118	-0.018	0.000	0.046
32.0	17.491	-0.993	-0.057	0.118	0.011	-0.025	0.061
34.0	18.711	-1.934	-0.103	0.070	0.066	0.070	0.062
36.0	20.472	-2.566	-0.125	0.016	0.107	0.115	0.067
38.0	21.415	-2.933	-0.137	0.016	0.144	0.129	0.072
40.0	22.553	-2.338	-0.104	-0.007	0.199	0.031	0.073
42.0	23.790	-3.777	-0.159	-0.027	0.251	0.101	0.075
44.0	25.424	-3.324	-0.131	-0.020	0.322	0.017	0.076
46.0	25.717	-3.926	-0.153	-0.037	0.357	-0.034	0.067
48.0	26.750	-3.506	-0.131	-0.092	0.402	-0.144	0.055
50.0	27.270	-2.841	-0.104	-0.147	0.449	-0.223	0.053
52.0	28.041	-1.181	-0.042	-0.181	0.520	-0.316	0.054
54.0	28.333	-0.669	-0.024	-0.216	0.533	-0.309	0.055
56.0	28.803	-0.614	-0.021	-0.234	0.567	-0.315	0.063
58.0	28.459	-0.814	-0.029	-0.277	0.547	-0.276	0.066
60.0	28.534	-0.931	-0.033	-0.335	0.554	-0.246	0.074
62.0	28.866	-0.687	-0.024	-0.377	0.506	-0.251	0.077
64.0	29.088	-1.188	-0.041	-0.419	0.489	-0.227	0.075
66.0	29.188	-2.143	-0.073	-0.478	0.433	-0.234	0.077
68.0	29.047	-1.628	-0.056	-0.525	0.376	-0.223	0.073
70.0	28.789	-1.686	-0.059	-0.545	0.315	-0.245	0.071
72.0	28.383	-1.507	-0.053	-0.587	0.236	-0.268	0.067
74.0	28.684	-1.731	-0.060	-0.575	0.150	-0.369	0.071
76.0	28.536	-0.637	-0.022	-0.605	0.055	-0.184	0.067
78.0	28.470	-1.349	-0.047	-0.615	-0.040	0.027	0.063
80.0	28.251	-1.528	-0.054	-0.588	-0.158	0.022	0.060
82.0	28.126	-1.338	-0.048	-0.560	-0.276	0.038	0.061
84.0	28.272	-1.284	-0.045	-0.514	-0.466	0.030	0.054
86.0	28.246	-1.651	-0.058	-0.385	-0.658	0.044	0.056
88.0	28.350	-1.610	-0.057	-0.223	-0.900	0.064	0.053
90.0	28.017	-1.399	-0.050	-0.121	-1.074	0.057	0.044
92.0	27.966	-1.387	-0.050	-0.098	-1.228	0.052	0.043
0.0	3.141	-1.702	-0.542	0.094	0.001	0.090	0.029
0.0	3.231	-1.644	-0.509	0.110	-0.002	0.092	0.032

RUNFILE> R1A802

AOA	Cn	Cy	Cy/Cn	Cax	Cpt	Crl	Cyw
0.0	-0.009	-0.032	3.600	-0.007	0.002	0.000	0.001
92.0	24.479	0.474	0.019	-0.255	-1.192	-0.039	0.015
90.0	24.751	0.447	0.018	-0.308	-1.018	-0.044	0.018
88.0	25.076	0.010	0.000	-0.397	-0.870	-0.033	0.019
86.0	24.939	0.208	0.008	-0.527	-0.694	-0.040	0.024
84.0	25.341	0.147	0.006	-0.643	-0.480	-0.036	0.027
82.0	25.655	0.263	0.010	-0.690	-0.340	-0.033	0.032
80.0	25.881	0.357	0.014	-0.701	-0.169	-0.051	0.034
78.0	26.141	-0.463	-0.018	-0.716	-0.075	-0.081	0.033
76.0	26.585	0.322	0.012	-0.719	0.028	-0.213	0.037
74.0	26.817	-0.783	-0.029	-0.643	0.103	-0.439	0.037
72.0	27.076	-0.386	-0.014	-0.606	0.195	-0.382	0.039
70.0	27.283	-0.612	-0.022	-0.554	0.281	-0.261	0.043
68.0	27.807	0.246	0.009	-0.507	0.342	-0.301	0.046
66.0	27.989	0.458	0.016	-0.456	0.413	-0.294	0.046
64.0	28.288	0.222	0.008	-0.383	0.471	-0.339	0.048
62.0	28.203	0.922	0.033	-0.306	0.484	-0.344	0.046
60.0	28.297	0.549	0.019	-0.260	0.478	-0.326	0.039
58.0	28.242	1.463	0.052	-0.196	0.489	-0.364	0.036
56.0	28.272	1.441	0.051	-0.155	0.484	-0.347	0.025
54.0	28.068	1.043	0.037	-0.111	0.487	-0.376	0.023
52.0	27.543	0.119	0.004	-0.066	0.423	-0.408	0.022
50.0	26.502	-0.340	-0.013	-0.052	0.399	-0.327	0.016
48.0	26.319	-1.843	-0.070	0.040	0.325	-0.205	0.015
46.0	25.950	-3.024	-0.117	0.093	0.286	-0.120	0.025
44.0	25.099	-1.959	-0.078	0.140	0.228	-0.030	0.019
42.0	23.911	-1.104	-0.046	0.218	0.155	-0.018	0.022
40.0	23.454	-1.328	-0.057	0.214	0.137	0.010	0.027
38.0	22.158	-1.139	-0.051	0.242	0.076	0.064	0.026
36.0	20.630	-0.499	-0.024	0.258	0.016	0.007	0.012
34.0	19.352	-0.339	-0.018	0.311	-0.009	0.029	0.030
32.0	17.870	0.366	0.020	0.341	-0.073	-0.022	0.020
30.0	16.441	0.710	0.043	0.387	-0.102	-0.041	0.010
28.0	14.870	0.423	0.028	0.411	-0.149	-0.038	0.000
26.0	13.694	0.830	0.061	0.452	-0.180	-0.039	-0.024
24.0	12.172	0.949	0.078	0.468	-0.200	-0.055	-0.021
22.0	10.786	0.593	0.055	0.476	-0.201	-0.027	-0.027
20.0	9.644	0.950	0.099	0.495	-0.197	-0.043	-0.034
18.0	8.450	0.862	0.102	0.501	-0.182	-0.035	-0.037
16.0	7.118	0.762	0.107	0.475	-0.166	-0.027	-0.045
14.0	6.117	0.756	0.124	0.478	-0.148	-0.019	-0.045
12.0	5.319	0.699	0.131	0.481	-0.136	-0.006	-0.048
10.0	4.474	0.665	0.149	0.481	-0.155	-0.003	-0.052
8.0	3.909	0.790	0.202	0.484	-0.170	0.014	-0.051
6.0	3.392	0.796	0.235	0.503	-0.175	0.022	-0.054
4.0	2.780	0.799	0.288	0.506	-0.158	0.029	-0.055
2.0	2.259	0.741	0.328	0.507	-0.131	0.027	-0.056
0.0	2.073	0.780	0.376	0.516	-0.115	0.044	-0.052
-2.0	1.658	0.738	0.445	0.520	-0.094	0.049	-0.050
-4.0	1.322	0.815	0.616	0.518	-0.075	0.051	-0.049
0.0	2.288	1.100	0.481	0.246	-0.120	0.009	-0.046
0.0	1.626	1.169	0.719	0.501	-0.173	0.012	-0.049

RUNFILE> R1A803

AOA	Cn	Cy	Cy/Cn	Cax	Cpt	Crl	Cyw
-5.0	0.063	0.015	0.237	0.012	0.001	0.000	0.003
-5.0	-1.246	-0.122	0.098	0.284	0.048	0.003	0.001
-4.0	-1.031	-0.196	0.191	0.283	0.042	0.008	0.000
-3.0	-0.666	-0.229	0.344	0.275	0.032	0.006	0.001
-2.0	-0.285	-0.256	0.895	0.273	0.024	0.003	0.003
-1.0	-0.021	-0.322	15.269	0.251	0.014	0.004	0.002
0.0	0.345	-0.317	-0.917	0.247	0.002	0.002	0.002
1.0	0.671	-0.257	-0.383	0.261	-0.008	-0.002	0.007
2.0	0.889	-0.331	-0.373	0.255	-0.020	-0.004	0.004
3.0	1.221	-0.302	-0.247	0.263	-0.031	-0.009	0.004
4.0	1.520	-0.372	-0.245	0.263	-0.045	-0.007	0.005
5.0	1.822	-0.364	-0.200	0.268	-0.059	-0.006	0.005
6.0	2.179	-0.361	-0.166	0.260	-0.065	-0.005	0.005
7.0	2.583	-0.315	-0.122	0.277	-0.067	-0.009	0.007
8.0	2.931	-0.335	-0.114	0.283	-0.060	-0.007	0.010
9.0	3.209	-0.327	-0.102	0.274	-0.057	-0.014	0.009
10.0	3.659	-0.498	-0.136	0.283	-0.046	-0.012	0.009
11.0	4.054	-0.392	-0.097	0.296	-0.042	-0.009	0.011
12.0	4.452	-0.408	-0.092	0.296	-0.047	-0.020	0.010
13.0	4.992	-0.388	-0.078	0.312	-0.059	-0.017	0.012
14.0	5.534	-0.373	-0.067	0.314	-0.067	-0.019	0.014
15.0	6.122	-0.338	-0.055	0.322	-0.081	-0.017	0.013
16.0	6.617	-0.372	-0.056	0.332	-0.099	-0.019	0.015
17.0	7.236	-0.416	-0.057	0.331	-0.102	-0.020	0.013
18.0	7.908	-0.394	-0.050	0.338	-0.113	-0.012	0.014
19.0	8.472	-0.428	-0.051	0.347	-0.127	-0.010	0.016
18.0	8.060	-0.440	-0.055	0.358	-0.119	-0.006	0.013
19.0	8.563	-0.365	-0.043	0.364	-0.130	-0.017	0.014
20.0	9.114	-0.232	-0.026	0.367	-0.135	-0.016	0.014
21.0	9.959	-0.295	-0.030	0.358	-0.148	-0.008	0.017
22.0	10.668	-0.241	-0.023	0.358	-0.157	-0.022	0.020
23.0	11.391	-0.520	-0.046	0.353	-0.157	-0.017	0.027
24.0	12.265	-0.269	-0.022	0.354	-0.154	-0.006	0.023
25.0	12.772	-0.183	-0.014	0.349	-0.147	-0.015	0.032
26.0	13.539	-0.572	-0.042	0.334	-0.136	0.001	0.026
27.0	14.176	-0.448	-0.032	0.312	-0.118	-0.019	0.030
28.0	14.990	-0.825	-0.055	0.296	-0.115	0.014	0.036
29.0	15.841	-0.521	-0.033	0.291	-0.086	-0.007	-0.010
30.0	16.696	-0.671	-0.040	0.284	-0.076	-0.011	-0.010
31.0	17.594	-1.137	-0.065	0.267	-0.054	0.041	0.047
32.0	18.600	-0.818	-0.044	0.249	-0.033	0.056	-0.001
33.0	19.250	-1.387	-0.072	0.246	-0.013	0.049	0.051
34.0	19.927	-1.668	-0.084	0.233	0.005	0.113	-0.001
35.0	20.635	-1.925	-0.093	0.205	0.029	0.141	0.000
36.0	21.418	-2.365	-0.110	0.210	0.058	0.128	-0.008
37.0	22.115	-1.494	-0.068	0.205	0.080	0.073	-0.013
38.0	22.691	-2.452	-0.108	0.183	0.127	0.092	0.063
39.0	23.398	-2.438	-0.104	0.204	0.134	0.129	-0.007
40.0	24.078	-3.199	-0.133	0.183	0.168	0.122	-0.011
41.0	24.674	-4.009	-0.162	0.182	0.190	0.138	-0.009
42.0	24.558	-3.221	-0.131	0.224	0.186	0.087	-0.006
43.0	25.459	-3.339	-0.131	0.176	0.227	0.049	-0.013

44.0	25.792	-3.378	-0.131	0.178	0.277	0.044	0.069
45.0	26.064	-3.347	-0.128	0.118	0.307	-0.047	0.066
46.0	26.713	-2.933	-0.110	0.111	0.327	-0.050	0.061
47.0	26.902	-2.644	-0.098	0.072	0.361	-0.142	0.058
48.0	27.339	-2.547	-0.093	0.059	0.398	-0.181	0.062
49.0	27.813	-1.883	-0.068	0.010	0.399	-0.150	0.057
50.0	28.135	-1.797	-0.064	-0.010	0.437	-0.243	0.056
51.0	28.410	-1.360	-0.048	-0.031	0.473	-0.298	0.085
52.0	28.616	-0.998	-0.035	-0.032	0.477	-0.261	0.075
53.0	28.837	-1.203	-0.042	-0.068	0.493	-0.287	0.079
54.0	28.867	-0.490	-0.017	-0.074	0.538	-0.281	-0.022
55.0	29.134	-0.669	-0.023	-0.093	0.534	-0.286	-0.025
56.0	29.184	-0.620	-0.021	-0.104	0.535	-0.282	-0.019
57.0	29.337	-0.131	-0.004	-0.098	0.525	-0.259	-0.015
58.0	29.336	-0.868	-0.030	-0.225	0.489	-0.228	3.217
59.0	29.216	-0.918	-0.031	-0.238	0.524	-0.237	1.232
60.0	29.500	-1.008	-0.034	-0.245	0.520	-0.243	1.163
58.0	28.560	-0.503	-0.018	0.123	0.487	-0.223	2.854
59.0	28.468	-0.791	-0.028	0.032	0.507	-0.227	2.209
60.0	28.232	-0.723	-0.026	-0.097	0.496	-0.259	1.966
61.0	28.613	-0.980	-0.034	-0.233	0.484	-0.212	1.892
62.0	28.694	-1.215	-0.042	-0.313	0.486	-0.228	1.844
63.0	29.068	-1.232	-0.042	-0.374	0.492	-0.228	3.775
64.0	29.182	-1.991	-0.068	-0.438	0.437	-0.219	4.976
65.0	29.186	-1.297	-0.044	-0.518	0.425	-0.216	10.150
66.0	28.885	-1.633	-0.057	-0.470	0.389	-0.215	0.062
67.0	28.964	-1.497	-0.052	-0.492	0.367	-0.215	0.265
68.0	28.802	-1.110	-0.039	-0.513	0.329	-0.206	0.213
69.0	28.852	-1.848	-0.064	-0.521	0.285	-0.225	0.172
70.0	28.925	-1.960	-0.068	-0.515	0.245	-0.267	0.059
71.0	28.921	-1.564	-0.054	-0.524	0.200	-0.301	0.037
72.0	29.082	-1.709	-0.059	-0.526	0.173	-0.347	0.006
73.0	29.053	-1.572	-0.054	-0.527	0.122	-0.373	-0.004
74.0	29.106	-1.596	-0.055	-0.535	0.073	-0.412	0.116
75.0	28.923	-1.532	-0.053	-0.559	0.016	-0.278	0.144
76.0	28.812	-0.821	-0.028	-0.561	-0.019	-0.155	2.054
77.0	29.052	-1.401	-0.048	-0.558	-0.073	-0.062	1.771
78.0	28.788	-0.333	-0.012	-0.562	-0.150	-0.003	1.696
79.0	28.335	-0.702	-0.025	-0.538	-0.205	-0.021	1.668
80.0	29.014	-0.874	-0.030	-0.527	-0.287	-0.009	1.532
81.0	28.787	-1.114	-0.039	-0.512	-0.365	-0.011	1.514
82.0	28.814	-1.106	-0.038	-0.485	-0.416	-0.002	1.510
83.0	28.609	-0.754	-0.026	-0.444	-0.504	-0.003	1.489
84.0	28.966	-0.854	-0.029	-0.397	-0.596	-0.008	1.327
85.0	28.781	-0.977	-0.034	-0.326	-0.718	0.001	1.300
86.0	28.255	-0.785	-0.028	-0.232	-0.853	-0.005	1.282
87.0	28.696	-1.174	-0.041	-0.160	-0.942	0.005	1.142
88.0	28.234	-1.185	-0.042	-0.093	-1.054	0.019	1.145
89.0	28.372	-1.090	-0.038	-0.062	-1.078	0.006	1.130
90.0	28.683	-0.943	-0.033	-0.053	-1.160	0.014	1.133
91.0	28.312	-1.232	-0.044	-0.041	-1.232	0.004	1.130
92.0	28.327	-1.233	-0.044	-0.047	-1.347	0.003	1.121
93.0	28.358	-1.041	-0.037	-0.020	-1.377	0.011	1.327
94.0	28.435	-1.111	-0.039	-0.008	-1.492	-0.003	1.294
95.0	28.265	-1.134	-0.040	0.002	-1.574	0.007	1.266
95.0	2.918	-1.229	-0.421	0.176	-0.058	0.018	1.307

-5.0	2.928	-1.165	-0.398	0.136	-0.061	0.020	0.677
0.0	2.984	-1.108	-0.371	0.155	-0.063	0.019	0.119

RUNFILE> R1A804

AOA	Cn	Cy	Cy/Cn	Cax	Cpt	Crl	Cyw
-5.0	0.107	0.052	0.485	0.018	0.000	0.000	0.003
-5.0	-1.227	-0.086	0.070	0.309	0.045	0.012	0.003
-4.0	-0.856	-0.122	0.143	0.310	0.036	0.010	0.001
-3.0	-0.683	-0.275	0.403	0.296	0.030	0.008	-0.002
-2.0	-0.106	-0.101	0.957	0.314	0.017	0.006	0.000
-1.0	0.130	-0.210	-1.619	0.304	0.004	0.000	-0.003
0.0	0.347	-0.249	-0.718	0.080	-0.007	-0.002	-0.006
1.0	0.805	-0.040	-0.050	0.313	-0.017	-0.010	-0.005
2.0	1.103	-0.112	-0.102	0.314	-0.027	-0.011	-0.005
3.0	1.331	-0.192	-0.144	0.312	-0.044	-0.014	-0.007
4.0	1.653	-0.113	-0.068	0.326	-0.059	-0.021	-0.009
5.0	1.889	-0.337	-0.178	0.316	-0.076	-0.015	-0.011
6.0	2.220	-0.259	-0.117	0.319	-0.085	-0.017	-0.013
7.0	2.568	-0.277	-0.108	0.321	-0.091	-0.014	-0.012
8.0	2.891	-0.163	-0.056	0.334	-0.086	-0.016	-0.013
9.0	3.272	-0.208	-0.064	0.326	-0.084	-0.023	-0.014
10.0	3.570	-0.284	-0.080	0.330	-0.076	-0.022	-0.016
11.0	3.957	-0.276	-0.070	0.330	-0.070	-0.024	-0.008
12.0	4.464	-0.200	-0.045	0.339	-0.075	-0.024	-0.002
13.0	4.951	-0.161	-0.032	0.331	-0.083	-0.029	0.006
14.0	5.421	-0.147	-0.027	0.347	-0.093	-0.029	0.012
15.0	5.611	-0.220	-0.039	0.325	-0.103	-0.033	-0.010
16.0	6.278	-0.217	-0.035	0.336	-0.122	-0.030	-0.025
17.0	6.887	-0.168	-0.024	0.341	-0.133	-0.036	0.000
18.0	7.630	-0.186	-0.024	0.355	-0.148	-0.014	-0.005
19.0	8.101	-0.083	-0.010	0.360	-0.164	-0.025	-0.005
20.0	8.595	-0.220	-0.026	0.345	-0.168	-0.015	-0.009
21.0	9.465	-0.182	-0.019	0.344	-0.181	-0.016	-0.010
22.0	10.052	-0.131	-0.013	0.341	-0.182	-0.014	-0.027
23.0	11.114	0.191	0.017	0.359	-0.182	-0.022	-0.024
24.0	11.605	0.020	0.002	0.337	-0.173	-0.018	-0.020
25.0	12.429	-0.287	-0.023	0.323	-0.172	-0.012	-0.018
26.0	13.132	-0.009	0.001	0.316	-0.164	-0.007	-0.027
27.0	13.968	-0.201	-0.014	0.327	-0.151	0.020	-0.020
28.0	14.718	-0.061	-0.004	0.323	-0.138	0.004	-0.015
29.0	15.593	-0.040	-0.003	0.306	-0.127	0.010	-0.013
30.0	16.628	-0.077	-0.005	0.327	-0.106	0.039	-0.013
31.0	16.952	-0.089	-0.005	0.257	-0.093	0.034	-0.024
32.0	17.609	-0.193	-0.011	0.254	-0.068	0.024	-0.031
33.0	18.776	-0.633	-0.034	0.273	-0.053	0.097	-0.021
34.0	19.793	-0.625	-0.032	0.261	-0.052	0.080	-0.020
35.0	20.484	-1.045	-0.051	0.244	-0.022	0.154	-0.017
36.0	21.189	-0.692	-0.033	0.246	0.014	0.134	-0.013
37.0	21.162	-1.732	-0.082	0.239	-0.021	0.182	-0.027
38.0	22.587	-1.824	-0.081	0.227	0.060	0.180	-0.031
39.0	23.335	-2.510	-0.108	0.198	0.066	0.188	-0.029
40.0	23.635	-2.630	-0.111	0.198	0.103	0.182	-0.030
41.0	24.467	-2.416	-0.099	0.221	0.122	0.164	-0.030
42.0	24.796	-1.967	-0.079	0.175	0.167	0.089	0.049
43.0	25.266	-2.054	-0.081	0.202	0.207	0.051	-0.036
44.0	25.721	-2.185	-0.085	0.196	0.235	0.062	-0.031
45.0	26.252	-2.216	-0.084	0.215	0.242	0.037	0.052

46.0	26.547	-2.238	-0.084	0.162	0.271	-0.030	0.043
47.0	27.016	-2.208	-0.082	0.156	0.305	-0.057	0.036
48.0	27.330	-2.307	-0.084	0.132	0.329	-0.146	0.037
49.0	27.512	-2.261	-0.082	0.092	0.342	-0.192	0.035
50.0	27.980	-1.183	-0.042	0.087	0.389	-0.205	0.041
51.0	28.184	-0.921	-0.033	0.047	0.420	-0.185	0.038
52.0	28.580	-0.812	-0.028	0.026	0.431	-0.231	0.044
53.0	29.002	-0.267	-0.009	0.004	0.471	-0.262	0.047
54.0	29.239	0.042	0.001	0.012	0.492	-0.250	0.050
55.0	29.145	0.524	0.018	0.008	0.493	-0.233	0.056
56.0	29.295	0.777	0.027	-0.009	0.489	-0.230	0.060
57.0	29.395	0.134	0.005	-0.026	0.501	-0.261	0.064
58.0	29.656	0.301	0.010	-0.019	0.476	-0.268	-0.046
59.0	29.556	0.754	0.026	-0.038	0.462	-0.250	-0.046
59.0	28.123	1.279	0.045	0.214	0.423	-0.228	-0.028
60.0	28.163	0.879	0.031	0.131	0.426	-0.213	-0.025
61.0	28.552	1.019	0.036	0.029	0.441	-0.240	-0.025
62.0	28.487	0.181	0.006	-0.074	0.423	-0.234	-0.022
63.0	29.067	0.466	0.016	-0.185	0.426	-0.230	-0.018
64.0	29.134	0.256	0.009	-0.275	0.405	-0.238	-0.021
65.0	29.213	-0.022	0.001	-0.297	0.368	-0.208	-0.014
66.0	29.227	0.040	0.001	-0.337	0.346	-0.229	-0.016
67.0	29.374	0.443	0.015	-0.366	0.342	-0.226	-0.016
68.0	29.509	-0.042	-0.001	-0.399	0.295	-0.232	-0.018
69.0	29.404	-0.231	-0.008	-0.388	0.261	-0.191	-0.012
70.0	29.263	-0.348	-0.012	-0.396	0.234	-0.261	-0.013
71.0	29.354	-0.797	-0.027	-0.420	0.183	-0.305	-0.016
72.0	29.447	-0.252	-0.009	-0.423	0.144	-0.321	-0.016
73.0	29.226	-0.546	-0.019	-0.439	0.098	-0.381	-0.019
74.0	29.427	-0.797	-0.027	-0.425	0.046	-0.390	-0.016
75.0	29.514	0.353	0.012	-0.423	-0.001	-0.243	-0.009
76.0	29.436	1.162	0.039	-0.449	-0.030	-0.086	-0.011
77.0	29.251	-0.024	0.001	-0.443	-0.090	-0.097	-0.006
78.0	29.078	0.303	0.010	-0.437	-0.160	-0.027	-0.005
79.0	29.362	0.443	0.015	-0.446	-0.211	-0.023	-0.006
80.0	29.237	0.106	0.004	-0.425	-0.292	-0.007	-0.005
81.0	29.393	0.083	0.003	-0.407	-0.351	0.003	-0.004
82.0	29.069	0.390	0.013	-0.401	-0.412	0.002	-0.006
83.0	29.231	0.401	0.014	-0.336	-0.504	-0.020	-0.001
84.0	29.338	0.177	0.006	-0.277	-0.617	0.003	-0.002
85.0	28.961	0.081	0.003	-0.201	-0.758	-0.014	-0.003
86.0	29.029	0.247	0.009	-0.125	-0.836	-0.004	-0.009
87.0	29.105	-0.019	0.001	-0.058	-0.929	-0.006	-0.007
88.0	29.606	0.045	0.002	0.007	-0.996	-0.013	-0.006
89.0	29.045	0.010	0.000	0.052	-1.086	-0.026	-0.004
90.0	28.969	-0.131	-0.005	0.015	-1.143	-0.006	-0.010
91.0	29.211	0.214	0.007	0.073	-1.238	-0.006	-0.010
92.0	29.344	0.220	0.007	0.052	-1.318	-0.027	-0.024
93.0	29.544	-0.157	-0.005	0.086	-1.424	-0.018	-0.025
94.0	28.959	-0.018	0.001	0.067	-1.482	-0.034	-0.036
95.0	28.692	-0.150	-0.005	0.079	-1.519	-0.028	-0.038
95.0	4.321	-0.376	-0.087	0.276	-0.084	0.016	0.029
-5.0	4.331	-0.297	-0.069	0.230	-0.086	0.019	0.031
0.0	4.332	-0.297	-0.069	0.271	-0.089	0.021	0.034
0.0	4.052	-0.177	-0.044	0.321	-0.100	0.024	0.029

RUNFILE> R2A801

AOA	Cn	Cy	Cy/Cn	Cax	Cpt	Crl	Cyw
-5.0	-0.003	0.012	-4.140	0.014	-0.002	0.001	0.000
-5.0	-1.389	-0.130	0.094	0.312	0.051	0.009	1.083
-4.0	-1.002	-0.115	0.115	0.345	0.049	0.009	0.033
-3.0	-0.702	-0.191	0.271	0.343	0.038	0.007	-0.030
-2.0	-0.304	-0.156	0.515	0.370	0.018	0.012	-0.028
-1.0	0.013	-0.178	-14.021	0.376	0.004	0.011	-0.074
0.0	0.394	-0.111	-0.283	0.399	-0.011	0.011	-0.100
1.0	0.545	-0.119	-0.219	0.397	-0.024	0.010	-0.117
2.0	0.823	-0.105	-0.127	0.418	-0.038	0.013	-0.119
3.0	1.097	-0.102	-0.093	0.423	-0.057	0.014	-0.127
4.0	1.482	-0.110	-0.074	0.438	-0.079	0.016	-0.126
5.0	1.797	-0.162	-0.090	0.440	-0.093	0.017	0.276
6.0	2.039	-0.179	-0.088	0.435	-0.100	0.021	0.163
7.0	2.358	-0.145	-0.061	0.435	-0.102	0.019	0.091
8.0	2.699	-0.164	-0.061	0.439	-0.095	0.022	0.073
9.0	3.130	-0.128	-0.041	0.449	-0.089	0.017	0.061
10.0	3.536	-0.110	-0.031	0.462	-0.083	0.020	0.052
11.0	3.870	-0.121	-0.031	0.465	-0.082	0.019	0.064
12.0	4.361	-0.046	-0.011	0.484	-0.086	0.029	0.011
13.0	4.855	-0.055	-0.011	0.498	-0.094	0.027	0.001
14.0	5.421	-0.082	-0.015	0.504	-0.111	0.023	-0.017
15.0	5.982	-0.001	0.000	0.519	-0.119	0.025	-0.019
16.0	6.567	-0.011	-0.002	0.528	-0.141	0.024	-0.025
17.0	7.201	0.070	0.010	0.530	-0.152	0.017	-0.032
18.0	7.775	0.136	0.017	0.528	-0.167	0.018	-0.037
19.0	8.392	0.135	0.016	0.531	-0.176	0.017	-0.042
20.0	9.065	0.172	0.019	0.531	-0.181	0.022	-0.046
21.0	9.785	0.169	0.017	0.529	-0.187	0.012	-0.067
22.0	10.484	0.082	0.008	0.521	-0.187	0.015	-0.085
23.0	11.071	0.137	0.012	0.517	-0.197	0.016	-0.096
24.0	12.034	-0.025	-0.002	0.523	-0.192	0.023	-0.090
25.0	12.847	0.267	0.021	0.527	-0.178	0.023	-0.091
26.0	13.608	0.289	0.021	0.511	-0.164	0.015	-0.090
27.0	14.506	0.096	0.007	0.507	-0.145	0.027	-0.096
28.0	15.236	-0.012	0.001	0.487	-0.120	0.028	-0.090
29.0	17.042	0.782	0.046	0.489	-0.113	0.002	0.034
30.0	17.688	0.383	0.022	0.462	-0.088	0.029	0.023
31.0	18.552	0.418	0.023	0.435	-0.063	0.011	-0.018
32.0	19.507	0.401	0.021	0.440	-0.042	0.025	0.000
33.0	20.558	0.561	0.027	0.421	-0.018	0.008	0.084
34.0	20.985	0.205	0.010	0.362	0.004	0.030	1.458
35.0	21.985	-0.184	-0.008	0.355	0.039	0.053	0.797
36.0	22.853	-1.339	-0.059	0.367	0.064	0.172	0.390
37.0	23.668	-1.070	-0.045	0.316	0.088	0.154	0.357
38.0	24.251	-1.085	-0.045	0.305	0.123	0.096	-0.117
39.0	24.961	-0.983	-0.039	0.341	0.171	0.150	-0.077
40.0	25.474	-1.434	-0.056	0.327	0.193	0.123	-0.087
41.0	26.132	-1.727	-0.066	0.326	0.233	0.116	-0.003
42.0	26.737	-1.472	-0.055	0.330	0.238	0.084	-0.006
43.0	27.163	-2.797	-0.103	0.313	0.277	0.128	-0.137
44.0	27.578	-2.648	-0.096	0.335	0.307	0.095	-0.208
45.0	27.955	-2.585	-0.092	0.303	0.324	0.007	-0.213

46.0	28.175	-3.390	-0.120	0.324	0.346	-0.107	-0.172
47.0	28.311	-2.894	-0.102	0.312	0.343	-0.050	-0.039
48.0	28.854	-3.456	-0.120	0.307	0.365	-0.116	-0.050
49.0	29.199	-2.542	-0.087	0.242	0.400	-0.141	-0.066
50.0	29.210	-3.003	-0.103	0.193	0.422	-0.223	-0.064
51.0	29.596	-2.908	-0.098	0.178	0.465	-0.282	-0.058
52.0	30.253	-2.051	-0.068	0.159	0.498	-0.303	-0.044
53.0	30.274	-1.675	-0.055	0.097	0.533	-0.357	0.098
54.0	30.661	-0.920	-0.030	0.067	0.564	-0.342	0.313
55.0	30.977	-1.182	-0.038	0.051	0.595	-0.405	0.342
56.0	31.002	-0.201	-0.006	0.053	0.628	-0.404	0.252
56.0	31.054	-0.280	-0.009	0.051	0.616	-0.385	0.674
57.0	31.296	-0.378	-0.012	0.045	0.605	-0.368	1.128
58.0	31.280	-0.499	-0.016	0.028	0.604	-0.381	0.996
59.0	31.207	-0.034	-0.001	-0.012	0.592	-0.323	0.914
60.0	30.983	0.166	0.005	-0.008	0.544	-0.329	0.897
61.0	31.320	0.112	0.004	-0.029	0.556	-0.344	0.825
62.0	31.001	-0.236	-0.008	-0.076	0.523	-0.301	0.810
63.0	30.988	-0.080	-0.003	-0.085	0.512	-0.286	0.654
64.0	31.196	-0.398	-0.013	-0.167	0.495	-0.286	0.642
65.0	31.279	-0.067	-0.002	-0.220	0.483	-0.283	0.633
66.0	31.315	-0.312	-0.010	-0.236	0.426	-0.308	0.606
67.0	31.090	-0.678	-0.022	-0.249	0.417	-0.316	0.597
68.0	31.290	-0.360	-0.012	-0.269	0.373	-0.289	0.596
69.0	31.120	-0.637	-0.020	-0.310	0.358	-0.323	0.586
70.0	31.085	-0.981	-0.032	-0.320	0.308	-0.386	0.583
71.0	31.001	-0.757	-0.024	-0.314	0.288	-0.410	0.584
72.0	30.888	-1.308	-0.042	-0.352	0.227	-0.500	0.585
73.0	30.904	-1.066	-0.034	-0.343	0.201	-0.541	0.582
74.0	30.691	-1.182	-0.039	-0.372	0.154	-0.530	0.571
75.0	30.689	-1.124	-0.037	-0.396	0.062	-0.190	0.530
76.0	30.785	0.084	0.003	-0.390	0.058	-0.146	0.524
78.0	30.646	0.509	0.017	-0.382	-0.027	0.009	0.549
79.0	30.428	0.221	0.007	-0.390	-0.120	-0.008	0.526
80.0	30.645	0.510	0.017	-0.353	-0.161	-0.011	0.461
81.0	30.377	0.428	0.014	-0.381	-0.255	0.002	0.472
82.0	30.365	0.236	0.008	-0.350	-0.332	-0.004	0.462
83.0	30.467	0.357	0.012	-0.327	-0.412	-0.007	0.460
84.0	29.929	0.219	0.007	-0.269	-0.511	0.001	0.447
85.0	30.144	0.327	0.011	-0.143	-0.652	0.020	0.637
86.0	29.905	0.416	0.014	0.098	-0.821	0.023	0.583
87.0	30.298	0.548	0.018	0.151	-0.934	0.005	0.980
88.0	30.636	0.390	0.013	0.229	-1.001	0.024	0.633
89.0	30.076	0.479	0.016	0.202	-1.101	0.010	0.411
90.0	30.098	0.339	0.011	0.243	-1.130	0.022	0.032
91.0	29.874	0.184	0.006	0.231	-1.261	0.027	-0.180
92.0	30.097	0.625	0.021	0.268	-1.320	0.011	-0.158
93.0	29.987	0.541	0.018	0.237	-1.412	0.030	-0.244
94.0	29.613	0.663	0.022	0.266	-1.475	0.028	-0.246
95.0	29.796	0.562	0.019	0.267	-1.590	0.017	-0.388
95.0	3.644	0.325	0.089	0.410	-0.082	0.019	0.171
-5.0	3.705	0.414	0.112	0.373	-0.084	0.018	-0.154
0.0	3.661	0.377	0.103	0.378	-0.084	0.018	-0.283

RUNFILE> R3A801

AOA	Cn	Cy	Cy/Cn	Cax	Cpt	Crl	Cyw
-5.0	0.055	0.012	0.213	0.013	0.001	-0.002	0.002
-5.0	-1.348	-0.117	0.086	0.273	0.065	0.006	0.004
-4.0	-0.856	-0.104	0.121	0.293	0.063	0.005	0.007
-3.0	-0.449	-0.026	0.059	0.298	0.057	-0.002	0.007
-2.0	-0.199	-0.165	0.829	0.276	0.039	0.001	0.000
-1.0	0.220	-0.104	-0.475	0.286	0.023	-0.002	0.005
0.0	0.391	-0.171	-0.437	0.282	0.006	-0.007	0.003
1.0	0.540	-0.183	-0.339	0.292	0.008	-0.006	0.004
2.0	1.028	-0.226	-0.220	0.305	-0.017	-0.013	0.004
3.0	1.357	-0.219	-0.161	0.315	-0.036	-0.010	0.004
4.0	1.611	-0.186	-0.115	0.328	-0.052	-0.017	0.002
5.0	1.926	-0.235	-0.122	0.327	-0.065	-0.014	0.001
6.0	2.130	-0.394	-0.185	0.316	-0.065	-0.015	0.001
7.0	2.537	-0.290	-0.114	0.332	-0.065	-0.013	0.002
8.0	2.866	-0.265	-0.092	0.334	-0.058	-0.020	0.003
9.0	3.144	-0.332	-0.106	0.336	-0.047	-0.019	0.000
10.0	3.582	-0.279	-0.078	0.337	-0.036	-0.023	0.003
11.0	4.007	-0.219	-0.055	0.376	-0.028	-0.028	0.004
12.0	4.473	-0.308	-0.069	0.390	-0.024	-0.028	0.004
13.0	5.012	-0.194	-0.039	0.402	-0.032	-0.030	0.002
14.0	5.603	-0.181	-0.032	0.420	-0.041	-0.035	0.002
15.0	6.123	-0.167	-0.027	0.432	-0.052	-0.029	0.004
16.0	6.659	-0.090	-0.014	0.443	-0.065	-0.037	0.003
17.0	7.315	-0.274	-0.037	0.433	-0.070	-0.027	0.001
18.0	7.804	-0.183	-0.023	0.435	-0.080	-0.033	-0.002
19.0	8.450	-0.208	-0.025	0.436	-0.083	-0.040	-0.003
20.0	9.224	-0.159	-0.017	0.450	-0.086	-0.044	0.000
21.0	9.886	-0.219	-0.022	0.448	-0.089	-0.039	-0.009
22.0	10.521	0.112	0.011	0.438	-0.085	-0.038	-0.004
23.0	11.318	-0.168	-0.015	0.431	-0.070	-0.052	-0.005
24.0	12.006	-0.276	-0.023	0.438	-0.056	-0.033	-0.007
25.0	12.938	-0.050	-0.004	0.437	-0.042	-0.025	-0.009
26.0	13.512	-0.077	-0.006	0.425	-0.018	-0.042	-0.021
27.0	14.374	-0.036	-0.002	0.423	0.005	-0.054	-0.013
28.0	15.140	-0.139	-0.009	0.413	0.031	-0.027	-0.015
29.0	15.851	-0.052	-0.003	0.393	0.055	-0.024	-0.011
30.0	16.328	0.099	0.006	0.379	0.078	-0.043	-0.016
31.0	17.352	-0.395	-0.023	0.361	0.098	-0.037	-0.024
32.0	18.027	-0.168	-0.009	0.343	0.119	-0.039	0.035
33.0	19.129	-0.190	-0.010	0.384	0.147	-0.025	-0.011
34.0	19.809	-1.183	-0.060	0.350	0.167	0.077	-0.012
35.0	20.480	-0.444	-0.022	0.329	0.195	0.016	-0.003
36.0	21.246	-0.372	-0.018	0.316	0.228	0.035	-0.012
37.0	21.972	-1.635	-0.074	0.297	0.256	0.078	0.005
38.0	22.588	-1.104	-0.049	0.292	0.289	0.069	-0.020
39.0	23.564	-1.158	-0.049	0.293	0.332	0.064	-0.003
40.0	24.182	-1.422	-0.059	0.280	0.352	0.085	-0.005
41.0	24.651	-1.823	-0.074	0.283	0.392	0.103	0.010
42.0	25.402	-1.623	-0.064	0.277	0.414	0.084	0.001
43.0	25.826	-2.682	-0.104	0.248	0.453	0.111	0.020
44.0	26.109	-2.982	-0.114	0.295	0.461	0.096	0.022
45.0	26.477	-3.200	-0.121	0.317	0.484	0.058	0.025

46.0	26.684	-3.961	-0.148	0.341	0.484	0.019	0.012
47.0	26.842	-4.237	-0.158	0.346	0.483	-0.066	0.005
48.0	26.925	-4.911	-0.182	0.320	0.461	-0.105	-0.010
49.0	27.231	-3.499	-0.128	0.296	0.478	-0.146	-0.019
50.0	27.579	-4.014	-0.146	0.266	0.512	-0.201	-0.025
51.0	27.532	-4.178	-0.152	0.234	0.509	-0.249	0.065
52.0	27.814	-4.777	-0.172	0.188	0.535	-0.387	0.059
53.0	27.680	-3.740	-0.135	0.147	0.549	-0.384	0.051
54.0	28.239	-3.686	-0.131	0.118	0.587	-0.424	0.052
55.0	28.439	-3.177	-0.112	0.094	0.616	-0.488	0.054
56.0	28.664	-2.573	-0.090	0.029	0.650	-0.517	0.053
57.0	28.970	-2.248	-0.078	0.037	0.684	-0.552	0.059
58.0	29.297	-1.925	-0.066	-0.006	0.718	-0.550	0.064
59.0	29.103	-0.898	-0.031	-0.007	0.722	-0.490	0.061
60.0	29.074	-1.432	-0.049	-0.039	0.723	-0.490	0.049
61.0	29.056	-1.149	-0.040	-0.035	0.710	-0.441	0.050
62.0	28.844	-1.450	-0.050	-0.065	0.683	-0.437	0.050
63.0	28.584	-1.214	-0.042	-0.073	0.635	-0.423	0.049
64.0	28.625	-1.342	-0.047	-0.169	0.612	-0.407	0.049
65.0	28.066	-1.216	-0.043	-0.163	0.556	-0.382	0.048
66.0	27.968	-1.582	-0.057	-0.196	0.510	-0.390	0.045
67.0	27.982	-2.008	-0.072	-0.217	0.458	-0.411	0.044
68.0	27.810	-1.961	-0.071	-0.215	0.413	-0.413	0.047
69.0	27.772	-1.784	-0.064	-0.252	0.383	-0.487	0.044
70.0	27.931	-2.256	-0.081	-0.264	0.346	-0.571	0.044
71.0	28.045	-2.298	-0.082	-0.301	0.353	-0.644	0.045
72.0	27.749	-2.203	-0.079	-0.318	0.336	-0.670	0.045
73.0	27.793	-1.840	-0.066	-0.334	0.303	-0.602	0.046
74.0	27.814	-0.939	-0.034	-0.368	0.263	-0.502	0.042
75.0	27.905	-1.859	-0.067	-0.376	0.236	-0.283	0.044
73.0	26.952	-1.300	-0.048	-0.045	0.285	-0.589	-0.046
74.0	26.563	-1.227	-0.046	-0.220	0.250	-0.539	0.048
75.0	26.335	-0.689	-0.026	-0.347	0.209	-0.291	0.039
76.0	26.561	0.214	0.008	-0.421	0.185	-0.066	0.044
77.0	24.911	0.122	0.005	-0.442	-0.021	-0.045	0.037
78.0	26.670	-0.321	-0.012	-0.475	0.081	0.003	0.041
79.0	26.761	-0.017	0.001	-0.454	0.033	0.025	0.041
80.0	26.831	-0.191	-0.007	-0.447	-0.022	0.000	0.040
81.0	26.468	-0.237	-0.009	-0.443	-0.092	-0.004	0.038
82.0	26.269	-0.190	-0.007	-0.409	-0.176	0.000	0.036
83.0	26.734	-0.175	-0.007	-0.378	-0.267	0.012	0.036
84.0	25.670	-0.251	-0.010	-0.322	-0.410	0.000	0.029
85.0	26.861	-0.281	-0.010	-0.232	-0.493	0.012	0.031
86.0	26.697	-0.312	-0.012	-0.029	-0.639	0.024	0.025
87.0	26.259	-0.377	-0.014	0.104	-0.813	0.026	0.020
88.0	26.401	-0.229	-0.009	0.189	-0.910	0.027	0.018
89.0	26.342	-0.228	-0.009	0.258	-0.990	0.027	0.019
90.0	26.320	-0.170	-0.006	0.256	-1.066	0.023	0.018
91.0	26.151	-0.188	-0.007	0.267	-1.143	0.027	0.017
92.0	25.995	-0.313	-0.012	0.266	-1.180	0.024	0.015
93.0	26.077	-0.220	-0.008	0.254	-1.262	0.020	0.011
94.0	26.255	-0.220	-0.008	0.255	-1.359	0.019	0.010
95.0	25.959	-0.356	-0.014	0.257	-1.421	0.018	0.007
95.0	1.258	-0.308	-0.245	0.362	-0.048	0.014	-0.008
-5.0	1.263	-0.286	-0.226	0.314	-0.049	0.015	-0.009
0.0	1.350	-0.274	-0.203	0.324	-0.048	0.016	-0.008

RUNFILE> R4A801

AOA	Cn	Cy	Cy/Cn	Cax	Cpt	Crl	Cyw
-5.0	0.033	0.023	0.705	0.010	-0.001	0.001	0.001
-5.0	-0.842	-0.047	0.056	0.215	0.064	0.010	0.004
-4.0	-0.734	-0.129	0.176	0.212	0.062	0.007	0.001
-3.0	-0.524	-0.059	0.113	0.210	0.048	0.004	0.002
-2.0	-0.144	-0.036	0.247	0.225	0.025	0.005	0.003
-1.0	0.107	-0.022	-0.208	0.224	0.008	0.005	0.001
0.0	0.239	-0.056	-0.236	0.221	-0.003	0.007	0.002
1.0	0.466	-0.019	-0.041	0.231	-0.013	0.006	0.002
2.0	0.687	-0.012	-0.017	0.231	-0.032	0.007	0.000
3.0	0.834	-0.069	-0.082	0.215	-0.054	0.001	0.025
4.0	1.383	0.029	0.021	0.250	-0.064	0.007	-0.027
5.0	1.595	0.158	0.099	0.242	-0.068	0.004	-0.017
6.0	1.811	0.041	0.022	0.247	-0.066	0.006	-0.006
7.0	1.939	0.037	0.019	0.245	-0.063	-0.002	-0.005
8.0	2.284	0.074	0.032	0.253	-0.048	-0.003	0.006
9.0	2.514	-0.021	-0.008	0.263	-0.042	0.000	0.007
10.0	2.810	0.017	0.006	0.269	-0.034	0.001	0.006
11.0	3.119	-0.112	-0.036	0.277	-0.035	-0.002	0.005
12.0	3.487	0.107	0.031	0.295	-0.028	-0.007	0.007
13.0	3.891	-0.182	-0.047	0.300	-0.036	0.005	0.027
14.0	4.280	-0.014	-0.003	0.309	-0.045	0.000	0.028
15.0	4.778	-0.190	-0.040	0.315	-0.054	0.004	0.028
16.0	5.292	-0.187	-0.035	0.319	-0.063	-0.004	0.026
17.0	5.866	0.037	0.006	0.335	-0.053	0.012	0.021
18.0	6.330	-0.047	-0.007	0.337	-0.069	0.002	0.027
19.0	6.664	-0.137	-0.021	0.332	-0.070	-0.011	0.021
20.0	7.364	-0.181	-0.025	0.342	-0.071	0.009	0.018
21.0	7.931	0.115	0.014	0.340	-0.063	-0.021	0.026
22.0	8.478	-0.385	-0.045	0.337	-0.052	0.012	0.021
23.0	8.988	0.216	0.024	0.337	-0.056	-0.034	0.005
24.0	9.663	-0.166	-0.017	0.332	-0.044	-0.010	0.027
25.0	10.497	-0.019	-0.002	0.341	-0.031	0.007	0.008
26.0	11.064	-0.036	-0.003	0.332	-0.025	0.018	0.025
27.0	11.949	-0.105	-0.009	0.345	-0.022	0.007	0.025
28.0	12.590	0.036	0.003	0.338	0.005	0.016	0.019
29.0	13.236	-0.133	-0.010	0.330	0.019	-0.003	0.016
30.0	13.795	-0.117	-0.008	0.324	0.054	0.010	0.028
31.0	14.266	-0.585	-0.041	0.302	0.044	0.013	0.015
32.0	15.157	0.305	0.020	0.307	0.065	-0.014	0.010
33.0	15.723	0.235	0.015	0.287	0.110	-0.022	0.023
34.0	16.590	0.825	0.050	0.274	0.139	-0.026	0.016
35.0	16.859	0.001	0.000	0.254	0.167	0.000	0.034
36.0	17.501	0.463	0.026	0.236	0.233	0.031	0.041
37.0	18.040	-0.348	-0.019	0.212	0.260	0.020	0.071
38.0	18.808	-1.194	-0.063	0.246	0.260	0.125	0.076
39.0	19.228	-0.570	-0.030	0.210	0.291	0.072	0.074
40.0	19.958	-1.846	-0.092	0.200	0.320	0.088	0.052
41.0	20.751	-1.689	-0.081	0.210	0.314	0.083	0.080
42.0	21.008	-2.569	-0.122	0.195	0.338	0.141	0.047
43.0	21.366	-1.445	-0.068	0.187	0.333	0.047	0.054
44.0	21.518	-2.195	-0.102	0.180	0.356	0.105	0.032
45.0	21.800	-2.218	-0.102	0.196	0.363	0.054	0.050

46.0	22.219	-2.178	-0.098	0.230	0.390	0.077	0.036
47.0	22.238	-3.791	-0.170	0.212	0.348	-0.014	0.025
48.0	22.551	-2.973	-0.132	0.211	0.330	0.041	0.019
49.0	22.791	-2.327	-0.102	0.194	0.348	-0.055	0.011
50.0	23.130	-2.326	-0.101	0.154	0.364	-0.099	0.004
51.0	23.516	-1.489	-0.063	0.127	0.366	-0.259	-0.005
52.0	23.656	-2.645	-0.112	0.119	0.350	-0.324	-0.007
53.0	23.790	-2.102	-0.088	0.084	0.363	-0.402	-0.026
54.0	23.902	-2.489	-0.104	0.033	0.322	-0.603	-0.027
55.0	24.324	-1.600	-0.066	0.025	0.334	-0.685	-0.025
56.0	24.434	-2.683	-0.110	0.000	0.384	-0.653	-0.020
57.0	24.299	-2.028	-0.083	-0.004	0.426	-0.644	-0.020
58.0	24.431	-1.118	-0.046	-0.010	0.478	-0.576	-0.020
59.0	24.213	-2.753	-0.114	-0.012	0.499	-0.556	-0.017
60.0	24.414	-1.536	-0.063	-0.113	0.503	-0.421	-0.008
61.0	24.485	0.067	0.003	-0.094	0.500	-0.263	-0.010
62.0	24.131	-1.193	-0.049	-0.114	0.497	-0.329	-0.004
63.0	23.917	0.499	0.021	-0.137	0.496	-0.272	-0.010
64.0	23.386	-0.929	-0.040	-0.137	0.471	-0.354	-0.017
65.0	23.285	-1.575	-0.068	-0.150	0.413	-0.480	-0.019
66.0	23.036	-1.731	-0.075	-0.151	0.366	-0.554	-0.016
67.0	22.921	-1.506	-0.066	-0.171	0.338	-0.524	-0.013
68.0	23.093	-1.532	-0.066	-0.187	0.304	-0.503	-0.013
69.0	23.362	-1.432	-0.061	-0.212	0.293	-0.516	-0.010
70.0	23.330	-1.220	-0.052	-0.223	0.286	-0.466	-0.009
71.0	23.460	-1.441	-0.061	-0.263	0.277	-0.266	-0.007
72.0	23.627	-2.593	-0.110	-0.290	0.263	-0.256	-0.003
73.0	23.463	-0.035	-0.001	-0.308	0.257	-0.011	-0.001
74.0	23.408	-0.145	-0.006	-0.339	0.227	0.053	0.000
75.0	23.475	0.236	0.010	-0.347	0.194	0.043	-0.003
76.0	23.133	0.240	0.010	-0.343	0.121	0.045	-0.002
77.0	23.197	0.181	0.008	-0.339	0.084	0.036	-0.005
78.0	22.989	0.035	0.002	-0.324	0.039	0.011	0.000
79.0	23.200	0.283	0.012	-0.324	0.011	0.021	-0.002
80.0	22.921	0.131	0.006	-0.317	-0.074	0.018	-0.003
81.0	22.936	0.113	0.005	-0.269	-0.138	0.027	-0.002
82.0	22.485	0.151	0.007	-0.238	-0.213	0.029	-0.005
83.0	22.283	0.120	0.005	-0.194	-0.257	0.030	-0.008
84.0	22.138	0.235	0.011	-0.149	-0.348	0.030	-0.006
85.0	22.152	0.073	0.003	-0.084	-0.452	0.044	-0.003
86.0	22.078	0.244	0.011	-0.018	-0.513	0.029	-0.003
87.0	22.413	0.182	0.008	0.035	-0.623	0.028	-0.006
88.0	22.472	0.029	0.001	0.132	-0.754	0.049	-0.010
89.0	21.989	0.001	0.000	0.202	-0.809	0.019	-0.009
90.0	22.391	-0.040	-0.002	0.225	-0.866	0.036	-0.007
91.0	22.264	0.159	0.007	0.224	-0.954	0.032	-0.010
92.0	22.348	0.084	0.004	0.251	-1.006	0.037	-0.009
93.0	22.285	0.066	0.003	0.248	-1.072	0.039	-0.012
94.0	22.233	-0.115	-0.005	0.240	-1.118	0.038	-0.011
95.0	22.216	0.145	0.007	0.247	-1.178	0.048	-0.010
95.0	1.531	0.058	0.038	0.311	-0.049	0.037	0.032
-5.0	1.466	0.014	0.009	0.244	-0.049	0.037	0.031
0.0	1.544	0.059	0.039	0.257	-0.049	0.038	0.033

RUNFILE> R0C801

AOA	Cn	Cy	Cy/Cn	Cax	Cpt	Crl	Cyw
0.0	-0.008	-0.013	1.695	-0.003	0.001	0.000	-0.002
0.0	0.126	-0.342	-2.715	0.349	-0.004	0.063	0.000
10.0	3.616	0.052	0.014	0.271	-0.130	-0.023	-0.002
20.0	7.671	-0.204	-0.027	0.375	0.124	-0.002	0.006
30.0	12.631	0.200	0.016	0.347	0.394	-0.014	0.001
35.0	15.264	-0.486	-0.032	0.271	0.493	-0.045	0.006
40.0	18.592	-0.498	-0.027	0.161	0.416	-0.229	-0.031
45.0	21.397	1.037	0.048	0.078	0.451	-0.449	-0.012
50.0	24.332	-0.133	-0.005	-0.081	0.545	-0.385	0.015
55.0	26.783	-2.625	-0.098	-0.230	0.670	-0.297	-0.007
60.0	29.142	0.815	0.028	-0.372	0.867	0.044	-0.043
65.0	30.947	-0.818	-0.026	-0.571	1.058	-0.725	0.045
70.0	31.683	-2.475	-0.078	-0.701	1.155	-0.947	-0.079
80.0	31.932	0.073	0.002	-0.780	0.800	-0.054	0.096
90.0	30.062	0.292	0.010	-0.241	-1.041	-0.028	0.122

RUNFILE> R0C802

AOA	Cn	Cy	Cy/Cn	Cax	Cpt	Crl	Cyw
-5.0	0.053	0.013	0.245	-0.006	0.001	0.000	0.001
-5.0	-1.357	-0.056	0.041	0.250	0.109	0.002	-0.004
-4.0	-0.939	-0.063	0.067	0.250	0.087	0.004	0.001
-3.0	-0.637	-0.131	0.205	0.247	0.073	0.012	0.001
-2.0	-0.442	-0.161	0.364	0.220	0.046	0.008	-0.004
-1.0	-0.021	-0.080	3.773	0.220	0.023	0.007	-0.019
0.0	0.110	-0.064	-0.583	0.212	0.008	0.008	-0.006
1.0	0.498	-0.088	-0.177	0.209	-0.014	0.010	0.000
2.0	0.820	0.047	0.057	0.220	-0.032	0.003	-0.003
3.0	1.082	0.025	0.023	0.215	-0.059	0.004	-0.005
0.0	1.279	-0.149	-0.117	0.213	-0.077	0.001	-0.006
4.0	1.292	-0.156	-0.121	0.213	-0.082	0.005	-0.007
5.0	1.610	0.063	0.039	0.227	-0.101	-0.009	-0.010
6.0	1.991	-0.051	-0.026	0.234	-0.114	-0.006	-0.005
7.0	2.328	0.087	0.037	0.235	-0.121	-0.001	-0.009
8.0	2.622	-0.212	-0.081	0.225	-0.125	0.001	-0.007
9.0	2.973	-0.036	-0.012	0.246	-0.124	-0.001	-0.004
10.0	3.183	-0.382	-0.120	0.224	-0.113	0.006	-0.013
11.0	3.439	-0.035	-0.010	0.241	-0.105	0.007	-0.015
12.0	3.984	-0.056	-0.014	0.273	-0.097	-0.004	-0.005
13.0	4.334	-0.052	-0.012	0.289	-0.085	-0.001	-0.006
14.0	4.731	-0.060	-0.013	0.304	-0.064	0.016	-0.006
15.0	4.880	0.034	0.007	0.304	-0.044	0.002	-0.011
16.0	5.266	-0.037	-0.007	0.321	-0.026	-0.003	-0.010
17.0	5.592	0.001	0.000	0.346	0.005	0.002	-0.008
18.0	5.918	0.076	0.013	0.355	0.023	0.001	-0.010
19.0	6.395	0.227	0.035	0.367	0.052	0.004	-0.003
20.0	6.317	0.259	0.041	0.364	0.063	-0.009	-0.015
21.0	6.735	0.038	0.006	0.389	0.095	-0.025	-0.013
22.0	7.303	0.194	0.027	0.417	0.119	-0.013	-0.003
23.0	7.617	-0.049	-0.006	0.435	0.135	-0.034	-0.016
24.0	7.948	-0.517	-0.065	0.444	0.144	-0.005	-0.002
25.0	8.388	0.295	0.035	0.460	0.154	-0.057	-0.010
26.0	8.409	0.236	0.028	0.435	0.181	-0.024	-0.003
27.0	9.041	0.081	0.009	0.462	0.203	-0.047	0.000
28.0	9.473	0.512	0.054	0.465	0.229	-0.058	-0.008
29.0	9.701	0.125	0.013	0.452	0.245	-0.021	-0.016
30.0	10.470	0.873	0.083	0.454	0.276	-0.073	-0.014
31.0	10.410	0.012	0.001	0.415	0.307	-0.016	-0.017
32.0	10.906	0.334	0.031	0.399	0.336	-0.018	-0.025
33.0	11.086	0.598	0.054	0.384	0.352	-0.066	-0.024
34.0	11.180	0.640	0.057	0.456	0.311	0.006	-0.083
35.0	12.185	0.603	0.049	0.370	0.373	-0.047	-0.019
36.0	12.780	0.302	0.024	0.366	0.374	-0.126	-0.024
37.0	12.671	0.687	0.054	0.433	0.315	-0.054	-0.099
38.0	13.622	1.026	0.075	0.334	0.357	-0.123	-0.047
39.0	14.113	2.940	0.208	0.312	0.356	-0.164	-0.061
40.0	14.465	-0.212	-0.015	0.302	0.357	-0.088	-0.028
41.0	15.264	-0.182	-0.012	0.312	0.336	-0.191	-0.030
42.0	15.868	-0.130	-0.008	0.301	0.330	-0.081	-0.047
43.0	15.947	0.222	0.014	0.263	0.347	-0.235	-0.070
44.0	16.521	1.160	0.070	0.261	0.342	-0.249	-0.043

45.0	17.044	-0.604	-0.035	0.278	0.268	-0.359	-0.095
46.0	17.858	0.366	0.021	0.228	0.343	-0.242	-0.072
47.0	18.653	2.334	0.125	0.233	0.372	-0.344	-0.049
48.0	18.423	1.255	0.068	0.212	0.315	-0.455	-0.168
49.0	19.061	1.003	0.053	0.203	0.342	-0.424	-0.094
50.0	20.536	-1.368	-0.067	0.165	0.446	-0.475	-0.131
51.0	20.620	-2.113	-0.102	0.102	0.428	-0.446	-0.066
52.0	21.165	-0.794	-0.038	0.094	0.499	-0.418	-0.062
53.0	21.478	-1.274	-0.059	0.065	0.548	-0.433	-0.054
54.0	22.105	-0.884	-0.040	0.050	0.606	-0.638	-0.110
55.0	22.632	-0.449	-0.020	0.034	0.636	-0.599	-0.121
56.0	22.901	-2.467	-0.108	-0.009	0.701	-0.779	-0.095
57.0	23.271	-1.777	-0.076	-0.040	0.740	-0.673	-0.091
58.0	23.550	-0.655	-0.028	-0.032	0.715	-0.602	-0.137
59.0	23.715	-0.150	-0.006	-0.070	0.724	-0.495	-0.125
60.0	23.996	-1.003	-0.042	-0.124	0.773	-0.551	-0.037
61.0	24.348	-2.703	-0.111	-0.195	0.777	-0.494	-0.133
62.0	24.531	-0.903	-0.037	-0.214	0.837	-0.588	-0.028
63.0	25.024	-1.780	-0.071	-0.234	0.863	-0.789	-0.132
64.0	25.142	-2.184	-0.087	-0.259	0.912	-0.901	-0.115
65.0	25.105	-2.262	-0.090	-0.288	0.938	-0.913	-0.106
66.0	25.403	-2.990	-0.118	-0.309	0.928	-0.862	-0.089
67.0	25.582	-3.194	-0.125	-0.343	0.944	-0.829	-0.082
68.0	25.623	-2.602	-0.102	-0.370	0.968	-0.745	-0.083
69.0	25.998	-2.126	-0.082	-0.400	1.000	-0.676	-0.087
70.0	25.854	-2.616	-0.101	-0.421	0.981	-0.660	-0.087
71.0	26.170	-1.590	-0.061	-0.443	0.973	-0.506	-0.085
72.0	26.269	-2.893	-0.110	-0.480	0.959	-0.234	-0.075
73.0	26.193	-0.033	-0.001	-0.524	0.940	-0.077	-0.074
74.0	26.386	-1.825	-0.069	-0.502	0.914	-0.018	-0.068
75.0	26.159	0.168	0.006	-0.527	0.881	0.074	-0.072
76.0	26.250	0.213	0.008	-0.505	0.820	0.002	-0.075
77.0	25.882	-0.482	-0.019	-0.500	0.766	0.070	-0.079
78.0	25.853	-0.015	0.001	-0.471	0.668	0.038	-0.084
79.0	25.704	0.171	0.007	-0.474	0.596	0.017	-0.084
80.0	25.426	0.049	0.002	-0.453	0.485	0.042	-0.089
81.0	25.675	0.088	0.003	-0.433	0.410	0.049	-0.087
82.0	25.107	-0.112	-0.004	-0.437	0.286	0.047	-0.095
83.0	25.641	0.006	0.000	-0.420	0.153	0.022	-0.094
84.0	25.359	-0.171	-0.007	-0.406	0.032	0.038	-0.068
85.0	25.365	-0.131	-0.005	-0.427	-0.065	0.033	-0.098
86.0	24.582	0.016	0.001	-0.400	-0.227	0.036	-0.092
87.0	24.776	-0.027	-0.001	-0.323	-0.333	0.044	-0.097
88.0	24.191	0.066	0.003	-0.243	-0.493	0.042	-0.110
89.0	24.274	0.054	0.002	-0.096	-0.611	0.051	-0.115
90.0	24.093	-0.116	-0.005	0.035	-0.867	0.047	-0.098
91.0	24.849	-0.043	-0.002	0.119	-1.097	0.057	-0.115
92.0	25.085	0.033	0.001	0.284	-1.318	0.070	-0.114
93.0	24.746	0.040	0.002	0.300	-1.322	0.063	-0.116
94.0	25.157	0.183	0.007	0.301	-1.390	0.059	-0.126
95.0	24.715	0.149	0.006	0.287	-1.390	0.067	-0.120
95.0	0.085	-0.271	-3.205	0.210	-0.060	0.047	-0.067
-5.0	0.213	-0.097	-0.455	0.189	-0.064	0.052	-0.066
0.0	0.140	-0.121	-0.864	0.179	-0.065	0.051	-0.070

RUNFILE> R1C801

AOA	Cn	Cy	Cy/Cn	Cax	Cpt	Crl	Cyw
-5.0	-0.056	-0.052	0.938	-0.009	0.002	0.000	-0.001
-5.0	-1.182	-0.127	0.108	0.287	0.050	-0.005	0.002
-4.0	-1.042	-0.197	0.189	0.271	0.040	-0.004	-0.001
-3.0	-0.643	-0.184	0.286	0.261	0.032	-0.002	-0.002
-2.0	-0.276	-0.159	0.576	0.259	0.016	-0.003	0.003
-1.0	0.056	-0.132	-2.354	0.258	0.007	-0.002	0.001
0.0	0.359	-0.186	-0.519	0.252	-0.003	-0.003	0.001
1.0	0.945	-0.011	-0.011	0.293	-0.015	-0.002	0.009
2.0	1.186	-0.015	-0.013	0.300	-0.025	0.002	0.004
3.0	1.558	0.032	0.020	0.333	-0.038	0.001	0.009
4.0	1.832	0.058	0.032	0.340	-0.052	0.003	0.009
5.0	2.132	0.127	0.060	0.363	-0.062	0.001	0.011
6.0	2.542	0.107	0.042	0.365	-0.074	0.002	0.011
7.0	2.844	0.129	0.045	0.390	-0.083	-0.002	0.013
8.0	3.266	0.093	0.028	0.400	-0.090	0.004	0.012
9.0	3.552	0.169	0.048	0.422	-0.089	-0.003	0.014
10.0	3.751	0.120	0.032	0.422	-0.092	-0.002	0.013
11.0	4.065	0.144	0.035	0.422	-0.086	-0.002	0.012
12.0	4.503	0.240	0.053	0.455	-0.082	-0.006	0.014
13.0	4.768	0.225	0.047	0.454	-0.071	-0.001	0.012
14.0	5.046	0.283	0.056	0.468	-0.062	-0.001	0.012
15.0	5.535	0.364	0.066	0.515	-0.058	0.000	0.015
16.0	5.869	0.269	0.046	0.507	-0.046	-0.001	0.014
17.0	6.311	0.448	0.071	0.542	-0.043	0.008	0.017
18.0	6.416	0.448	0.070	0.524	-0.033	0.001	0.012
19.0	6.811	0.288	0.042	0.536	-0.028	0.011	0.011
20.0	7.202	0.547	0.076	0.575	-0.022	0.009	0.018
21.0	7.552	0.608	0.080	0.567	-0.012	-0.009	0.015
22.0	8.076	0.638	0.079	0.608	-0.011	-0.001	0.018
23.0	8.460	0.601	0.071	0.631	0.000	0.008	0.016
24.0	8.670	0.796	0.092	0.635	0.002	-0.002	0.011
25.0	8.951	0.545	0.061	0.622	0.016	0.004	0.011
26.0	9.350	0.552	0.059	0.631	0.034	0.008	0.006
27.0	9.658	0.490	0.051	0.634	0.040	0.012	0.006
28.0	9.997	0.651	0.065	0.655	0.053	0.001	0.012
29.0	10.579	0.682	0.064	0.657	0.080	0.011	0.010
30.0	10.907	0.686	0.063	0.645	0.104	-0.010	0.005
31.0	11.087	0.487	0.044	0.638	0.115	0.002	0.004
32.0	11.482	0.633	0.055	0.630	0.140	-0.009	0.000
33.0	12.000	0.862	0.072	0.621	0.172	-0.012	0.000
34.0	12.086	0.783	0.065	0.612	0.186	-0.020	-0.002
35.0	12.676	0.968	0.076	0.628	0.200	-0.023	0.003
36.0	13.080	0.791	0.060	0.607	0.212	-0.021	0.001
37.0	13.529	0.910	0.067	0.599	0.222	-0.038	-0.001
38.0	14.060	0.527	0.037	0.586	0.220	-0.054	0.001
39.0	14.361	1.249	0.087	0.559	0.230	-0.012	-0.003
40.0	14.843	0.700	0.047	0.571	0.217	-0.050	-0.002
41.0	15.529	0.570	0.037	0.563	0.224	-0.019	0.005
42.0	15.866	0.717	0.045	0.551	0.234	-0.023	-0.001
43.0	16.289	0.290	0.018	0.545	0.236	0.026	0.011
44.0	16.645	-0.213	-0.013	0.532	0.237	-0.025	0.011
45.0	17.021	0.288	0.017	0.525	0.248	0.015	0.012

46.0	17.664	0.187	0.011	0.500	0.260	0.009	0.009
47.0	17.899	-0.030	-0.002	0.500	0.281	0.015	0.019
48.0	18.241	-0.010	0.001	0.485	0.283	0.025	-0.003
49.0	18.547	-0.261	-0.014	0.479	0.294	0.045	0.014
50.0	19.069	-0.764	-0.040	0.481	0.319	0.010	0.012
51.0	19.377	-0.087	-0.005	0.459	0.332	0.001	0.022
52.0	19.422	-0.159	-0.008	0.432	0.345	-0.017	0.010
53.0	19.889	-0.571	-0.029	0.417	0.345	-0.040	0.006
54.0	20.149	-0.376	-0.019	0.395	0.368	-0.031	0.006
55.0	20.468	-0.086	-0.004	0.373	0.381	-0.018	0.001
56.0	20.929	-0.255	-0.012	0.335	0.383	-0.050	-0.003
57.0	20.874	-0.201	-0.010	0.318	0.406	-0.050	0.005
58.0	21.143	-0.407	-0.019	0.303	0.410	-0.074	0.006
59.0	21.501	-0.052	-0.002	0.290	0.418	-0.063	0.002
60.0	21.525	-0.485	-0.023	0.288	0.411	-0.072	0.011
61.0	21.730	-0.253	-0.012	0.235	0.415	-0.065	0.009
62.0	22.176	-0.313	-0.014	0.233	0.425	-0.062	0.012
63.0	22.308	-0.506	-0.023	0.226	0.414	-0.074	0.008
64.0	22.625	-0.055	-0.002	0.211	0.399	-0.050	0.009
65.0	22.919	-0.110	-0.005	0.217	0.405	-0.057	0.013
66.0	22.766	-0.456	-0.020	0.167	0.383	-0.065	0.005
67.0	23.253	-0.280	-0.012	0.182	0.379	-0.075	0.014
68.0	23.402	-0.290	-0.012	0.160	0.361	-0.074	0.008
69.0	23.408	-0.180	-0.008	0.150	0.358	-0.080	0.008
70.0	23.606	-0.757	-0.032	0.125	0.348	-0.152	0.007
71.0	23.834	-0.519	-0.022	0.112	0.349	-0.154	0.009
72.0	24.149	0.043	0.002	0.125	0.333	-0.218	0.006
73.0	24.185	-0.822	-0.034	0.114	0.330	-0.250	0.003
74.0	24.485	-0.715	-0.029	0.107	0.306	-0.291	0.008
75.0	24.745	-0.889	-0.036	0.113	0.261	-0.337	0.004
76.0	24.944	-1.313	-0.053	0.106	0.205	-0.223	0.008
77.0	24.901	-0.352	-0.014	0.095	0.184	-0.126	0.012
78.0	25.099	-0.223	-0.009	0.084	0.116	0.081	0.011
79.0	24.925	0.460	0.018	0.110	0.046	0.029	0.016
80.0	25.468	-0.124	-0.005	0.117	-0.037	0.052	0.025
81.0	25.207	0.391	0.016	0.120	-0.090	0.061	0.025
82.0	25.318	-0.071	-0.003	0.087	-0.214	0.056	0.029
83.0	25.517	0.117	0.005	0.088	-0.312	0.099	0.029
84.0	25.578	0.140	0.005	0.067	-0.430	0.070	0.025
85.0	25.839	0.154	0.006	0.107	-0.513	0.072	0.027
86.0	25.514	0.690	0.027	0.121	-0.591	0.088	0.017
87.0	25.435	0.371	0.015	0.208	-0.720	0.091	0.024
88.0	25.596	0.452	0.018	0.230	-0.809	0.072	0.021
89.0	25.588	0.146	0.006	0.283	-0.897	0.080	0.027
90.0	25.873	0.289	0.011	0.346	-0.994	0.092	0.030
91.0	25.618	0.418	0.016	0.382	-1.044	0.098	0.024
92.0	25.663	0.487	0.019	0.423	-1.121	0.114	0.028
93.0	25.890	0.757	0.029	0.427	-1.186	0.094	0.029
94.0	25.599	0.661	0.026	0.444	-1.254	0.108	0.032
95.0	25.897	0.702	0.027	0.458	-1.307	0.091	0.034
95.0	3.775	0.613	0.162	0.505	-0.084	0.070	0.063
-5.0	3.916	0.729	0.186	0.553	-0.104	0.071	0.129
0.0	3.634	0.632	0.174	0.500	-0.088	0.072	0.066
45.0	18.053	0.649	0.036	0.659	0.231	0.034	0.059
72.0	24.535	-0.731	-0.030	0.254	0.324	-0.195	0.049

RUNFILE> R1C802

AOA	Cn	Cy	Cy/Cn	Cax	Cpt	Crl	Cyw
-5.0	-0.046	0.005	-0.114	0.005	-0.001	0.001	0.007
-5.0	-1.059	0.088	-0.084	0.297	0.042	0.002	0.006
-4.0	-0.710	0.080	-0.113	0.331	0.035	0.002	0.001
-3.0	-0.474	0.059	-0.125	0.334	0.024	0.003	0.001
-2.0	-0.294	-0.030	0.102	0.327	0.016	0.003	0.003
-1.0	0.017	-0.020	-1.141	0.332	0.000	0.002	0.005
0.0	0.246	-0.032	-0.131	0.342	-0.010	0.004	0.006
1.0	0.596	0.024	0.041	0.365	-0.020	0.001	0.007
2.0	0.815	-0.086	-0.105	0.358	-0.031	0.001	0.008
3.0	1.023	-0.010	-0.010	0.355	-0.047	-0.003	0.004
4.0	1.165	-0.090	-0.077	0.350	-0.056	-0.005	0.000
5.0	1.526	-0.058	-0.038	0.369	-0.070	-0.004	0.004
6.0	1.696	-0.086	-0.051	0.354	-0.078	-0.012	0.000
7.0	2.156	0.006	0.003	0.378	-0.088	-0.012	0.006
8.0	2.516	-0.024	-0.010	0.385	-0.093	-0.009	0.007
9.0	2.554	-0.134	-0.052	0.371	-0.099	-0.010	0.005
10.0	2.792	-0.041	-0.015	0.381	-0.092	-0.017	0.004
11.0	3.236	0.014	0.004	0.397	-0.094	-0.018	0.007
12.0	3.404	-0.199	-0.058	0.385	-0.086	-0.013	0.002
13.0	3.794	-0.138	-0.036	0.396	-0.076	-0.012	0.003
14.0	4.061	-0.060	-0.015	0.400	-0.069	-0.020	0.003
15.0	4.417	0.002	0.000	0.417	-0.062	-0.007	0.005
16.0	4.819	0.036	0.007	0.442	-0.056	-0.008	0.008
17.0	5.247	0.012	0.002	0.445	-0.043	-0.008	0.011
18.0	5.561	0.126	0.023	0.447	-0.039	-0.014	0.011
19.0	5.928	0.049	0.008	0.462	-0.033	-0.012	0.008
20.0	6.226	0.196	0.032	0.470	-0.032	-0.021	0.010
21.0	6.584	0.060	0.009	0.476	-0.022	-0.013	0.010
22.0	6.923	0.153	0.022	0.481	-0.018	-0.013	0.011
23.0	7.333	0.140	0.019	0.499	-0.007	-0.017	0.013
24.0	7.887	0.404	0.051	0.538	0.000	-0.024	0.016
25.0	8.073	0.279	0.035	0.522	0.014	-0.017	0.016
26.0	8.414	0.267	0.032	0.535	0.013	-0.028	0.018
27.0	8.764	0.150	0.017	0.525	0.042	-0.021	0.015
28.0	9.243	0.020	0.002	0.534	0.054	-0.005	0.017
29.0	9.509	0.040	0.004	0.518	0.071	-0.009	0.012
30.0	9.898	0.084	0.009	0.513	0.089	-0.017	0.013
31.0	10.255	0.145	0.014	0.512	0.109	-0.010	0.011
32.0	10.446	0.060	0.006	0.495	0.134	-0.029	0.010
33.0	10.849	-0.084	-0.008	0.491	0.165	-0.030	0.012
34.0	11.290	0.232	0.021	0.485	0.185	-0.037	0.011
35.0	11.809	0.319	0.027	0.485	0.202	-0.058	0.019
36.0	12.142	0.371	0.031	0.472	0.210	-0.042	0.019
37.0	12.615	0.084	0.007	0.459	0.209	-0.046	0.021
38.0	13.052	0.311	0.024	0.446	0.223	-0.054	0.016
39.0	13.395	0.021	0.002	0.439	0.212	-0.046	0.019
40.0	13.912	0.017	0.001	0.426	0.211	-0.050	0.019
41.0	14.394	0.342	0.024	0.425	0.214	-0.036	0.038
42.0	14.740	0.036	0.002	0.397	0.227	-0.032	0.021
43.0	15.099	-0.444	-0.029	0.399	0.227	0.007	0.029
44.0	15.548	-0.217	-0.014	0.398	0.239	-0.035	0.028
45.0	16.014	-0.554	-0.035	0.382	0.243	-0.010	0.035

46.0	16.405	-0.828	-0.050	0.390	0.255	-0.004	0.028
47.0	16.773	-1.024	-0.061	0.382	0.264	0.017	0.036
48.0	16.906	-1.485	-0.088	0.364	0.272	0.030	0.044
49.0	17.492	-0.649	-0.037	0.359	0.307	0.005	0.044
50.0	17.845	-1.313	-0.074	0.335	0.317	0.033	0.051
51.0	18.062	-1.358	-0.075	0.331	0.316	0.001	0.039
52.0	18.488	-0.917	-0.050	0.308	0.328	0.017	0.049
53.0	18.880	-1.352	-0.072	0.291	0.345	-0.009	0.050
54.0	18.958	-1.405	-0.074	0.250	0.350	-0.023	0.045
55.0	19.281	-1.231	-0.064	0.246	0.370	-0.065	0.049
56.0	19.530	-0.907	-0.046	0.223	0.376	-0.058	0.052
57.0	19.548	-0.730	-0.037	0.191	0.375	-0.039	0.053
58.0	19.780	-1.406	-0.071	0.181	0.402	-0.059	0.055
59.0	20.110	-1.209	-0.060	0.155	0.384	-0.067	0.060
60.0	20.045	-0.828	-0.041	0.139	0.401	-0.081	0.056
61.0	20.484	-0.587	-0.029	0.127	0.402	-0.060	0.061
62.0	20.863	-0.975	-0.047	0.115	0.393	-0.082	0.059
63.0	21.066	-0.963	-0.046	0.140	0.393	-0.085	0.062
64.0	21.285	-1.028	-0.048	0.097	0.395	-0.084	-0.020
65.0	21.490	-0.791	-0.037	0.072	0.368	-0.055	0.063
66.0	21.603	-0.997	-0.046	0.060	0.372	-0.069	-0.018
67.0	21.855	-1.072	-0.049	0.057	0.372	-0.063	-0.018
68.0	21.900	-0.692	-0.032	0.044	0.357	-0.096	-0.017
69.0	22.534	-0.368	-0.016	0.059	0.330	-0.082	-0.014
70.0	22.772	-0.800	-0.035	0.048	0.334	-0.104	-0.016
71.0	22.955	-0.436	-0.019	0.014	0.332	-0.153	-0.022
72.0	23.083	-1.129	-0.049	-0.009	0.322	-0.186	-0.021
73.0	22.967	-1.326	-0.058	-0.078	0.324	-0.212	-0.026
74.0	23.271	-1.608	-0.069	0.001	0.287	-0.303	-0.022
75.0	23.596	-1.539	-0.065	-0.072	0.244	-0.288	-0.027
76.0	23.361	-1.729	-0.074	-0.016	0.223	-0.239	-0.026
77.0	23.805	0.014	0.001	-0.080	0.174	-0.100	-0.022
78.0	23.633	-0.752	-0.032	-0.083	0.093	-0.027	-0.020
79.0	23.728	-0.852	-0.036	-0.024	0.048	0.038	-0.013
80.0	24.178	-0.819	-0.034	-0.014	-0.061	0.058	-0.007
81.0	24.196	-0.599	-0.025	-0.064	-0.146	0.017	-0.011
82.0	24.430	-0.771	-0.032	-0.017	-0.227	0.046	-0.004
83.0	24.325	-0.676	-0.028	-0.017	-0.340	0.040	-0.007
84.0	24.685	-0.555	-0.022	0.013	-0.425	0.032	-0.001
85.0	24.627	-0.944	-0.038	-0.016	-0.487	0.042	-0.011
86.0	24.744	-0.628	-0.025	0.052	-0.606	0.067	-0.007
87.0	24.406	-0.830	-0.034	0.080	-0.736	0.066	-0.010
88.0	24.610	-0.757	-0.031	0.148	-0.828	0.054	-0.008
89.0	24.673	-0.639	-0.026	0.216	-0.915	0.055	-0.007
90.0	24.446	-0.746	-0.031	0.244	-1.007	0.071	-0.010
91.0	24.343	-1.014	-0.042	0.262	-1.038	0.066	-0.012
92.0	24.552	-0.948	-0.039	0.276	-1.140	0.055	-0.017
93.0	24.885	-0.550	-0.022	0.310	-1.189	0.062	-0.007
94.0	24.342	-0.753	-0.031	0.332	-1.221	0.065	-0.010
95.0	24.468	-0.623	-0.025	0.344	-1.300	0.071	-0.006
95.0	2.479	-0.708	-0.285	0.291	-0.081	0.041	0.022
-5.0	2.503	-0.426	-0.170	0.264	-0.091	0.050	0.025
0.0	2.191	-0.455	-0.208	0.368	-0.099	0.054	0.014
0.0	2.182	0.081	0.037	0.515	-0.106	0.057	0.031

RUNFILE> R2C801

AOA	Cn	Cy	Cy/Cn	Cax	Cpt	Crl	Cyw
-5.0	-0.042	-0.032	0.771	0.001	0.001	0.000	0.001
-5.0	-1.283	-0.260	0.203	0.251	0.054	-0.009	-0.002
-4.0	-0.967	-0.294	0.304	0.252	0.052	-0.004	-0.003
-3.0	-0.613	-0.291	0.476	0.258	0.039	-0.006	0.001
-2.0	-0.202	-0.245	1.212	0.259	0.023	0.001	0.001
-1.0	-0.040	-0.291	7.275	0.254	0.013	-0.003	-0.004
0.0	0.241	-0.331	-1.374	0.246	-0.003	-0.002	-0.005
1.0	0.395	-0.316	-0.800	0.242	-0.017	-0.002	-0.007
2.0	0.845	-0.289	-0.342	0.274	-0.029	0.001	-0.004
3.0	1.016	-0.334	-0.329	0.274	-0.040	0.005	-0.006
4.0	1.340	-0.277	-0.207	0.288	-0.057	0.001	-0.007
5.0	1.580	-0.289	-0.183	0.300	-0.074	0.001	-0.007
6.0	1.888	-0.402	-0.213	0.300	-0.090	0.003	-0.008
7.0	2.205	-0.410	-0.186	0.308	-0.094	0.001	-0.007
8.0	2.582	-0.358	-0.139	0.330	-0.103	0.001	-0.008
9.0	2.925	-0.333	-0.114	0.337	-0.104	-0.003	-0.010
10.0	3.388	-0.182	-0.054	0.373	-0.102	0.001	-0.008
11.0	3.648	-0.274	-0.075	0.375	-0.100	0.002	-0.008
12.0	3.933	-0.292	-0.074	0.379	-0.090	0.001	-0.010
13.0	4.378	-0.195	-0.045	0.410	-0.081	0.000	-0.011
14.0	4.608	-0.300	-0.065	0.422	-0.074	0.004	-0.011
15.0	4.916	-0.145	-0.029	0.435	-0.065	0.003	-0.011
16.0	5.313	-0.203	-0.038	0.461	-0.055	0.004	-0.008
17.0	5.851	-0.017	-0.003	0.494	-0.042	0.010	0.001
18.0	5.968	-0.301	-0.050	0.466	-0.037	0.020	-0.006
19.0	6.247	-0.182	-0.029	0.471	-0.031	0.014	-0.006
20.0	6.566	-0.160	-0.024	0.486	-0.025	0.012	-0.009
21.0	6.753	-0.476	-0.071	0.485	-0.018	0.029	-0.014
22.0	7.163	-0.159	-0.022	0.501	-0.010	0.021	-0.011
23.0	7.231	-0.246	-0.034	0.486	0.001	0.016	-0.022
24.0	7.606	-0.322	-0.042	0.495	0.015	0.033	-0.022
25.0	7.988	-0.327	-0.041	0.523	0.027	0.035	-0.017
26.0	8.455	-0.195	-0.023	0.535	0.042	0.026	-0.018
27.0	8.883	-0.173	-0.019	0.539	0.057	0.027	-0.015
28.0	9.034	-0.309	-0.034	0.519	0.084	0.036	-0.022
29.0	9.433	-0.197	-0.021	0.535	0.100	0.026	-0.023
30.0	9.813	-0.028	-0.003	0.541	0.132	0.024	-0.024
31.0	10.022	-0.182	-0.018	0.527	0.149	0.024	-0.027
32.0	10.660	-0.228	-0.021	0.530	0.186	0.025	-0.030
33.0	10.797	-0.006	0.001	0.504	0.201	0.021	-0.036
34.0	11.187	-0.153	-0.014	0.489	0.220	0.000	-0.040
35.0	11.713	-0.164	-0.014	0.482	0.232	-0.007	-0.038
36.0	12.078	0.277	0.023	0.481	0.243	-0.021	-0.043
37.0	12.535	0.171	0.014	0.462	0.239	-0.044	-0.046
38.0	12.880	0.215	0.017	0.462	0.236	-0.033	-0.035
39.0	13.278	-0.011	0.001	0.432	0.233	-0.059	-0.050
40.0	14.027	-0.298	-0.021	0.444	0.227	-0.083	-0.043
41.0	14.323	-0.071	-0.005	0.420	0.224	-0.076	-0.053
42.0	16.817	-1.074	-0.064	0.253	0.339	-0.101	-0.008
41.0	14.552	0.243	0.017	0.438	0.215	-0.059	-0.054
42.0	14.925	-0.232	-0.016	0.423	0.233	-0.034	-0.059
43.0	15.331	-0.210	-0.014	0.430	0.236	-0.042	-0.052

44.0	15.888	-0.458	-0.029	0.431	0.241	-0.083	-0.064
45.0	16.294	-0.119	-0.007	0.427	0.249	-0.098	-0.066
46.0	16.612	-0.765	-0.046	0.397	0.264	-0.074	0.001
47.0	17.155	-0.576	-0.034	0.413	0.279	-0.067	-0.056
48.0	17.595	-0.720	-0.041	0.397	0.303	-0.076	-0.065
49.0	17.972	-0.594	-0.033	0.397	0.316	-0.089	-0.068
50.0	18.440	-0.550	-0.030	0.387	0.332	-0.111	-0.068
51.0	18.699	-1.340	-0.072	0.377	0.343	-0.107	0.005
52.0	19.081	-1.305	-0.068	0.341	0.363	-0.176	0.001
53.0	19.501	-0.691	-0.035	0.313	0.379	-0.113	-0.002
54.0	19.935	-0.723	-0.036	0.297	0.411	-0.154	0.013
55.0	20.048	-1.218	-0.061	0.260	0.419	-0.196	0.010
56.0	20.449	-1.360	-0.067	0.253	0.445	-0.178	-0.065
57.0	20.576	-1.179	-0.057	0.228	0.461	-0.171	-0.066
58.0	20.927	-1.098	-0.052	0.196	0.477	-0.176	-0.062
59.0	21.166	-1.219	-0.058	0.163	0.487	-0.181	-0.058
60.0	21.272	-1.414	-0.066	0.147	0.499	-0.176	-0.055
61.0	21.588	-1.435	-0.066	0.124	0.491	-0.165	-0.048
62.0	21.668	-1.714	-0.079	0.124	0.491	-0.188	-0.045
63.0	21.893	-1.293	-0.059	0.095	0.515	-0.198	-0.045
64.0	22.083	-1.183	-0.054	0.073	0.506	-0.129	-0.044
65.0	22.559	-1.221	-0.054	0.050	0.508	-0.154	-0.040
66.0	22.654	-0.759	-0.033	0.026	0.492	-0.145	-0.037
67.0	22.721	-1.098	-0.048	0.006	0.479	-0.169	-0.038
68.0	22.972	-1.314	-0.057	-0.020	0.481	-0.197	-0.036
69.0	23.156	-1.489	-0.064	-0.038	0.477	-0.212	-0.043
70.0	23.170	-1.631	-0.070	-0.077	0.483	-0.222	-0.046
71.0	23.478	-1.422	-0.061	-0.071	0.482	-0.283	-0.049
72.0	23.712	-1.323	-0.056	-0.068	0.469	-0.286	-0.051
73.0	23.768	-1.567	-0.066	-0.080	0.474	-0.374	-0.056
74.0	24.206	-1.361	-0.056	-0.069	0.450	-0.403	-0.048
75.0	24.659	-1.465	-0.059	-0.070	0.413	-0.363	-0.047
76.0	24.718	-1.575	-0.064	-0.063	0.373	-0.184	-0.039
77.0	24.841	-1.360	-0.055	-0.069	0.295	-0.082	-0.033
78.0	24.346	-1.189	-0.049	-0.080	0.279	-0.014	-0.029
79.0	24.713	-0.455	-0.018	-0.072	0.206	0.014	-0.031
80.0	24.881	-0.424	-0.017	-0.097	0.097	0.011	-0.037
81.0	24.646	-0.055	-0.002	-0.088	0.040	0.061	-0.029
82.0	25.088	-0.659	-0.026	-0.081	-0.075	0.055	-0.030
83.0	24.964	-0.154	-0.006	-0.093	-0.183	0.057	-0.029
84.0	24.863	-0.266	-0.011	-0.103	-0.259	0.101	-0.032
85.0	24.543	0.005	0.000	-0.110	-0.359	0.060	-0.023
86.0	25.195	-0.407	-0.016	-0.083	-0.490	0.078	-0.026
87.0	24.550	-0.036	-0.001	-0.038	-0.593	0.080	-0.034
88.0	24.740	-0.392	-0.016	0.065	-0.760	0.089	-0.028
89.0	24.481	-0.213	-0.009	0.164	-0.875	0.062	-0.034
90.0	24.854	-0.424	-0.017	0.215	-0.985	0.101	-0.036
91.0	24.998	-0.469	-0.019	0.256	-1.051	0.088	-0.037
92.0	25.065	-0.495	-0.020	0.304	-1.100	0.087	-0.026
93.0	24.901	-0.393	-0.016	0.323	-1.186	0.096	-0.030
94.0	25.160	-0.187	-0.007	0.336	-1.264	0.091	-0.026
95.0	24.688	-0.483	-0.020	0.331	-1.267	0.099	-0.029
95.0	2.441	-0.458	-0.187	0.339	-0.092	0.069	0.007
-5.0	2.574	-0.347	-0.135	0.330	-0.096	0.070	0.010
0.0	2.652	-0.322	-0.121	0.342	-0.096	0.069	0.010

RUNFILE> R3C801

AOA	Cn	Cy	Cy/Cn	Cax	Cpt	Crl	Cyw
-5.0	-0.067	-0.039	0.583	-0.024	0.000	0.000	-0.001
-5.0	-1.075	-0.039	0.036	0.240	0.060	-0.003	0.000
-4.0	-0.871	-0.144	0.165	0.234	0.051	0.001	-0.001
-3.0	-0.494	-0.196	0.396	0.235	0.040	0.001	0.001
-2.0	-0.218	-0.123	0.565	0.233	0.024	0.001	-0.003
-1.0	0.025	-0.185	-7.271	0.227	0.011	0.003	-0.005
0.0	0.379	-0.100	-0.264	0.237	-0.001	0.003	-0.002
1.0	0.662	-0.083	-0.126	0.245	-0.018	0.001	0.001
2.0	0.948	-0.072	-0.076	0.255	-0.030	0.001	-0.002
3.0	1.150	-0.094	-0.082	0.265	-0.041	0.003	-0.005
4.0	1.444	-0.133	-0.092	0.284	-0.059	0.006	-0.005
5.0	1.720	-0.148	-0.086	0.298	-0.074	0.003	-0.004
6.0	2.082	-0.122	-0.059	0.310	-0.085	0.000	-0.004
7.0	2.383	-0.052	-0.022	0.315	-0.096	-0.006	-0.006
8.0	2.674	-0.099	-0.037	0.314	-0.098	0.001	-0.007
8.0	3.008	-0.144	-0.048	0.339	-0.101	-0.001	-0.007
9.0	3.454	-0.108	-0.031	0.370	-0.097	-0.003	-0.004
11.0	3.816	-0.024	-0.006	0.385	-0.089	0.006	-0.004
12.0	4.015	-0.007	-0.002	0.386	-0.082	-0.002	-0.007
13.0	4.353	-0.136	-0.031	0.399	-0.070	0.001	-0.009
14.0	4.692	0.028	0.006	0.405	-0.059	0.001	-0.011
15.0	5.017	-0.083	-0.016	0.432	-0.050	0.003	-0.010
16.0	5.404	0.025	0.005	0.472	-0.041	0.002	-0.008
17.0	5.716	0.047	0.008	0.462	-0.024	0.009	-0.011
18.0	6.039	0.193	0.032	0.491	-0.014	0.000	-0.008
19.0	6.339	0.131	0.021	0.492	-0.006	0.003	-0.008
20.0	6.547	0.062	0.010	0.485	0.004	0.010	-0.015
21.0	6.907	0.300	0.043	0.507	0.014	-0.004	-0.020
22.0	7.251	0.012	0.002	0.517	0.029	0.012	-0.020
23.0	7.678	0.339	0.044	0.549	0.046	0.003	-0.017
24.0	7.960	0.087	0.011	0.561	0.066	0.006	-0.015
25.0	8.263	0.217	0.026	0.569	0.078	0.020	-0.020
26.0	8.612	0.381	0.044	0.589	0.097	-0.002	-0.022
27.0	9.010	0.404	0.045	0.578	0.117	0.014	-0.023
28.0	9.110	0.296	0.032	0.561	0.143	0.018	-0.025
29.0	9.521	0.173	0.018	0.562	0.165	0.016	-0.024
30.0	9.959	0.340	0.034	0.567	0.200	0.006	-0.029
31.0	10.254	0.105	0.010	0.562	0.224	0.018	-0.032
32.0	10.644	0.379	0.036	0.557	0.257	0.008	-0.028
33.0	10.877	0.295	0.027	0.542	0.275	0.024	-0.027
34.0	11.313	0.302	0.027	0.514	0.301	0.023	-0.032
35.0	11.656	0.278	0.024	0.509	0.307	0.018	-0.026
36.0	12.095	0.235	0.019	0.501	0.316	0.013	-0.024
37.0	12.503	0.368	0.029	0.489	0.321	0.026	-0.025
38.0	12.894	0.305	0.024	0.482	0.313	0.048	-0.028
39.0	13.350	-0.106	-0.008	0.452	0.297	0.048	-0.024
40.0	13.765	0.450	0.033	0.430	0.288	0.028	-0.034
41.0	14.235	-0.192	-0.013	0.424	0.282	0.014	-0.031
42.0	14.624	0.301	0.021	0.417	0.277	0.020	-0.024
43.0	15.338	-0.521	-0.034	0.418	0.286	0.008	-0.021
44.0	15.635	-0.263	-0.017	0.410	0.294	0.039	-0.033
45.0	16.100	-0.678	-0.042	0.394	0.295	-0.021	-0.047

46.0	16.558	-0.357	-0.022	0.398	0.303	-0.047	-0.044
47.0	17.125	-1.273	-0.074	0.396	0.313	-0.029	-0.040
48.0	17.554	-0.658	-0.038	0.397	0.322	-0.089	-0.061
49.0	18.043	-0.662	-0.037	0.394	0.351	-0.100	0.002
50.0	18.389	-0.597	-0.032	0.359	0.358	-0.103	-0.001
51.0	18.904	-0.206	-0.011	0.347	0.395	-0.175	-0.006
52.0	19.292	-1.267	-0.066	0.339	0.405	-0.187	-0.012
53.0	19.853	-0.664	-0.033	0.317	0.433	-0.226	-0.027
54.0	20.178	-1.607	-0.080	0.274	0.456	-0.311	-0.025
55.0	20.701	-1.035	-0.050	0.268	0.483	-0.341	-0.028
56.0	21.043	-1.685	-0.080	0.215	0.514	-0.404	-0.028
57.0	21.063	-1.371	-0.065	0.189	0.534	-0.381	-0.029
58.0	21.427	-1.816	-0.085	0.175	0.565	-0.414	-0.019
59.0	21.625	-1.559	-0.072	0.157	0.578	-0.434	-0.001
60.0	21.840	-1.582	-0.072	0.125	0.593	-0.439	-0.003
61.0	22.019	-1.689	-0.077	0.116	0.606	-0.430	0.011
62.0	22.173	-1.583	-0.071	0.081	0.607	-0.414	0.018
63.0	22.387	-1.492	-0.067	0.052	0.622	-0.427	-0.070
64.0	22.731	-1.374	-0.060	0.070	0.628	-0.411	-0.060
65.0	22.695	-1.670	-0.074	0.033	0.614	-0.429	-0.056
66.0	22.916	-1.522	-0.066	0.004	0.620	-0.402	-0.047
67.0	23.190	-1.803	-0.078	-0.005	0.613	-0.402	-0.042
68.0	23.490	-1.778	-0.076	-0.002	0.612	-0.400	-0.036
69.0	23.650	-1.927	-0.082	-0.029	0.617	-0.432	-0.037
70.0	23.835	-1.993	-0.084	-0.043	0.628	-0.442	-0.036
71.0	24.148	-1.903	-0.079	-0.059	0.635	-0.480	-0.039
72.0	24.271	-1.907	-0.079	-0.067	0.640	-0.500	-0.040
73.0	24.484	-1.740	-0.071	-0.067	0.649	-0.465	-0.040
74.0	24.378	-1.847	-0.076	-0.087	0.631	-0.429	-0.041
75.0	24.629	-1.314	-0.053	-0.095	0.601	-0.363	-0.037
76.0	24.691	-0.508	-0.021	-0.090	0.565	-0.212	-0.032
77.0	24.702	-1.265	-0.051	-0.110	0.520	-0.097	-0.029
78.0	24.950	-0.653	-0.026	-0.084	0.462	0.018	-0.024
79.0	24.719	-0.882	-0.036	-0.099	0.410	0.023	-0.020
80.0	25.209	-0.826	-0.033	-0.066	0.312	0.054	-0.022
81.0	25.164	-0.819	-0.033	-0.076	0.233	0.081	-0.019
82.0	25.126	-0.679	-0.027	-0.117	0.139	0.073	-0.018
83.0	24.822	-0.713	-0.029	-0.139	0.044	0.036	-0.024
84.0	25.254	-0.733	-0.029	-0.142	-0.077	0.053	-0.026
85.0	25.085	-0.714	-0.028	-0.162	-0.193	0.068	-0.030
86.0	24.659	-0.544	-0.022	-0.165	-0.265	0.046	-0.032
87.0	24.678	-0.629	-0.026	-0.125	-0.403	0.039	-0.039
88.0	25.123	-0.506	-0.020	-0.055	-0.580	0.050	-0.033
89.0	24.597	-0.846	-0.034	0.106	-0.731	0.053	-0.038
90.0	24.578	-0.589	-0.024	0.249	-0.880	0.063	-0.034
91.0	24.453	-0.656	-0.027	0.340	-0.932	0.075	-0.029
92.0	24.738	-0.623	-0.025	0.348	-1.046	0.067	-0.034
93.0	24.470	-0.524	-0.021	0.358	-1.100	0.074	-0.030
94.0	24.741	-0.243	-0.010	0.373	-1.163	0.061	-0.029
95.0	24.650	-0.584	-0.024	0.399	-1.205	0.081	-0.025
95.0	3.174	-0.387	-0.122	0.420	-0.063	0.050	0.025
-5.0	3.231	-0.326	-0.101	0.393	-0.065	0.049	0.031
0.0	3.119	-0.389	-0.125	0.354	-0.065	0.049	0.028

RUNFILE> R4C801

AOA	Cn	Cy	Cy/Cn	Cax	Cpt	Crl	Cyw
-5.0	-0.012	-0.001	0.122	0.016	0.001	0.000	0.002
-5.0	-0.844	-0.003	0.003	0.220	0.067	-0.004	0.005
-4.0	-0.571	0.029	-0.051	0.239	0.056	-0.007	0.008
-3.0	-0.343	0.013	-0.037	0.238	0.042	0.002	0.011
-2.0	-0.159	-0.084	0.528	0.237	0.024	0.004	0.013
-1.0	0.006	-0.004	-0.670	0.230	0.007	-0.002	0.003
0.0	0.232	0.021	0.091	0.249	-0.002	0.003	0.008
1.0	0.436	0.006	0.013	0.244	-0.010	0.004	0.009
2.0	0.668	0.064	0.096	0.254	-0.025	0.004	0.008
3.0	0.943	0.029	0.031	0.264	-0.041	0.004	0.008
4.0	1.067	0.121	0.113	0.262	-0.061	0.001	0.005
5.0	1.466	-0.015	-0.010	0.281	-0.064	0.012	0.009
6.0	1.585	0.112	0.071	0.274	-0.074	0.001	0.006
7.0	1.900	0.130	0.068	0.269	-0.085	0.001	0.006
8.0	2.178	0.187	0.086	0.285	-0.087	0.005	0.007
9.0	2.437	0.012	0.005	0.284	-0.089	0.003	0.005
10.0	2.640	0.018	0.007	0.293	-0.086	-0.003	0.003
11.0	2.866	-0.032	-0.011	0.285	-0.080	-0.005	0.001
12.0	3.053	0.130	0.042	0.306	-0.070	0.001	0.000
13.0	3.264	0.024	0.007	0.311	-0.061	0.005	-0.001
14.0	3.510	0.091	0.026	0.321	-0.051	0.001	-0.002
15.0	3.722	0.061	0.016	0.325	-0.035	0.003	-0.004
16.0	4.169	0.141	0.034	0.348	-0.012	-0.008	0.010
17.0	4.383	0.129	0.029	0.375	0.002	-0.002	0.000
18.0	4.617	0.152	0.033	0.402	0.020	-0.004	0.001
19.0	4.812	-0.138	-0.029	0.407	0.024	-0.007	-0.014
20.0	5.025	0.090	0.018	0.416	0.048	-0.006	-0.003
21.0	5.290	-0.113	-0.021	0.435	0.062	0.010	0.001
22.0	5.636	0.057	0.010	0.464	0.071	-0.001	-0.006
23.0	5.901	0.180	0.030	0.483	0.094	-0.014	-0.011
24.0	6.103	-0.213	-0.035	0.487	0.107	0.006	-0.009
25.0	6.264	0.159	0.025	0.478	0.125	-0.028	-0.009
26.0	6.643	-0.147	-0.022	0.494	0.137	-0.004	-0.017
27.0	6.936	-0.011	-0.002	0.505	0.158	-0.009	-0.009
28.0	7.075	-0.229	-0.032	0.494	0.178	-0.008	-0.016
29.0	7.413	0.115	0.016	0.499	0.202	-0.024	-0.014
30.0	7.505	-0.435	-0.058	0.483	0.219	0.022	-0.020
31.0	7.991	0.474	0.059	0.482	0.245	-0.031	-0.015
32.0	8.179	0.330	0.040	0.465	0.249	-0.018	-0.020
33.0	8.548	0.217	0.025	0.470	0.259	-0.039	-0.023
34.0	8.677	-0.432	-0.050	0.453	0.273	-0.012	-0.018
35.0	8.994	-0.049	-0.005	0.449	0.268	-0.029	-0.038
36.0	9.381	0.612	0.065	0.447	0.259	-0.068	-0.021
37.0	9.621	-0.118	-0.012	0.423	0.258	-0.053	-0.040
38.0	10.097	-0.272	-0.027	0.410	0.244	-0.130	-0.050
39.0	10.334	0.379	0.037	0.412	0.250	-0.172	-0.036
40.0	10.876	0.696	0.064	0.406	0.239	-0.191	-0.051
41.0	11.011	0.265	0.024	0.389	0.234	-0.260	-0.060
42.0	11.499	0.238	0.021	0.404	0.245	-0.103	-0.053
43.0	11.959	0.781	0.065	0.377	0.237	-0.253	-0.059
44.0	12.174	1.039	0.085	0.369	0.257	-0.179	-0.066
45.0	12.525	-0.507	-0.040	0.363	0.244	-0.158	-0.036

46.0	12.853	0.493	0.038	0.361	0.247	-0.101	-0.047
47.0	14.101	1.070	0.076	0.382	0.210	-0.181	-0.040
48.0	14.075	0.670	0.048	0.352	0.269	-0.251	-0.021
49.0	14.187	0.831	0.059	0.333	0.288	-0.186	-0.074
50.0	14.522	0.632	0.044	0.334	0.295	-0.143	-0.059
51.0	14.926	0.462	0.031	0.307	0.348	-0.250	-0.033
52.0	14.946	0.271	0.018	0.291	0.335	-0.245	-0.060
53.0	15.575	0.011	0.001	0.281	0.371	-0.305	-0.054
54.0	16.188	-1.159	-0.072	0.246	0.426	-0.492	-0.084
55.0	16.545	-1.544	-0.093	0.209	0.460	-0.511	-0.097
56.0	16.581	-0.949	-0.057	0.209	0.475	-0.543	-0.112
57.0	16.992	-1.608	-0.095	0.171	0.512	-0.580	-0.077
58.0	17.399	-1.332	-0.077	0.158	0.530	-0.593	-0.076
59.0	17.495	-1.215	-0.069	0.144	0.563	-0.617	-0.083
60.0	17.692	0.829	0.047	0.131	0.553	-0.524	-0.060
61.0	17.542	-0.829	-0.047	0.111	0.538	-0.489	-0.043
62.0	17.997	-0.533	-0.030	0.071	0.585	-0.479	-0.058
63.0	18.161	0.811	0.045	0.092	0.594	-0.522	-0.017
64.0	18.442	-0.069	-0.004	0.089	0.614	-0.540	-0.020
65.0	18.520	-0.776	-0.042	0.060	0.632	-0.602	-0.005
66.0	18.592	-1.032	-0.056	0.051	0.643	-0.577	0.006
67.0	18.638	-1.467	-0.079	-0.029	0.644	-0.559	-0.074
68.0	18.731	-1.672	-0.089	-0.064	0.641	-0.507	-0.074
69.0	18.749	-1.509	-0.081	-0.075	0.657	-0.484	-0.075
70.0	18.996	-1.436	-0.076	-0.086	0.678	-0.452	-0.075
71.0	19.067	-1.493	-0.078	-0.073	0.668	-0.447	-0.072
72.0	19.301	-0.362	-0.019	-0.111	0.669	-0.152	-0.068
73.0	19.364	0.407	0.021	-0.142	0.656	-0.080	-0.071
74.0	19.460	-0.450	-0.023	-0.152	0.657	0.019	-0.067
75.0	19.245	-0.423	-0.022	-0.174	0.632	-0.017	-0.068
76.0	19.331	-0.320	-0.017	-0.133	0.579	0.039	-0.066
77.0	19.298	-0.110	-0.006	-0.110	0.529	0.046	-0.065
78.0	19.401	0.182	0.009	-0.066	0.449	0.027	-0.065
79.0	19.164	0.287	0.015	-0.067	0.401	0.036	0.003
80.0	19.121	0.487	0.025	-0.065	0.334	0.050	-0.072
81.0	19.468	0.178	0.009	-0.046	0.271	0.027	-0.073
82.0	19.218	0.037	0.002	-0.055	0.175	0.037	-0.073
83.0	19.034	-0.016	0.001	-0.067	0.107	0.056	-0.071
84.0	18.971	0.213	0.011	-0.066	0.000	0.033	-0.075
85.0	18.973	0.088	0.005	-0.038	-0.086	0.040	-0.074
86.0	18.792	0.304	0.016	-0.054	-0.181	0.045	-0.077
87.0	18.303	0.192	0.011	-0.015	-0.284	0.054	-0.023
88.0	18.352	0.313	0.017	-0.007	-0.367	0.048	-0.080
89.0	18.388	0.256	0.014	0.124	-0.495	0.039	-0.034
90.0	18.568	0.204	0.011	0.214	-0.662	0.045	-0.036
91.0	18.591	-0.008	0.000	0.323	-0.824	0.041	-0.042
92.0	18.395	0.318	0.017	0.371	-0.874	0.053	-0.032
93.0	18.358	0.344	0.019	0.353	-0.945	0.052	-0.042
94.0	18.396	0.361	0.020	0.390	-0.996	0.061	-0.087
95.0	18.351	0.311	0.017	0.378	-1.025	0.073	-0.041
95.0	0.690	0.091	0.132	0.386	-0.055	0.049	-0.053
-5.0	0.739	0.117	0.158	0.348	-0.057	0.052	-0.050
0.0	0.768	0.137	0.178	0.325	-0.057	0.052	-0.049

RUNFILE> R0B801

AOA	Cn	Cy	Cy/Cn	Cax	Cpt	Crl	Cyw
-5.0	-0.032	-0.017	0.540	-0.006	0.001	0.000	0.001
-5.0	-0.572	-0.038	0.066	0.122	-0.099	-0.006	-0.006
-4.0	-0.353	-0.067	0.189	0.115	-0.077	0.001	-0.006
-3.0	-0.217	-0.081	0.376	0.129	-0.061	-0.005	-0.004
-2.0	-0.215	-0.105	0.487	0.121	-0.051	-0.008	-0.007
-1.0	-0.138	-0.219	1.583	0.126	-0.027	-0.010	-0.005
0.0	0.013	-0.100	-7.709	0.126	-0.014	-0.007	-0.006
1.0	0.083	-0.114	-1.363	0.125	0.006	-0.006	-0.005
2.0	0.153	-0.054	-0.352	0.124	0.020	-0.004	-0.005
3.0	0.238	-0.150	-0.630	0.128	0.035	-0.012	-0.004
4.0	0.427	-0.024	-0.057	0.148	0.054	-0.001	0.001
5.0	0.356	-0.090	-0.253	0.140	0.074	-0.006	-0.004
6.0	0.452	-0.119	-0.263	0.150	0.087	-0.005	-0.004
7.0	0.527	-0.071	-0.135	0.164	0.098	-0.002	-0.003
8.0	0.618	-0.033	-0.054	0.169	0.110	-0.005	-0.001
9.0	0.756	0.024	0.032	0.184	0.124	0.001	-0.001
10.0	0.859	0.004	0.004	0.190	0.137	0.002	0.001
11.0	1.113	0.050	0.045	0.217	0.154	0.001	0.002
12.0	1.170	0.041	0.035	0.214	0.169	0.004	0.005
13.0	1.333	0.018	0.013	0.224	0.188	0.005	0.002
14.0	1.560	0.049	0.031	0.226	0.212	0.009	0.001
15.0	1.719	0.221	0.129	0.235	0.229	-0.008	0.002
16.0	1.803	-0.045	-0.025	0.234	0.250	0.011	0.000
17.0	1.929	-0.023	-0.012	0.253	0.264	0.008	0.001
18.0	2.211	0.082	0.037	0.271	0.301	0.017	0.000
19.0	2.394	0.122	0.051	0.285	0.326	-0.008	-0.003
20.0	2.616	0.117	0.045	0.304	0.350	0.004	-0.002
21.0	2.820	0.263	0.093	0.312	0.387	-0.005	-0.004
22.0	3.037	-0.067	-0.022	0.326	0.423	0.004	-0.004
23.0	3.195	-0.072	-0.022	0.335	0.451	0.008	-0.004
24.0	3.503	0.003	0.001	0.352	0.480	0.011	-0.003
25.0	3.690	-0.048	-0.013	0.348	0.510	0.032	-0.004
26.0	3.946	0.102	0.026	0.365	0.550	0.036	-0.002
27.0	4.179	-0.375	-0.090	0.381	0.586	0.061	0.001
28.0	4.499	-0.061	-0.014	0.395	0.623	0.073	0.001
29.0	4.793	-0.262	-0.055	0.399	0.650	0.062	0.001
30.0	5.033	0.152	0.030	0.404	0.676	0.095	0.001
31.0	5.205	-0.161	-0.031	0.412	0.709	0.090	0.000
32.0	5.468	-0.322	-0.059	0.412	0.747	0.110	0.000
33.0	5.859	-0.257	-0.044	0.408	0.777	0.108	-0.002
34.0	5.883	-0.659	-0.112	0.411	0.825	0.131	-0.003
35.0	6.205	-0.670	-0.108	0.408	0.858	0.122	-0.003
36.0	6.400	-1.189	-0.186	0.418	0.897	0.069	-0.004
37.0	6.526	-0.783	-0.120	0.410	0.930	0.114	-0.005
38.0	7.170	-0.372	-0.052	0.419	0.978	0.141	0.004
39.0	7.200	-1.094	-0.152	0.392	0.996	0.014	0.002
40.0	7.447	-0.169	-0.023	0.383	1.042	0.086	0.003
41.0	7.724	-0.647	-0.084	0.383	1.055	0.104	0.005
42.0	7.914	-1.224	-0.155	0.338	1.083	0.052	-0.002
43.0	8.274	-1.924	-0.233	0.340	1.091	-0.054	0.001
44.0	8.682	-1.479	-0.170	0.323	1.144	-0.097	-0.004
45.0	8.872	-1.677	-0.189	0.313	1.163	-0.121	-0.004

46.0	9.353	-1.294	-0.138	0.300	1.175	-0.185	-0.002
47.0	9.709	-2.156	-0.222	0.286	1.212	-0.245	-0.002
48.0	10.009	-3.233	-0.323	0.273	1.231	-0.349	-0.001
49.0	10.545	-2.497	-0.237	0.256	1.247	-0.434	-0.005
50.0	10.913	-2.784	-0.255	0.258	1.259	-0.407	-0.005
51.0	11.238	-0.778	-0.069	0.256	1.263	-0.387	-0.007
52.0	11.859	-2.298	-0.194	0.241	1.271	-0.577	-0.009
53.0	12.308	-2.120	-0.172	0.239	1.264	-0.618	-0.008
54.0	12.688	-2.675	-0.211	0.236	1.260	-0.602	-0.002
55.0	12.969	-2.533	-0.195	0.189	1.262	-0.715	-0.010
56.0	13.578	-2.931	-0.216	0.187	1.266	-0.717	-0.006
57.0	14.087	-1.914	-0.136	0.141	1.238	-0.735	-0.012
58.0	14.407	-2.303	-0.160	0.122	1.233	-0.711	-0.010
59.0	14.528	-2.424	-0.167	0.088	1.211	-0.535	-0.010
60.0	14.856	-1.898	-0.128	0.093	1.198	-0.541	-0.006
61.0	15.119	-1.023	-0.068	0.069	1.191	-0.454	-0.011
62.0	15.223	-2.118	-0.139	0.058	1.191	-0.388	-0.008
63.0	15.594	-1.365	-0.088	0.060	1.177	-0.331	-0.004
64.0	15.841	-0.284	-0.018	0.062	1.169	-0.291	-0.003
65.0	15.974	-0.494	-0.031	0.055	1.189	-0.335	-0.003
66.0	15.636	0.082	0.005	0.021	1.222	-0.347	-0.005
67.0	15.753	0.520	0.033	-0.011	1.234	-0.342	-0.006
68.0	15.796	1.081	0.068	-0.030	1.257	-0.212	-0.004
69.0	15.723	1.103	0.070	-0.041	1.272	-0.126	0.001
70.0	15.816	-0.013	0.001	-0.068	1.296	0.026	0.005
71.0	16.047	0.659	0.041	-0.172	1.333	0.051	0.004
72.0	16.182	-0.124	-0.008	-0.169	1.379	0.073	0.009
73.0	16.176	0.691	0.043	-0.232	1.375	0.002	0.003
74.0	16.284	0.647	0.040	-0.253	1.372	0.031	0.003
75.0	16.393	-0.213	-0.013	-0.226	1.373	-0.022	0.006
76.0	16.427	0.372	0.023	-0.233	1.360	-0.009	0.007
77.0	16.161	0.906	0.056	-0.260	1.338	-0.007	0.005
78.0	15.836	0.801	0.051	-0.267	1.301	0.004	0.003
79.0	15.972	0.545	0.034	-0.294	1.298	-0.012	0.003
80.0	16.056	0.856	0.053	-0.299	1.275	0.009	0.006
81.0	15.900	0.796	0.050	-0.300	1.235	0.016	0.004
82.0	15.762	0.523	0.033	-0.307	1.192	0.012	0.007
83.0	15.965	0.534	0.033	-0.302	1.146	0.012	0.007
84.0	16.060	0.786	0.049	-0.357	1.105	0.010	0.008
85.0	15.922	0.786	0.049	-0.339	1.028	-0.017	0.006
86.0	15.431	0.939	0.061	-0.389	0.983	-0.013	0.006
87.0	15.335	0.924	0.060	-0.339	0.875	0.026	0.008
88.0	15.396	0.656	0.043	-0.254	0.800	0.006	0.004
89.0	15.108	0.975	0.065	0.002	0.687	-0.116	0.000
90.0	15.282	1.020	0.067	0.093	0.632	-0.102	-0.001
91.0	15.341	1.520	0.099	0.120	0.567	-0.104	0.002
92.0	15.319	1.386	0.090	0.107	0.525	-0.126	-0.002
93.0	15.365	1.210	0.079	0.126	0.470	-0.148	-0.006
94.0	15.272	1.587	0.104	0.130	0.420	-0.144	-0.009
95.0	15.496	1.469	0.095	0.136	0.382	-0.151	-0.011
95.0	1.060	1.025	0.967	0.241	-0.036	0.009	0.011
-5.0	1.152	1.056	0.917	0.200	-0.036	0.010	0.013
0.0	1.075	1.003	0.934	0.192	-0.037	0.009	0.011

RUNFILE> R0B802

AOA	Cn	Cy	Cy/Cn	Cax	Cpt	Crl	Cyw
0.0	0.008	-0.013	-1.634	-0.002	0.000	0.000	0.000
95.0	0.076	0.017	0.221	0.007	0.000	0.001	0.001
95.0	14.342	0.289	0.020	-0.099	0.393	-0.114	-0.020
94.0	14.298	0.587	0.041	-0.093	0.439	-0.115	-0.018
93.0	14.261	0.254	0.018	-0.102	0.473	-0.119	-0.021
92.0	14.318	0.337	0.024	-0.105	0.538	-0.110	-0.017
91.0	14.444	0.363	0.025	-0.109	0.592	-0.123	-0.017
90.0	14.491	0.130	0.009	-0.129	0.638	-0.164	-0.020
89.0	14.511	-0.042	-0.003	-0.208	0.694	-0.165	-0.020
88.0	14.516	-0.391	-0.027	-0.485	0.788	-0.015	-0.012
87.0	15.060	-0.742	-0.049	-0.670	0.964	0.001	-0.009
86.0	15.171	0.220	0.014	-0.660	1.041	-0.065	-0.012
85.0	15.189	-0.146	-0.010	-0.611	1.088	-0.044	-0.010
84.0	15.623	-0.572	-0.037	-0.520	1.144	0.009	-0.005
83.0	15.480	-0.469	-0.030	-0.494	1.182	-0.003	-0.006
82.0	15.726	-0.476	-0.030	-0.443	1.222	0.018	-0.002
81.0	15.718	-0.287	-0.018	-0.414	1.233	0.027	-0.003
80.0	15.787	-0.349	-0.022	-0.404	1.270	0.022	-0.005
79.0	15.796	-0.384	-0.024	-0.377	1.295	0.042	-0.003
78.0	15.770	0.173	0.011	-0.376	1.323	0.025	-0.005
77.0	15.946	-0.325	-0.020	-0.335	1.337	0.028	-0.002
76.0	15.977	-0.636	-0.040	-0.322	1.351	0.032	-0.004
75.0	15.798	-0.430	-0.027	-0.306	1.353	0.013	-0.004
74.0	15.993	-0.509	-0.032	-0.284	1.366	0.000	-0.004
73.0	16.053	-0.255	-0.016	-0.218	1.385	-0.017	-0.006
72.0	15.936	-0.279	-0.018	-0.175	1.399	-0.042	-0.005
71.0	15.762	-0.660	-0.042	-0.128	1.381	-0.045	-0.002
70.0	15.860	-0.751	-0.047	-0.109	1.341	-0.013	-0.003
69.0	15.619	-0.293	-0.019	-0.106	1.301	-0.043	-0.005
68.0	15.707	-1.040	-0.066	-0.077	1.262	-0.239	-0.006
67.0	15.796	-1.110	-0.070	-0.033	1.248	-0.284	-0.012
66.0	15.709	-1.915	-0.122	-0.019	1.227	-0.341	-0.012
65.0	15.670	-2.209	-0.141	-0.007	1.195	-0.305	-0.013
64.0	15.549	-1.399	-0.090	0.028	1.192	-0.492	-0.018
63.0	15.649	-1.128	-0.072	0.051	1.182	-0.336	-0.014
62.0	14.812	-0.821	-0.055	0.067	1.170	-0.410	-0.017
61.0	15.153	-0.169	-0.011	0.075	1.181	-0.312	-0.016
60.0	14.723	-1.316	-0.089	0.070	1.193	-0.326	-0.015
59.0	14.552	-2.105	-0.145	0.100	1.222	-0.329	-0.009
58.0	14.241	-2.950	-0.207	0.107	1.200	-0.574	-0.015
57.0	14.156	-2.947	-0.208	0.141	1.204	-0.735	-0.019
56.0	13.460	-4.077	-0.303	0.170	1.246	-0.799	-0.018
55.0	13.192	-2.563	-0.194	0.183	1.273	-0.618	-0.017
54.0	12.395	-3.332	-0.269	0.209	1.328	-0.646	-0.014
53.0	12.003	-1.921	-0.160	0.238	1.328	-0.597	-0.013
52.0	11.244	-3.201	-0.285	0.244	1.351	-0.451	-0.011
51.0	10.872	-3.159	-0.291	0.257	1.339	-0.324	-0.007
50.0	10.754	-2.286	-0.213	0.302	1.270	-0.315	-0.009
49.0	9.984	-3.681	-0.369	0.306	1.296	-0.374	-0.010
48.0	9.966	-3.326	-0.334	0.318	1.278	-0.273	-0.006
47.0	9.543	-3.597	-0.377	0.339	1.235	-0.264	-0.006
46.0	9.210	-2.616	-0.284	0.339	1.229	-0.277	-0.009

45.0	8.921	-1.436	-0.161	0.352	1.196	-0.155	-0.008
44.0	8.795	-2.062	-0.234	0.377	1.161	-0.157	-0.003
43.0	8.457	-1.125	-0.133	0.379	1.138	-0.037	-0.003
42.0	8.008	-1.910	-0.238	0.379	1.097	-0.080	-0.006
41.0	7.758	-0.891	-0.115	0.409	1.065	0.050	-0.003
40.0	7.757	-0.867	-0.112	0.414	1.033	0.030	-0.003
39.0	7.240	-0.251	-0.035	0.421	1.013	0.094	-0.003
38.0	6.968	-1.342	-0.193	0.446	0.972	0.044	-0.002
37.0	6.966	-0.916	-0.131	0.460	0.933	0.051	0.000
36.0	6.674	-0.835	-0.125	0.469	0.902	0.076	-0.001
35.0	6.534	-0.772	-0.118	0.457	0.864	0.021	-0.002
34.0	6.052	-0.785	-0.130	0.561	0.817	0.048	-0.003
33.0	5.968	-0.468	-0.078	0.468	0.784	0.057	-0.002
32.0	5.989	-0.509	-0.085	0.472	0.745	0.080	0.000
31.0	5.619	-0.239	-0.042	0.468	0.700	0.099	0.000
30.0	5.426	-0.470	-0.087	0.460	0.671	0.089	0.001
29.0	5.295	-0.762	-0.144	0.466	0.646	0.032	0.000
28.0	5.078	-0.221	-0.044	0.468	0.598	0.049	0.002
27.0	4.984	-0.136	-0.027	0.462	0.585	0.053	0.001
26.0	4.732	-0.158	-0.033	0.451	0.538	0.035	0.001
25.0	4.505	-0.418	-0.093	0.443	0.504	0.027	0.002
24.0	4.244	-0.302	-0.071	0.439	0.473	0.033	0.001
23.0	4.109	-0.301	-0.073	0.433	0.441	0.039	0.000
22.0	3.912	-0.296	-0.076	0.420	0.404	0.043	-0.002
21.0	3.753	-0.375	-0.100	0.417	0.376	0.038	0.000
20.0	3.491	-0.107	-0.031	0.418	0.336	0.044	0.001
19.0	3.302	-0.203	-0.061	0.395	0.311	0.043	-0.004
18.0	3.099	-0.325	-0.105	0.404	0.279	0.040	0.001
17.0	3.002	-0.376	-0.125	0.382	0.258	0.030	-0.005
16.0	2.837	-0.058	-0.020	0.391	0.222	0.041	-0.004
15.0	2.683	-0.234	-0.087	0.381	0.192	0.042	-0.003
14.0	2.553	-0.200	-0.078	0.377	0.171	0.040	-0.006
13.0	2.407	-0.246	-0.102	0.377	0.156	0.045	-0.001
12.0	2.198	-0.292	-0.133	0.365	0.134	0.041	-0.003
11.0	2.105	-0.289	-0.137	0.376	0.117	0.047	-0.002
10.0	2.070	-0.275	-0.133	0.380	0.103	0.046	-0.002
9.0	1.872	-0.238	-0.127	0.361	0.082	0.041	-0.004
8.0	1.865	-0.164	-0.088	0.359	0.070	0.042	-0.003
7.0	1.811	-0.211	-0.116	0.359	0.060	0.042	-0.003
6.0	1.756	-0.234	-0.133	0.364	0.044	0.043	-0.003
5.0	1.653	-0.294	-0.178	0.347	0.030	0.042	-0.006
4.0	1.490	-0.376	-0.252	0.335	0.019	0.038	-0.007
3.0	1.594	-0.215	-0.135	0.342	0.000	0.046	-0.005
2.0	1.504	-0.239	-0.159	0.344	-0.019	0.046	-0.006
1.0	1.446	-0.404	-0.279	0.353	-0.031	0.042	-0.004
0.0	1.528	-0.270	-0.177	0.363	-0.050	0.039	-0.004
-1.0	1.525	-0.208	-0.137	0.369	-0.072	0.039	-0.003
-2.0	1.332	-0.259	-0.195	0.358	-0.090	0.043	-0.004
-3.0	1.339	-0.231	-0.173	0.364	-0.107	0.045	-0.003
-4.0	1.339	-0.180	-0.135	0.376	-0.121	0.045	-0.002
-5.0	1.267	-0.191	-0.151	0.384	-0.135	0.044	-0.002
-5.0	1.635	-0.179	-0.109	0.240	-0.046	0.048	0.001
95.0	1.675	-0.165	-0.099	0.297	-0.043	0.047	0.001

RUNFILE> R1B801

AOA	Cn	Cy	Cy/Cn	Cax	Cpt	Crl	Cyw
-5.0	-0.013	-0.009	0.691	0.011	-0.002	0.000	0.000
-5.0	-0.251	0.017	-0.067	0.200	-0.087	-0.003	0.000
-4.0	-0.201	-0.031	0.156	0.201	-0.070	-0.002	-0.002
-3.0	-0.190	-0.068	0.357	0.193	-0.059	-0.003	-0.003
-2.0	-0.063	-0.084	1.334	0.196	-0.044	-0.003	-0.002
-1.0	0.127	-0.068	-0.536	0.206	-0.030	-0.002	-0.002
0.0	0.212	-0.110	-0.519	0.200	-0.015	0.001	-0.004
1.0	0.390	-0.058	-0.148	0.227	0.001	0.004	-0.001
2.0	0.504	-0.135	-0.268	0.226	0.017	0.001	-0.002
3.0	0.637	-0.073	-0.115	0.240	0.030	0.002	-0.001
4.0	0.818	-0.067	-0.082	0.258	0.043	0.003	0.001
5.0	0.878	-0.085	-0.097	0.269	0.057	0.007	-0.002
6.0	0.982	-0.098	-0.100	0.286	0.067	0.007	-0.003
7.0	1.148	-0.106	-0.093	0.302	0.079	0.004	-0.002
8.0	1.246	-0.116	-0.093	0.318	0.090	0.008	-0.002
9.0	1.436	-0.023	-0.016	0.345	0.103	0.011	0.001
10.0	1.563	-0.085	-0.054	0.358	0.114	0.010	0.001
11.0	1.642	-0.093	-0.056	0.360	0.125	0.005	0.000
12.0	1.887	-0.014	-0.008	0.395	0.135	0.009	0.003
13.0	1.986	-0.042	-0.021	0.400	0.149	0.007	0.002
14.0	2.016	-0.067	-0.033	0.397	0.163	0.012	0.000
15.0	2.133	-0.037	-0.017	0.409	0.180	0.017	-0.001
16.0	2.187	-0.115	-0.053	0.419	0.186	0.014	-0.005
17.0	2.238	-0.182	-0.081	0.419	0.203	0.017	-0.007
18.0	2.538	-0.088	-0.035	0.449	0.222	0.014	-0.005
19.0	2.684	-0.132	-0.049	0.470	0.242	0.015	-0.004
20.0	2.809	-0.115	-0.041	0.467	0.260	0.014	-0.007
21.0	3.084	-0.125	-0.041	0.502	0.277	0.015	-0.004
22.0	3.211	-0.094	-0.029	0.506	0.297	0.015	-0.006
23.0	3.367	-0.201	-0.060	0.511	0.322	0.015	-0.008
24.0	3.490	-0.162	-0.046	0.510	0.344	0.005	-0.009
25.0	3.749	-0.122	-0.033	0.529	0.373	0.006	-0.008
26.0	4.015	-0.115	-0.029	0.551	0.402	0.010	-0.006
27.0	4.287	-0.092	-0.021	0.563	0.427	-0.001	-0.006
28.0	4.521	0.029	0.006	0.567	0.463	-0.005	-0.007
29.0	4.710	-0.267	-0.057	0.567	0.490	-0.005	-0.007
30.0	4.961	-0.168	-0.034	0.584	0.514	-0.012	-0.004
31.0	5.231	-0.048	-0.009	0.590	0.551	-0.015	-0.006
32.0	5.499	0.065	0.012	0.603	0.577	-0.023	-0.004
33.0	5.611	-0.351	-0.063	0.586	0.609	-0.020	-0.008
34.0	5.788	-0.144	-0.025	0.572	0.642	-0.025	-0.010
35.0	6.169	-0.137	-0.022	0.598	0.666	-0.028	-0.006
36.0	6.521	-0.009	-0.001	0.616	0.702	-0.042	-0.003
37.0	6.578	-0.128	-0.019	0.591	0.730	-0.042	-0.009
38.0	6.833	-0.056	-0.008	0.596	0.745	-0.040	-0.007
39.0	6.963	-0.093	-0.013	0.594	0.778	-0.023	-0.006
40.0	7.354	-0.071	-0.010	0.595	0.812	-0.056	-0.005
41.0	7.527	0.039	0.005	0.588	0.834	-0.050	-0.007
42.0	7.725	-0.419	-0.054	0.573	0.850	-0.053	-0.008
43.0	7.729	-0.354	-0.046	0.548	0.866	-0.069	-0.012
44.0	8.069	-0.248	-0.031	0.536	0.899	-0.078	-0.014
45.0	8.197	-0.613	-0.075	0.543	0.908	-0.080	-0.011

46.0	8.494	-0.360	-0.042	0.521	0.923	-0.089	-0.011
47.0	8.679	-0.388	-0.045	0.516	0.949	-0.092	-0.013
48.0	8.984	-0.775	-0.086	0.502	0.945	-0.137	-0.015
49.0	9.288	-0.215	-0.023	0.499	0.969	-0.111	-0.014
50.0	9.360	-0.675	-0.072	0.499	0.988	-0.154	-0.013
51.0	9.655	-0.496	-0.051	0.476	0.988	-0.150	-0.013
52.0	9.729	-0.456	-0.047	0.465	1.008	-0.122	-0.013
53.0	9.943	-0.900	-0.091	0.444	1.004	-0.166	-0.014
54.0	10.184	-0.833	-0.082	0.434	1.018	-0.154	-0.013
55.0	10.323	-0.258	-0.025	0.418	1.034	-0.147	-0.014
56.0	10.627	-0.306	-0.029	0.394	1.030	-0.162	-0.014
57.0	10.688	-0.228	-0.021	0.376	1.050	-0.150	-0.014
58.0	11.122	-0.557	-0.050	0.363	1.048	-0.173	-0.012
59.0	11.066	-0.307	-0.028	0.323	1.059	-0.162	-0.017
60.0	11.143	-0.027	-0.002	0.319	1.044	-0.169	-0.016
61.0	11.485	-0.249	-0.022	0.295	1.047	-0.166	-0.015
62.0	11.502	-0.440	-0.038	0.279	1.060	-0.174	-0.015
63.0	11.648	-0.746	-0.064	0.270	1.057	-0.166	-0.013
64.0	11.867	-0.047	-0.004	0.248	1.048	-0.188	-0.015
65.0	11.999	-0.292	-0.024	0.247	1.044	-0.165	-0.014
66.0	12.128	-0.382	-0.032	0.213	1.033	-0.180	-0.014
67.0	12.106	-0.850	-0.070	0.223	1.025	-0.175	-0.011
68.0	12.348	-0.224	-0.018	0.205	1.023	-0.153	-0.013
69.0	12.505	-0.701	-0.056	0.202	1.017	-0.167	-0.011
70.0	12.467	-0.152	-0.012	0.196	1.010	-0.159	-0.012
71.0	12.789	-0.398	-0.031	0.196	1.014	-0.178	-0.008
72.0	12.738	-0.856	-0.067	0.185	1.001	-0.226	-0.010
73.0	12.860	-0.455	-0.035	0.176	1.011	-0.220	-0.012
74.0	12.926	-0.428	-0.033	0.190	0.990	-0.242	-0.010
75.0	12.844	-0.078	-0.006	0.170	0.980	-0.218	-0.014
76.0	13.013	-0.876	-0.067	0.157	0.965	-0.137	-0.011
77.0	12.914	0.524	0.041	0.140	0.972	-0.033	-0.012
78.0	12.948	0.286	0.022	0.127	0.931	-0.014	-0.011
79.0	13.016	0.163	0.013	0.112	0.915	-0.019	-0.010
80.0	13.108	0.380	0.029	0.111	0.898	0.000	-0.008
81.0	13.121	-0.162	-0.012	0.099	0.879	-0.012	-0.008
82.0	13.256	0.261	0.020	0.097	0.846	0.020	-0.007
83.0	13.316	0.026	0.002	0.097	0.810	0.018	-0.006
84.0	13.348	-0.252	-0.019	0.096	0.786	0.009	-0.004
85.0	13.419	0.200	0.015	0.112	0.748	0.014	-0.002
86.0	13.465	-0.186	-0.014	0.113	0.721	0.012	-0.003
87.0	13.428	0.218	0.016	0.145	0.676	0.016	-0.003
88.0	13.652	0.182	0.013	0.154	0.631	0.031	-0.003
89.0	13.646	0.068	0.005	0.200	0.610	0.001	-0.003
90.0	13.492	0.105	0.008	0.201	0.563	0.012	-0.002
91.0	13.635	0.179	0.013	0.207	0.557	0.016	-0.002
92.0	13.436	0.251	0.019	0.202	0.530	0.030	-0.003
93.0	13.512	-0.049	-0.004	0.192	0.521	0.015	0.001
94.0	13.345	0.333	0.025	0.183	0.488	0.020	-0.003
95.0	13.284	0.293	0.022	0.186	0.468	0.029	-0.003
95.0	2.777	0.209	0.075	0.460	-0.054	0.051	0.010
-5.0	2.827	0.372	0.131	0.418	-0.056	0.057	0.012
0.0	2.738	0.494	0.180	0.474	-0.061	0.059	0.014

RUNFILE> R2B801

AOA	Cn	Cy	Cy/Cn	Cax	Cpt	Crl	Cyw
-5.0	-0.066	-0.016	0.248	0.010	-0.006	0.001	0.000
-5.0	-0.142	0.077	-0.542	0.208	-0.080	-0.009	0.001
-4.0	-0.239	-0.100	0.419	0.191	-0.069	-0.008	-0.003
-3.0	0.102	0.042	0.409	0.229	-0.057	-0.006	0.003
-2.0	0.143	0.017	0.121	0.225	-0.046	-0.005	0.000
-1.0	0.116	-0.067	-0.576	0.216	-0.032	-0.008	-0.001
0.0	0.347	-0.029	-0.083	0.235	-0.018	-0.005	0.000
1.0	0.427	0.030	0.069	0.243	-0.005	0.000	0.000
2.0	0.409	-0.092	-0.225	0.233	0.005	-0.004	-0.005
3.0	0.567	-0.022	-0.038	0.248	0.021	0.001	-0.002
4.0	0.676	-0.020	-0.030	0.259	0.034	0.000	0.000
5.0	0.785	0.018	0.023	0.271	0.044	0.001	0.000
6.0	0.951	0.018	0.019	0.297	0.055	0.005	0.001
7.0	0.945	-0.016	-0.017	0.286	0.069	0.007	-0.004
8.0	1.070	-0.009	-0.009	0.305	0.078	0.008	-0.001
9.0	1.184	-0.022	-0.018	0.319	0.087	0.011	0.001
10.0	1.264	-0.015	-0.012	0.319	0.098	0.010	-0.003
11.0	1.319	-0.077	-0.059	0.321	0.109	0.012	-0.004
12.0	1.487	0.049	0.033	0.347	0.120	0.019	-0.002
13.0	1.720	-0.011	-0.007	0.366	0.133	0.014	0.001
14.0	1.713	-0.006	-0.004	0.365	0.145	0.020	-0.003
15.0	1.946	0.048	0.025	0.391	0.159	0.022	-0.003
16.0	1.996	0.034	0.017	0.377	0.179	0.020	-0.009
17.0	2.200	0.064	0.029	0.395	0.197	0.021	-0.009
18.0	2.314	-0.018	-0.008	0.404	0.211	0.025	-0.009
19.0	2.512	-0.008	-0.003	0.422	0.229	0.027	-0.009
20.0	2.556	-0.105	-0.041	0.424	0.247	0.024	-0.011
21.0	2.893	0.054	0.019	0.459	0.270	0.030	-0.006
22.0	3.022	-0.026	-0.008	0.463	0.288	0.030	-0.007
23.0	3.288	-0.048	-0.015	0.475	0.316	0.030	-0.008
24.0	3.377	-0.010	-0.003	0.479	0.333	0.033	-0.007
25.0	3.734	0.194	0.052	0.510	0.364	0.032	-0.003
26.0	4.027	0.041	0.010	0.520	0.394	0.024	-0.001
27.0	4.224	0.048	0.011	0.515	0.424	0.020	-0.005
28.0	4.522	0.012	0.003	0.529	0.455	0.015	-0.004
29.0	4.699	-0.031	-0.007	0.533	0.486	0.010	-0.003
30.0	4.922	0.085	0.017	0.549	0.515	0.009	-0.006
31.0	5.062	-0.039	-0.008	0.536	0.545	0.003	-0.009
32.0	5.297	-0.092	-0.017	0.522	0.580	0.004	-0.010
33.0	5.565	-0.043	-0.008	0.529	0.620	0.007	-0.009
34.0	5.915	-0.113	-0.019	0.544	0.643	-0.008	-0.006
35.0	6.030	-0.181	-0.030	0.533	0.676	-0.013	-0.007
36.0	6.214	-0.029	-0.005	0.527	0.707	-0.013	-0.009
37.0	6.473	-0.385	-0.059	0.542	0.730	-0.015	-0.003
38.0	6.790	-0.016	-0.002	0.540	0.761	-0.014	-0.004
39.0	6.879	-0.138	-0.020	0.511	0.789	-0.031	-0.007
40.0	7.277	-0.218	-0.030	0.520	0.815	-0.016	-0.002
41.0	7.340	-0.011	-0.001	0.486	0.843	-0.033	-0.007
42.0	8.465	-0.525	-0.062	0.542	0.963	-0.059	-0.008
43.0	7.880	-0.004	0.001	0.492	0.884	-0.061	-0.004
44.0	8.090	-0.686	-0.085	0.474	0.904	-0.069	-0.006
45.0	8.257	-0.800	-0.097	0.452	0.929	-0.092	-0.007

46.0	8.690	-0.404	-0.047	0.505	0.949	-0.079	-0.005
47.0	8.740	-0.400	-0.046	0.456	0.960	-0.097	-0.006
48.0	9.199	-0.536	-0.058	0.441	0.984	-0.111	-0.006
49.0	9.334	-0.436	-0.047	0.433	0.992	-0.117	-0.004
50.0	9.724	-0.808	-0.083	0.421	1.007	-0.160	-0.004
51.0	9.881	-0.615	-0.062	0.418	1.020	-0.172	-0.003
52.0	9.960	-0.108	-0.011	0.399	1.045	-0.175	-0.004
53.0	10.366	-0.468	-0.045	0.361	1.052	-0.160	-0.005
54.0	10.609	-0.412	-0.039	0.388	1.068	-0.197	0.001
55.0	10.633	-0.357	-0.034	0.344	1.072	-0.193	-0.001
56.0	11.070	-0.504	-0.046	0.346	1.090	-0.204	0.001
57.0	11.108	-0.691	-0.062	0.287	1.090	-0.220	-0.004
58.0	11.191	-0.206	-0.018	0.267	1.098	-0.229	-0.004
59.0	11.612	-0.672	-0.058	0.260	1.095	-0.200	-0.003
60.0	11.382	-0.891	-0.078	0.230	1.090	-0.216	-0.003
61.0	11.742	-0.367	-0.031	0.221	1.100	-0.228	-0.002
62.0	11.872	-0.419	-0.035	0.196	1.094	-0.186	-0.003
63.0	12.285	-0.925	-0.075	0.182	1.093	-0.232	-0.002
64.0	12.067	-0.258	-0.021	0.156	1.089	-0.239	-0.005
65.0	12.164	-0.764	-0.063	0.153	1.065	-0.251	-0.002
64.0	11.491	-0.011	0.001	0.420	1.054	-0.217	0.023
65.0	11.242	0.158	0.014	0.355	1.042	-0.213	0.016
65.0	11.479	-0.409	-0.036	0.235	1.070	-0.275	0.009
66.0	11.379	0.006	0.001	0.165	1.072	-0.261	0.006
67.0	11.758	-0.429	-0.036	0.108	1.065	-0.249	0.008
68.0	12.131	-0.393	-0.032	0.067	1.062	-0.252	0.008
69.0	12.159	-0.882	-0.073	0.041	1.067	-0.247	0.009
70.0	12.440	-1.174	-0.094	0.027	1.061	-0.273	0.009
71.0	12.542	-1.062	-0.085	0.004	1.047	-0.307	0.005
72.0	12.717	-0.835	-0.066	0.005	1.050	-0.292	0.006
73.0	13.043	-0.708	-0.054	0.012	1.045	-0.303	0.007
74.0	13.015	-0.321	-0.025	0.010	1.034	-0.297	0.008
75.0	13.459	-0.451	-0.034	0.015	1.034	-0.191	0.014
76.0	13.307	-0.305	-0.023	0.000	1.003	-0.136	0.015
77.0	13.643	0.107	0.008	-0.005	1.004	-0.070	0.017
78.0	13.588	0.152	0.011	0.002	0.992	0.041	0.020
79.0	13.721	-0.691	-0.050	0.001	0.957	0.001	0.021
80.0	13.749	-0.277	-0.020	-0.019	0.935	0.024	0.020
81.0	13.846	-0.022	-0.002	-0.049	0.908	0.012	0.018
82.0	13.689	-0.143	-0.010	-0.054	0.880	0.025	0.019
83.0	14.181	-0.137	-0.010	-0.055	0.884	0.039	0.022
84.0	14.186	-0.157	-0.011	-0.070	0.847	0.037	0.020
85.0	14.205	-0.189	-0.013	-0.076	0.800	0.036	0.022
86.0	14.372	-0.189	-0.013	-0.077	0.763	0.035	0.019
87.0	14.224	-0.302	-0.021	-0.057	0.735	0.023	0.019
88.0	14.122	-0.171	-0.012	-0.073	0.684	0.007	0.012
89.0	14.194	-0.241	-0.017	-0.023	0.619	0.013	0.010
90.0	14.169	-0.340	-0.024	0.008	0.587	0.021	0.012
91.0	14.162	-0.290	-0.020	0.117	0.568	0.022	0.022
92.0	14.383	0.245	0.017	0.117	0.548	0.026	0.020
93.0	14.191	-0.039	-0.003	0.113	0.517	0.029	0.021
94.0	14.012	-0.118	-0.008	0.120	0.498	-0.008	0.021
95.0	14.073	0.024	0.002	0.137	0.495	0.026	0.023
95.0	2.602	-0.185	-0.071	0.352	-0.068	0.035	0.034
-5.0	2.729	-0.101	-0.037	0.316	-0.066	0.034	0.037
0.0	2.636	-0.116	-0.044	0.324	-0.068	0.034	0.036

RUNFILE> R3B801

AOA	Cn	Cy	Cy/Cn	Cax	Cpt	Crl	Cyw
-5.0	-0.053	-0.016	0.295	-0.005	-0.002	0.000	-0.003
-5.0	-0.311	-0.101	0.324	0.139	-0.079	-0.007	-0.007
-4.0	-0.218	-0.056	0.257	0.163	-0.070	-0.005	-0.003
-3.0	-0.144	0.008	-0.054	0.172	-0.060	-0.003	-0.003
-2.0	-0.109	-0.096	0.887	0.160	-0.044	-0.006	-0.005
-1.0	0.000	-0.096	373.742	0.166	-0.031	-0.004	-0.004
0.0	0.146	-0.069	-0.474	0.173	-0.019	-0.004	-0.002
1.0	0.212	-0.061	-0.289	0.165	-0.005	0.001	-0.003
2.0	0.274	-0.089	-0.324	0.166	0.013	0.001	-0.003
3.0	0.404	-0.032	-0.078	0.172	0.023	-0.002	-0.002
4.0	0.426	-0.025	-0.059	0.178	0.034	0.002	-0.001
5.0	0.552	-0.034	-0.062	0.183	0.049	0.006	-0.001
6.0	0.614	-0.023	-0.037	0.195	0.062	0.004	-0.002
7.0	0.627	-0.090	-0.143	0.189	0.071	0.005	-0.005
8.0	0.721	-0.094	-0.131	0.191	0.082	0.009	-0.006
9.0	0.916	-0.044	-0.048	0.212	0.095	0.010	-0.006
10.0	1.022	-0.049	-0.048	0.222	0.101	0.012	-0.007
11.0	1.212	-0.006	-0.005	0.246	0.112	0.013	-0.006
12.0	1.284	-0.010	-0.008	0.254	0.123	0.017	-0.007
13.0	1.553	0.040	0.026	0.286	0.139	0.019	-0.002
14.0	1.604	0.079	0.049	0.289	0.154	0.023	-0.002
15.0	1.699	0.037	0.022	0.300	0.167	0.021	-0.003
16.0	1.732	-0.046	-0.026	0.288	0.189	0.024	-0.009
17.0	1.994	-0.055	-0.027	0.313	0.208	0.032	-0.005
18.0	2.057	-0.048	-0.023	0.304	0.221	0.022	-0.008
19.0	2.258	-0.006	-0.003	0.326	0.244	0.034	-0.008
20.0	2.477	-0.056	-0.023	0.340	0.268	0.030	-0.009
21.0	2.678	-0.003	-0.001	0.351	0.292	0.031	-0.010
22.0	2.803	-0.058	-0.021	0.359	0.314	0.040	-0.010
23.0	2.909	-0.118	-0.041	0.358	0.344	0.040	-0.012
24.0	3.225	-0.115	-0.036	0.367	0.369	0.036	-0.011
25.0	3.493	-0.022	-0.006	0.387	0.397	0.042	-0.009
26.0	3.691	-0.110	-0.030	0.391	0.431	0.046	-0.010
27.0	3.951	0.012	0.003	0.406	0.461	0.051	-0.009
28.0	4.091	-0.130	-0.032	0.413	0.492	0.043	-0.010
29.0	4.397	-0.027	-0.006	0.421	0.530	0.050	-0.009
30.0	4.544	-0.161	-0.035	0.416	0.567	0.048	-0.011
31.0	4.787	-0.169	-0.035	0.420	0.596	0.047	-0.010
32.0	5.121	-0.053	-0.010	0.432	0.630	0.047	-0.008
33.0	5.278	-0.346	-0.066	0.425	0.659	0.054	-0.007
34.0	5.483	-0.286	-0.052	0.429	0.690	0.047	-0.006
35.0	5.628	-0.275	-0.049	0.418	0.712	0.043	-0.007
36.0	5.834	-0.365	-0.063	0.411	0.745	0.039	-0.008
37.0	5.986	-0.573	-0.096	0.408	0.767	0.025	-0.008
38.0	6.240	-0.422	-0.068	0.402	0.793	0.029	-0.008
39.0	6.320	-0.645	-0.102	0.292	0.819	0.033	-0.009
40.0	6.668	-0.541	-0.081	0.399	0.840	0.028	-0.006
41.0	6.930	-0.599	-0.086	0.388	0.867	0.007	-0.006
42.0	7.059	-0.384	-0.054	0.379	0.887	0.033	-0.006
43.0	7.309	-0.736	-0.101	0.372	0.913	-0.012	-0.006
44.0	7.541	-0.531	-0.070	0.359	0.933	-0.004	-0.005
45.0	7.936	-0.962	-0.121	0.362	0.957	-0.020	-0.003

46.0	8.270	-0.816	-0.099	0.361	0.975	-0.066	-0.001
47.0	8.420	-0.866	-0.103	0.347	0.996	-0.078	0.000
48.0	8.719	-0.891	-0.102	0.330	1.018	-0.112	0.001
49.0	8.983	-0.949	-0.106	0.315	1.041	-0.147	-0.004
50.0	9.275	-1.189	-0.128	0.308	1.058	-0.185	-0.002
51.0	9.514	-1.379	-0.145	0.294	1.079	-0.197	-0.001
52.0	9.633	-0.830	-0.086	0.272	1.091	-0.200	-0.005
53.0	9.969	-1.360	-0.136	0.255	1.106	-0.273	-0.003
54.0	10.205	-1.404	-0.138	0.231	1.118	-0.291	-0.002
55.0	10.311	-1.460	-0.142	0.208	1.131	-0.320	-0.003
56.0	10.562	-1.540	-0.146	0.198	1.135	-0.361	0.001
57.0	10.844	-1.294	-0.119	0.170	1.143	-0.348	0.000
58.0	11.047	-1.320	-0.119	0.153	1.133	-0.363	0.000
59.0	11.249	-1.625	-0.144	0.136	1.125	-0.348	0.001
60.0	11.633	-1.560	-0.134	0.139	1.112	-0.311	0.005
61.0	11.597	-1.939	-0.167	0.112	1.109	-0.281	0.002
62.0	11.940	-1.627	-0.136	0.102	1.075	-0.243	0.002
63.0	11.911	-1.037	-0.087	0.075	1.079	-0.249	0.000
64.0	12.231	-1.185	-0.097	0.058	1.066	-0.288	0.000
65.0	12.089	-0.916	-0.076	0.042	1.078	-0.305	0.000
66.0	12.596	-1.371	-0.109	0.021	1.071	-0.403	0.008
67.0	12.969	-1.774	-0.137	0.039	1.052	-0.449	0.016
65.0	11.496	0.064	0.006	0.258	1.057	-0.319	0.040
66.0	11.478	-1.986	-0.173	0.139	1.057	-0.398	0.040
67.0	11.651	-1.396	-0.120	0.061	1.051	-0.425	0.035
68.0	11.989	-1.560	-0.130	0.001	1.042	-0.424	0.034
69.0	12.341	-1.513	-0.123	-0.042	1.042	-0.398	0.034
70.0	12.548	-1.183	-0.094	-0.058	1.043	-0.362	0.035
71.0	12.865	-0.987	-0.077	-0.079	1.043	-0.289	0.036
72.0	12.985	-0.858	-0.066	-0.096	1.038	-0.252	0.036
73.0	13.099	-1.054	-0.080	-0.108	1.027	-0.206	0.040
74.0	13.238	-0.974	-0.074	-0.098	1.020	-0.096	0.046
75.0	13.397	-0.473	-0.035	-0.110	1.034	-0.076	0.044
76.0	13.506	-0.392	-0.029	-0.108	1.016	-0.020	0.048
77.0	13.689	-0.722	-0.053	-0.143	1.008	0.005	0.046
78.0	13.725	-0.888	-0.065	-0.128	0.990	0.030	0.047
79.0	13.896	-0.592	-0.043	-0.122	0.964	0.028	0.050
80.0	13.857	-1.119	-0.081	-0.136	0.945	0.018	0.049
81.0	14.067	-0.692	-0.049	-0.165	0.927	0.033	0.048
82.0	14.144	-0.613	-0.043	-0.158	0.895	0.031	0.051
83.0	14.295	-0.524	-0.037	-0.176	0.869	0.058	0.051
84.0	14.197	-0.416	-0.029	-0.194	0.845	0.044	0.049
85.0	14.490	-0.734	-0.051	-0.197	0.812	0.058	0.050
86.0	14.457	-0.354	-0.025	-0.218	0.771	0.041	0.046
87.0	14.382	-0.457	-0.032	-0.229	0.723	0.005	0.044
88.0	14.286	-0.873	-0.061	-0.223	0.656	-0.002	0.044
89.0	14.631	-0.259	-0.018	-0.135	0.615	-0.006	0.043
90.0	14.809	-0.336	-0.023	-0.088	0.568	-0.033	0.046
91.0	14.634	-0.445	-0.030	-0.038	0.526	-0.026	0.046
92.0	14.466	-0.482	-0.033	0.042	0.485	-0.027	0.043
93.0	14.402	-0.502	-0.035	0.058	0.464	-0.013	0.047
94.0	14.269	-0.359	-0.025	0.082	0.437	0.018	0.046
95.0	14.253	-0.594	-0.042	0.075	0.428	0.010	0.048
95.0	2.099	-0.701	-0.334	0.229	-0.070	0.026	0.061
-5.0	2.270	-0.676	-0.298	0.197	-0.075	0.025	0.065
0.0	2.238	-0.580	-0.259	0.217	-0.077	0.027	0.066

RUNFILE> R4B801

AOA	Cn	Cy	Cy/Cn	Cax	Cpt	Crl	Cyw
-5.0	0.065	0.020	0.308	0.004	0.001	0.001	0.000
-5.0	-0.008	0.031	-3.973	0.111	-0.061	-0.003	0.000
-4.0	-0.037	0.041	-1.105	0.110	-0.051	-0.004	-0.001
-3.0	0.057	0.018	0.322	0.112	-0.039	0.001	-0.002
-2.0	0.057	-0.046	-0.813	0.115	-0.031	-0.001	-0.003
-1.0	0.108	-0.026	-0.236	0.105	-0.019	0.001	-0.006
0.0	0.164	0.048	0.292	0.116	-0.003	0.001	-0.004
1.0	0.360	0.016	0.045	0.136	0.007	0.001	-0.002
2.0	0.463	-0.015	-0.033	0.143	0.018	-0.002	0.001
3.0	0.679	0.183	0.269	0.173	0.028	0.005	0.005
4.0	0.573	0.011	0.020	0.149	0.040	0.001	-0.001
5.0	0.536	0.018	0.034	0.147	0.047	0.002	-0.002
6.0	0.680	0.030	0.044	0.151	0.061	0.005	-0.001
7.0	0.772	-0.015	-0.019	0.169	0.071	0.001	0.001
8.0	0.808	0.044	0.054	0.169	0.083	0.002	-0.002
9.0	0.897	-0.007	-0.008	0.182	0.091	0.004	0.000
10.0	0.975	0.065	0.067	0.182	0.100	0.005	0.000
11.0	1.074	0.043	0.040	0.194	0.108	0.006	0.001
12.0	1.214	-0.019	-0.015	0.203	0.119	0.009	0.003
13.0	1.347	0.117	0.087	0.211	0.135	0.013	0.003
14.0	1.448	0.107	0.074	0.217	0.147	0.007	0.003
15.0	1.938	0.108	0.056	0.197	0.158	0.003	-0.005
16.0	1.455	-0.333	-0.229	0.202	0.188	0.024	0.000
17.0	1.595	-0.100	-0.063	0.217	0.208	0.032	0.000
18.0	1.787	-0.155	-0.087	0.226	0.227	0.023	0.000
19.0	1.898	-0.293	-0.154	0.229	0.252	0.025	0.001
20.0	2.115	-0.124	-0.059	0.237	0.276	0.019	-0.002
21.0	2.257	-0.244	-0.108	0.253	0.290	0.026	0.001
22.0	2.437	-0.264	-0.108	0.273	0.308	0.034	0.001
23.0	2.547	-0.319	-0.125	0.274	0.329	0.033	0.000
24.0	2.697	-0.322	-0.120	0.275	0.363	0.023	0.001
25.0	2.894	-0.169	-0.058	0.303	0.377	0.034	0.002
26.0	3.001	-0.102	-0.034	0.304	0.406	0.025	0.002
27.0	3.150	-0.176	-0.056	0.314	0.435	0.022	0.002
28.0	3.250	-0.181	-0.056	0.304	0.452	0.014	0.000
29.0	3.296	-0.340	-0.103	0.291	0.478	0.014	-0.003
30.0	3.611	-0.229	-0.063	0.318	0.492	-0.002	0.000
31.0	3.666	-0.068	-0.019	0.315	0.534	0.020	-0.001
32.0	3.757	-0.232	-0.062	0.306	0.551	0.011	-0.004
33.0	3.942	-0.156	-0.040	0.315	0.576	0.016	-0.002
34.0	4.145	-0.362	-0.087	0.319	0.602	-0.029	-0.003
35.0	4.335	-0.644	-0.148	0.317	0.619	-0.025	-0.001
36.0	4.358	-0.648	-0.149	0.317	0.637	-0.050	-0.004
37.0	4.670	-0.589	-0.126	0.329	0.671	-0.016	-0.002
38.0	4.863	-0.875	-0.180	0.323	0.690	-0.117	-0.003
39.0	5.066	-0.923	-0.182	0.334	0.709	-0.092	0.001
40.0	5.156	-0.327	-0.063	0.314	0.730	-0.126	-0.004
41.0	5.496	-0.383	-0.070	0.316	0.762	-0.141	-0.002
42.0	5.629	-1.066	-0.189	0.307	0.785	-0.141	-0.002
43.0	5.705	0.051	0.009	0.290	0.796	-0.070	-0.004
44.0	5.891	0.165	0.028	0.286	0.825	-0.125	-0.005
45.0	6.014	-0.933	-0.155	0.268	0.834	-0.162	-0.004

46.0	6.246	-1.133	-0.181	0.245	0.859	-0.224	-0.008
47.0	6.579	-0.513	-0.078	0.266	0.881	-0.198	-0.004
48.0	6.826	-0.777	-0.114	0.256	0.906	-0.203	-0.004
49.0	7.009	-1.458	-0.208	0.230	0.918	-0.234	-0.007
50.0	7.088	-1.591	-0.225	0.224	0.931	-0.226	-0.007
51.0	7.276	-0.140	-0.019	0.210	0.943	-0.186	-0.007
52.0	7.475	-1.500	-0.201	0.199	0.953	-0.313	-0.007
53.0	7.859	-1.345	-0.171	0.176	0.953	-0.263	-0.009
54.0	8.036	-1.096	-0.136	0.186	0.952	-0.334	-0.010
55.0	8.251	-1.109	-0.134	0.169	0.960	-0.379	-0.012
56.0	8.696	-1.722	-0.198	0.152	0.953	-0.520	-0.012
57.0	9.117	-1.808	-0.198	0.169	0.925	-0.578	-0.016
58.0	9.634	-1.785	-0.185	0.157	0.851	-0.534	-0.016
59.0	10.085	-1.061	-0.105	0.139	0.834	-0.374	-0.015
60.0	10.299	-0.925	-0.090	0.126	0.830	-0.300	-0.014
61.0	10.484	-0.510	-0.049	0.145	0.804	-0.301	-0.010
62.0	10.372	0.198	0.019	0.116	0.807	-0.258	-0.013
63.0	10.345	-0.586	-0.057	0.071	0.807	-0.281	-0.019
64.0	10.386	0.232	0.022	0.082	0.808	-0.216	-0.016
65.0	10.530	0.962	0.091	0.068	0.807	-0.127	-0.016
66.0	10.887	-0.014	-0.001	0.088	0.823	-0.137	-0.009
67.0	11.079	-0.642	-0.058	0.060	0.842	-0.172	-0.008
68.0	11.114	-0.480	-0.043	0.055	0.842	-0.012	-0.004
69.0	11.161	-0.083	-0.007	0.027	0.856	-0.019	-0.009
70.0	11.081	-0.823	-0.074	0.014	0.879	0.040	-0.008
71.0	11.183	-0.319	-0.029	-0.006	0.911	0.060	-0.008
72.0	11.288	-0.093	-0.008	-0.008	0.930	0.055	-0.007
73.0	11.193	-0.320	-0.029	-0.052	0.934	-0.011	-0.010
74.0	11.311	-0.286	-0.025	-0.066	0.923	-0.021	-0.008
75.0	11.408	-0.355	-0.031	-0.061	0.925	0.032	-0.007
76.0	11.448	-0.315	-0.028	-0.049	0.916	0.029	-0.006
77.0	11.443	-0.422	-0.037	-0.051	0.906	0.046	-0.006
78.0	11.299	-0.307	-0.027	-0.072	0.882	0.035	-0.007
79.0	11.493	-0.239	-0.021	-0.080	0.863	0.047	-0.006
80.0	11.278	-0.146	-0.013	-0.091	0.842	0.050	-0.005
81.0	11.216	-0.111	-0.010	-0.096	0.821	0.047	-0.007
82.0	11.295	-0.178	-0.016	-0.128	0.800	0.039	-0.010
83.0	11.478	0.092	0.008	-0.133	0.780	0.028	-0.008
84.0	11.238	-0.178	-0.016	-0.223	0.767	0.025	-0.009
85.0	11.438	-0.243	-0.021	-0.233	0.742	0.034	-0.007
86.0	11.288	-0.084	-0.007	-0.292	0.708	0.060	-0.006
87.0	11.082	0.103	0.009	-0.252	0.629	0.063	-0.003
88.0	10.896	-0.252	-0.023	-0.127	0.560	0.062	-0.004
89.0	10.979	-0.176	-0.016	-0.054	0.495	0.050	-0.006
90.0	10.944	-0.125	-0.011	0.047	0.448	0.012	-0.007
91.0	11.230	0.136	0.012	0.088	0.400	-0.011	-0.009
92.0	10.973	0.113	0.010	0.111	0.358	-0.007	-0.010
93.0	11.082	0.213	0.019	0.130	0.322	-0.026	-0.010
94.0	11.085	-0.058	-0.005	0.171	0.283	-0.036	-0.008
95.0	10.980	0.071	0.006	0.146	0.244	-0.048	-0.013
95.0	1.092	-0.028	-0.025	0.234	-0.035	0.032	0.003
-5.0	0.964	-0.072	-0.075	0.172	-0.043	0.034	0.001
0.0	1.015	-0.133	-0.131	0.176	-0.035	0.033	0.003

APPENDIX D. DATA ACQUISITION PROGRAM

The following computer program was originally written by Sestak [Ref. 47] in BASIC and modified by the author for use with this experiment. This program follows a data aquisition *shell program* which allows the data acquisition program to control the Hewlett-Packard data acquisition hardware. The original program implemented automatic data input for angle of attack and tare values. Angle of attack is manually input to this program by the operator.

Preliminary test runs indicated a larger than desired variation in the balance readings. The program was modified to average ten separate readings per channel and calculate the mean and standard deviation. Any readings which were greater than one standard deviation from the mean were discarded. The program was also modified to allow the operator to recycle the balance reading routine without having to leave the program. This was necessary to enable the operator to reject all balance readings during a current read cycle after viewing the data.

Since the missile model pitched in the horizontal direction, only one tare reading was necessary, eliminating the original routine for recording tare values at each angle of attack. Additional information for the program procedure is contained in the the program listing.

```
1000 'Program to scan with the DMM and RELAY.MUX.01
1010 'This program was writen by T.SESTAK and modified by
1020 'P. RABANG for use with the VLSAM model.
1030 '
1040 'This section after the SHELL program directs reading
1050 'the voltages from the balance, computes forces measured
1060 'by the strain guages, then stores the values in two arrays,
1070 'one for the TARE one for FORCE.  This data file can then
1080 'be used for graphs or other displays.  Each test run
1090 'will generate a windtun.dat file which should be copied
1100 'under another name before the next test run so that it
1110 'will not be overwritten.
1120 '
1130    'dimension arrays
1140 DIM READING[7],FORCE[140,8],TARE[8],TREAD[7,10]
1150 COLOR 14,1,1
1160 CLS
1170 '
1180 AOA=0
1190 VALUE=5
1200 LOCATE 12,28
1210 PRINT"SETTING UP DATA FILES"
1220 '
1230    'The program will write the data to several files.
1240 STATEFILE$ = "C:  PCIB WIND.HPC"     'stored in PCIB subdirectory
1250 DATAFILE$ = "C: WINDTUN.DAT"         'stored on disc C
1260 DISKFILE$ = "A: WINDTUN.DAT"         'stored on disc A
1270 BALANFILE$ = "C:  MISSILE BALANCE.DAT    'stored on disc C
1280 '
1290 RELAY.SETTLING.TIME = .8             '800 ms
1300 LOCATE 16,35: PRINT"D O N E"
1310 CALL DELAY(VALUE)
1320 '
1330 CLS: LOCATE 12,28: PRINT"INITIALIZING INSTRUMENTS"
1340 CALL INITIALIZE.SYSTEM(STATEFILE$)
1350 IF PCIB.ERR <> 0 THEN ERROR PCIB.BASERR
1360 CALL ENABLE.SYSTEM
1370 IF PCIB.ERR <> 0 THEN ERROR PCIB.BASERR
1380 LOCATE 16,35:PRINT"D O N E"
1390 CALL DELAY(VALUE)
1400 '
1410 'This part of the program is to preserve the data if
1420 'if the program is aborted in mid run.  Parity errors
1430 'in the Hewlett Packard PC Instruments setup caused by
1440 'electrical noise and undervoltage at NPS requires
1450 'this.  A voltage regulated, uninteruptible power source
1460 'would ameliorate this problem. Just in case- this little
1470 'sequence allows reentry into the program and the data
1480 'arrays with minimal inconvenience.
1490 '
1500 CLS: LOCATE 12,20: INPUT"WERE YOU INTERRUPTED (Y OR N)";A$
1510 IF A$="Y" GOTO 1670
1520 '
1530 'The next three variables are counters in the arrays
1540 'FORCE and TARE
1550 '
```

```
1560 TRIAL = 0
1570 TRY = 0
1580 '
1590 'open the datafile so each scan can be recorded
1600 '
1610 OPEN DATAFILE$ FOR OUTPUT AS #1
1620 CLOSE #1
1630 OPEN BALANFILE$ FOR OUTPUT AS #3
1640 CLOSE #3
1650 GOTO 1800
1660 '
1670 OPEN DATAFILE$ FOR INPUT AS #1
1680 INPUT #1, TARE(1),TARE(2),TARE(3),TARE(4),TARE(5),TARE(6),
     TARE(7),TARE(8)
1690 FOR X = 1 TO 140
1700    INPUT #1, FORCE(X,1),FORCE(X,2),FORCE(X,3),FORCE(X,4),
     FORCE(X,5),FORCE(X,6),FORCE(X,7),FORCE(X,8)
1710 NEXT X
1720 CLOSE #1
1730 '
1740 GOTO 1800
1750 'A$ is used as a marker for interrupted run sequences
1760 'in the program, it is set to <>"Y" so the
1770 'uninterrupted sequences are used unless otherwise directed
1780 '
1790 A$="N"
1800 KEY OFF
1810 '
1820 'prompt to begin each scan or quit program if desired
1830 '
1840 CLS: LOCATE 12,10
1850 INPUT "TO START SCAN ENTER ANY KEY EXCEPT Q, Q TO QUIT";ANSWER$
1860 IF ANSWER$ = "Q" THEN GOTO 4730
1870 '
1880 'THIS ENTERS THE AOA FOR EACH TRIAL AND DISPLAYS IT ON THE CRT
1890 '
1900 CLS: LOCATE 12,10
1910 PRINT "THE CURRENT ANGLE OF ATTACK IS ";AOA
1920 '
1930 '
1940 LOCATE 15,10: PRINT "INPUT THE ANGLE OF ATTACK (AOA) FOR THE
     NEXT TRIAL"
1950 INPUT AOA          'READING(1)
1960 GOTO 1970
1970 '
1980 READING(1)=AOA
1990 '
2000 'This variable is a marker in the iteration loop
2010 'interaction equations for convergence.
2020 '
2030 CYCLE = 0
2040 '
2050 'This loop scans the pitch angle and 6 balance channels
2060 'and stores the values in the array READING
2070 'Each channel is read ten times and averaged.
2080 'The user may reject the current readings and input a new set.
```

```
2090 '
2100 CLS
2110 PRINT"********************** DIRECT BALANCE READINGS *****
     **********************
2120 PRINT"                      CHECK OF SYSTEM OPERATION
2130 PRINT
     " IN VOLTS       N1          N2          S1          S2          A          R  "
2140 PRINT
     " **********     *******     *******     *******     *******     *******     *******"
2150 '
2160 'This file is for storing the direct voltage readings and averages.
2170 'The data file is continually appended.
2180 'The data is for further analysis of the direct voltage readings.
2190 OPEN BALANFILE$ FOR APPEND AS #3
2200 '
2210 FOR CNT = 1 TO 10
2220 FOR CHANNEL = 2 TO 7
2230    CALL OUTPUT(RELAY.MUX.01, CHANNEL)
2240            IF PCIB.ERR <> 0 THEN ERROR PCIB.BASERR
2250    CALL DELAY(RELAY.SETTLING.TIME)
2260            IF PCIB.ERR <> 0 THEN ERROR PCIB.BASERR
2270    CALL MEASURE(DMM.01, READING[CHANNEL])
2280            IF PCIB.ERR <> 0 THEN ERROR PCIB.BASERR
2290 TREAD(CHANNEL,CNT) = READING(CHANNEL)
2300 NEXT CHANNEL
2310 PRINT USING
     "             +.######   +.######   +.######   +.######   +.######   +.######";
     READING(2),READING(3),READING(4),READING(5),READING(6),READING(7)
2320 PRINT #3, USING
     "    +###.#   +.######   +.######   +.######   +.######   +.######   +.######";
     READING(1),READING(2),READING(3),READING(4),READING(5),READING(6),
     READING(7)
2330 NEXT CNT
2340 '
2350 '  CALL SUBROUTINE TO AVERAGE READINGS
2360 GOSUB 4790
2370 '
2380 PRINT"- - - - - - - - - - - - - - - - - - - - - - - - - - - -
     - - - - - - - - - -"
2390 PRINT USING
     "MEAN VALUE +.######   +.######   +.######   +.######   +.######   +.######";
     READING(2),READING(3),READING(4),READING(5),READING(6),READING(7)
2400 PRINT #3, USING
     "    +###.#   +.######   +.######   +.######   +.######   +.######   +.######";
     READING(1),READING(2),READING(3),READING(4),READING(5),READING(6),
     READING(7)
2410 CLOSE #3
2420 PRINT" ": BEEP
2430 PRINT"<CR> TO CONTINUE, "1" TO GET NEW READINGS"
2440 INPUT XYZ
2450 IF XYZ=1 GOTO 2040
2460 '
2470 'These equations take voltage readings from the balance,
2480 'converts them to counts, then applys the primary force
2490 'equations to the results.  These values are applied to
2500 'the balance interaction equations. Each channel has
```

```
2510 'separate equations for positive and negative readings and
2520 'may have a "+" or "-" reading on any test run so the
2530 'rather involved logic path below is my solution to the
2540 'problem.  For more information consult Calibration laboratory
2550 'guidelines at NASA Ames Research Facility for TASK balances
2560 '
2570 '*************** CONVERT SIGNAL TO FORCES ***************
2580 '********************************************************
2590 '
2600 'Direct balance readings are multiplied by a scale factor
2610 '5000000 then divided by the balance exitation voltage to
2620 'get a readiing in COUNTS. The program will send each reading
2630 'to the appropriate equation and convert to force or moment
2640 'then return to send the next reading for calculation
2650 'The data acquisition system for using this program used an
2660 'amplifier with 1000 gain. The scale factor is divided by 1000.
2670 '
2680 VEX=5                          'Excitation Voltage
2690 N1=READING(2)*5000!/VEX
2700 N2=READING(3)*5000!/VEX
2710 S1=READING(4)*5000!/VEX
2720 S2=READING(5)*5000!/VEX
2730 A=READING(6)*5000!/VEX
2740 R=READING(7)*416.67#/VEX
2750 '
2760 'send each reading to the appropriate equation
2770 '
2780 IF READING(2)>0 THEN GOTO 2870 ELSE GOTO 3020
2790 IF READING(3)>0 THEN GOTO 2890 ELSE GOTO 3040
2800 IF READING(4)>0 THEN GOTO 2930 ELSE GOTO 3080
2810 IF READING(5)>0 THEN GOTO 2950 ELSE GOTO 3100
2820 IF READING(6)>0 THEN GOTO 2910 ELSE GOTO 3060
2830 IF READING(7)>0 THEN GOTO 2970 ELSE GOTO 3120
2840 '
2850 '*************** POSITIVE FORMULAS ***************
2860 '
2870 EN1 = .050861*N1 - 5.4826E-09*(N1*N1)
2880 GOTO 2790
2890 EN2 = .047211*N2 - 1.7015E-08*(N2*N2)
2900 GOTO 2800
2910 EA = .014309*A - 7.1962E-10*(A*A)
2920 GOTO 2830
2930 ES1 = .031309*S1 - 3.8153E-08*(S1*S1)
2940 GOTO 2810
2950 ES2 = .030366*S2 - 3.8607E-08*(S2*S2)
2960 GOTO 2820
2970 ER = .0030885*R + 2.5672E-09*(R*R)
2980 GOTO 3130
2990 '
3000 '*************** NEGATIVE FORMULAS ***************
3010 '
3020 EN1 = .051591*N1 + 1.7157E-08*(N1*N1)
3030 GOTO 2790
3040 EN2=.047763*N2+8.915299E-09*(N2*N2)
3050 GOTO 2800
3060 EA = .01429*A - 1.3322E-09*(A*A)
```

```
3070 GOTO 2830
3080 ES1 = .032073*S1 - 8.931601E-09*(S1*S1)
3090 GOTO 2810
3100 ES2 = .031167*S2 - 7.2517E-09*(S2*S2)
3110 GOTO 2820
3120 ER = .0030908*R - 2.4769E-09*(R*R)
3130 '
3140 '
3150 'a heading for the iteration values
3160 '
3170 PRINT" "
3180 PRINT"************************ FORCE INTERACTION ITERATIONS
     ************************
3190 PRINT"                          CHECK FOR CONVERGENCE
3200 PRINT
     "  CYCLE    AOA      N1        N2        S1        S2        A         R "
3210 PRINT
     "    #      DEG    POUNDS    POUNDS    POUNDS    POUNDS    POUNDS    FT-LBS"
3220 PRINT
     "  ******    ****    ********  ********  ********  ********  ********  ********"
3230 '
3240 'The loop that controls the balance interaction
3250 'equations and allows a visual convergence check
3260 '
3270 FOR I = 1 TO 10
3280 IF READING(2)>0 THEN GOTO 3370 ELSE GOTO 3570
3290 IF READING(3)>0 THEN GOTO 3400 ELSE GOTO 3600
3300 IF READING(4)>0 THEN GOTO 3460 ELSE GOTO 3660
3310 IF READING(5)>0 THEN GOTO 3490 ELSE GOTO 3690
3320 IF READING(6)>0 THEN GOTO 3430 ELSE GOTO 3630
3330 IF READING(7)>0 THEN GOTO 3520 ELSE GOTO 3720
3340 '
3350 '*****************POSITIVE FORMULAS*****************
3360 '
3370 XN1= EN1+.0058036*N2+.0041655*S1+.058079*R-7.1926E-07*(N2*N2)
     +4.0352E-06*(S1*S1)-.0006786*(R*R)
3380 GOTO 3290
3390 '
3400 XN2= EN2+.046218*N1-.0028393*A-.0081694*S1+.0041463*S2+.077279
     *R-6.8577E-07*(N1*N1)-1.7755E-05*(A*A)+2.1719E-06*(S1*S1)+1.8582E-06
     *(S2*S2)-.0019294*(R*R)
3410 GOTO 3300
3420 '
3430 XA= EA+8.6893E-04*N1+6.0359E-04*S1+7.7722E-05*S2-.11115*R
     +4.4537E-07*(N1*N1)+4.7936E-06*(S1*S1)-4.1033E-06*(S2*S2)+2.0697E-04
     *(R*R)
3440 GOTO 3330
3450 '
3460 XS1 = ES1-6.3459E-04*N1-.11148*R+5.535E-06*(N1*N1)+.0024592*(R*R)
3470 GOTO 3310
3480 '
3490 XS2= ES2-.0024237*N1+.0022455*A+.0066785*S1-.26377*R+1.7099E-06
     *(N1*N1)+1.2072E-05*(A*A)-2.7825E-06*(S1*S1)+.0062217*(R*R)
3500 GOTO 3320
3510 '
3520 XR= ER-1.9928E-04*N2-2.5893E-04*S2+1.1512E-07*(N2*N2)-5.156E-08
```

```
     *(S2*S2)
3530 GOTO 3730
3540 '
3550 '****************** NEGATIVE FORMULAS **************
3560 '
3570 XN1= EN1+.010257*N2-.0045396*S1-.04494*R+7.9499E-07*(N2*N2)
     -1.967E-06*(S1*S1)-.0003232*(R*R)
3580 GOTO 3290
3590 '
3600 XN2= EN2+.051778*N1-.0044056*A-9.038499E-03*S1-.061125*R
     +5.2897E-06*(N1*N1)+1.0467E-05*(A*A)-4.8493E-07*(S1*S1)-.0011773*(R*R)
3610 GOTO 3300
3620 '
3630 XA= EA-.0021217*N1+9.1524E-04*N2-.097148*R-4.2547E-06*(N1*N1)
     +4.5846E-06*(N2*N2)-7.5001E-04*(R*R)
3640 GOTO 3330
3650 '
3660 XS1= ES1-.0071275*N1-.0089235*A-.05268*R-1.2923E-05*(N1*N1)
     -4.0345E-05*(A*A)-9.3969E-04*(R*R)
3670 GOTO 3310
3680 '
3690 XS2= ES2-.0037176*N1-.0052619*N2+.0072915*A+.006856*S1-.062581
     *R-5.211E-07*(N1*N1)-8.6265E-06*(N2*N2)+3.7054E-05*(A*A)+9.983001E-06
     *(S1*S1)+8.0007E-04*(R*R)
3700 GOTO 3320
3710 '
3720 XR= ER+3.5945E-04*N1+1.5497E-07*(N1*N1)
3730 '
3740 'Shift all the new variables back to the old name
3750 'for the next iteration
3760 N1=XN1
3770 N2=XN2
3780 A=XA
3790 S1=XS1
3800 S2=XS2
3810 R=XR
3820 '
3830 'A marker for the interations
3840 CYCLE = CYCLE + 1
3850 'print the iterations to watch for convergence
3860 '
3870 PRINT USING
     "   ##    +##.#   +###.##   +###.##   +###.##   +###.##   +###.##   +###.##";
     CYCLE,AOA,N1,N2,S1,S2,A,R
3880 NEXT I
3890 '
3900 INPUT "IF CONVERGENCE IS ADEQUATE ENTER Y, IF ANOTHER RUN
     IS DESIRED ENTER N";ANSWR$
3910 IF ANSWR$ = "N" THEN GOTO 3160
3920 '
3930 NORMAL = N1 + N2
3940 SIDE = S1 + S2
3950 AXIAL = A
3960 PITCH = (N1-N2) * .0854
3970 ROLL = (S1-S2) * .0698
3980 YAW = R*12
```

```
3990 '
4000 TRIAL = TRIAL + 1
4010 INPUT;"IS THIS A TARE READING, Y OR N";AN$
4020 IF AN$ <> "Y" GOTO 4290
4030 COLOR 10,4,1
4040 TRIAL = 0
4050 TRY = TRY + 1
4060 IF A$<>"Y" GOTO 4100
4070 CLS: LOCATE 12,10
4080 INPUT"ENTER THE VALUE OF THE LAST TRY BEFORE INTERRUPT";ITRY
4090 TRY = ITRY + 1
4100 TARE(1) = TRY
4110 TARE(2) = AOA
4120 TARE(3) = NORMAL
4130 TARE(4) = SIDE
4140 TARE(5) = AXIAL
4150 TARE(6) = PITCH
4160 TARE(7) = ROLL
4170 TARE(8) = YAW
4180 '
4190 PRINT" "
4200 PRINT"* * * * * * * * * * * * * TARE CALCULATIONS * * * *
     * * * * * * * * * *
4210 PRINT
     "  TRIAL    AOA    NORMAL    SIDE     AXIAL    PITCH    ROLL     YAW"
4220 PRINT
     "    #      DEG    POUNDS    POUNDS   POUNDS   FT-LBS   FT-LBS   FT-LBS"
4230 PRINT
     "  ******   ******   *******   *******   *******   *******   *******   *******"
4240     'A loop to list all values so far
4250 FOR J = 1 TO TRY
4260 PRINT USING"    ##    +###.##    ###.##    ###.##    ###.##    ###.##
     ###.##    ###.##";TARE(1),TARE(2),TARE(3),TARE(4),TARE(5),TARE(6),
     TARE(7),TARE(8)
4270 NEXT J
4280 GOTO 4550
4290 '
4300 IF A$<>"Y" GOTO 4340
4310 CLS: LOCATE 12,10
4320 INPUT"ENTER THE VALUE OF THE LAST TRIAL BEFORE INTERRUPT";ITRIAL
4330 TRIAL = ITRIAL + 1
4340 FORCE(TRIAL,1) = TRIAL
4350 FORCE(TRIAL,2) = AOA
4360 FORCE(TRIAL,3) = NORMAL - TARE(3)
4370 FORCE(TRIAL,4) = SIDE - TARE(4)
4380 FORCE(TRIAL,5) = AXIAL - TARE(5)
4390 FORCE(TRIAL,6) = PITCH - TARE(6)
4400 FORCE(TRIAL,7) = ROLL - TARE(7)
4410 FORCE(TRIAL,8) = YAW - TARE(8)
4420 '
4430 'print the values and store in file
4440 '
4450 PRINT" "
4460 PRINT"* * * * * * * * * * * * * FORCE CALCULATIONS * * *
     * * * * * * * * * *
4470 PRINT
```

```
    " TRIAL   AOA    NORMAL    SIDE     AXIAL    PITCH    ROLL     YAW"
4480 PRINT
    "    #     DEG    POUNDS   POUNDS   POUNDS   FT-LBS   FT-LBS   FT-LBS"
4490 PRINT
    " ******  ******  *******  *******  *******  *******  *******  *******"
4500 'a loop to list all values so far
4510 '
4520 FOR J = 1 TO TRIAL
4530 PRINT USING"   ##   +###.#  +###.##  +###.##  +###.##  +###.##
    +###.##  +###.##";FORCE(J,1),FORCE(J,2),FORCE(J,3),FORCE(J,4),
    FORCE(J,5),FORCE(J,6),FORCE(J,7),FORCE(J,8)
4540 NEXT J
4550 '
4560 'Write the data to the output data files
4570 COLOR 14,1,1
4580 OPEN DATAFILE$ FOR OUTPUT AS #1
4590  WRITE #1, TARE(1),TARE(2),TARE(3),TARE(4),TARE(5),TARE(6),
    TARE(7),TARE(8)
4600 FOR X = 1 TO 140
4610    WRITE #1, FORCE(X,1),FORCE(X,2),FORCE(X,3),FORCE(X,4),
    FORCE(X,5),FORCE(X,6),FORCE(X,7),FORCE(X,8)
4620 NEXT X
4630 CLOSE #1
4640 '
4650 OPEN DISKFILE$ FOR OUTPUT AS #2
4660  WRITE #2, TARE(1),TARE(2),TARE(3),TARE(4),TARE(5),TARE(6),
    TARE(7),TARE(8)
4670 FOR X = 1 TO 140
4680    WRITE #2, FORCE(X,1),FORCE(X,2),FORCE(X,3),FORCE(X,4),
    FORCE(X,5),FORCE(X,6),FORCE(X,7),FORCE(X,8)
4690 NEXT X
4700 CLOSE #2
4710 '
4720    'Prompt for next scan
4730 '
4740 INPUT "DO YOU WANT ANOTHER SCAN (Y OR N)";ANSW$
4750 IF ANSW$ <>"N" THEN GOTO 1790
4760 '
4770 END
4780 '
4790    'This subroutine averages the balance voltage readings
4800    'by computing the mean and standard deviation.
4810    'Any readings less or greater than one standard deviation
4820    'are thrown out and a new mean is computed
4830 '
4840 FOR CHANNEL = 2 TO 7
4850 N=10
4860 SREAD=0
4870 SSDEV=0
4880 '
4890    'Mean of balance voltage readings
4900 FOR CNT = 1 TO 10
4910 SREAD = SREAD + TREAD(CHANNEL,CNT)
4920 NEXT CNT
4930 MEAN = SREAD/N
4940 READING(CHANNEL) = MEAN
```

```
4950 IF(N < 10) THEN GOTO 5120
4960 '
4970    'Standard deviation routine
4980 FOR CNT = 1 TO 10
4990 DIF = TREAD(CHANNEL,CNT) - MEAN
5000 SDEV = DIF * DIF
5010 SSDEV = SSDEV + SDEV
5020 NEXT CNT
5030 DEV = SQR(SSDEV/N)
5040 HI = MEAN + DEV
5050 LO = MEAN - DEV
5060 FOR CNT = 1 TO 10
5070 ARG = TREAD(CHANNEL,CNT)
5080 IF (ARG < HI) AND (ARG > LO) THEN GOTO 5110
5090 TREAD(CHANNEL,CNT) = 0!
5100 N = N - 1
5110 NEXT CNT
5120 NEXT CHANNEL
5130 RETURN
5140 END
```

APPENDIX E. COEFFICIENTS TRANSLATION PROGRAM

This program was written by the author for use with this thesis experiment. The program reads a data file containing force and moment values and converts these into a coefficient form taking into account:

Test conditions.

Body configuration for blockage.

Screen number.

The results are written into a data file which are used to produce graphs and plots.

```
1000 '  PROGRAM BY M.P. RABANG TO READ FORCE AND MOMENT VALUES FROM
1010 '  A DATA FILE CREATED BY THE DATA ACQUISITION PROGRAM.
1020 '
1030 COLOR 10,4,1
1040 '
1050 DIM TARE[8], FORCE[140,8], COEF[140,9]
1060 '
1070 CLS
1080 LOCATE 5
1090 INPUT"ENTER THE NAME OF THE INPUT FILE";INFILE$
1100 INPUT"ENTER THE NAME OF THE OUTPUT FILE";OUTFILE$
1110 INPUT"ENTER THE MINIMUM TEMPERATURE (F)";TMIN
1120 INPUT"ENTER THE MAXIMUM TEMPERATURE (F)";TMAX
1130 INPUT"ENTER THE BODY TYPE, A=+, B=0, C=X ";BOD$
1140 IF BOD$="A" THEN BODY=1: GOTO 1180
1150 IF BOD$="B" THEN BODY=3: GOTO 1180
1160 IF BOD$="C" THEN BODY=2: GOTO 1180
1170 GOTO 1130
1180 INPUT"ENTER THE SCREEN NUMBER, 0-4";SCR
1190 IF SCR=0 THEN GOTO 1250
1200 IF SCR=1 THEN Q=15.35: GOTO 1260
1210 IF SCR=2 THEN Q=14.882: GOTO 1260
1220 IF SCR=3 THEN Q=16.38: GOTO 1260
1230 IF SCR=4 THEN Q=15.605: GOTO 1260
1240 GOTO 1180
1250 INPUT"ENTER THE WIND TUNNEL VELOCITY (cm H20)";PH20
1260 INPUT"DO YOU WANT TO VIEW OUTPUT";PANS$
1270 INPUT"DO YOU WANT A HARDCOPY";ANS$
1280 '
1290 '  OPEN THE DATA FILE SO EACH SCAN IS RECORDED
1300 TRANSFILE$="C:MISSILE TRANS.DAT"
1310 OPEN OUTFILE$ FOR OUTPUT AS #2
1320 CLOSE #2
1330 '
1340 '  READ THE FORCE VALUES FROM THE DATA FILE
1350 OPEN INFILE$ FOR INPUT AS #1
1360 INPUT #1, TARE(1),TARE(2),TARE(3),TARE(4),TARE(5),TARE(6),
     TARE(7),TARE(8)
1370 FOR X = 1 TO 140
1380 INPUT #1, FORCE(X,1),FORCE(X,2),FORCE(X,3),FORCE(X,4),
     FORCE(X,5),FORCE(X,6),FORCE(X,7),FORCE(X,8)
1390 IF FORCE(X,1)=0! THEN GOTO 1410
1400 NEXT X
1410 CLOSE #1
1420 IF PANS$<>"Y" THEN GOTO 1610
1430 '
1440 '  DISPLAY FORCE VALUES
1450 COLOR 14,1,1
1460 CLS
1470 PRINT"FILE NAME: ";INFILE$
1480 PRINT" "
1490 PRINT"* * * * * * * * * * * * * * * FORCE READINGS
     * * * * * * * * * * * * * * * * * *
1500 PRINT" "
1510 PRINT
     " TRIAL   AOA    NORMAL      SIDE       AXIAL      PITCH
```

```
     ROLL        YAW"
1520 PRINT
     "   #      DEG     POUNDS      POUNDS      POUNDS      FT-LBS
     FT-LBS      FT-LBS"
1530 PRINT
       ******  ******  *********   *********   *********   *********
     *********   *********"
1540 '
1550 FOR J = 1 TO 140
1560 IF FORCE(J,1)=0 THEN GOTO 1590
1570 PRINT USING"  ### +###.#    +##.####    +##.####    +##.####
     +##.####    +##.####    +##.####";FORCE(J,1),FORCE(J,2),FORCE(J,3),
     FORCE(J,4),FORCE(J,5),FORCE(J,6),FORCE(J,7),FORCE(J,8)
1580 NEXT J
1590 '
1600 INPUT"ENTER <CR> TO CONTINUE";INPT$
1610 '
1620 '  BEGIN COEFFICIENTS CALCULATION
1630 A=.0167
1640 MU=3.719E-07
1650 TAV=(TMIN+TMAX)/2!
1660 RHO=2116.22/(1545*(459.7+TAV))
1670 IF SCR>0 GOTO 1740
1680 VE=(2!*2.046*PH20)/(.93*RHO)
1690 VEL=SQR(VE)
1700 RED=(RHO*VEL*(1.75/12))/MU
1710 Q=(RHO*VEL*VEL)/2!
1720 GOTO 1800
1730 '
1740 VE=2*Q/RHO
1750 VEL=SQR(VE)
1760 RED=(RHO*VEL*(1.75/12))/MU
1770 PH20=Q*.93/2.046
1780 '
1790 '  WRITE THE COEFFICIENTS TO THE OUTPUT FILE
1800 OPEN OUTFILE$ FOR OUTPUT AS #2
1810 OPEN TRANSFILE$ FOR APPEND AS #3
1820 WRITE #3, OUTFILE$
1830 FOR X = 1 TO 140
1840 FOR Y = 3 TO 8
1850 IF FORCE(X,1)=0 THEN GOTO 2040
1860 '  ROUTINE TO CORRECT THE DYNAMIC PRESSURE FOR BLOCKAGE
1870 '  AND BODY TYPE
1880 COEF(X,1)=FORCE(X,1)
1890 COEF(X,2)=FORCE(X,2)
1900 ALPHA = FORCE(X,2)
1910 IF FORCE(X,2) < 0 THEN ALPHA = ABS(FORCE(X,2))
1920 IF FORCE(X,2) > 90 THEN ALPHA = 180-FORCE(X,2)
1930 IF BODY=1 THEN EPS=.0000126*ALPHA+.007759
1940 IF BODY=2 THEN EPS=.0000101*ALPHA+.007759
1950 IF BODY=3 THEN EPS=.0000908*ALPHA+.007759
1960 D = A*Q*(1+(2*EPS))
1970 COEF(X,Y) = FORCE(X,Y)/D
1980 COEF(X,9)=COEF(X,4)/COEF(X,3)
1990 NEXT Y
```

```
2000 IF FORCE(X,1)=0 THEN GOTO 2040
2010  WRITE #2, COEF(X,1),COEF(X,2),COEF(X,3),COEF(X,4),COEF(X,9),
     COEF(X,5),COEF(X,6),COEF(X,7),COEF(X,8)
2020  WRITE #3, COEF(X,1),COEF(X,2),COEF(X,3),COEF(X,4),COEF(X,9),
     COEF(X,5),COEF(X,6),COEF(X,7),COEF(X,8)
2030 NEXT X
2040 CLOSE #2
2050 CLOSE #3
2060 IF PANS$<>"Y" THEN GOTO 2300
2070 '
2080 '  DISPLAY ROUTINE
2090 COLOR 10,4,1
2100 CLS
2110 PRINT"FILE NAME: ";OUTFILE$
2120 PRINT" "
2130 PRINT"AVERAGE TEMPERATURE (F)                ";TAV
2140 PRINT"WIND TUNNNEL VELOCITY (FT/SEC)         ";VEL
2150 PRINT"WIND TUNNNEL VELOCITY (cmH2O)          ";PH20
2160 PRINT"AIR DENSITY (LBM/FT3)                  ";RHO
2170 PRINT"REYNOLDS NUMBER                        ";RED
2180 PRINT"DYNAMIC PRESSURE (LB/FT2)              ";Q
2190 PRINT" "
2200 PRINT"* * * * * * * * * * * * * * * FORCE COEFFICIENTS
     * * * * * * * * * * * * * * * * *
2210 PRINT" "
2220 PRINT
     " TRIAL   AOA     NORMAL       SIDE        AXIAL       PITCH
     ROLL        YAW"
2230 PRINT
     " ******  ******  *********    *********   *********   *********
     *********   *********"
2240 FOR X = 1 TO 140
2250 IF COEF(X,3)=0 THEN GOTO 2280
2260 PRINT USING" ###   +###.#    +##.####    +##.####    +##.####
     +##.####    +##.####    +##.####";COEF(X,1),COEF(X,2),COEF(X,3),
     COEF(X,4),COEF(X,5),COEF(X,6),COEF(X,7),COEF(X,8)
2270 NEXT X
2280 '
2290 PRINT" "
2300 IF ANS$<>"Y" THEN GOTO 2640
2310 '  HARDCOPY ROUTINE
2320 LPRINT"INPUT FILENAME: ";INFILE$
2330 LPRINT"OUTPUT FILENAME: ";OUTFILE$
2340 LPRINT" "
2350 LPRINT"INITIAL TEMPERATURE (F)                ";TMIN
2360 LPRINT"FINAL TEMPERATURE (F)                  ";TMAX
2370 LPRINT"AVERAGE TEMPERATURE (F)                ";TAV
2380 LPRINT"WIND TUNNEL VELOCITY (FT/SEC)         ";VEL
2390 LPRINT"WIND TUNNEL VELOCITY (cmH2O)          ";PH20
2400 LPRINT"AIR DENSITY (LBM/FT3)                  ";RHO
2410 LPRINT"REYNOLDS NUMBER                        ";RED
2420 LPRINT"DYNAMIC PRESSURE (LB/FT2)              ";Q
2430 LPRINT" "
2440 LPRINT" "
2450 LPRINT"* * * * * * * * * * * * * * * FORCE READINGS
```

```
     * * * * * * * * * * * * * * * * * *
2460 LPRINT" "
2470 LPRINT
     " TRIAL   AOA     NORMAL       SIDE        AXIAL       PITCH
     ROLL        YAW"
2480 LPRINT
     "   #      DEG     POUNDS      POUNDS      POUNDS      FT-LBS
     FT-LBS      FT-LBS"
2490 LPRINT
     " ******  ******  **********   **********  **********  **********
     **********  **********"
2500 FOR J = 1 TO 140
2510 IF FORCE(J,1)=0 THEN GOTO 2540
2520 LPRINT USING" ###  +###.#   +##.####   +##.####   +##.####
     +##.####   +##.####   +##.####";FORCE(J,1),FORCE(J,2),FORCE(J,3),
     FORCE(J,4),FORCE(J,5),FORCE(J,6),FORCE(J,7),FORCE(J,8)
2530 NEXT J
2540 LPRINT" "
2550 LPRINT" "
2560 LPRINT"* * * * * * * * * * * * * * * FORCE COEFFICIENTS
     * * * * * * * * * * * * * * * *
2570 LPRINT" "
2580 LPRINT
     " TRIAL   AOA     NORMAL       SIDE        AXIAL       PITCH
     ROLL        YAW"
2590 LPRINT
     " ******  *****   **********   **********  **********  **********
     **********  **********"
2600 FOR X = 1 TO 140
2610 IF COEF(X,3)=0! THEN GOTO 2640
2620 LPRINT USING" ###  +###.#   +##.####   +##.####   +##.####
     +##.####   +##.####   +##.####";COEF(X,1),COEF(X,2),COEF(X,3),
     COEF(X,4),COEF(X,5),COEF(X,6),COEF(X,7),COEF(X,8)
2630 NEXT X
2640 '
2650 INPUT"DO YOU WANT TO EXIT THE PROGRAM";AANS$
2660 IF AANS$<>"Y" THEN GOTO 1060
2670 END
```

LIST OF REFERENCES

1. Friedman, Norman, *Naval Vertical Launch Missile Systems*, Military Technology, pp. 24-31, May 1985.

2. Gregoriou, Gregor and Knoche, H.G., *High Incidence Aerodynamics of Missiles During Launch Phase*, MBB GMBH Report UA-523/80, January 1980.

3. Roane, Donald P., *The Effect of a Turbulent Airstream on a Vertically-Launched Missile at High Angles of Attack*, M.S. Thesis, Naval Postgraduate School, Monterey, CA, December 1987.

4. Dahlem, Valentine, and others, *High Angle of Attack Missile Aerodynamics at Mach Numbers 0.3 to 1.5*, AFWAL-TR-80-3070, November 1980.

5. Sheffield, J. Steven, and Deffenbaugh, F.D., *A Three Dimensional Vortex Wake Model for Missiles at High Angles of Attack*, NASA Contractor Report 3208, January 1980.

6. Sheppard, N.M. and Shenton, P.H., *The Asymmetric Shedding of Vortices form an Ogive-Nose Slender Cylinder at Incidence to a Uniform Flow*, Paper, University of Bristol, Bristol, U.K., June 1976.

7. Ericsson, Lars E. and Redding J. Peter, *Asymmetric Vortex Shedding from Bodies of Revolution*, Tactical Missile Aerodynamics, American Institute of Aeronautics and Astronautics, Inc., 1986.

8. Przirembel, C.E.G. and Sherda, Donald E., *Aerodynamics of Slender Bodies at High Angles of Attack*, Journal of Spacecraft, Volume 14, Number 3, pp. 10-14, March 1977.

9. Gregoriou, Gregor, *Modern Missile Design for High Angle-of-Attack*, AGARD/VKI Lecture Series No. 121, High Angle of Attack Aerodynamics, March 1982.

10. Chapman, Gary T., and Keener, Earl R., *The Aerodynamics of Bodies of Revolution at Angles of Attack to 90°*, AIAA Paper 79-0023, 1979.

11. Keener, Earl R., *Flow Separation Patterns on Symmetric Forebodies*, NASA TM 86016, January 1986.

12. Wardlaw, Andrew B., Jr. and Yanta, William J., *Multistable Vortex Patterns on Slender, Circular Bodies at High Incidence*, AIAA Journal, Volume 20, Number 4, pp. 509-515, April 1982.

13. Achenbach, Elmar, *Influence of Surface Roughness on the Cross-Flow Around a Circular Cylinder*, Journal of Fluid Mechanics, pp. 321-335, Volume 46, Part 2, 1971.

14. Ericsson, Lars E. and Redding J. Peter, *Dynamics of Forebody Flow Separation and Associated Vortices*, AIAA Paper 83-2118, August 1983.

15. Reding, J. Peter and Ericsson, Lars E., *Maximum Vortex-Induced Side Forces on Slender Bodies*, AIAA Paper 77-1155, 1977.

16. Lamont, P.J., *Pressure Measurements on an Ogive-Cylinder at High Angles of Attack With Laminar, Transitional, or Turbulent Separation*, AIAA Paper 80-1556, 1980.

17. Yanta, William J. and Wardlaw, Andrew B., Jr. *Flowfield About and Forces on Slender Bodies at High Angles of Attack*, AIAA Journal, Volume 19, Number 3, pp. 296-302, March 1981.

18. Jorgensen, Leland H. and Nelson, Edgar R., *Experimantal Aerodynamic Characteristics for a Cylindrical Body of Revolution With Side Strakes and Various Noses at Angles of Attack From 0° to 58° and Mach Numbers from 0.6 to 2.0*, NASA TM X-3130, March 1975.

19. Deffenbaugh, F.D., and Koerner, *Asymmetric Vortex Wake Development on Missiles at High Angles of Attack*, Journal of Spacecraft, Volume 14, Number 3, pp. 155-162, March 1977.

20. Wardlaw, Andrew B., Jr., and Morrison, Alfred M., *Induced Side Forces on Bodies of Revolution at High Angles of Attack*, NSWC/WOL/TR 75-176, November 1975.

21. Fidler, J.E. and Bateman, M.C., *Asymmetric Vortex Effects on Missile Configurations*, Journal of Spacecraft, Volume 12, Number 11, pp. 674-681, November 1975.

22. Keener, Earl R. and Chapman, Gary T., *Onset of Aerodynamic Side Forces at Zero Sideslip on Symmetric Forebodies at High Angles of Attack*, AIAA Paper 74-770, August 1974.

23. Keener, Earl R., and others, *Side Forces on Forebodies at High Angles of Attack and Mach Numbers from 0.1 to 0.7: Two Tangent Ogives, Paraboloid and Cone*, NASA TM X-3438, February 1977.

24. Wu, J.M., and others, *Some Aerodynamic Performance Calculations on Missile Configurations*, Report, University of Tennessee Space Institute, Tullahoma, TN, May 1979.

25. Kruse, Robert L., Keener, Earl R., and Chapman, Gary T., *Investigation of the Asymmetric Aerodynamic Characteristics of Cylindrical Bodies of Revolution With Various Variations in Nose Geometry and Rotational Orientation*, NASA TM 78533, September 1979.

26. Pick, George S., *Investigation of Side Forces on Ogive-Cylinder Bodies at High Angles of Attack in the M = 0.5 to 1.1 Range*, AIAA Paper 71-570, 1971.

27. Deane, J.R., *Missile Body Vortices and Their Interaction With Lifting Surfaces*, AGARD/VKI Lecture Series No. 121, High Angle of Attack Aerodynamics, March 1982.

28. Neilson, Jack N., *Missile Aerodynamics - Past, Present, Future*, Journal of Spacecraft, Volume 17, Number 3, pp. 165-176, May-June 1980.

29. *On the Development of a Unified Theory for Vortex Flow Phenomena for Aeronautical Applications*, Office of Naval Research, Massachusetts Institute of Technology, April 1975.

30. Vandeput, Fernand, *Aerodynamics of a Missile Fitted With Strakes*, Katholieke Universiteit te Leven, 1980.

31. Schlichting, Hermann, *Boundary Layer Theory*, Seventh Edition, McGraw Hill Book Company, 1979.

32. Tieleman, H.W., *A Survey of the Turbulence in the Marine Surface Layer for the Operation of Low-Reynolds Number Aircraft*, Virginia Polytechnic Institute Report VPI-E-85-10., Blacksburg, VA, March 1985.

33. Castro, I.P., *Effects of Free Stream Turbulence on Low Reynolds Number Boundary Layers*, Journal of Fluids Engineering, Volume 106, pp.298-306, September 1984.

34. Bradshaw, P., *An Introduction to Turbulence and it's Measurement*, Pergamon Press, 1971.

35. Meier, H.U. and Kreplin, H.P., *Influence of Freestream Turbulence on Boundary-Layer Development*, AIAA Journal, Volume 18, Number 1, pp. 11-15, January 1980.

36. Modi, V.J., and others, *Aerodynamics of Pointed Forebodies at High Angles of Attack*, Journal of Aircraft, Volume 21, Number 6, pp. 428-431, June 1984.

37. Bush, N.E., and Jensen, N.O., *Atmospheric Turbulence*, Engineering Meteorology, Elsevier Scientific Publishing Company, 1982.

38. Arya, S.P., *Atmospheric Boundary Layers Over Homogeneous Terrain*, Engineering Meteorology, Elsevier Scientific Publishing Company, 1982.

39. Healey, J. Val, *Simulating the Helicopter-Ship Interface as an Alternative to Current Methods of Determining the Safe Operating Envelopes*, Naval Postgraduate School, Report NPS67-86-003, September, 1986.

40. Bertin, John J., Bertin, Randolph S., Yung, Anne, and Soohoo, George, *The Launch-Tube Flow-Field for a Vertical Launching System*, NSWC Dahlgren Contract Report SCEEE/NWSC/84-B032 and 86-B046, 1986.

41. *Laboratory Manual for Low-Speed Wind-Tunnel Testing*, Department of Aeronautics, Naval Postgraduate School, Monterey, CA, 1983.

42. *Calibration for TASK Mark 14-C Balance*, Balance Calibration Laboratory, NASA-Ames Research Facility, July 1987.

43. Aiello, Gennaro F. and Bateman, Michael C., *Aerodynamic Stability Technology for Maneuverable Missiles*, AFFDL-TR-76-55, March, 1979.

44. Rae, William H. Jr., and Pope, Alan, *Low-Speed Wind Tunnel Testing*, 2nd Ed., John Wiley and Sons, New York, 1984.

45. Clark, W.H., *Body Vortex Formation on Missiles in Incompressible Flows*, AIAA Paper 77-1154, August 1977.

46. Jorgensen, Leland H., *Prediction of Static Aerodynamic Characteristics for Slender Bodies Alone and With Lifting Surfaces to Very High Angles of Attack*, NASA TR R-474, September 1977.

47. Sestak, Timothy A., *Measurement of the Aerodynamic Forces Generated by Flight Crew Helmets in Supercitical Subsonic Flow*, M.S. Thesis, Naval Postgraduate School, Monterey, CA, March 1987.

INITIAL DISTRIBUTION LIST

		No. Copies
1.	Defense Technical Information Center Cameron Station Alexandria, VA 22304-6145	2
2.	Library, Code 0142 Naval Postgraduate School Monterey, CA 93943-5002	2
3.	Chairman Department of Aeronautics, Code 67 Naval Postgraduate School Monterey, CA 93943-5000	1
4.	Commander Naval Sea Systems Command SEA 62Z31 Washington, D.C. 20362-5001	2
5.	Commander Naval Air Systems Command Washington, D.C. 20360	1
6.	Commander Naval Surface Warfare Center Code G20 Dahlgren, VA 22448	2
7.	Commander Naval Weapons Center Code 406 China Lake, CA 93555	1
8.	Commander Naval Surface Weapons Center White Oak Laboratory 10901 New Hampshire Avenue Silver Spring, MD 20903-5000	1
9.	Commander Naval Missile Center Point Mugu, CA 93041	1

10. Commander
Naval Ship Research and Development Center
Bethesda, MD 20035 — 1

11. Office of Naval Research
ONR 100
800 N. Quincy Street
Arlington, VA 22217 — 1

12. Headquarters
Arnold Engineering Development Center
Library Documents
Arnold Airforce Station, TN 37389 — 1

13. NASA Langley Research Center
MS 185 Technical Library
Hampton, VA 23665 — 1

14. NASA Ames Research Center
Technical Library
Moffett Field, CA 94035 — 1

15. NASA Lewis Research Center
Technical Library 60-3
21000 Brookpart Rd.
Cleveland, OH 44135 — 1

16. Prof. R.M. Howard
Department of Aeronautics, Code 67Ho
Naval Postgraduate School
Monterey, CA 93943-5000 — 7

17. Prof. J.V. Healey
Department of Aeronautics, Code 67He
Naval Postgraduate School
Monterey, CA 93943-5000 — 1

18. LT. M. Peter Rabang, USN
5348 Cape Henry Ave.
Norfolk, Va 23513 — 2

20. Dra. Helena Rosa Campos Rabang
Caixa Postal 56022
Praia Vermelha
22292 Rio de Janeiro, RJ BRAZIL — 1

Thesis
R122 Rabang
c.1 Turbulence effects on
the high angle of attack
aerodynamics of a verti-
cally launched missile.
13 SEP 90
35466

Thesis
R122 Rabang
c.1 Turbulence effects on
the high angle of attack
aerodynamics of a verti-
cally launched missile.

DEMCO

AMERICAN BINDERY
TOPEKA, KANSAS

ThesR122
Turbulence effects on the high angle of
3 2768 000 84337 9
DUDLEY KNOX LIBRARY